

Megalin Cytoplasmic Tail Phosphorylation and Function in Kidney Proximal Tubular Cells.

Thesis submitted for the degree of Doctor of Philosophy at the University of
Leicester

By

Richard John Baines B.Sc (Leicester) MB ChB (Leicester) MRCP (UK)
Department of Infection, Immunity and Inflammation
University of Leicester
November 2010

Megalin Cytoplasmic Tail Phosphorylation and Function in Kidney Proximal Tubular Cells.

Richard John Baines

A hallmark of progressive renal disease in man is the presence of abnormal urinary constituents termed proteinuria. These substances include proteins, of which albumin predominates and are derived from the serum but are present in the urine because of abnormal glomerular permeability. Such macromolecules are bioactive and interact with proximal tubular cells (PTC) to activate intracellular signalling cascades. The result is a PTC phenotype that stimulates localised renal inflammation and fibrosis which are characteristic pathological changes of proteinuric nephropathy.

A PTC albumin receptor is a complex that includes megalin, a member of the low-density lipoprotein (LDL-R) family. The paradigm regarding LDL-R family members is that they are cargo receptors which transport ligand from one epithelial surface to another. The cytoplasmic domains of some members of the LDL-R mediate important signalling functions. Therefore, it is postulated that the cytoplasmic tail of megalin (MegCT) might link PTC albumin exposure with signalling effects within the cell. As signalling cascades and protein-protein interactions are regulated by protein phosphorylation studies in this thesis were designed to address whether MegCT is phosphorylated.

Potential agents of MegCT phosphorylation were used to stimulate PTC in culture and stimulated cell lysate tested for its ability to phosphorylate a MegCT-GST fusion protein. Human serum albumin (HSA), epidermal growth factor (EGF) and activators of Protein kinase C (PKC) were all identified to increase the substantial basal phosphorylation of MegCT. Using specific kinase inhibitors phosphoinositide 3-kinase (PI 3-kinase), epidermal growth factor receptor (EGF-R) and PKC were all identified as important mediators of MegCT phosphorylation. MegCT immunoprecipitated from intact cells demonstrated an identical pattern of phosphorylation. To overexpress MegCT a MegCT-CD8 chimaeric protein was developed and demonstrated to associate with the cell membrane and phosphorylate identically to MegCT-GST. Using mass spectrometry of phosphorylated peptides derived from MegCT-GST six sites of MegCT phosphorylation were identified under basal and stimulated conditions.

By measuring FITC-albumin uptake agents stimulating MegCT phosphorylation were identified to be functionally associated with attenuated albumin endocytosis.

In summary this is the first description of the regulated phosphorylation of MegCT in PTC and indicates a number of sites of potential pharmacological inhibition to abrogate the progression of proteinuric nephropathy.

Acknowledgements

I would like to thank Professor Nigel Brunskill who whether to his credit or not has encouraged me in my renal career since I first set foot on the renal unit as a medical student in 1995. More recently he has been an excellent role model demonstrating what a clinician scientist can achieve and without his wisdom and encouragement the project would not have got to this point.

The Consultant staff of the John Walls Renal Unit have been consistently supportive during the (considerable) entirety of my training. The late Professor John Walls was, and still is a huge influence on my career. As my training comes to an end I would like to thank Professor John Feehally and Drs. Kevin Harris, Graham Warwick, Sue Carr, Peter Topham, Jonathan Barratt, James Medcalf, Reem Al-Jayyousi and Rachel Westacott for all they have taught me. It has perhaps taken some gentle cajoling from some of them to make this thesis the printed word rather than a neural pattern.

The financial support of the University Hospitals of Leicester is gratefully acknowledged in funding my training fellowship.

The laboratory has moved a number of times over the years but the friendship and generosity of Ravi, Jen, James, Claire, Kate and Clement has remained constant. Numerous other members of the departments of Infection, Immunity and Inflammation and Cell Physiology and Pharmacology have helped me and I thank them. Drs Blair Grubb, Andrew Bottrill and Professor Andrew Tobin have in particular been generous with their time and expertise.

I would like to thank my family. It has perhaps taken some time to realise that if I have achieved anything it was because I was stood on their shoulders. As I get frustrated by the competing influences on my time I realise how much they gave up for me.

Finally, thanks to my wife Joey for her love, support and the future.

List of abbreviations

ACEi	Angiotensin converting enzyme inhibitor
ANKRA	Ankyrin-repeat family A protein
AOPP	Advanced oxidation protein product
ARB	Angiotensin II receptor antagonist
ASK-1	Apoptosis signal-regulating kinase-1
ATP	Adenosine triphosphate
BMP-4/7	Bone morphogenic peptide-4/7
BSA	Bovine serum albumin
CD2AP	CD2-associated protein
CK I/II	Caesin kinase I/II
CIC-5	Calcium activated chloride channel-5
CUB	C1r/s, Uegf, bone morphogenic peptide-1
DBP	Vitamin D binding protein
DN	Diabetic nephropathy
ECL	Enhanced chemiluminescence
EDTA	Ethylenediaminetetraacetic acid
EEV	Early endocytic vesicle
EGF	Epidermal growth factor
EGTA	Egtazic acid
ELISA	Enzyme linked immunosorbent assay
ERK	Extracellular signal regulated kinase
ESL	Endothelial cell surface layer
ESRF	End stage renal failure
FcRn	Neonatal Fc receptor
FCS	Foetal calf serum
FITC-BSA	Fluorescein 5(6)-isothiocynate labelled albumin
GFR	Glomerular filtration rate
GN	Glomerulonephritis
GSC	Glomerular sieving coefficient
GSK	Glycogen synthase kinase
GST	Glutathione-S-transferase
HK-2	Human kidney-2 cell line
HMG-CoA	Hydroxymethylglutarate CoA
hPTC	Human proximal tubular cell line
HRP	Horseradish peroxidase
HSA	Human serum albumin
ICAM-1	Intercellular adhesion molecule-1
IGF-1	Insulin-like growth factor-1
IL-6	Interleukin-6
IPTG	Isopropyl β -D-thigalactopyranoside
Jak-STAT	Janus kinase signal transducer and activator of transcription pathway
JNK	C-Jun terminal kinase
Kim-1	Kidney injury molecule-1
LDL-R	Low-density lipoprotein receptor
LRP1	Low-density lipoprotein like receptor protein-1
MA	Microalbuminuria

MAPK	Mitogen activated protein kinase
MCP-1	Monocyte chemoattractant protein-1
MegBP	Megalyn binding protein
MegCT	Megalyn cytoplasmic tail
MEK	MAPK kinase
MHC	Major histocompatibility complex
MMP	Matrix metalloproteinase
NAG	N-acetyl glucuronidase
NF-κB	Nuclear factor κB
NHE-3	Sodium-hydrogen exchanger-3
NHERF	NHE regulatory factor
OCRL-1	Occulo-cerebello-renal poetin of Lowe
OK	Opossum kidney
OxLDL	Oxidised low-density lipoprotein
PAGE	Polyacrylamide gel electrophoresis
PAN	Puromycin aminonucleoside
PCR	Polymerase chain reaction
PDBu	Phorbol ester 12,13-dibutyrate
PDGF	Platelet derived growth factor
PI 3-kinase	Phosphoinositide 3-kinase
PIP-4	Phosphoinositide 4-kinase
PKA	Cyclic AMP dependent protein kinase
PKB	Protein kinsase B
PKC	Protein kinase C
PKG	Cyclic GMP dependent protein kinase
PMSF	Phenylmethylsulphonyl fluoride
PTB	Phosphotyrosine binding domain
PTC	Proximal tubular cell
RANTES	Regulated upon activation normal T cell expressed and secreted
RAP	Receptor associated protein
RE	Recycling endosome
RIP	Regulated inramembrane proteolysis
RME	Receptor mediated endocytosis
ROS	Reactive oxygen species
RRT	Renal replacement therapy
SDS	Sodium dodecylsulphate
SE	Sorting endosome
SH2	Src-homology domain-2
SH3	Src-homology domain-3
SKIP	SKI-interacting protein
TGF-β	Transforming growth factor-β
UPE	Urinary protein excretion
VCAM-1	Vascular cell adhesion molecule-1
ZO-1	Zona occludens-1

Table of Contents

1 Introduction.	10
1.1 The epidemiology and natural history of end stage renal failure.	10
1.2 The relationship between tubulointerstitial scarring and progression of renal failure.	12
1.3 Potential mechanisms linking glomerular injury and tubulointerstitial fibrosis.	13
1.4 The role of proteinuria in the development of renal scarring.	15
<i>1.4.1 The relationship between proteinuria and progressive renal failure.</i>	<i>15</i>
1.5 Evidence for toxicity of filtered proteins to PTC.	23
<i>1.5.1 N-acetyl-β-glucosaminidase (NAG)</i>	<i>23</i>
<i>1.5.2 Kidney injury molecule-1 (Kim-1).</i>	<i>24</i>
1.6 The physiology of renal handling of proteins.	25
<i>1.6.1 Glomerular filtration.</i>	<i>25</i>
1.7 Proximal tubular handling of filtered albumin	31
<i>1.7.1 Mechanisms of endocytosis.</i>	<i>33</i>
<i>1.7.2 Fluid phase endocytosis</i>	<i>33</i>
<i>1.7.3 Clathrin mediated endocytosis</i>	<i>34</i>
1.8 The identification of the PTC binding sites for albumin.	34
<i>1.8.1 Megalin and the low-density lipoprotein receptor gene superfamily.</i>	<i>36</i>
<i>1.8.2 Cubilin</i>	<i>38</i>
<i>1.8.3 Amnionless.</i>	<i>39</i>
<i>1.8.4 Evidence for non-megalin/cubilin mediated uptake of albumin in PTC.</i>	<i>43</i>
<i>1.8.5 Other protein components of the albumin endocytic apparatus in PTC.</i>	<i>45</i>
1.9 Regulation of PTC albumin endocytosis.	48
1.10 Phenotypic changes stimulated by proteinuria in PTC.	50
<i>1.10.1 Signalling pathways activated by albumin in PTC.</i>	<i>52</i>
<i>1.10.2 Transcription factors activated by albumin in PTC.</i>	<i>56</i>
<i>1.10.3 Genes regulated by albumin in PTC.</i>	<i>57</i>
<i>1.10.4 Protein expression up-regulated in PTC by albumin.</i>	<i>58</i>
<i>1.10.5 The effect of proteinuria on PTC viability.</i>	<i>59</i>
<i>1.10.6 The axolotl</i>	<i>59</i>
<i>1.10.7 Albumin endocytosis may not be a pre-requisite for signalling effects.</i>	<i>60</i>
1.11 The crucial biological role of megalin.	63
<i>1.11.1 The megalin knockout mouse.</i>	<i>63</i>

1.11.2	<i>Megalin as a regulator of apoptosis.</i>	65
1.11.3	<i>Megalin regulates vitamin D metabolism.</i>	66
1.11.4	<i>Other pathways potentially regulated by megalin.</i>	66
1.11.5	<i>Regulated intramembrane proteolysis (RIP) of megalin.</i>	67
1.12	Potential signalling role of megalin in PTC.	68
1.12.1	<i>Signalling functions of LRP-1.</i>	69
1.12.2	<i>LRP-1 is phosphorylated.</i>	69
1.12.3	<i>The effect of LRP-1 phosphorylation on receptor mediated endocytosis.</i>	71
1.12.4	<i>Megalin as a putative phospho-acceptor protein and modulator of signalling pathways.</i>	71
1.12.5	<i>The sequence of the MegCT.</i>	74
1.13	Aims.	75
1.14	Hypothesis.	76
2	Materials and Methods.	77
2.1	Materials.	77
2.2	General methods.	79
2.2.1	<i>Cell culture.</i>	79
2.2.2	<i>Isolation and culture of human PTC.</i>	80
2.2.3	<i>Culture of OK cells.</i>	82
2.2.4	<i>Culture of HK-2 cells.</i>	83
2.2.5	<i>Preparation of human renal cortex homogenate.</i>	83
2.2.6	<i>Polyacrylamide gel electrophoresis and immunoblotting.</i>	83
2.2.7	<i>Transfection of chemically competent E. Coli, bacterial culture and formation of glycerol stocks.</i>	85
2.2.8	<i>Large and small scale plasmid DNA preparation.</i>	86
2.2.9	<i>Determination of protein concentration.</i>	86
2.2.10	<i>Determination of DNA concentration.</i>	87
2.2.11	<i>Statistical analysis.</i>	87
3	Phosphorylation Studies of a MegCT-GST Fusion Protein.	89
3.1	Introduction.	89
3.2	Aims of these studies.	91
3.3	Methods.	91
3.3.1	<i>Rationale for use of a MegCT-GST fusion protein.</i>	91
3.3.2	<i>Generation of a MegCT-GST fusion protein.</i>	92
3.3.3	<i>Expression, purification and collection of MegCT-GST fusion protein.</i>	92
3.3.4	<i>Stimulation of MegCT-GST fusion protein phosphorylation.</i>	93

3.4 Results.	95
3.4.1 <i>A MegCT-GST fusion protein is phosphorylated in vitro.</i>	95
3.4.2 <i>Multiple kinases regulate MegCT-GST fusion protein phosphorylation.</i>	102
3.5 Discussion.	102
4 Characterisation of Polyclonal Rabbit anti-MegCT Antisera.	110
4.1 Introduction.	110
4.2 Aims.	110
4.3 Materials and Methods.	110
4.3.1 <i>Immunisation of rabbits against human MegCT.</i>	111
4.3.2 <i>Determination of antibody titre.</i>	111
4.3.3 <i>Characterisation of rabbit anti-human MegCT antisera.</i>	112
4.4 Results.	112
4.4.1 The immunoreactivity of rabbit serum anti-MegCT.	112
4.4.2 <i>Rabbit anti-sera recognised the megalin component of a MegCT-GST fusion protein.</i>	113
4.4.3 <i>Intact megalin was detected in human renal cortex homogenate by rabbit anti-sera.</i>	113
4.4.4 <i>Rabbit antisera is immunoreactive against intact megalin in HK2 cell lysate.</i>	116
4.5 Discussion.	116
5 Studies of Megalin Phosphorylation in Intact Cells.	119
5.1 Introduction.	119
5.2 Aims.	119
5.3 Methods.	119
5.3.1 <i>Stimulation of [³²P]-Orthophosphate loaded PTC.</i>	119
5.3.2 <i>Immunoprecipitation of radiolabelled MegCT.</i>	120
5.3.3 <i>Analysis of immunoprecipitated proteins.</i>	121
5.4 Results.	121
5.4.1 <i>MegCT is phosphorylated in intact cells.</i>	121
5.4.2 <i>Kinase regulation of MegCT in intact cells.</i>	123
5.5 Discussion.	123
6 Development and Phosphorylation of a MegCT-CD8 Chimaeric Protein.	129
6.1 Introduction.	129
6.2 Strategy for the development of a MegCT-CD8 chimaeric protein.	130
6.3 Aims.	130
6.4 Methods.	131

6.4.1	<i>Primer design and conditions for the PCR.</i>	131
6.4.2	<i>Separation and Visualisation of DNA products.</i>	137
6.4.3	<i>Gel Extraction of DNA bands.</i>	137
6.4.4	<i>Restriction endonuclease digestion of DNA.</i>	137
6.4.5	<i>Ligation of DNA fragments.</i>	138
6.4.6	<i>DNA sequencing.</i>	140
6.4.7	<i>Transfection MegCT-CD8 Chimaeric construct into OK cells.</i>	141
6.4.8	<i>Visualisation of OK cells transiently transfected with MegCT-CD8 chimaeric protein.</i>	142
6.4.9	<i>Phosphorylation of MegCT-CD8 Transiently expressed in OK Cells.</i>	143
6.5	Results.	144
6.5.1	<i>Propagation of pGEX-4T1-MegCT.</i>	144
6.5.2	<i>Propagation of pBS SKII-CD8.</i>	144
6.5.3	<i>Amplification of MegCT cDNA by PCR from pGEX-4T1-MegCT.</i>	147
6.5.4	<i>Amplification of CD8 cDNA from BS-SKII-CD8 using PCR.</i>	147
6.5.5	<i>Subcloning of CD8 and MegCT cDNA into SacII/XhoI digested pCMV-Script.</i>	151
6.5.6	<i>Sall digestion of MegCT and CD8 and ligation.</i>	154
6.5.7	<i>Attempted ligation of NotI/AflIII digested MegCT cDNA into NotI/AflIII digested BS-SKII-CD8.</i>	155
6.5.8	<i>Introduction of greater 5' and 3' overhang into CD8 and MegCT cDNA.</i>	157
6.5.9	<i>Cloning of CD8 cDNA and MegCT cDNA into pCRII-TOPO.</i>	161
6.5.10	<i>Subcloning of CD8 cDNA into pCMV-Script.</i>	163
6.5.11	<i>Subcloning of MegCT cDNA into pCMV-Script-CD8.</i>	163
6.5.12	<i>Preparation of Sall/ApaI MegCT cDNA and Sall/ApaI pCMV-Script-CD8 for ligation.</i>	166
6.5.13	<i>Introduction of a full Kozak initiation sequence into the CD8-MegCT cDNA.</i>	171
6.5.14	<i>Sequencing of pCMV-Script-CD8-MegCT.</i>	173
6.5.15	<i>Transient expression of MegCT-CD8 chimaeric protein in OK cells.</i>	173
6.5.16	<i>Stable transfection of MegCT-CD8 and CD8.</i>	176
6.5.17	<i>A MegCT-CD8 chimaeric protein transiently expressed in OK cells was associated with the cell membrane.</i>	180
6.5.18	<i>MegCT-CD8 chimeric proteins transiently transfected into OK cells are phosphorylated.</i>	180
6.6	Discussion.	185
7	PTC functional associations of MegCT phosphorylation.	191
7.1	Introduction.	191

7.2 Aim.	193
7.3 Methods.	193
7.3.1 <i>The assay of endocytosis.</i>	193
7.4 Results.	194
7.4.1 <i>Effect of agents that stimulate MegCT phosphorylation on albumin endocytosis.</i>	194
7.4.2 <i>Effect of inhibitors of megalin RIP on endocytosis.</i>	194
7.4.3 <i>The effect of transient overexpression of MegCT-CD8 on albumin endocytosis.</i>	198
7.4.4 <i>Investigations on OK cells stably expressing MegCT-CD8.</i>	198
7.4.5 <i>The role of the proteasome in albumin endocytosis.</i>	201
7.5 Discussion.	203
8 Determination of phosphorylation sites in MegCT.	209
8.1 Introduction.	209
8.2 Aim.	209
8.3 Methods	209
8.3.1 <i>Phosphorylation of MegCT-GST by HK-2 cell lysate.</i>	209
8.3.2 <i>LC-MS/MS.</i>	210
8.4 Results.	212
8.4.1 <i>Identification of phospho-acceptor sites in MegCT.</i>	212
8.5 Discussion.	218
9 Final discussion, summary and indications for future work.	225
10 Appendices.	234
10.1 Appendix A – Buffers used in these studies.	234
10.2 Appendix B. Vector maps of plasmids used in these studies.	238
11 References.	242

1 Introduction.

“When bubbles settle on the surface of the urine, they indicate disease of the kidneys and that the complaint will be protracted.”

Corpus Hippocratium. Circa 430 BC
(Diamandopoulos et al., 2009)

This aphorism from Hippocrates is perhaps the first recording of the link between proteinuria and renal disease. As true today as it was then, a holy grail of the modern nephrologist is to understand and limit the mechanisms that lead to the progressive loss of renal function.

1.1 The epidemiology and natural history of end stage renal failure.

The replacement of renal function by dialysis is imperfect and socio-economically costly. The need for renal replacement therapy continues to rise globally and applies great pressure to health services where dialysis and transplantation are available.

In 2008 the United Kingdom acceptance rate onto renal replacement programmes was 108 patients per million of population (pmp). The prevalence of those requiring renal replacement therapy (RRT) was 774 pmp with an annual increase in this figure of approximately 4.4% (Byrne et al., 2010a, Byrne et al., 2010b). The basic cost per person on dialysis is between £15,000 and £35,000 (Baboolal et al., 2008) and previous estimates have equated this to total 1.5% of the overall health budget (Nicholson and Roderick, 2007).

The treatment itself is imperfect. The one year survival from the date of the first dialysis is 79%, the median life years remaining for a 25-29 year old on haemodialysis is 20 years (Ansell et al., 2010). It is estimated that 320,000

hospital days a year in the UK are used in dealing with the consequences and complications of haemodialysis alone (Roderick et al., 2005).

Although the stark economic costs are relatively easy to quantify, what is more difficult are the personal costs to individuals affected with end-stage renal failure (ESRF), their families and communities. There is not a facet of their life that the illness does not pervade.

Therefore, it would be desirable to halt or slow the progression of renal disease at an early stage. Recommended screening of high risk groups has facilitated the diagnosis of renal disease earlier in its natural history. However, identifying those with progressive renal disease is insufficient. The therapeutic armoury of the nephrologist is limited and the treatments relatively non-specific. There is a pressing need to understand the underlying patho-physiology of progressive renal disease with the expectation that new, more targeted interventions will be developed.

A multiplicity of renal diseases can initiate renal damage and in many cases the nature of the original pathology is well characterised. Often, even if this insult is removed the kidneys progressively fail over time and this culminates with the need for renal replacement therapy. This continuing progression may, in some way reflect the kidneys maladaptive response to injury, and the decline in function could be due to a common perpetuating factor. The uniformity of this secondary process may explain how the diverse histological patterns associated with primary glomerular diseases ultimately end in the strikingly similar macro- and microscopic appearance of the end-stage kidney.

The end-stage kidney has a characteristic appearance (Heptinstall, 1983). On a macroscopic level the failed kidney is small and shrunken. Microscopically, the

glomeruli demonstrate a loss of capillary structure with localised areas of cell proliferation. Progressive scarring results in deformation, collapse and sclerosis of the capillary bed. Tubular atrophy is marked, especially in those tubules downstream of scarred glomeruli and there is a significant inflammatory infiltrate around the tubules. The interstitium displays prominent fibrosis with deposition of collagen and lipids and large numbers of fibroblasts are visible.

These changes are seen in kidneys of humans and in animal models of progressive renal failure. The extent of these inflammatory, and pro-scarring changes, are strongly correlated with the degree by which renal function is impaired.

1.2 The relationship between tubulointerstitial scarring and progression of renal failure.

A consistent finding in humans and animals is that the degree of renal impairment is closely associated with the extent of tubulointerstitial scarring rather than glomerular damage. This observation is true even in the case of primary glomerular diseases and therefore, it has been suggested that the events in the tubulointerstitium are critical in mediating progressive renal dysfunction.

Over forty years ago Risdon (Risdon et al., 1968) found a highly significant correlation between the degree of tubular damage in a series of renal biopsies and various measures of renal function from the same patients. The same relationship was not found between glomerular damage and renal failure and of particular note was the finding that individuals with severe glomerular damage maintained a relatively normal serum creatinine providing the tubulointerstitium was undamaged. Later work confirmed this finding and extended the

observation to show that irrespective of the original cause of the renal dysfunction the relationship between tubulointerstitial damage and overall function held true (Schainuck et al., 1970). Over time, the correlation between tubulointerstitial damage and renal function has been described for focal segmental glomerulosclerosis, diabetic nephropathy, membrano-proliferative glomerulonephritis, IgA nephropathy, membranous glomerulonephritis, renal amyloidosis, chronic interstitial nephritis and Alport's disease (Bohle et al., 1979, Bohle et al., 1991, Park et al., 1986, Hooke et al., 1987, Cameron, 1989, Alexopoulos et al., 1990, Kim et al., 1995).

1.3 Potential mechanisms linking glomerular injury and tubulointerstitial fibrosis.

Whilst the degree of renal impairment most closely correlates with the degree of tubulointerstitial damage a large number of renal pathologies primarily affect the glomeruli. A number of theories postulate how glomerular lesions result in tubulointerstitial fibrosis, and whilst these remain contentious they have been summarised and evaluated (Kriz and LeHir, 2005). In brief, the proposed mechanisms are;

- *Transfer via the vascular route.* The efferent arteriole of the glomerulus gives rise to capillaries that perfuse the tubulointerstitium. Therefore, harmful factors within the vascular system of the glomerulus would be transported to the tubulointerstitium. Furthermore, if a glomerulus were rendered hypoxic by vascular injury the downstream tubulointerstitium would be even more oxygen deficient. There is little evidence that this occurs *in vivo* (Kang et al., 2002).

- *Encroachment of crescentric lesions on the tubule.* If a crescent is formed at the glomerulo-tubular junction, obstruction results and there is misdirected flow of filtrate around the tubule (Kriz et al., 2001). This leads to an inflammatory response to agents in the filtrate, tubular obstruction and degeneration. A second consequence of obstruction at the tubulo-glomerular junction may be an effectively aglomerular tubular segment which subsequently degenerates (Le Hir and Besse-Eschmann, 2003)
- *Protein leakage into the tubular urine.* This is thought to contribute to tubular damage by three mechanisms. (i) The excessive reabsorption of protein by PTC as a result of glomerular damage may result in cell stress and either the spillage of lysosomal enzymes into the cytoplasm and/or the generation of reactive oxygen species (Morigi et al., 2002) (ii) Factors toxic to PTC may be present in the proximal tubular filtrate such as complement proteins (Hsu and Couser, 2003), albumin and albumin-bound fatty acids (see below). Alternatively, one of the effects of increased lysosomal degradation of reabsorbed proteins may be ammonia generation that has been shown to activate complement (Nath et al., 1985) (iii) Finally, excess lysosomal degradation of filtered protein may stimulate cytokine secretion by PTC that initiates peri-tubular fibrosis and in this context albumin itself may act as a cytokine. The evidence for this will be discussed in far more detail below.

These theories need not of course be mutually exclusive and may be more or less prominent in different disease states. It is however important to recognise that not all glomerular lesions are crescentic in nature and yet a progressive decline in renal function is still observed.

1.4 The role of proteinuria in the development of renal scarring.

1.4.1 The relationship between proteinuria and progressive renal failure.

A hallmark of progressive renal dysfunction is proteinuria. Glomerular proteinuria arises as the result of circulating proteins passing from the vasculature across an inflamed or injured glomerulus into the urine. Whilst glomerular proteinuria is predominantly manifest as albuminuria, a cocktail of potentially bioactive macromolecules are abnormally filtered by the glomerulus and are present in the urine. The number of triggers for initiating glomerular damage is large but the pattern of tubulointerstitial inflammation is much more limited. This has led investigators to hypothesise that irrespective of the initiator of renal damage a perpetuating factor may be responsible for stimulating tubulo-interstitial damage and the corresponding loss of renal function. As proteinuria is an almost universal finding in progressive renal disease it has been asked whether filtered proteins interact with PTC and result in pro-inflammatory changes. In this model, proteins filtered by the glomerulus – predominantly albumin – would be the perpetuating factor and the histological pattern that results has been termed proteinuric nephropathy (Brunskill, 2004). In the following sections evidence arising from studies on humans and animals will be described that support this theory.

1.4.1.1 Evidence from animal studies

Five stages have been identified that are important to the development of tubulointerstitial fibrosis (Jernigan and Eddy, 2000). These are (i) the initial renal insult (ii) cellular release of fibrogenic factors (iii) accumulation of intracellular matrix proteins (iv) obliteration of peritubular capillaries and (v) death of PTC

and progressive renal insufficiency. In order to associate this series of events with the development of proteinuria a number of experimental models have been developed.

1.4.1.1.1 Purinomycin nucleoside induced nephrosis.

A single administration of puromycin aminonucleoside (PAN) to rats has a toxic effect on the podocyte following which heavy proteinuria develops. Proteinuria peaks 14 days after administration and abates thereafter. This is a useful model in which the time courses of the development of proteinuria and inflammatory infiltrate can be compared. There is a clear relationship between the two (Eddy et al., 1991) and both are reduced by provision of a low protein diet, thereby reducing proteinuria (Eddy, 1994). Following an initial inflammatory infiltrate, foci of tubulointerstitial fibrosis develop and expression of a number of pro-fibrotic and pro-inflammatory proteins (e.g. extracellular matrix proteins, metalloproteinases, MCP-1 and TGF- β) are increased. In this model administering enalapril did not reduce proteinuria and had no effect on the tubulointerstitial changes.

1.4.1.1.2 Protein overload nephropathy.

Proteinuria can also be induced in rats by the intra-peritoneal injection of between 2 and 5 g/day of BSA. These animals rapidly develop proteinuria and widespread foot process effacement. There is no evidence of either an immune system mediated glomerular injury or immune-complex deposition due to anti-BSA antibodies (Davies et al., 1978, Eddy, 1989, Andrews, 1977). Heterologous excretion of albumin ceases within 48 hours of the last injection of BSA although homologous albuminuria persists (Davies *et al.*, 1978). Following induction of proteinuria there is an influx of chronic inflammatory cells into the

interstitium and an accumulation of extracellular matrix proteins (Eddy, 1989, Eddy and Giachelli, 1995). There is also an increase in PTC expression of the chemotactic substances MCP-1 and osteopontin (Eddy *et al.*, 1995).

1.4.1.1.3 *Sub-total nephrectomy*

In the remnant kidney model surgical reduction of renal mass by 3/4 to 5/6 is followed by the development of proteinuria, hypertension and progressive renal failure with histological evidence of glomerulosclerosis and tubulointerstitial fibrosis (Chanutin A, 1932). Hyperperfusion of the remaining nephrons increases intraglomerular pressure and is associated with proteinuria and systemic hypertension (Hostetter *et al.*, 1981, Anderson *et al.*, 1985a, Anderson *et al.*, 1985b). A reduction in proteinuria as a result of dietary modification (El-Nahas *et al.*, 1983, Williams *et al.*, 1987), or inhibition of the renin-angiotensin system (Anderson *et al.*, 1986) reduces proteinuria, attenuates tubulointerstitial fibrosis and overall is reno-protective. The beneficial effects of antagonising the renin-angiotensin system are independent of an effect on systemic blood pressure.

1.4.1.2 Evidence from human studies and clinical trials.

In individuals with diabetes the development of proteinuria is the hallmark of diabetic nephropathy (Mogensen, 2000, Williams, 2005). As a consequence, this group of patients have featured in many of the landmark studies that have related degree of proteinuria to renal prognosis. Although subject to individual variation, as a population the pattern of change of proteinuria in diabetic patients is predictable. In the early years (up to year five) following diagnosis there is a subtle increase in the level of microalbuminuria (MA), that is an

excretion of albumin of less than 300 µg/day. The onset of nephropathy is marked by glomerular hyperfiltration and a rise in GFR with a continuing increase in the urinary protein excretion (UPE). As GFR starts to fall the UPE is about 1 g/day. Progressive azotaemia is matched by a rise in UPE to roughly 6g/day which falls abruptly as end stage renal disease (ESRD) develops. It should be noted that in some individuals MA will not progress and may, in fact, regress. So, whilst these observations do not prove a causative role for proteinuria in diabetic nephropathy (DN) the natural history has lent itself to a number of observational and interventional studies that indicate proteinuria to be a key mediator in progressive kidney disease.

It has been realised for some time that in individuals with type 1 diabetes the presence of proteinuria indicates a poor prognosis (Gellman et al., 1959, Watkins et al., 1972). However, only in recent years have well constructed randomised controlled trials (RCT) addressed this issue more systematically.

One arm of the Diabetes Control and Complications Trial (DCCT) received intensive glycaemic control compared to a then standard treatment group (DCCT, 1993) and the incidence of macro- and micro-vascular complications of both groups recorded. In terms of renal outcome intensive glycaemic control reduces the progression from MA to more florid proteinuria and in more long term follow up lessened renal impairment (DCCT, 2003). The Collaborative Study Group noted that in a group of patients that reached the primary end point of a doubling of serum creatine the baseline proteinuria was 4.99 g/day compared to 2.34 g/day in those whose serum creatinine was more stable (Breyer et al., 1996).

The same pattern is seen in people affected by type 2 diabetes where baseline albuminuria predicts renal outcome (Lebovitz et al., 1994). In the United Kingdom Prospective Diabetes Study (UKPDS) tight glycaemic control in individuals with type 2 diabetes attenuated the progression through MA to macroalbuminuria (Adler et al., 2003). A number of studies relate risk of progression of renal disease to baseline proteinuria in individuals affected by type 2 diabetes (de Zeeuw et al., 2004, Atkins et al., 2005, Eijkelkamp et al., 2007).

Proteinuria has also long been recognised to be an adverse prognostic feature in non-diabetic renal disease (Hostetter et al., 1982, Mallick et al., 1987). In people with progressive CKD protein excretion correlates with rate of loss of renal function and proteinuria was the only predictive variable of renal failure in a multi-variate analysis that included blood pressure, calcium/phosphate product and dietary protein intake. (Wight et al., 1992, Williams et al., 1988). The modification of diet in renal disease study (MDRD) is a landmark randomised controlled trial that enrolled 840 patients with non-diabetic renal disease to study the effect of dietary protein modification and blood pressure management on progression of renal disease (Klahr et al., 1994). Baseline proteinuria was a strong predictor of a decline in renal function. Other investigators have studied the prognostic utility of albuminuria in a population unrecognised to have renal disease. The Prevention of REnal and Vascular ENd-stage Disease (PREVEND) group collected urine samples from over 40,000 members of the general population of Groningen (the Netherlands). MA predicted the development of stage 3 CKD at year 4. Moreover, even at levels of MA

conventionally regarded as normal (that is less than 30 mg/day of albumin excretion) there was a rise in risk of developing CKD (Verhave et al., 2004).

The studies referred to above indicate an association between proteinuria and progressive renal disease. Establishing a causative role of proteinuria in driving progressive renal disease is less straightforward but hinted at by intervention studies in which strategies that reduce UPE are, in general, renoprotective.

Low protein diets reduce proteinuria in patients with chronic glomerulonephritis, and, the extent of reduction predicts a favourable outcome in terms of renal function (El Nahas et al., 1984). A similar finding was observed in a *post hoc* analysis of the MDRD data in which a reduction in dietary protein, attenuation of UPE and renoprotective effect all correlated (Hunsicker et al., 1997). Adverse nutritional effects have limited dietary modification as a therapeutic approach in modern practice. Instead, pharmacological agents, particularly those that interrupt the renin–angiotensin system are more commonly used.

Interruption of the renin-angiotensin system is thought to reduce urinary protein excretion via several mechanisms (Brenner and Zagrobelny, 2003) These include:

- Alteration of renal and systemic haemodynamics with a reduction in the intraglomerular filtration pressure.
- Reducing the permeability of the glomerular filtration barrier.
- Blockade of the angiotensin II mediated growth stimulating actions within the kidney.

Diabetic nephropathy and proteinuria are strongly linked and many of the earliest reports of the anti-proteinuric and renoprotective effect of angiotensin

converting enzyme inhibition (ACEi) involved patients with type 1 diabetes. In a study of patients with diabetes and nephrotic range proteinuria (>3.5 g/day) there was remission of proteinuria in 16.5% of people receiving captopril compared to 1.5% in those receiving placebo (Hebert et al., 1994). In that study captopril treatment was associated with a lower blood pressure. In the Heart Outcomes Prevention Evaluation (HOPE), ramipril reduced the primary outcome measure of a reduction in cardiovascular endpoints, and in addition lessened the risk of overt nephropathy and lowered albuminuria independent of blood pressure reduction (HOPE, 2000).

In patients with type 2 diabetes and nephropathy the anti-proteinuric effects of angiotensin receptor blockers (ARB) have been tested. Both irbesartan (Lewis et al., 2001) and losartan (Brenner et al., 2001) reduce proteinuria and retard renal failure again, independent of an improvement in blood pressure control.

Similar patterns are observed in populations with non-diabetic proteinuric renal disease. A landmark study demonstrating a reno-protective effect of ramipril over and above an effect on blood pressure is the Ramipril Efficacy in Nephropathy (REIN) study (Ruggenenti et al., 1999b, Ruggenenti et al., 1999a, Ruggenenti et al., 1998). Ramipril reduced both proteinuria and the risk of doubling of serum creatinine and/or ESRF in populations that had non-nephrotic UPE rates. This effect could not be attributed to blood pressure reduction and furthermore, the initial response to ramipril was prognostically significant. That is, a swift reduction in proteinuria was associated with reno-protection.

In a pooled analysis of 11 trials the benefit of ACEi in non-diabetic patients divided into quartiles of risk of progressive renal disease and baseline levels of proteinuria was studied. At UPE of > 500 mg/day ACEi were beneficial across

risk groups, whereas, no benefit was seen when protein excretory rates were less than 500 mg/day (Kent et al., 2007). This contrasts with another study in a similar population in which a reduction of MA by 50% was specifically targeted as a therapeutic aim. Over an 8 year period a 50% reduction in MA was associated with a rate of eGFR loss of 1.8/year compared to 4.4/year in the standard treatment group (Araki et al., 2007). In specifically reducing albumin excretion to levels below 500 mg/day published reports have used high doses of benazepril (Hou et al., 2007), with benefit in terms of UPE reduction and a reduction in renal outcomes (doubling of serum creatinine/ESRD).

The Ongoing Telmisartan Alone or in combination with Ramipril Global Endpoint Trial (ONTARGET) was a large RCT designed to investigate potential superiority of combined telmisartan and ramipril compared to monotherapy in over 25,000 individuals with atherosclerotic disease. ONTARGET's major endpoints were cardiovascular in nature and no benefit was found for combination therapy (Yusuf et al., 2008). In a subsequent report the same investigators described that combination treatment was associated with a reduction of proteinuria but significantly more adverse renal events which included the need for dialysis, a doubling of serum creatinine or death (Mann et al., 2008). Some caveats are needed in interpreting this data. The majority of the adverse renal events arose from a need for dialysis because of acute kidney injury, perhaps not surprising as the studied population probably had an occult burden of renovascular disease. It should also be noted that that the number of people enrolled in this study with proteinuria was relatively small and perhaps underpowered to detect an effect of UPE on renal and/or cardiovascular outcome.

In summary, there is a broad body of evidence that events occurring in the renal tubulointerstitium are critical to the progression of renal disease. In rats induction of proteinuria is associated with tubulointerstitial fibrosis, and in humans anti-proteinuric strategies are renoprotective. As PTCs are the most abundant cell in the tubulointerstitium investigators have studied the effect of proteinuric urine, or its components on markers of tubular cell injury.

1.5 Evidence for toxicity of filtered proteins to PTC.

The evidence outlined above that relates proteinuria to renal toxicity is associative and does not prove a cause and effect relationship. To develop this association studies have utilised the fact that PTC injury results in macromolecule release which can be used as biomarkers of renal damage. This characteristic has been used *in vitro* and *in vivo* to investigate the potential reno-toxicity of a number of agents, including albumin.

1.5.1 N-acetyl- β -glucosaminidase (NAG)

NAG is a urinary enzyme originating from the lysosome that has a molecular mass of 130kDa. It is normally excreted in the urine in a small amount as a result of the normal exocytosis process as opposed to glomerular filtration. When PTC are damaged it is present in the proximal tubular filtrate at an increased concentration (Guder and Hofmann, 1992). NAG is elevated by several agents toxic to the proximal tubular epithelium including lead, solvents, contrast media, aminoglycoside antibiotics and chemotherapeutic agents (Price, 1992, Pergande et al., 1994). NAG levels are elevated in proteinuric conditions, including diabetes, and positively correlate with UPE (Rustom et al., 1998, Bazzi et al., 2002).

1.5.2 *Kidney injury molecule-1 (Kim-1).*

Kim-1 is a recently discovered proximal tubular protein that is induced after tubular injury caused by ischaemia-reperfusion and nephrotoxic injury (Ichimura et al., 1998, Ichimura et al., 2004). Renal expression can be assessed by immunohistochemistry of renal biopsy specimens, or by measuring the large cleaved extracellular domain of Kim-1 that may be excreted in the urine. Urinary assays for Kim-1 might detect early renal damage (Vaidya et al., 2006). Urinary Kim-1 levels are more sensitive and specific in predicting acute kidney injury than NAG, blood urea or serum creatinine (Vaidya et al., 2010). In rats induction of proteinuria using the protein overload model increases urinary Kim-1 levels in proportion to the UPE (van Timmeren et al., 2006). Studies of proteinuric rats demonstrate co-localisation of renal Kim-1 expression at areas of tubulointerstitial fibrosis. In PAN induction of proteinuria increases urinary Kim-1 levels and tubulointerstitial fibrosis. Co-administration of enalapril reduces proteinuria, renal Kim-1 expression and urinary Kim-1 secretion (Kramer et al., 2009).

In humans, Kim-1 may be an early biomarker of renal graft loss as a high urinary Kim-1 excretion is associated with a falling creatinine clearance and high proteinuria (van Timmeren et al., 2007a). Renal Kim-1 expression and urinary Kim-1 secretion correlate and are elevated in proteinuric states including minimal change disease, membranous GN, diabetic nephropathy and IgAN. However, there is no direct correlation between degree of proteinuria and renal Kim-1 expression and secretion (van Timmeren et al., 2007b). More recently, it was reported that anti-proteinuric strategies reduce UPE and urinary Kim-1 levels in non-diabetic proteinuric patients (Waanders et al., 2009).

To summarise, there is strong evidence to link proteinuria, PTC damage, tubulointerstitial fibrosis and progressive renal failure. The following sections will consider how proteinuria arises and how filtered macromolecules interact with PTC.

1.6 The physiology of renal handling of proteins.

1.6.1 Glomerular filtration.

1.6.1.1 Glomerular structure (Figs. 1.1 A and B).

A single glomerulus is comprised of a tuft of specialised capillaries supplied by an afferent arteriole. An efferent arteriole facilitates drainage from the glomerulus and the structure is covered by Bowmans capsule.

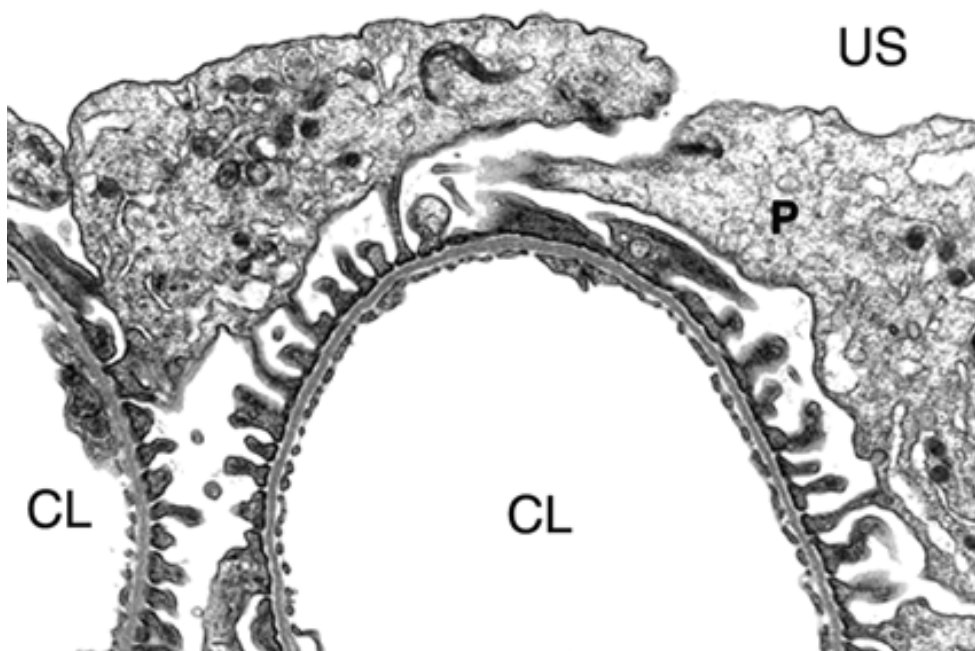


Figure 1.1 A. Cross section of a rat glomerular capillary loop. The podocyte (P) cell body extends into the urinary space (US). CL capillary lumen. Taken from Kerjaschki (2001).

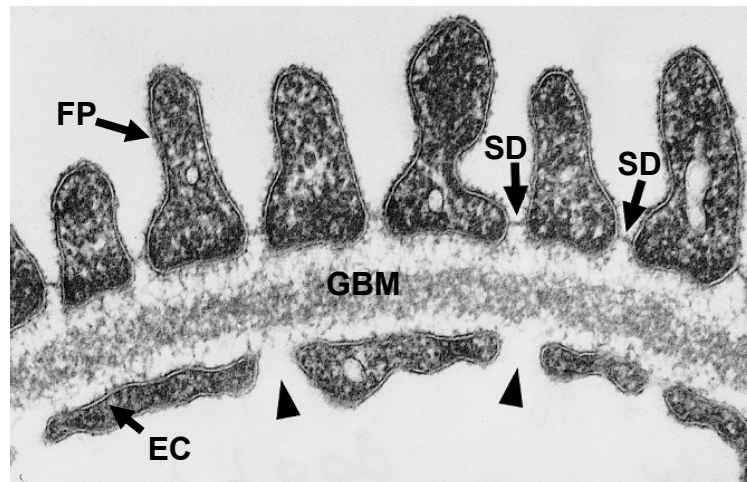


Figure 1.1 B. Glomerular filtration barrier. FP podocyte foot process, SD slit diaphragm, GMB glomerular basement membrane, EC endothelial cell, arrow heads endothelial fenestrae. Taken from Mathieson (2004).

glomerular basement membrane consists of type IV collagens, heparin sulphate proteoglycans and laminin (Abrahamson 1987).

The fenestrated areas of the endothelium are extremely attenuated and possess oval or round shaped pores of up to 100nm in diameter (Larsson and Maunsbach, 1980). Compared to other fenestrated endothelia at different sites these pores are mostly wide open and lack a diaphragm (Jorgensen, 1966). Projecting into the lumen of the capillary is the endothelial cell surface layer (ESL). This layer coats the entire endothelium, including the fenestrations, and has two components; the glycocalyx, that is predominantly bound to the plasma membrane and a more loosely associated endothelial cell coat (Jeansson and Haraldsson, 2006, Jeansson and Haraldsson, 2003). The ESL is strongly negatively charged and has a potential thickness of 1 μm (Haraldsson et al., 2008). Adriamycin treatment of rats depletes the ESL and results in proteinuria (Jeansson et al., 2009).

The glomerular basement membrane separates the glomerular capillary endothelium from the visceral epithelial cell layer that is comprised of

podocytes. With contributions from both the capillary endothelium and visceral epithelium (Abrahamson, 1987) the basement membrane consists of three layers. These layers are distinguished on the basis of their different electron densities and are arranged such that an electron dense lamina densa is bounded by the electron lucent areas termed the lamina rara externa and lamina rara interna. The composition of this basement membrane does not differ markedly from other basement membranes (Mohan and Spiro, 1986, Timpl and Dziadek, 1986).

The tuft of glomerular capillaries is covered by glomerular epithelial cells (the podocyte). These cells possess an exquisitely intricate architecture. The voluminous cell body projects into the urinary space and from it arise primary processes that extend to the capillary wall to which they are attached by numerous secondary foot processes. These inter-digitate with the processes from neighbouring cells and form an intricate network of slits termed filtration slits. The slits are narrowest at their bases where they have a diameter of 25-65 nm (Bulger, 1988). The filtration slits are bridged by an extracellular slit diaphragm with a regular subunit structure a major component of which is nephrin (Tryggvason, 1999). A number of other proteins such as ZO-1, P-cadherin, CD2AP, podocin and catenins are important in maintaining the integrity of this structure (D'Amico and Bazzi, 2003).

The spaces between these subunits have an area of about 14 nm, roughly equivalent to the size of an albumin molecule (Rodewald and Karnovsky, 1974). At the vascular pole the visceral epithelium is in continuity with the parietal epithelium which is a simple squamous layer. At the urinary pole the simple squamous epithelia gives way to the tall columnar epithelia of the proximal

tubule. Between the parietal and visceral epithelial layers is the urinary space from which filtrate exits via the urinary pole into the proximal tubule.

The glomerular filtration barrier is thus formed by the ESL, the capillary endothelium with its wide open pores, the glomerular basement membrane and the slits between the podocyte foot processes covered by the slit membrane. Recently attention has turned to a potential fifth layer of this barrier formed by sub-podocyte spaces that may have a role in controlling hydraulic filtration (Salmon et al., 2007).

These distinct anatomical layers provide a functional barrier to molecules based on their size and charge. Overall this allows the free movement of water and small molecules whilst restraining larger molecules. Various models have been proposed as to how this occurs derived from studies of the fractional excretion of biologically inert molecules such as dextrans and ficoll whose size and charge can be manipulated (see D'Amico and Bazzi 2003 for review). In a mathematical model of glomerular permeability it is postulated that a group of small restrictive pores allow free movement of molecules up to around 40Å and larger pores enable movement of molecules up to 80Å in size. This is purely a model with no structural evidence that functional pores exist. The relative ratio of the small and large pores determines the overall permeability of the filtration barrier. As the smaller pores prevail they offer the major barrier to filtration. Size however, is not the only factor determining glomerular filtration. Albumin is a molecule whose diameter approximates to 36Å and as such could be expected to be freely filtered at the glomerular filtration barrier. However, compared to ficoll, a molecule of comparable size to albumin the sieving coefficient of the latter is much reduced (Ruggenti et al., 1999) implying filtration of the

negatively charged albumin is hampered by the overall negative charge of the glomerular filtration barrier.

The impedance to traffic of albumin offered by the glomerular filtration barrier is a source of much controversy. Some investigators believe there to be only a size restriction to free flow of albumin from the circulation into the proximal tubule and the following section describes these competing theories.

1.6.1.2 Significant amounts of protein are filtered by the glomerulus in health.

In health the amount of albumin lost in the urine is small and approximates to 100 mg/day (Maack et al., 1992). The fractional filtration of albumin is the concentration ratio between the proximal tubular filtrate and blood and in rats this is estimated by micropuncture studies to range between 0.0005 and 0.0007 (Maack et al., 1992, Tojo and Endou, 1992, Lund et al., 2003). Indirect measures of the proximal tubular filtrate composition suggest that the fractional filtration of albumin in humans is 0.0001 (Norden et al., 2001). Assuming a serum albumin concentration of 45g/L, this equates to a proximal tubular filtrate concentration of albumin of 22-32 mg/L a value broadly similar to micropuncture studies in rats (Lund et al., 2003). In healthy humans the daily glomerular filtration is about 150-180L and this approximates to a filtered load of albumin of 3300 to 5760 mg (Gekle, 2005). As this far exceeds the 100 mg/day that appears in the urine an efficient retrieval system of filtered macromolecules must exist.

An alternative, and controversial model of glomerular filtration has been proposed. It is suggested that the fractional filtration of albumin is actually much higher and is largely size dependent. In this model the vast majority of filtered

albumin would be retrieved intact by the proximal tubule with a small fraction being degraded within PTC and expelled back into the filtrate as its component polypeptides (Russo et al., 2002, Russo et al., 2007, Comper et al., 2008a, Comper et al., 2008b, Comper and Russo, 2009). Under these circumstances it is suggested that albuminuria arises not because of a loss of glomerular permselectivity but a failure of the proximal tubule to maintain a high capacitance for albumin retrieval. Using fluorescently labelled albumin and two photon microscopy a GSC of 0.031 for albumin was calculated (Russo et al., 2007).

The model of a high permeability of the glomerular filtration barrier for albumin – the so called Comper model - has been much criticised. An assertion of the Comper model is that significant amounts of albumin are fragmented in the proximal tubule and secreted in the urine. The polypeptide fragments of albumin are not detected by conventional measures of proteinuria but can be detected using the biuret reaction (Russo et al., 2002). The detection of urinary peptides using the biuret reaction has been criticised as it may be subject to cross reactivity (Hortin and Meilinger, 2005) and examination of the urinary proteome using mass spectrometry failed to demonstrate in significant quantities the presence of albumin degradation products greater than 750 Da in size (Norden et al., 2004). The counter argument to that was that many of the degradation products were less than 75 Da (Comper et al., 2008).

Independent investigators using 2-photon microscopy have been unable to reproduce the high GSC for albumin demonstrated by Russo *et al.* Variables relating to animal husbandry such as hypothermia, volume depletion along with physiological variables such as blood pressure and GFR all affected the

apparent results (Tanner, 2009). Technical issues relating to 2-photon microscopy itself are also relevant. Scattering of fluorescence means that only superficial glomeruli that are not entirely physiologically relevant are imaged. Furthermore, the dynamic range of the fluorescence intensity measurements might be insufficient in the published studies (Peti-Peterdi, 2009, Peti-Peterdi et al., 2009). In summary there is no evidence from 2 photon microscopy studies in which physiological and technical variables are adequately controlled that supports a GSC for albumin that is significantly different from micropuncture studies.

The debate centres around the amount of albumin PTC are exposed to. What is clear is that in health, compared to the amount filtered, renal losses of albumin are small. Therefore, an efficient retrieval system of macromolecules must exist within the kidney that prevents significant losses.

1.7 Proximal tubular handling of filtered albumin

As less than 1% of filtered albumin is excreted in the urine it must be removed from the proximal tubule in an efficient manner. Indeed, it has been recognised for over seventy years that proteins entering the proximal tubule are re-absorbed (Lambert, 1932). Subsequently, it was demonstrated that the hyaline droplets commonly seen within proximal tubular cells in renal biopsy specimens represented re-absorbed proteins (Oliver et al., 1954). Numerous electron microscopy studies show that macromolecules including albumin (Maunsbach, 1966, Maunsbach, 1970, Bourdeau et al., 1972, Park and Maack, 1984, Schwegler et al., 1991), lysozyme (Christensen and Maunsbach, 1974), haemoglobin (Miller, 1960), horseradish peroxidase (Graham and Karnovsky,

1966) and β 2-microglobulin (Sundin et al., 1994) are re-absorbed by the proximal tubular epithelium.

These studies have provided information on the morphological aspects of uptake of proteins at the cell membrane (summarised in Geckle, 2005). During endocytosis small cell membrane invaginations are formed at the microvillar base entrapping an aliquot of tubular fluid within an endocytic vesicle. This structure is internalised and termed an early endosomal vesicle (EEV), and as a result of acidification of the EEV lumen the endocytosed cargo is detached from its receptor. The contents of the EEV are then delivered to the sorting endosome (SE) where because of sorting peptide sequences of the endocytosed receptors the majority is re-targeted back to the plasma membrane via recycling endosomes (RE). Endocytosed cargo destined for lysosomal degradation is trafficked to the lysosomal compartment via late endosomes (LE). Once in the lysosome cargo is digested into small fragments and returned to the circulation. It is apparent that subcellular endocytic structures are more evident in the early proximal tubule (the pars convoluta or S1/S2 segments) and sparser in the more distal pars recta (or S2/S3 segments) (Christensen and Nielsen, 1991, Clapp et al., 1988) .

The albumin concentration in early endosomes is about 40 fold greater than that of the proximal tubule filtrate (Gekle, 2005). The concentration of albumin must result from a molecular interaction between albumin and the plasma membrane. This concentration theoretically may be the result of albumin binding to the negatively charged microvilli. In the case of the negatively charged albumin this is unlikely as neutralisation of the negative surface charge of the microvilli of the PTC increases albumin uptake (Gekle, 2005). It is more likely that albumin

resorption by the PTC is specific and a consequence of receptor mediated endocytosis (RME). This is evidenced by the inhibition of binding of labelled albumin by unlabelled albumin (Gekle et al., 1995, Brunskill et al., 1997) but not other protein macromolecules such as transferrin or lactalbumin (Gekle et al., 1996).

1.7.1 Mechanisms of endocytosis.

Endocytosis is a complex process that regulates diverse biological events including development, intracellular communication, signal transduction, cellular homeostasis and neurotransmission. As such it is highly regulated and coordinated to the cell's overall requirements. There are a number of mechanistically diverse processes that function in mammals namely micropinocytosis, clathrin-mediated endocytosis, caveolae-mediated endocytosis and clathrin and caveolin independent endocytosis. The latter two are not thought to have a significant role within the proximal tubule and will be discussed no further (Gekle et al., 1997).

1.7.2 Fluid phase endocytosis

Fluid phase endocytosis, or micropinocytosis, accompanies membrane ruffling and is a response to cell stimulation by a variety of growth factor and involves modulation of the actin cytoskeleton by the Rho-family GTPases (Conner and Schmid, 2003).

Endocytosis is achieved as the ruffle collapses and fuses with the membrane below sampling the fluid contained within. This process is non-specific and contents are endocytosed at the same concentration as the bathing fluid, and

therefore, because of the concentration increase of albumin in the PTC is thought to have only a small role in the proximal tubule.

1.7.3 Clathrin mediated endocytosis

The proximal tubular uptake of albumin is an example of clathrin-mediated endocytosis (Gekle et al., 1997, Christensen et al., 1998). Clathrin-mediated endocytosis has a critical role in regulating cell signalling and development (Di Fiore and De Camilli, 2001, Seto et al., 2002) as it regulates the clearance and down regulation of plasma membrane associated activated signalling molecules. Receptors cluster in pits and are associated with clathrin. Under physiological conditions clathrin forms a polygonal cage which serves to facilitate the formation of endocytic invaginations. The structure of the cage is dependent on an association with adapter proteins (AP) such as AP180 and AP1-4, of which AP2 is the most important in the retrieval of extracellular ligands. AP2 consists of four subunits, and one of these, the μ 2 protein interacts with the NPXY region contained within some receptors and anchors them to the clathrin coat (Collins et al., 2002). This interaction modulates receptor shuttling between the membrane and the endosomal compartment and is regulated by changes to the phosphorylation status of μ 2 (Slepnev and De Camilli, 2000, Di Fiore and De Camilli, 2001). Clathrin-mediated endocytosis is the major mechanism of uptake in resorptive epithelia including the proximal tubule (Gekle et al., 1997, Christensen et al., 1998).

1.8 The identification of the PTC binding sites for albumin.

A number of albumin binding proteins have been identified in the plasma membrane of PTC that contribute to RME. Two different transport mechanisms

for albumin exist in the rabbit proximal tubule that are distinguishable in terms of both the receptor affinity (K_d) and capacity (V_{max}). One mechanism is of high affinity and low capacity and the other of low affinity and high capacity (Park and Maack, 1984). It would therefore follow that more than one population of receptors for albumin is likely to exist in PTC. Affinity chromatography studies have identified two albumin binding proteins of approximately 55 and 31 kDa in size (Cessac-Guillemet et al., 1996) This was in broad agreement with a study of opossum kidney membranes in which somewhat smaller albumin binding proteins of between 14 and 30 kDa in size exist (Brunskill et al., 1997). Binding studies of opossum membranes suggest that the two binding sites differ in their affinity constants and are consistent with the model proposed by Park and Maack (Brunskill et al., 1997).

Megalin, a 660 kDa glycosylated protein, is a member of the low-density lipoprotein-receptor (LDL-R) family is expressed on secretory epithelia including the proximal tubule (Christensen et al., 1995). Studies of megalin's role in the PTC indicate that it mediates the uptake of a large number of ligands including plasminogen complexes and gentamycin (Willnow et al., 1992, Moestrup et al., 1995). Functional studies identified megalin as a PTC albumin receptor (Cui et al., 1996). Uptake of albumin is blocked by co-administration of megalin antibodies and receptor associated protein (RAP) which is a competitive antagonist for binding of all known megalin ligands (Cui et al., 1996).

Cubilin is a 460 kDa protein that in enterocytes functions as the intestinal receptor for the intrinsic factor B₁₂ complex (Seetharam et al., 1997), and in PTC and the yolk sac epithelium co-localises with megalin (Moestrup et al.,

1998). In addition to co-localising with megalin, cubilin is also an albumin binding protein that facilitates PTC endocytosis (Zhai et al., 2000).

It is unclear as to why there should be such a large difference in the molecular size of megalin and cubilin and the albumin proteins identified in the early studies (Cessac-Guillemat et al., 1996, Brunskill et al., 1997). Other PTC albumin receptors are described and these are discussed below, but alternatively, the smaller albumin binding proteins could be fragments of cubilin (Birn et al., 2000a). The role of the LDL-R family member, megalin, is crucial in mediating endocytosis of albumin.

1.8.1 Megalin and the low-density lipoprotein receptor gene superfamily.

In mammals there are seven core members of the LDL-R family and these include the low density lipoprotein receptor (LDLR), the LDLR related protein (LRP1), a closely related receptor LRP1b, megalin (LRP2), The VLDL receptor (VLDLR), Apolipoprotein E receptor-2 (ApoER2) and MEGF7. Core members fulfil five requirements of their structural properties which are:

1. Ligand binding type cysteine rich repeats.
2. Epidermal growth factor cysteine rich repeats.
3. YWTD domains that form a fold of β -pleated sheet that results in a propeller like structure formation.
4. A single membrane spanning segment.
5. A cytoplasmic tail containing one or more NPXY domains that mediate interaction with clathrin coated vesicles or phospho-tyrosine interaction domains (Herz et al., 2000).

For each member of the LDL-R family RAP is a ligand. Functionally, this acts as a biological chaperone during intracellular transport and prevents the premature

binding of the proteins to one of their numerous biological ligands (Willnow et al., 1996b, Birn et al., 2000b). The extended LDL-R family include LRP-5, LRP-6 and Sorla, and these proteins share some characteristics with the main members of the LDL-R family (May et al., 2007).

1.8.1.1 Megalin: Structure and function.

Megalin has been of interest to nephrologists for many years as a potential antigen in membranous glomerulonephritis (GN). Rats injected with a crude extract of renal cortex develop clinical and histological features of membranous GN due to antibodies raised against megalin expressed on the glomerular podocyte (Kerjaschki and Farquhar, 1982). There is, however, no evidence that megalin is involved in human membranous GN. Based on partial sequencing and motif homology megalin is placed as a member of the LDL-R (Raychowdhury et al., 1989). Subsequently, full length megalin has been cloned and sequenced in rats (Saito et al., 1994) and humans (Hjalm et al., 1996). The human gene has been localised to chromosome 2q24-q31 (Korenberg et al., 1994) and loss of function mutations have recently been identified as being responsible for the Donnai-Barrow and facio-oculo-acoustico-renal syndromes (Kantarci et al., 2007). The clinical features of both disorders include tubular proteinuria. Case reports indicate that one patient carrying the Donnai-Barrow syndrome mutation developed end-stage renal failure (Stora et al., 2009) and another person developed focal and segmental glomerulosclerosis (Shaheen et al., 2010).

1.8.1.1.1 *The structure and function of the extracellular domain of megalin.*

Akin to other members of the LDL-R family megalin is a type 1 transmembrane receptor composed of a huge extracellular domain, a transmembrane region and a relatively small, though important cytoplasmic tail of 209 amino acids in humans (Christensen and Birn, 2002).

The extracellular domain consists of four cysteine rich complement repeats which, as in LRP, mediate ligand binding. These are separated by seventeen EGF-like repeats and eight cysteine poor spacer regions (**Fig. 1.2**) that contain YWTD motifs that are involved in the pH-dependent release of ligands in endosomal compartments (Davis et al., 1987). There are an enormous number of extracellular ligands for megalin (Christensen et al., 2009) (**Table 1.1**) but two particularly worthy of mention are albumin (Cui et al., 1996) and EGF (Orlando et al., 1997).

1.8.2 *Cubilin*

Cubilin binds megalin by a calcium dependent, high affinity interaction (Moestrup et al., 1998). Whilst cubilin does not span the plasma membrane it does possess a membrane anchoring region (**Fig. 1.2**). This is followed by eight EGF-like repeats and 27 complement subcomponents **C1r/C1s**, **Uegf** and **Bone morphogenic peptide-1 (CUB)**. These regions facilitate binding to a wide range of extracellular ligands and it is likely that the CUB1-2 regions of cubilin mediate the interaction with megalin (Yammani et al., 2001). Loss of function mutations of cubilin in humans result in the Imerslund-Gräsbeck syndrome which is characterised by vitamin B₁₂ deficiency and significant proteinuria (Imerslund, 1960, Grasbeck et al., 1960, Aminoff et al., 1999). Animal studies in which targeted disruption of cubilin is inherited demonstrate a lack of apical

expression of the protein in enterocytes and PTC and again, appreciable proteinuria (Birn et al., 2000a, Fyfe et al., 1991).

As cubilin lacks an intracellular domain its correct cellular trafficking is dependent on megalin. Megalin, cubilin and bound albumin localise to the apical membrane of the proximal tubule in dogs (Birn et al., 2000). A loss of function mutation of cubilin results in retention of cubilin in intracellular compartments and a 5 fold increase in the rate of proteinuria. Apical expression of cubilin is critically dependent on correct expression of megalin. In megalin deficient mice, cubilin is correctly distributed but in significantly reduced amounts (Birn et al., 2000).

1.8.3 Amnionless.

Cubilin also associates with the transmembrane protein amnionless (**Fig. 1.2**). This association is probably responsible for the small amount of apical expression of cubilin seen in conditions of megalin deficiency (Coudroy et al., 2005). Amnionless contains a transmembrane domain and facilitates the translocation of the cubilin-amnionless complex from the ER to the cell membrane (Fyfe et al., 2004). Point mutations of the amnionless gene in three Norwegian families result in proteinuria (Tanner et al., 2003). To date, it has not been shown that amnionless is itself an albumin binding protein and therefore it seems likely that the association between proteinuria and loss of function of amnionless is due to a reduced apical expression of cubilin.

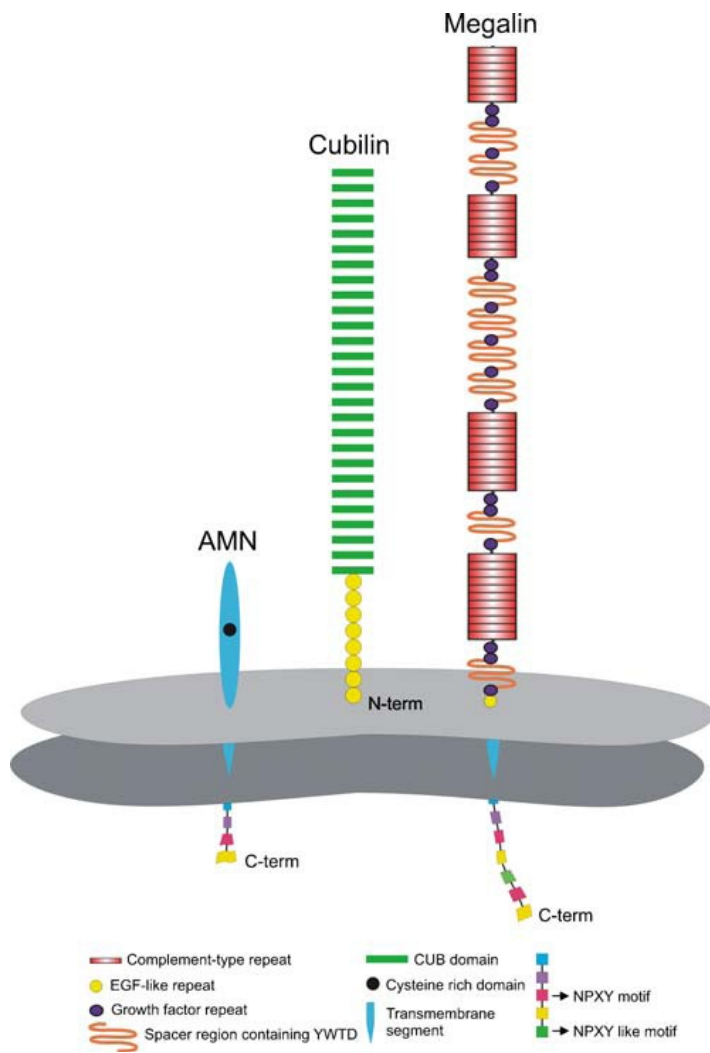


Figure 1.2. The structure of megalin, cubilin and amnionless showing known motifs and domains. *From Nielsen and Christensen (2010).*

Table 1.1 Identified ligands for the megalin and cubilin complex. *From;* Receptor-mediated endocytosis in renal proximal tubule. E.I. Christensen *et al.*, *Pflugers Arch.* (2009) 458: 1039-1048

Megalyn	Cubilin
Vitamin carrier proteins	
Transcobalamin–vitamin B12	Intrinsic factor–vitamin B12
Vitamin D-binding protein	Vitamin D-binding protein
Retinol-binding protein	
Folate-binding protein	
Other carrier proteins	
Albumin	Albumin
Myoglobin	Myoglobin
Hemoglobin	Hemoglobin
Lactoferrin	Transferrin
Selenoprotein P	
Metallothionein	
Neutrophil gelatinase-associated lipocalin	
Oderant-binding protein	
Transthyretin	
Liver-type fatty acid-binding protein	
Sex hormone-binding globulin	
Lipoproteins	
Apolipoprotein B	Apolipoprotein AI
Apolipoprotein E	High-density lipoprotein
Apolipoprotein J/clusterin	
Apolipoprotein H	
Apolipoprotein M	
Hormones, hormone precursors, and signaling proteins	
Parathyroid hormone	
Insulin	
Epidermal growth factor	
Prolactin	
Thyroglobulin	
Hedgehog protein	
Angiotensin II	
Leptin	
Bone morphogenic protein 4	

Enzymes and enzyme inhibitors	
Plasminogen activator inhibitor-type 1	
Plasminogen activator inhibitor-type 1–urokinase	
Plasminogen activator inhibitor-type 1–tissue plasminogen activator	
Pro-urokinase	
Lipoprotein lipase	
Plasminogen	
α -Amylase	
α_1 -Microglobulin	
Lysozyme	
Cathepsin b	
α -Galactosidase A	
Immune- and stress-response related proteins	
Immunoglobulin light chains	Immunoglobulin light chains
Pancreatitis-associated protein 1	Clara cell secretory protein
Advanced glycation end products	
α_2 -Microglobulin	
Receptors and transmembrane proteins	
Cubilin	Megalyn
Heavy metallothionein	AMN
Cation-independent mannose-6-phosphate receptor	
TCII–B12 receptor	
Drugs and toxins	
Aminoglycosides	Aminoglycosides
Polymyxin B	
Aprotinin	
Trichosantin	
Others	
RAP (receptor-associated protein)	RAP
Ca ²⁺	
Cytochrome c	
Receptor for seminal vesicle secretory protein II	
Coagulation factor VIII	

1.8.4 Evidence for non-megalin/cubilin mediated uptake of albumin in PTC.

Conservative estimates of glomerular permeability suggest that between 3 and 5 g/day of protein permeates the glomerular filter. Loss of function of megalin, cubilin or amnionless is associated with tubular proteinuria but not, in general, at levels associated with the nephrotic syndrome.

Renal specific loss of megalin in mice occurs in a mosaic pattern allowing a comparison of megalin expressing and non-expressing tubules (Theilig et al., 2007, Motoyoshi et al., 2008). In megalin deficient tubules accumulation of fluorescently labelled albumin is reduced to about 15% but is not entirely absent. In PTC megalin deficiency is associated with a widespread endocytic defect (Theilig et al., 2007). The mechanism of this might be related to the observation that megalin-mediated reclamation of lysosomal enzymes is an important generator of lysosomes in PTC (Nielsen et al., 2007). Thus, the reduction of lysosomes may adversely affect non-megalin mediated endocytic pathways and therefore the estimated reduction of albumin endocytosis associated with megalin deficiency may represent an under-estimation.

1.8.4.1 Neonatal Fc Receptor (FcRn).

FcRn is responsible for the bidirectional transfer of maternal IgG across epithelial barriers, thereby providing fetal humoral immunity. High affinity binding of IgG to FcRn occurs at pH <6.5 but not physiological pH (Roopenian and Akilesh, 2007). However, a wider biological role for FcRn must exist as there is continued

expression into adulthood. To date expression has been shown in the vascular endothelium, antigen presenting cells, adult gut, blood-brain barrier, podocytes and PTC (Roopenian and Akilesh, 2007, Haymann et al., 2000).

FcRn also binds albumin and in mice deficient in FcRn exhibit a reduced half life of circulating albumin and IgG by between 25% and 50%. Isolated renal FcRn deficiency in mice is associated with hypoalbuminaemia and nephrotic level proteinuria (Sarav et al., 2009).

These findings suggest a PTC retrieval system for albumin dependent on FcRn that is active under physiological conditions. A number of aspects of the mechanism behind this remain unexplained. Firstly, FcRn functions to mediate transcytosis and yet intact albumin has never convincingly been found on the basolateral surface of the PTC, and secondly albumin binds FcRn at pH 6.5 that may not be encountered in the proximal tubular lumen. It is possible that albumin delivered to the acidic endosomal compartment of PTC may be salvaged by an FcRn dependent pathway.

1.8.4.2 CD36.

CD36 is a class B scavenger receptor that has a widespread tissue distribution including PTC, and an important role in the uptake of oxidised lipoproteins (OxLDL) and long chain fatty acids by macrophages (Febbraio et al., 1999). Ligation of OxLDL to CD36 stimulates signalling pathways leading to pro-inflammatory cytokine synthesis.

In human diabetic nephropathy there is a positive association between PTC CD36 levels and apoptosis (Susztak et al., 2005), an effect ascribed to fatty acids and

advanced glycation end product-bovine serum albumin. Expression of CD36 in PTC is increased by high glucose (Susztak et al., 2005), after exposure to advanced oxidation protein products (AOPP) (Iwao et al., 2008), and by dyslipidaemia (Okamura et al., 2009). AOPP-modified human serum albumin is subject to CD36 dependent endocytosis by immortalised human PTCs (Iwao et al., 2008). Downstream CD36 stimulated signalling events in PTC include activation of Src, p38 MAPK, and caspase-3 pathways, and consequently superoxide production and secretion of fibronectin and TGF- β secretion (Yang et al., 2007). In hypercholesterolaemic mice CD36 deficiency attenuates TGF- β signalling, NF- κ B activity and renal fibrosis (Okamura et al., 2009). Whether filtered unmodified albumin binds to, and is endocytosed by CD36 in the proximal tubule to elicit these actions remains to be fully elucidated.

1.8.5 Other protein components of the albumin endocytic apparatus in PTC.

The correct composition of a multi-molecular endocytic complex is recognised to be critical in regulating albumin endocytosis in PTC. As well as the albumin binding receptors described the proteins calcium activated chloride channel-5 (CLC-5) and NHE-3 are recognised to have significant functions in regulating protein uptake.

1.8.5.1 CLC-5: Function in PTC and disease correlates.

CLC-5 functions alongside the V type H⁺-ATPase (Gunther et al., 1998) to create an electro-neutral shunt by which the early endosome is acidified resulting in ligand detachment from endocytosed receptors. However, albumin endocytosis still proceeds when the V type H⁺-ATPase is pharmacologically inhibited (Wang et al.,

2005b) and this suggests a wider role for CLC-5 in the endocytic process in ensuring the correct intracellular trafficking of other proteins. Loss of function of CLC-5 results in a failure of delivery of membrane bound proteins, including megalin and cubilin to the cell membrane (Gunther et al., 2003, Christensen et al., 2003). CLC-5 regulates the actin cytoskeleton via an interaction with the protein cofilin (Hryciw et al., 2003). Phosphorylated cofilin binds CLC-5, which favours actin polymerisation and maintains the structure of the endocytic complex and dephosphorylation of cofilin reverses this process (Ashworth et al., 2003). Exposure of PTC in culture to albumin at concentrations up to 100 µg/ml increases CLC-5 surface expression. It is thought that PTC exposure to albumin stimulates ubiquitination of CLC-5 by the enzyme Nedd 4-2. This targets the CLC-5/Nedd 4-2 complex for degradation within the proteasome which, by an unknown mechanism upregulates CLC-5 and Nedd 4-2 gene transcription and expression (Hryciw et al., 2004).

Dent's disease is a predominantly X-linked inherited condition that results in a loss of function of CLC-5. In addition to tubular proteinuria the clinical features include renal stones, hypokalaemia, nephrocalcinosis and renal failure (Pook et al., 1993, Wrong et al., 1994). In Dent's disease the urinary excretion of megalin is reduced indicating that a defective endocytic process fails to cycle receptor proteins back to the membrane (Norden et al., 2002). The urinary proteome of individuals affected by Dent's disease has been assessed and based on a different profile of urinary protein losses when compared to other causes of tubular proteinuria might offer a diagnostic utility and mechanistic insight into proteinuric disease (Cutillas et al., 2004, Vilasi et al., 2007).

1.8.5.2 Na⁺/H⁺-Exchanger-3 (NHE-3)

Na⁺/H⁺ exchangers (NHE) are plasma membrane transport proteins that are involved in cellular pH homeostasis and volume regulation. To date there are likely to be over eight members of the family and the predominant isoform in the apical membrane of the PTC is NHE-3. Along with the CLC-5/V-type H⁺ATPase complex NHE-3 contributes to early endosomal acidification in the proximal tubule and prevents premature fusion of the EEV to the plasma membrane (Gekle et al., 2002). At this stage of the endocytic process the electro-chemical gradient of protons favours such an acidification function for NHE-3 (D'Souza et al., 1998).

A failure of endosomal acidification attenuates vesicle fusion and flow through the endocytic pathway (Gekle et al., 2001) and this may explain the aberrant trafficking of megalin and cubulin observed with pharmacological inhibition of NHE-3 (Christensen et al., 2003). This is physiologically relevant because proteinuria is the consequence of loss of function mutations, and pharmacological inhibition of NHE-3 (Gekle et al., 2004).

NHE-3 is regulated by NHERF (NHE-regulatory factor) which is a PDZ module containing protein (Weinman et al., 2001). PDZ proteins are so named because of sequence homology between PSD-95, the *Drosophila* junctional protein Disc-large and the tight junctional protein ZO1. Such proteins serve to maintain large functional units such as that required for albumin endocytosis in the proximal tubule.

It is therefore of some interest that there is a specific interaction between megalin and NHE-3 in rabbit PTC (Biemesderfer et al., 1999). The interaction involves the

carboxyl terminus of NHE-3 and as this entirely intracellular probably involves the MegCT. Furthermore, megalin associated NHE-3 is inactive whereas, non-megalín associated NHE-3 is active (Biemesderfer et al., 2001). A number of studies have demonstrated albumin stimulation of NHE-3 activity in PTC in culture (Lee et al., 2003, Drumm et al., 2003) and it is reasonable to speculate that this is mediated via megalín. This may, at least in part explain the salt and water retention seen in nephrotic syndrome. Also, this makes the potentially regulated interaction between the PTC receptor for albumin and NHE-3 a point of potential therapeutic intervention.

1.9 Regulation of PTC albumin endocytosis.

The components of the endocytic process are dynamically regulated to match the extra-cellular conditions to the cellular needs. Low extracellular calcium inhibits albumin binding to PTC (Gekle et al., 1995) as the ligand interaction with the megalín/cubilín complex is calcium dependent (Christensen et al., 1998). G-proteins are recognised to have a significant regulatory role on endocytosis in a variety of tissues and are abundantly expressed in the proximal tubule (Brunskill et al., 1991). Over-expression of the $G_{\alpha_{i3}}$ in OK cells increases albumin uptake and inhibition of the $G_{\alpha_{i3}}$ subunit with pertussis toxin has the opposite effect (Brunskill et al., 1996). One effect of the hydroxyl-methyl-glutarate CoA (HMGCoA)–reductase inhibitors is to reduce post translational prenylation of G-proteins altering G-protein localisation to phospholipid membranes. Such agents are associated with reduced albumin endocytosis (Sidaway et al., 2004). A point of action of G-proteins is the control of the actin/microtubule cytoskeleton. Depolymerisation of the actin

cytoskeleton and inhibition of microtubule formation reduces albumin endocytosis by 95% and 55% respectively (Gekle et al., 1997). Stimulation of protein kinases A (PKA) and C (PKC) also reduces endocytic rate. The role of the latter is likely to be isoform specific as activation of PKC- α augments albumin endocytosis in OK cells (Hryciw et al., 2005).

Activity of phospho-inositide-3 kinase (PI-3K) augments albumin endocytosis by PTC (Brunskill et al., 1998) an effect that could be mediated by NHE-3 (Shiue et al., 2005). PI 3-kinase catalyses the phosphorylation of phosphatidylinositides at the 3' position. It is a heterodimer consisting of a p110 catalytic and p85 regulatory subunit. The p110 domain contains binding sites for the p85 regulatory subunit, a C2 and Ras-binding region and a catalytic domain. The catalytic area bears homology to serine/threonine kinases and is capable of phosphorylating those residues along with phosphoinositides. The p85 regulatory subunit inhibits basal catalytic activity of the p110 subunit. Binding of the regulatory subunit to tyrosine phosphorylated residues of other proteins detaches it from and stimulates the catalytic subunit. The p85 region has several domains including a Rho-GAP homology domain. Also, there is a SH3 consensus sequence, two proline rich regions that themselves mediate interaction with SH3 regions and two SH2 regions that bind to phosphoTyr-XX-Met regions on activated receptors. PI 3-kinase participates in a number of growth factor signalling pathways as well as regulating endocytosis (Cantley, 2002). An inducible, dominant-negative mutant of PI 3-kinase inhibits PTC albumin uptake by PTC (Brunskill et al., 1998).

It is recognised that the phospholipid composition of the cell membrane is a crucial regulator of endocytosis. Phospho-inositide 4-phosphate (PIP-4) recruits adapter

proteins such as AP1 and these have been implicated in scission of the golgi apparatus to the plasma membrane carrier system (Levine and Munro, 2002). In turn, this is regulated by the enzyme polyphosphate 5-phosphatase which is abundantly expressed in the golgi apparatus and binds clathrin (Olivos-Glander et al., 1995, Ungewickell et al., 2004). The gene OCRL1 encodes a protein homologous for polyphosphate 5-phosphatase, loss of function of which results in Lowes syndrome (Lowe, 2005). Reduced urinary excretion of megalin is reported in individuals affected by Lowes syndrome (Norden et al., 2002) and this may reflect reduced megalin recycling and be responsible for the tubular proteinuria observed in affected individuals. However, *in vitro* loss of function of OCRL is associated with normal megalin trafficking (Cui et al., 2010). So, at present the full mechanism behind the tubular proteinuria seen in Lowes syndrome is unclear.

Physiological processes such as signalling through phospholipase C result in local changes in phosphoinositide concentrations. Phospholipase C activity attenuates apical membrane clathrin-mediated endocytosis of insulin (Carvou et al., 2007).

1.10 Phenotypic changes stimulated by proteinuria in PTC.

To explain the relationship between proteinuria, tubulo-toxicity and tubulointerstitial fibrosis investigators postulated that components of the proteinuric urine altered function of PTCs. This hypothesis has been extensively tested and there is a broad body of evidence that albumin modulates signalling pathways, transcription factor activation, chemokine secretion and apoptosis/growth of PTC *in vitro* and *in vivo* (summarised in **Table 1.2**).

Table 1.2 Alterations in PTC signalling, transcription factor activity and secretory phenotype demonstrated under proteinuric conditions *in-vitro* and *in-vivo*.

Signalling Mediators Stimulated	Transcription Factors Altered	Mediators Released
ERK 1 and 2 MEK1 p38 MAP kinase c-jun n-terminal kinase Ribosomal p70 ^{S6} kinase Protein kinase C Protein kinase B PI 3-kinase NAD(P)H oxidase Intracellular [Ca ²⁺] (increased)	NFκB AP-1 Elk-1 STAT HIF/HRE (reduced) PPARγ (by albumin bound fatty acids)	Endothelin-1 MCP-1 RANTES Fractalkine Interleukin-8 Osteopontin TGF-β TNF-α Connective tissue growth factor Fibronectin Collagen Complement Reactive oxygen species Clusterin

1.10.1 Signalling pathways activated by albumin in PTC.

1.10.1.1 PI 3-kinase.

The dependence of PTC albumin endocytosis on PI 3-kinase has been described in section **1.10**. PTC albumin endocytosis is both regulated by and stimulatory to PI 3-kinase activity providing a clear nexus between endocytosis control and cell signalling. A subsequent study confirmed this finding and extended it to show that the mitogenic effect of albumin on PTC is dependent on PI 3-kinase activity (Dixon and Brunskill, 1999). The stimulation of mitogenesis by albumin also results in the phosphorylation of pp70^{s6} kinase, an enzyme involved in the translational control of mRNA encoding components of the protein synthetic apparatus. Activity of both PI 3-kinase and pp70^{s6} are necessary for mitogenesis to proceed suggesting that they operate in a linear pathway.

1.10.1.2 Extracellular-signal-regulated-mitogen activated protein kinase (ERK).

Mitogen activated protein kinases (MAPKs) include the ERK 1 and 2 (also known as p42 and p44 MAPK), stress activated c-Jun terminal kinase and p38 MAPK. These enzymes play a key role in intracellular signal transduction cascades to integrate the transcription of genes for a variety of responses (Tian et al., 2000). These molecules are serine/threonine kinases and their phosphorylation status regulates their translocation to the nucleus where they modulate activity of transcription factors.

The classic MAPKs, ERK-1 and -2 are activated through Ras dependent transduction pathways and mediate cellular proliferation and differentiation by stimulating the transcription factors *c-fos* and other growth responsive genes (Cobb et al., 1994). In contrast, JNK and p38 MAPK leads to apoptotic cell death and are activated by ultraviolet light and oxidants to name but two (Alberts, 2008). Incubation of OK cells with recombinant human albumin time and dose dependently increases ERK activation (Dixon and Brunskill, 2000). A maximal effect was seen at a dose of albumin between 1 and 10 mg/ml. In HK-2 cells the albumin stimulated secretion of fractalkine involved activation of p38 MAPK. As well as modulating cell growth it has been suggested that MAP kinases play an important role in regulating apoptosis in the kidney as pharmacological inhibition of JNK inhibits renal fibrosis and apoptosis in PTC. Targeted deletion of JNK failed to effect the fibrotic changes but did result in a significant reduction in the rate of apoptosis (Ma et al., 2007).

1.10.1.3 Protein kinase C.

Protein kinases C (PKC) are a family of serine/threonine kinases with at least twelve isoforms. On the basis of common structural themes they can be sub-classified as:

- Classical PKC enzymes are composed of two cysteine rich zinc finger like motifs (C1 region), which are essential for interaction with phorbol ester and diacylglycerol (DAG), and a calcium binding domain (C2 region) in their regulatory area.

- The novel PKC enzymes do not require calcium as their C2 region is absent. The novel PKC enzymes are activated by phosphatidylserine, diacylglycerol or phorbol esters.
- The atypical PKC enzymes which lack the C2 region and one of the cysteine rich finger-like motifs in the C1 region are not activated by calcium, diacylglycerol or phorbol esters. Instead, their activation depends on phosphatidylserine and cis-unsaturated fatty acids (Steinberg, 2008).

In HK-2 cells albumin stimulates PKC activity and inflammatory cytokine production whereas, inhibition of PKC has the opposite effect (Morigi et al., 2002). Downstream events of PKC activity are reactive oxygen species generation and NF- κ B activation, both of which will be discussed in more detail below. In PTC PKC activity is not always contributory to the pro-inflammatory phenotype. PKC-epsilon knockout mice develop albuminuria and tubulointerstitial fibrosis without evidence of damage to other organs. It may be that PKC-epsilon exerts an inhibitory effect on the TGF- β pathway as components of this pathway were up-regulated in this model (Meier et al., 2007). In streptozotocin treated diabetic mice PKC- δ deletion is associated reduced PTC apoptosis in response to albuminuria (Li et al., 2010). The specific isoforms of PKC activated by albumin in PTC have not been fully characterised though it is probable that there will be tension between different isoforms of PKC in regulating overall PTC function.

1.10.1.4 Reactive oxygen species.

Exposure to albumin of PTC *in vitro* results in a sustained production of superoxide ions/reactive oxygen species (ROS) which is catalysed by superoxide dismutase to

form hydrogen peroxide. In a reaction favoured by catalase, hydrogen peroxide is converted to water and oxygen (Morigi et al., 2002, Imai et al., 2004). In addition, other filtered proteins relevant to proteinuric diseases, such as immunoglobulin light chains stimulate ROS generation *in vitro* (Wang and Sanders, 2007, Basnayake et al., 2010). The precise stimulant of albumin induced superoxide generation in PTC is not known. However, it is recognised that some interactions between ligand and receptor, by the nature of the physico-chemical association generate ROS (DeYulia et al., 2005). Superoxide generation is a product of the enzyme NADPH oxidase which is itself regulated by recruitment from the cytosol of two components. The translocation of these two components termed p47phox and p67phox is stimulated by PKC and Akt and appears to involve Rac1 (a small Rho-family GTPase) (Whaley-Connell et al., 2007). Hydrogen peroxide stimulates a variety of intracellular signalling cascades including c-Src (Giannoni et al., 2005), ERK 1/2, JNK, p38 MAP kinases, PI 3-kinase (Rhee, 2006) with downstream effects on the transcription factors NF- κ B (Morigi et al., 2002) and the Jak-STAT pathway (Imai et al., 2004). Akt/PKB as well as stimulating superoxide generation can inhibit ASK-1 (apoptosis signal-regulating kinase-1) (Bedard and Krause, 2007). ASK-1 is a positive regulator of p38 MAP kinase, a protein that generates a pro-apoptotic signal. Therefore, in the same cell superoxide generation can both stimulate and inhibit apoptosis, and it is thought that the overall outcome reflects the relative flux through these pathways and is itself regulated by the degree of oxidative stress placed on the cell (Imai et al. 2004).

The fatty acids bound to, and not necessarily albumin *per se* have been shown to be major contributors to the development of oxidative stress (Ishola et al., 2006).

Modulation of superoxide concentration was shown to have a corresponding effect on IL-6 protein expression. The mechanism of IL-6 production has not been fully elucidated though it appears to involve PKC and NF- κ B activity (Morigi et al., 2002) acting in a linear pathway.

1.10.2 Transcription factors activated by albumin in PTC.

1.10.2.1 Nuclear factor kappa B (NF- κ B).

NF- κ B proteins are dimeric sequence-specific transcription factors involved in the activation of a large number of genes in response to inflammation (Rothwarf and Karin, 1999). In a resting state NF- κ B is rendered inactive by virtue of its association with an inhibitory molecule I- κ B. Activation results in phosphorylation, ubiquitination and ultimately proteolytic degradation of I- κ B. NF- κ B is then free to translocate to the nucleus and regulate gene transcription.

Activation of NF- κ B has been found in a large number of studies using PTC. Albumin uptake induces NF- κ B in a human PTC line (Drumm et al., 2003), a process that is PKC and H₂O₂ dependent (Morigi et al., 2002). Downstream events include MCP-1 and fractalkine secretion (Wang et al., 1999, Donadelli et al., 2003). Inhibition and loss of function of NF- κ B reduces cortical tubulointerstitial injury (Panzer et al., 2009) further emphasising the critical role of this molecule in regulating tubulointerstitial fibrosis.

1.10.2.2 Signal transducer and activator of transcription pathway (STAT)

The Jak (Janus kinase)-STAT signalling pathway is one of the most direct routes to regulating gene transcription in biology and is a recognised feature of cytokine signalling. Activated receptors oligomerise allowing Jaks to bind to the receptor and cross-phosphorylate adjacent Jaks. Activated Jaks phosphorylate the host receptor enabling SH2 domain containing STAT proteins to bind. The STATs undergo a further phosphorylation event catalysed by Jak. The STATs then dissociate from the receptors and dimerise via a link between their SH2 domains and phospho-tyrosine residues. Following translocation to the nucleus they are able to bind regulatory proteins to facilitate gene transcription. There are four known Jaks and seven STATs which enables a degree of specificity (Alberts et al., 2008).

Albumin has been found to activate the Jak-STAT pathway and therefore act in the manner of a cytokine in PTC. The activation relies on the generation of reactive oxygen species, a process dependent not only on stimulation of NADPH oxidase but also reduced activity of glutathione peroxidase and catalase (Nakajima et al., 2004). The activation of a 'cytokine' signalling pathway enables the transcription of immuno-modulatory genes (i.e. MCP-1 and RANTES).

1.10.3 Genes regulated by albumin in PTC.

In cultured PTC albumin dose dependently increases the activity of NF- κ B and the expression of RANTES (Zoja et al., 1998), MCP-1 (Wang et al., 1999), IL-8 (Tang et al., 2003) and fractalkine (Donadelli et al., 2003).

In vivo proteinuria induces upregulation of MCP-1, TGF- β and osteopontin mRNA. Gene transcription precedes an inflammatory cell infiltration of the tubulointerstitium (Eddy and Giachelli, 1995). These effects are downstream of NF- κ B activation (Wang et al., 1997, Zoja et al., 1998). Using the protein overload model in rats, pro-inflammatory gene transcription is greater when lipidated-albumin compared to a fatty acid free preparation is administered (Thomas et al., 2002).

In PTC taken from human renal biopsy specimens from patients with proteinuric nephropathy 168 genes were identified to be differentially regulated (Rudnicki et al., 2007). Up-regulated genes included a number of chemokines and transcription factors emphasising the relevance of previous experimental observations.

1.10.4 Protein expression up-regulated in PTC by albumin.

The *in vitro* studies described in the previous section matched increased protein expression to gene transcription. In addition to those proteins secreted by PTC, components of the proteinuric urine stimulate production of fibronectin, fractalkine, complement C3 (C3), interleukins 6 and 8, TGF- β , collagens I and IV and clusterin (Burton et al., 1996, Donadelli et al., 2003, Tang et al., 2003, Yard et al., 2001, Wohlfarth et al., 2003, Takase et al., 2008). Albumin also signals to increase cell membrane expression of TGF- β receptor II (Wolf et al., 2004). Therefore, in addition to stimulating inflammatory cells around them PTC can autologously up-regulate inflammatory signalling cascades.

In addition to the *in vivo* studies of up-regulated genes in animal models of proteinuric nephropathy, other mediators are over-expressed in response to

proteinuria. Particular attention has focused on TGF- β which stimulates peritubular myofibroblasts to a pro-fibrotic phenotype (Abbate et al., 2002). The TGF- β pathway is a point of potential therapeutic intervention in reducing renal fibrosis. This includes using bone morphogenic peptide-7 (BMP-7), a renal developmental morphogen (Klahr, 2003) and an antagonist of the TGF- β pathway. Infusion of BMP-7 in a model of renal injury was anti-fibrotic and reno-protective (Zeisberg et al., 2007).

1.10.5 The effect of proteinuria on PTC viability.

Other studies have focused on the effect of albumin on cell growth and viability. In OK cells recombinant human albumin stimulates growth in a dose dependent way (Dixon and Brunskill, 1999). Albumin at 1mg/ml increases thymidine incorporation three fold. In a different PTC line, recombinant albumin concentrations between 10 and 100 mg/ml induce apoptosis (Caruso-Neves et al., 2006). These studies are particularly interesting as these effects cannot be ascribed to serum proteins other than albumin.

1.10.6 The axolotl

A limitation of *in vivo* studies is that a loss of glomerular permeselectivity has to be induced to expose the PTC to proteinuria. Axolotls (*Amblystoma mexicanum*) circumvent this problem as they have an almost unique and experimentally advantageous structure to their nephrons. The kidney of the axolotl represents an amphibian opisthonephros in which ciliated funnels connect the peritoneum and the proximal tubule distal to the glomerulus. A second population of nephrons are

conventionally structured compared to mammalian systems except axolotls lack a loop of Henle. This structure enables investigators to have direct access to a sub-population of proximal tubules via the coelaemic cavity.

Injection of foetal bovine serum into the peritoneum of axolotls results in an uptake of protein droplets into PTC, tubular luminal dilation and sludging of protein. This is closely followed by the development of an inflammatory infiltrate around the protein laden tubules and immunohistological detection of TGF- β , fibronectin and collagen I (Gross et al., 2002). The findings are repeatable with specific proteins (transferrin, LDL, IgG, all of human origin) but not human albumin. Nevertheless, the general trajectory of these experiments is consistent with the hypothesis that proteins are inherently tubulo-toxic even in the absence of glomerular damage.

1.10.7 Albumin endocytosis may not be a pre-requisite for signalling effects.

The evidence that albumin modulates PTC function is clear and compelling. What is less obvious is whether albumin endocytosis is obligate for these effects and whether albumin stimulated signalling events at the apical cell membrane may be important in regulating intracellular signalling cascades.

Activation of NF- κ B, and stimulated secretion of MCP-1 and collagen types I, III and IV are reliant on albumin endocytosis (Wang et al., 1997, Drumm et al., 2001 and Wohlfarth et al., 2003). Whereas, albumin induced secretion of TGF- β at least *in vitro*, is independent of uptake (Diwakar et al., 2007). Furthermore, pharmacological activation of the peroxisome proliferator receptor- γ using thiazolidinediones inhibits albumin endocytosis but does not affect PTC MCP-1 and RANTES secretion (Chana et al., 2008).

Some effects of albumin are more likely to be mediated by events at the cell membrane rather than being dependent on endocytosis. *In vitro* albumin stimulates ERK induced IL-8 production in PTC via the native EGF-R. Pharmacological inhibition of the EGF-R phosphorylation attenuates this effect (Reich et al., 2005) and downstream NF-κB activation and cell proliferation (Lee and Han, 2008). The EGF-R is patho-physiologically relevant in progressive renal disease as EGF-R deficiency in knockout mice is reno-protective (Terzi et al., 2000). Mechanistically, this process is poorly understood, but ligand binding to another member of the LDL-R family, LRP1, transactivates the neurotrophic Trk receptor (Shi et al., 2009). Inhibition of ligand binding by RAP reduces receptor transactivation thereby implicating the extracellular domain of LRP in Trk activation. This may involve ROS as ligand binding to some receptors generates H₂O₂, which *in vitro* stimulates EGF-R phosphorylation and activation (DeYulia et al., 2005).

1.10.7.1 Megalin deficiency attenuates inflammatory cytokine production.

The best characterised mechanism of albumin uptake in PTC is via the megalin/cubilin complex. To test the hypothesis that albumin endocytosis is not necessary to elicit signalling, experiments using a renal specific megalin knockout mouse model have been undertaken. An assumption of this approach is that the megalin/cubilin complex is the sole system that results in albumin uptake in PTC. Mice exhibit a mosaic pattern of megalin loss such that 20-40% of tubules will continue to express megalin. Two groups have utilised this model with contradictory and not easily explicable results.

A crescentic form of glomerulonephritis was induced in renal specific knockout mice by injecting mouse anti-glomerular basement serum. After 18 days the mice developed proteinuria with histology confirming the crescentic glomerular changes but also tubulointerstitial damage. Tubular damage was related to severely damaged glomeruli but not, albumin endocytosis. In fact, megalin expressing, and therefore albumin endocytic-competent cells secreted enhanced quantities of TGF- β , intercellular adhesion molecule-1 (ICAM-1) and vascular cell adhesion molecule-1 (VCAM-1). Secretion of these proteins was reduced but not abolished in megalin deficient cells. However, as it was glomerular damage, rather than megalin expression that predicted tubular damage the authors suggested that inflammatory mediator production was in some way protective (Theilig et al., 2007).

Using the same renal specific megalin knockout mice, but a different mechanism of proteinuria induction led others to come to a contrary conclusion. Unselective proteinuria with little histological evidence of glomerular damage was induced in renal specific megalin knockout mice. Markers of PTC damage (heme-oxygenase-1), inflammatory cytokine production (MCP-1) and apoptosis were all more marked in megalin-expressing cells compared with non-megalín expressing segments (Motoyoshi et al., 2008).

Taken together these studies place megalin as an important molecule in mediating the pro-inflammatory effects of albumin. Some of these effects can be attributed to megalin's established role as a cargo receptor but they are also consistent with cell regulatory properties that will be considered in the following section.

1.11 The crucial biological role of megalin.

There is clear evidence that albumin is able to stimulate a number of signalling pathways within PTC with distinct, and patho-physiologically relevant consequences. It may of course be that these effects are reliant on more than one mechanism but it is clear that albumin binding and/or uptake by PTC via megalin is critical. The traditional view of megalin is that it is essentially biologically inert and simply functions as a cargo receptor which facilitates the uptake of an array of ligands. However, the phenotype of megalin knockout mice and humans with megalin loss of function mutations is severe, suggesting that megalin has a much more crucial biological role and as a signalling molecule may link PTC albumin exposure and albumin-induced cellular events.

1.11.1 The megalin knockout mouse.

The role of megalin in development is exemplified by the phenotype of the megalin knockout mouse. These mice demonstrate a severe forebrain abnormality termed holoprosencephaly (Willnow et al., 1996a). This is characterised by an absence of the corpus callosum, microphthalmia, a common ventricular system and a prolapse of the choroids plexus. This is such a lethal phenotype that only 2% of the pups survive the perinatal period. The neurological phenotype is not the only defect. A major contributant to the perinatal lethality of this phenotype is respiratory failure and those pups that do survive demonstrate appreciable proteinuria. Targeted disruption of *megalyn* in the embryo but not the yolksac, results in a similar phenotype indicating that failure of endocytic uptake of essential nutrients from the

maternal circulation is not the underlying mechanism of the debilitating phenotype (Spoelgen et al., 2005).

The sonic hedgehog (Shh) signalling pathway gives an interesting insight into how megalin may regulate extracellular signalling pathways and give rise to the severe phenotype seen. Disruption of the Shh pathway in the developing embryo results in holoprosencephaly (Farese and Herz, 1998). Furthermore, Shh binds to megalin with high affinity and in contrast to other megalin ligands is not destined for lysosomal degradation (McCarthy et al., 2002). It may be that megalin regulates Shh signalling (a) directly by transducing a signal (b) indirectly by limiting the availability of Shh at its recognised receptor, patched (Ptc) or (c) by transcytosing Shh so it is transported for long range signalling and neural arrangement. A further level of complexity is added with the recognition that bone morphogenic peptide 4 (BMP4) is both a megalin ligand and a negative regulator of Shh. Overexpression of BMP4 results in a holoprosencephalic phenotype very similar to that seen in Shh and megalin deficiency (Farese and Herz 1998). Therefore, it may be that megalin regulates signals by limiting the availability of extra-cellular binding partners that positively or negatively regulate intracellular signalling pathways.

Megalín knockout mice are useful as a model of low molecular weight proteinuria (Leheste et al., 1999). The role of the PTC in the retrieval of the considerable amount of protein filtered by the glomerulus has been discussed previously. In megalín knockout mice the specific molecules excreted in increased amounts were the plasma carriers of lipophilic compounds such as vitamin D binding protein and retinol binding protein. As such urinary losses of retinol and 25-OH vitamin D₃ were increased in megalín deficiency. Overall, megalín has a crucial role in vitamin

homeostasis. The total amounts of albumin excreted were similar between wild type and knockout mice indicating that some other retrieval system must operate as well.

1.11.2 Megalin as a regulator of apoptosis.

Apoptosis contributes to a loss of functional PTC in proteinuric nephropathy. The role of albumin in regulating an apoptotic signalling pathway involving PKB/akt, PI-3 kinase and megalin is crucial in this regard (Caruso-Neves et al., 2006). In the LLC-PK1 PTC line megalin anchors PKB to the region of the cell membrane where the latter is active, and stimulates a survival pathway involving PI-3 kinase. Low concentrations of albumin support this pathway by promoting membrane association of megalin. Conversely, high concentrations of albumin downregulate megalin expression at the plasma membrane and consequently PKB activity is also reduced, and pro-apoptotic pathways stimulated.

Clusterin is a secreted glycoprotein whose role in regulating apoptosis is variable and cell-type specific. In cell culture studies albumin stimulates PTC secretion of clusterin which inhibits NF-KB dependent survival pathways (Takase et al., 2008). Secreted clusterin is a megalin ligand and may act in a paracrine/juxtacrine fashion (Christensen *et al.*, 2009), though whether megalin is the sole clusterin receptor in these cells is unclear. Therefore, PTC megalin may modulate apoptosis and clusterin bioactivity by (a) mediating PTC-albumin interactions; (b) directly mediating clusterin uptake; or (c) by limiting availability of clusterin at a second receptor.

1.11.3 Megalin regulates vitamin D metabolism.

The renal specific megalin KO mouse described earlier was generated introducing a lox P recombination site into the murine megalin gene. Simultaneously, a strain of mouse with a renal specific expression of Cre recombinase was developed. Subsequent generations that were doubly transgenic had a Cre mediated inactivation of the megalin gene and less than 10% megalin protein expression within the kidney (Leheste et al., 2003).

The phenotype of the renal specific megalin knockout mouse is very similar to mice lacking vitamin D binding protein (DBP). That is, renal specific megalin deficiency is associated with severe plasma vitamin D deficiency, hypocalcaemia and osteomalacia and increased urinary levels of DBP. This emphasises the crucial role that tubular retrieval of proteins filtered by the glomerulus fulfils in physiology. Although, this process reflects an endocytic function of megalin the relationship between vitamin D and the TGF- β pathway is described in **1.12.4** and **1.13.6**.

1.11.4 Other pathways potentially regulated by megalin.

Expression profiling using microarray has confirmed an essential role for megalin in vitamin D₃ metabolism (Hilpert et al., 2002). In megalin deficient mice there is a down-regulation of the mRNA encoding 25-OH vitamin D-24-hydroxylase and 25-(OH) vitamin D-1 α -hydroxylase. In addition a number of genes relating to the TGF- β pathway are up-regulated in knockout mice although TGF- β levels are similar between the groups with no evidence of renal fibrosis. The explanation for this may

be that one of cofactors activated by TGF- β (SMAD3) is also a coactivator of the vitamin D₃ receptor (Yanagisawa et al., 1999). Convergence of the pathways on SMAD3 may, when both pathways are active in the same cell be mutually regulating. Therefore, in the converse situation to that described above increased activity through the vitamin D pathway attenuates the activity of TGF- β (Aschenbrenner et al., 2001). In megalin knockout mice there is renal up-regulation of the enzyme HMG CoA-reductase. This enzyme, which is involved in cholesterol biosynthesis has become a major therapeutic target in contemporary medicine. HMG-CoA reductase inhibitors have a wide use in reducing cardiovascular risk but in PTC and podocytes reduce albumin uptake (Sidaway et al., 2004, Eyre et al., 2007).

1.11.5 Regulated intramembrane proteolysis (RIP) of megalin.

RIP is a widely conserved process that links cell surface receptor function to gene transcription. Initially, PKC dependent matrix metalloproteinase (MMP) mediates ectodomain cleavage of the receptor. Subsequently the remaining transmembrane–cytosolic receptor fragment is cleaved by the γ -secretase family of proteases, and for several receptors the released cytosolic fragment translocates to the nucleus where it regulates gene transcription (Biemesderfer, 2006).

In cell culture studies using the opossum kidney (OK) derived proximal tubular cell line, megalin has been found to be processed in this way. In this cell culture model, RIP of megalin appears to occur both constitutively and in response to ligation of the receptor by one of its known ligands, vitamin D binding protein (Zou et al.,

2004). Although it is entirely possible that other megalin ligands such as albumin stimulate RIP of megalin, this remains to be determined. To date, nuclear translocation of the cytosolic fragment of megalin has not been directly observed. However overexpression of the transmembrane/cytosolic fragment of megalin in OK cells inhibits transcription of the megalin and NHE-3 genes, and inhibition of γ -secretase attenuates this effect (Li et al., 2008).

Whilst these studies rely on *in vitro* observations, there is some evidence that RIP of megalin may also occur in proteinuric patients. Individuals with diabetic nephropathy and albuminuria display enhanced urinary shedding of the extracellular fragment of megalin compared to non-albuminuric diabetic patients, and it could be speculated that this is mediated by increased MMP activity in the albuminuric diabetic kidney (Thraill et al., 2009).

In vivo over-expression of the transmembrane and cytoplasmic tail of megalin (MegCT) has recently been reported to have no effect on the apical expression levels of native megalin and endocytic capacity of the proximal tubule (Christ et al., 2010). The different findings of the *in vitro* and *in vivo* studies may reflect the difference between acute and chronic changes in the intracellular concentration of MegCT.

1.12 Potential signalling role of megalin in PTC.

The severe phenotype of megalin deficient mice and the evidence that megalin is processed by RIP, suggests divergent roles for megalin as a mediator of endocytosis and as a regulator of signalling pathways. The concept of other

members of the LDL-R family functioning as signalling pathway regulators is better developed than is the case for megalin and will be considered first.

1.12.1 Signalling functions of LRP-1.

LRP-1 is a 600 kDa ubiquitously expressed type 1 transmembrane receptor (Herz et al., 1988). It exists as a heterodimer in which a large 515kDa extracellular subunit and is non-covalently linked to a subunit of 85kDa that contains a small extracellular region, a transmembrane region and a cytoplasmic tail. In the liver, LRP-1 functions in co-operation with LDL-R in the removal of cholesterol containing lipoproteins from the circulation (Willnow et al., 1995). The phenotype of LRP-1 knockout mice indicates a wider biological role. These mice have a high periimplantation mortality and those that survive have severe cephalic abnormalities (Lillis et al., 2008). LRP-1 has a critical role in maintaining the blood brain barrier (Herz, 2003), regulation of the inflammatory response in the lung (Gardai et al., 2003) and modulating vascular tone (Nassar et al., 2004). Targeted disruption to LRP-1 in vascular smooth muscle cells results in smooth muscle cell proliferation, aneurysm formation and an increased susceptibility to cholesterol induced atherosclerosis (Boucher et al., 2003). It is believed that changes to the phosphorylation status of the cytoplasmic tail of LRP-1 are crucial in initiating some of the biological effects associated with LRP-1.

1.12.2 LRP-1 is phosphorylated.

Tyrosine phosphorylation of LRP1 occurs as a result of transformation of fibroblasts with v-Src (Barnes et al., 2001) which may be a critical step in

tumorigenesis. One of the two NPXY regions in the cytoplasmic tail of LRP-1 act as a binding site for the PTB region of another adapter protein SHC. It is thought that localisation of SHC to the cell membrane results in tyrosine phosphorylation of SHC. Such phosphorylation modulates the interaction with the Grb10-Sos complex. This provides a platform from which the Ras and MAP kinase signalling pathway can be activated (Barnes et al., 2003).

Tyrosine phosphorylation of LRP-1 is dependent on an interaction with the PDGF β receptor dimer (Loukinova et al., 2002, Boucher et al., 2002). Stimulation of vascular smooth muscle cells with PDGF (but not other growth factors such as EGF and IGF) results in PI-3 kinase and Src dependent tyrosine phosphorylation of LRP-1 in the second NPXY domain. PKC α stimulated phosphorylation of serine and threonine residues in the cytoplasmic tail of LRP-1 may have a permissive effect on subsequent tyrosine phosphorylation (Ranganathan et al., 2004). Mutation of the serine and threonine residues results in greatly diminished tyrosine phosphorylation and impaired binding to SHC.

Physiologically, the interaction of LRP-1 and the PDGF-R may underlie the observation that ApoE as a ligand of LRP-1 inhibits vascular smooth muscle migration in response to PDGF (Swertfeger et al., 2002). In a vascular smooth muscle specific LRP-1 knockout mouse the loss of function of LRP-1 results in increased smooth muscle migration, disruption to the elastic lamina and aneurysm formation (Boucher et al., 2003). All these changes are abrogated by the administration of the PDGF-R inhibitor gleevec. The mechanism of the LRP-1 modulation of the PDGF derived signal is unclear. A further effect of ApoE is to diminish the PDGF stimulated activation of MAP kinase (Ishigami et al., 1998) the

activity of which regulates smooth muscle migration (Cospedal et al., 1999). Mechanistically, the cytoplasmic domain of LRP-1 sequesters JIP-1 and JNK and inhibits the JNK-MAP kinase pathway (Lutz et al., 2002).

Taken together this data indicates that there is a marked cross talk between LRP-1 and the PDGF-R. Not only is the phosphorylation of LRP-1 at least in part dependent on the PDGF-R but events downstream of the PDGF signal can be modulated by the cytoplasmic tail of LRP-1.

1.12.3 The effect of LRP-1 phosphorylation on receptor mediated endocytosis.

Studies link LRP-1 phosphorylation with receptor function. Potentially, phosphorylation of the NPXY motif may alter the interaction of LRP-1 with clathrin coated pits and therefore endocytosis. However, the predominant endocytosis signal for LRP-1 is a YXXL motif and a dileucine sequence (Li et al., 2000). PKA stimulated phosphorylation of the cytoplasmic tail of LRP-1 at the serine 76 enhances endocytic rate (Li et al., 2001). These results are incongruent with other reports in the literature where mutation of 4 phospho-acceptor sites in LRP-1, including serine 76, augment endocytosis (Ranganathan et al., 2004). So, at present, the relationship between phospho-status of LRP-1 and endocytic rate is not clear.

1.12.4 Megalin as a putative phospho-acceptor protein and modulator of signalling pathways.

Having established that other members of the LDL-R have important signalling functions the evidence favouring a similar role for megalin will be considered.

Some knowledge of the signalling pathways potentially modulated by megalin can be inferred from the binding partners of the MegCT. Using MegCT as bait in yeast two hybrid screening several binding partners for megalin have been identified. Protein/protein interaction was confirmed using GST pulldown assays and SEMCAP-1, JIP-1 and 2, PSD-95, OMP-25, PIP4,5-kinase, ICAP-1 and Dab1 have been identified as binding partners of MegCT. Based on the known biological functions of these binding proteins megalin may have a role in regulating G-protein signalling, MAP kinase activity, synaptic organisation, cytoskeletal attachment, phosphoinositide signalling, integrin signalling and cell differentiation. This study was based on biochemical and genetic techniques and did not confirm an interaction in intact cells. Nevertheless, there is a clear implication that megalin has some function in cell signalling (Gotthardt et al., 2000).

Other molecules interacting with MegCT include disabled-2 (Dab-2) (Oleinikov et al., 2000), ankyrin-repeat family A protein (ANKRA) (Rader et al., 2000) and the megalin-binding protein (MegBP) (Petersen et al., 2003).

Dab-2 is a molecule that is downregulated in a number of malignancies (Morris et al., 2002). Through its phospho-tyrosine binding (PTB) modules Dab2 modulates signal transduction pathways and/or regulates protein trafficking within cells. Targeted disruption of the dab2 gene in mice results in a very similar phenotype to those in which there is a lack of TGF- β signal (Morris et al., 2002). Dab-2 is known to interact with the transforming growth factor- β (TGF- β) pathway and this is recognised to be altered in proteinuric renal disease (Hocevar et al., 2001, Bottinger and Bitzer, 2002). The finding, using a variety of techniques that MegCT (through its third NPXY domain) interacts with Dab-2 is particularly interesting

(Oleinikov et al., 2000). There is a mutual regulation of protein expression and subcellular distribution between megalin and Dab-2 (Nagai et al., 2005). It is likely that the MegCT-Dab-2 interaction regulates endocytic activity as anti-Dab-2 antisera transfected into BN16 cells attenuates RAP (a high affinity ligand of megalin) uptake. In addition in visceral endoderm cells internalisation of megalin requires Dab-2 (Maurer and Cooper, 2005). From these data it is possible to appreciate that MegCT via its interaction with dab2 may be able to regulate diverse signalling pathways.

In further studies using the yeast two hybrid system the ankyrin containing protein ANKRA was identified as a binding partner for MegCT (Rader et al., 2000). Ankyrin is a cytoskeletal protein that functions to link transmembrane proteins with actin (Sedgwick and Smerdon, 1999). Rader and colleagues postulated that via its interaction with ANKRA MegCT may be able to modulate the Raf-1 kinase pathway. Active Raf-1 kinase stimulates anti-apoptotic pathways in mouse fibroblasts (Kebache et al., 2007).

There is a very limited literature around ANKRA. In rats it has been shown to modulate the α -subunit of the calcium activated potassium channel (Lim and Park, 2005). In a further role distinct from any aspect of the endocytic pathway ANKRA up-regulates major histocompatibility complex class II antigens (MHCII) via an interaction with human histone deacetylases (HDACs) which serve as signal responsive transcription repressors (Wang et al., 2005a).

Therefore, this interaction between ANKRA and megalin is intriguing as it potentially regulates gene transcription.

Megalin binding protein (MegBP) interacts with MegCT using a yeast two hybrid screen. An interaction in intact cells (BN16) has been shown using fluorescently tagged MegBP and immunofluorescently labelled megalin. Interestingly, overexpression of MegBP does not affect endocytic rate (as measured by uptake of fluorescently labelled RAP) but is associated with non-apoptotic cell death within 24 hours (Petersen et al., 2003). Further studies using MegBP as bait in a yeast two hybrid screen identified a number of transcriptional regulators as binding partners. Amongst these is SKI-interacting protein (SKIP) that functions as a transcriptional co-activator of the vitamin D receptor (Zhang *et al* 2002). SKI family members are also known to down regulate the TGF β signalling pathway (Wu *et al.* 2002).

1.12.5 The sequence of the MegCT.

At 209 amino acids in length the human MegCT is much larger than equivalent regions in other LDL-R family members. The cytoplasmic tail of LRP1 for example consists of 110 amino acids. MegCT has unique sequence motifs (Hjälml et al., 1996, Saito et al., 1994) that may mediate interaction with intracellular binding partners. These motifs include three NPXY domains serving to mediate endocytosis within clathrin coated pits (Chen et al., 1990) or interaction with phospho-tyrosine interaction domains (Songyang et al., 1995b), four Src homology-3 (SH3 binding regions conforming to the XpFPpXP SH3-binding site) consensus recognition motif (Yu et al., 1994) and one Src homology-2 (SH2) recognition motif for, amongst other molecules the p85 regulatory subunit of PI 3-kinase (Songyang et al., 1993). In addition there are numerous consensus

sequences for phosphorylation by protein kinase C, casein kinase II and cyclicAMP/GMP dependent kinases (PKA/PKG) (Rader et al., 2000). The functional significance of these regions remains to be determined.

1.13 Aims.

Proteinuric nephropathy is associated with a significant mortality and morbidity and accompanies common medical conditions such as diabetes and hypertension. There is a pressing need to better understand the mechanisms of progressive renal disease.

Albumin, other filtered proteins and growth factors (a) bind and are endocytosed by receptors on the PTC and (b) stimulate an array of intracellular signalling cascades that has a distinct effect on PTC phenotype ultimately favouring a loss of renal function. Albumin binding to its established PTC receptor megalin may stimulate intracellular events. Traditional dogma has it that megalin functions solely as a cargo receptor, reclaiming nutrients that would otherwise be lost in the urine. The signalling function of megalin suggested by the severe phenotype of the megalin knockout mouse and identification of a number of signalling related binding partners for the megCT argues that the paradigm that megalin is a cargo receptor is no longer appropriate.

The aim of this project was to identify whether megalin functioned as a phospho-acceptor protein and in particular establish:

- Does phosphorylation of megCT occur?
- If so, what agents present in the proteinuric urine regulate phosphorylation of megCT?

- What kinases are responsible?
- Are there any functional associations of megCT phosphorylation?

1.14 Hypothesis.

Megalin is an agonist regulated phospho-acceptor protein whose post-translational modification has distinct functional consequences on PTC.

2 Materials and Methods.

2.1 Materials.

Standard chemical reagents of analytical grade were obtained from Sigma (Poole, UK) and Elgastat purified water was used throughout. DMEM:F12, Hanks balanced salt solution (HBSS), penicillin/streptomycin, L-glutamine and foetal calf serum and all other tissue culture reagents were purchased from Invitrogen Life Technologies (Paisley, UK).

Wild-type OK cells were a gift from Dr. J. Caverzasio (University Hospital, Geneva, Switzerland). Human proximal tubular cells were obtained from the normal pole of nephrectomy samples taken from people with renal cell carcinoma. HK-2 cells were given by Dr. M. Dockrell, SW Thames Institute for Renal Research, St. Helier Hospital, Carshalton, Surrey.

Essentially-fatty acid free recombinant human albumin was purchased from Sigma (Poole, UK). Epidermal growth factor, insulin-like growth factor-1, phorbol-12,13 dibutyrate, AG1478, wortmannin, Ro-31 8220, carbobenoxyl-L-leucyl-leucyl-L-leucinal (MG-132), protease inhibitor cocktail III and gamma-secretase inhibitor X were bought from Calbiochem (Nottingham, UK). FITC-labelled bovine serum albumin was obtained from Sigma (Poole, Dorset). Glutathione sepharoseTM and protein A sepharose were bought from GE Healthcare (Uppsala, Sweeden).

[³²P]-ATP was purchased from Perkin Elmer Life Sciences (Cambridge, UK) and ³²P-orthophosphate obtained from Amersham Pharmacia Biotech (Little Chalfont, UK).

All PCR primers were synthesised by Invitrogen Life Technologies (Paisley, UK) and restriction enzymes and DNA T4 ligase purchased from New England Biolabs (Hitchin, Herts, UK) or Invitrogen (Paisley, UK). Endo-free Plasmid maxi and mini kits, QIAquick PCR purification kit, QIAquick gel extraction kit and QIAquick reaction cleanup kit were obtained from Qiagen Ltd (Crawley, UK). Fugene-6 transfection reagent was purchased from Roche Diagnostics (Lewes, UK).

Anti-megalin-CT rabbit serum was produced by CovalAb UK Ltd (Cambridge, UK) and goat anti-CD8 antibody bought from Santa Cruz Biotechnology Inc. (Santa Cruz, CA, USA). HRP-labelled goat anti-rabbit and HRP labelled rabbit anti-goat secondary antibodies were purchased from Sigma (Poole, UK).

The TOPO TA cloning kit was bought from Invitrogen Life Technologies (Paisley, UK) and the plasmid pCMV-Script purchased from Stratagene (La Jolla, CA, USA). The vectors pGEX-4T-MegCT and pBS-SKII-CD8 were kind gifts from Dr. A. Oleinikov (University of California) and Prof. F. Karet (University of Cambridge, UK) respectively.

All tissue culture plastic ware was from Nuncleon (Denmark). Four well chamber slides were from Sigma (Poole, UK) and glass coverslips from Chance Proper (UK).

Protein electrophoresis gel equipment and PRECISION PLUS protein blue standard markers were from Bio-Rad (Hercules, USA). Nitrocellulose membrane (0.4 μm pore size) was supplied by Schleicher and Schuel (London, UK). Hyperfilm-ECL and chemiluminescence (ECL) reagents were from Amersham Pharmacia Biotech (Little Chalfont, UK).

MS/MS spectrometry was performed by the Protein and Nucleic Acid Laboratory at the University of Leicester. Reagents and equipment were MonoTip (GL Sciences Inc), chymotrypsin (Roche Applied Science), Voyager DE-STR MALDI-TOF mass spectrometer (Applied Biosystems, Warrington, UK), 4000 Q-Trap mass spectrometer (Applied Biosystems, Warrington, UK), C18 300 Å Acclaim PepMap media (Dionex), Jupiter Proteo 4 µM 90 Å media (Phenomenex, UK) and the MASCOT search tool (Matrix Science Ltd., London, UK).

2.2 General methods.

2.2.1 Cell culture.

2.2.1.1 Choice of cell type.

Three different kidney proximal tubular cell lines were chosen for these experiments. To ensure biological applicability of the early studies to the proteinuric state in man human primary cell cultures were used. These were derived from tissue taken from the unaffected poles of kidneys removed because of renal cell cancer. When considering functional associations of MegCT phosphorylation albumin endocytosis was studied as this process may have a significant patho-physiological role in the development of proteinuric renal disease. Primary cell cultures exhibit little endocytic activity and therefore the immortalised opossum kidney (OK) derived cell line was used. The OK cell line maintains characteristics of the proximal tubular epithelium (Malstrom et al., 1987, Nakai et al., 1987) and had been used previously in the host laboratory and demonstrates avid albumin endocytosis (Brunskill et al., 1996). To achieve over-expression of

the MegCT in intact cells a chimaeric CD8-MegCT protein was developed. This was transiently and stably transfected into OK derived cells instead of primary human PTC lines for the following reasons:

- During the course of this work urological practice changed such that most nephrectomies were performed laparoscopically. Associated with this was a long warm ischaemic time of the kidney and an inability to salvage tissue from which viable cell lines could be established.
- Primary cell lines would not retain their PTC phenotype over sufficient passages to develop stably transfected cell lines.
- Expression of the chimaeric protein may affect albumin uptake and a model consistent with previous studies was needed.

As using a human primary PTC line was no longer feasible to continue the studies of megalin phosphorylation the immortalised human PTC line HK-2 was used.

2.2.2 Isolation and culture of human PTC.

This was based on an established method (Detrisac et al., 1984). The tissue was obtained from the unaffected pole of kidneys removed because of renal cell carcinoma. A sample of kidney weighing approximately 50g was removed and transferred to a sterile container holding HBSS supplemented with benylpenicillin (100 IU/ml) and streptomycin (50µg/ml) at 4°C.

The kidney was transferred to a tissue culture cabinet and the renal capsule removed using sterile forceps. The outer cortex was removed and diced using a sterile scalpel blade. The diced tissue was placed in 30ml universal containers, suspended in HBSS and centrifuged at 1000rpm for 5 minutes at 4°C. The HBSS

was aspirated and this washing procedure repeated 3 times. The tissue was then transferred to a 60ml sterile container and suspended in 30ml of HBSS containing 30mg of collagenase type II. With the lid loosely applied to allow gas exchange the container was placed in the tissue culture incubator. The mixture was stirred with a sterile bar for 30 minutes. The collagenase reaction was stopped by the addition of 10ml of HBSS containing 40mg/ml of BSA. The digested kidney was then washed twice with HBSS and then added to the top of a sieve of 500 μ m mesh size. The tissue was forced through the sieve using the plunger from a 10ml syringe. It was then passed successively through 250 μ m and 90 μ m sieves. The glomeruli were retained on top of the 90 μ m sieve whilst the tubular fragments passed through and were collected. The tubular fragments were washed twice with HBSS before seeding into four prepared 75cm² flasks.

The flasks were prepared by coating with collagen type I and foetal calf serum. 50 μ g/ml of bovine collagen type I solution was prepared in 0.1M acetic acid. 7.5ml was placed in each flask to produce 50 μ g collagen/cm². The flasks were left in the cell culture cabinet overnight to allow evaporation of the acetic acid and adherence of the collagen to the plastic. The collagen solution was aspirated and the flasks washed three times with HBSS. Heat inactivated foetal calf serum was then added to each plate in sufficient quantity to cover the bottom of the flasks which were then incubated at 4°C overnight. The foetal calf serum was then removed by aspiration and the flasks washed three times with HBSS before storage at 4°C and use within 1 month.

The cells were grown in the following medium: DMEM:F12 with the addition of 25 mM HEPES buffer, recombinant human epidermal growth factor (10 ng/ml), bovine

insulin (5 µg/ml), transferrin (human, iron free, 5 µg/ml) sodium selenite (5 ng/ml), tri-iodo-thyronine (4 pg/ml), hydrocortisone (36 ng/ml), benzylpenicillin (100 IU/ml) and streptomycin (50 µg/ml). This media was termed defined growth media (DGM). The media was changed after 3 days and then on alternate days until confluence was reached. Typically, this was after 10 to 14 days.

Confluent monolayers of cells were then passaged. The media was removed from each flask and the cells washed three times with calcium and magnesium free HBSS. 5ml of trypsin/EDTA (0.25% trypsin, 1 mM EDTA) solution was added to each flask which was then incubated for 5 minutes at 37°C. The reaction was stopped by the addition of 10ml of DGM supplemented with 10% foetal calf serum. Trypsinised cells were collected by centrifugation at 1000rpm, the pellet re-suspended in DGM supplemented with 5% foetal calf serum and plated out in 6 well plates at a concentration of 2×10^5 cells/well. The plated cells were allowed to reach confluence, typically after two or three days. Cell monolayers produced this way have previously been characterised as proximal tubular in origin in the host laboratory (Burton et al., 1996).

2.2.3 Culture of OK cells.

Wild type OK derived cells were maintained in DMEM:F12 supplemented with 10% FCS, 2 mM L-glutamine, 100 U/ml penicillin, 100 µg/ml streptomycin and 10 mM HEPES. OK derived cells were passaged (typically split 1:5) exactly as described for hPTC. Cells were used between the passage numbers 65 and 87. Passaged cells reached confluence after a week and the culture media was changed on

alternate days. Prior to experimentation cells were cultured in DMEM/F12 low glucose (5 mM) for 48 h.

2.2.4 Culture of HK-2 cells.

HK-2 cells (passages 18-30) were maintained in DMEM/Ham's F12 (DMEM/F12) medium, supplemented with 10% FCS, glutamine (2 mM), penicillin (100 IU/ml), and streptomycin (100 µg/ml). Cells were cultured at 37°C in a humidified atmosphere of 5% CO₂ in air. Cells were passaged weekly and typically split 1 in 4. Media was replaced on alternate days. Before treatment, cells were cultured in DMEM/F12 low glucose (5 mM) for 48 h.

2.2.5 Preparation of human renal cortex homogenate.

Polyclonal anti-MegCT antisera were characterised using renal cortex homogenate as a source of intact megalin. The homogenisation procedure was performed on ice or at 4°C. The renal capsule was removed and the remaining tissue diced into 2 mm pieces. 5 ml of ice cold homogenisation buffer was added. The tissue was homogenised with 20 manual strokes of a tissue homogeniser. The homogenate was centrifuged at 50g for 5 minutes and the supernatant collected. The pellet was homogenised once again following the same procedure and the supernatants combined and frozen at -80°C until further use.

2.2.6 Polyacrylamide gel electrophoresis and immunoblotting.

2.2.6.1 Preparation of proteins for electrophoresis.

Proteins were suspended in 2x gel loading buffer and boiled for 5 minutes.

2.2.6.2 Polyacrylamide gel electrophoresis of proteins.

Cell proteins in loading buffer were then applied to a well of a polyacrylamide gel and electrophoresed at 200V for approximately 45 minutes according to the method of Laemmli (Laemmli, 1970). At least one lane of each gel was reserved for the application of pre-stained molecular weight standards to determine the molecular weights of proteins of interest in the cell lysates. Separated proteins were analysed in gels by Coomassie staining, or after transferring to a nitrocellulose membrane for immunoblotting.

2.2.6.3 Coomassie staining, Gel Drying and Autoradiography.

Proteins separated by PAGE were visualised by soaking the entire gel in Coomassie staining solution followed by submersion in Coomassie destaining solution. Stained gels were dried on blotting paper before being exposed to autoradiograph film for varying times at -80°C.

2.2.6.4 Immunoblotting of Proteins after PAGE.

Separated proteins were transferred from polyacrylamide gels to nitrocellulose membranes in a semi-dry transfer cell according to the method of Towbin *et al.* (Towbin *et al.*, 1979). The polyacrylamide gel was placed on a nitrocellulose membrane and sandwiched between three sheets of blotting paper pre-soaked in transfer buffer. Transfer of proteins from the gel to the nitrocellulose membrane was stimulated by the application of a current of 0.65 mamps/cm² for 120 minutes at room temperature. During this time the nitrocellulose membrane was orientated

towards the anode and the gel towards the cathode. Efficacy of transfer was confirmed by assessing the transfer of the pre-stained molecular weight standards from the gel to the nitrocellulose membrane.

Membranes were then washed for 5 minutes at room temperature in Tris buffered saline (TBS); followed by a second 5 minute wash in TBST. To prevent non-specific antibody binding, membranes were blocked by immersion in 5% milk in TTBS for 1 hour at room temperature.

Nitrocellulose membranes were then incubated with the primary antibody diluted in blocking solution for either 1 hour at room temperature or overnight at 4°C. Following this incubation the nitrocellulose membranes were washed three times with TBST for 10 minutes. Horseradish peroxidase (HRP) conjugated secondary antibodies were suspended in blocking solution and applied to the nitrocellulose membranes with the second incubation proceeding for 60 minutes at room temperature. Following the final wash ECL plus reagents were added to the membrane and drained off after 5 minutes. Each nitrocellulose membrane was then sealed in Saran wrap and exposed to photographic film for varying times in order to achieve optimal visualization of the protein bands of interest.

2.2.7 Transfection of chemically competent E. Coli, bacterial culture and formation of glycerol stocks.

Competent cells were thawed on ice and to a 100 µl aliquot of cell suspension was added 1 ng of plasmid DNA. After gentle agitation the mixture was incubated on ice for 30 minutes before being heat shocked for exactly 45 seconds at 42°C. Following a further 2 minute incubation on ice 900 µl of SOC media was added.

Each transfection was incubated horizontally in a shaking incubator at 225 rpm at 37°C for 1 hour. Individual colonies of transfected DH5α cells were grown by spreading 100 µl of the transfection mixture on LB agar plates (containing 50 µg/ml ampicillin) and incubating overnight at 37°C.

An individual colony was selected and used to inoculate 100 ml of 2X YTA media and grown overnight at 37°C with shaking.

Glycerol stocks of transfected bacteria were made by combining 10 ml of the overnight culture with 4.5 ml of a 50:50 mixture of sterile culture media and glycerol. Stocks were stored at -80°C.

2.2.8 Large and small scale plasmid DNA preparation.

Two to five ml of Luria Broth supplemented with either ampicillin or kanamycin was inoculated with a single colony of bacteria and incubated at 37°C on a rotator platform at 220 rpm for 8 hours. This starter culture was diluted 1 in 1000 and incubated overnight, with shaking at 37°C. Bacteria were pelleted by centrifugation at 6000g for 15 minutes at 4°C and plasmid DNA purified using a Qiagen maxi or midi prep kit following exactly the manufacturers instructions.

2.2.9 Determination of protein concentration.

Total protein content was determined by the method of Lowry *et al* (1951). Briefly, duplicate protein standards were created by dilution of 1 mg/ml BSA from 0-200 µg/ml in a volume of 250 µl. The unknown samples with an approximate concentration of protein between 0-200 µg/ml were prepared in volume made up to 250 µl with distilled water. Thereafter, to each tube, 1ml of alkaline copper sulphate

reagent was added, vortexed and incubated for 10 minutes at room temperature. Folin-Ciocalteu reagent was diluted with distilled water 1:3 and 100 μ l added to each tube, vortexed and incubated at room temperature for 15 minutes. Finally 1 ml of distilled water was added to each tube before the absorbance of the developed blue/purple colour was measured at 750 nm using a spectrophotometer.

The absorbance versus the protein concentration of each standard was plotted using GraphPad Prism software to give a standard curve from which the protein concentrations of the unknown samples were determined.

2.2.10 Determination of DNA concentration.

DNA absorbs light with a wavelength of 260 nm (A_{260}). To calculate DNA concentration sample was diluted by a factor of between 50 and 100 by suspending in 1 ml of DNAase free water, gently mixing and allowing to stand for 10 minutes. The suspension was applied to a glass cuvette and the absorbance measured. A DNA concentration of 50 μ g/ml records an absorbance of 1, by relating the absorbance of the sample to this the DNA concentration was calculated. A second absorbance was measured at 280 nm (A_{280}). This is the wavelength at which cellular debris is maximally absorbent. Measuring the ratio of A_{260} and A_{280} indicated the purity of the DNA. A ratio of 1.5 was acceptable.

2.2.11 Statistical analysis.

Data are expressed as mean \pm SE. Where required, statistical analysis of multiple

comparisons was performed using one-way analysis of variance with Tukey's correction. Differences were considered significant at $p < 0.05$.

3 Phosphorylation Studies of a MegCT-GST Fusion Protein.

3.1 Introduction.

The 209 amino acid MegCT is longer than the equivalent region in other LDL-R family members and possesses unique sequence motifs (**Fig. 3.1**). Human MegCT contains three NPxY domains that act as coated pit internalisation sequences (Chen et al., 1990) and/or mediate interaction with phospho-tyrosine interaction domains (Songyang et al., 1995a), three Src homology-3 (SH3) binding regions conforming to the XpFPpXP SH3 binding site consensus motif (Yu et al., 1994), one Src-homology-2 (SH2) recognition motif for the p85 regulatory subunit of PI 3-kinase (Songyang et al., 1993) and one RXXX(p)SXP site for binding 14-3-3 domain containing proteins (Aitken, 2006).

A number of intracellular binding partners of the MegCT have been identified including the MAP kinase scaffold proteins JIP-1 and -2 (JNK interacting proteins) (Gotthardt et al., 2000), post synaptic density protein-95 (PSD-95) like membrane associated guanylate kinase proteins (Larsson et al., 2003) and adapter molecules such as SEMCAP-1 (semaphorin binding protein) (Gotthardt et al., 2000), disabled-2 (Dab-2) (Oleinikov et al., 2000), autosomal recessive hypercholesterolaemia (ARH) (Nagai et al., 2003), megalin binding protein (megBP) (Petersen et al., 2003) and ankyrin-repeat family A protein (ANKRA) (Rader et al., 2000). Whilst some of these proteins have a role in regulating endocytosis they also imply a role of MegCT in Ras and ERK signalling,

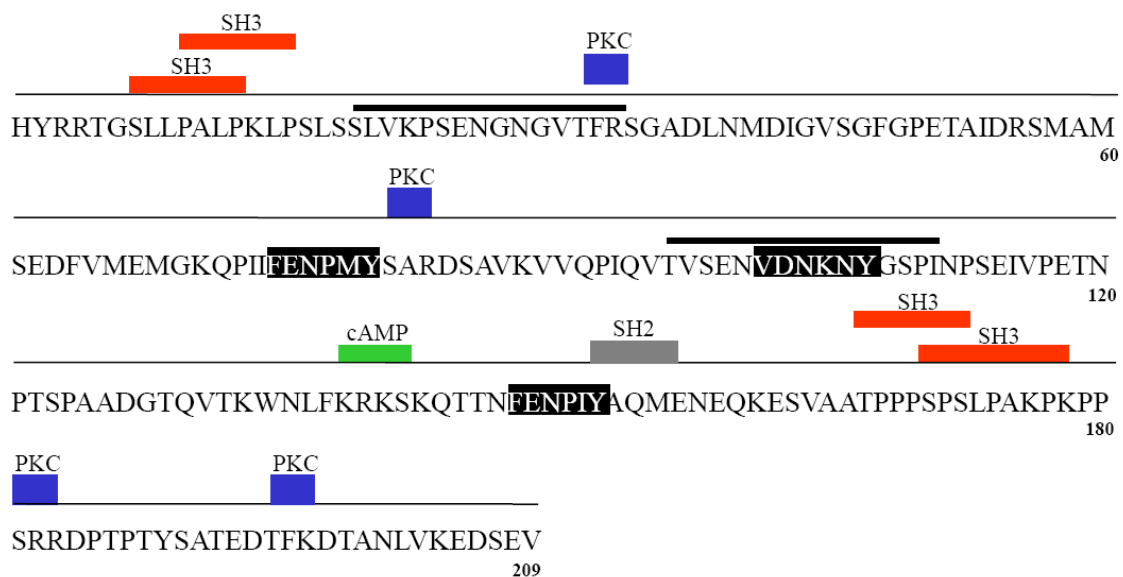


Figure 3.1 Amino acid sequence of the megalin cytoplasmic tail. The 209 amino acid sequence of the human MegCT is depicted and shows the presence of sequence motifs potentially involved in signalling. The thick black lines are above the peptide sequences that were used to immunise rabbits in the production of polyclonal antisera described in chapter 4.

GTP-binding protein signalling, JNK scaffold assembly, inositol metabolism and Raf-1 kinase binding.

In addition there are multiple potential phosphorylation sites in MegCT including consensus sites for PKC, casein kinase II, glycogen synthase kinase-3 (GSK-3), protein kinase B and cAMP/cGMP-dependent protein kinase (Hjalm et al., 1996).

3.2 Aims of these studies.

The aim of these studies was to determine using an *in vitro* approach whether MegCT is a phospho-acceptor protein and if so, to determine potential kinases that regulate phosphorylation.

The essence of the studies described in this chapter is that by using cell lysate from agonist stimulated PTC only kinases that mediate MegCT phosphorylation that are relevant to PTC function would be tested. That is, a degree of specificity is maintained as kinases are present at intracellular concentrations even if MegCT is more abundant. At the outset it was postulated that MegCT phosphorylation may occur following ligation of megalin or other receptors and this assay enabled that hypothesis to be tested.

3.3 Methods.

3.3.1 Rationale for use of a MegCT-GST fusion protein.

Recombinant proteins, or fragments of protein fused to glutathione-S-transferase (GST) are easily and rapidly purified. GST fusion proteins have been widely used as an *in vitro* method of detecting with a degree of specificity protein/protein

interactions and post translational modifications of proteins (Smith and Johnson, 1988). Typically GST fusion proteins bound to glutathione sepharose beads are easily manipulated and collected by centrifugation from reaction mixtures.

3.3.2 Generation of a MegCT-GST fusion protein.

To generate a MegCT-GST fusion protein the Glutathione-S-transferase Gene Fusion System (Amersham Pharmacia Biotech) was used. The pGEX vectors allow for inducible, high level expression of genes as fusions with *Schistosoma japonicum* GST. MegCT cDNA as supplied was ligated between the *EcoRI/XhoI* sites of pGEX-4T1 (**Fig. 10.1**). Propagation of pGEX-4T1 in bacterial culture was achieved by transfecting the *E. Coli* strain DH5 α as described in chapter 2.

3.3.3 Expression, purification and collection of MegCT-GST fusion protein.

A scraping of frozen glycerol stock of pGEX-4T1-MegCT transfected DH5 α *E. Coli* was used to inoculate 200 ml of 2X YTA media which was incubated at 37°C with shaking overnight. The overnight culture was diluted 1:100 into fresh pre-warmed 2X YTA media and grown at 30°C until the A600 reached 1 (typically 4 hours). Sterile IPTG was added to a final concentration of 1 mM and incubation continued for a further 2 hours whilst expression of the fusion protein was induced. Bacteria were collected by centrifugation at 8000 rpm at 4°C for 10 minutes. The supernatant was discarded and the pellet resuspended in 5 ml of ice cold PBS. The cell wall of the bacteria was disrupted by brief sonications on ice until partial clearing of the cell suspension was observed. The fusion protein was solubilised by the addition of 20% Triton X-100 to a final concentration of 1% followed by

gentle mixing for 30 minutes. Insoluble cell debris was removed by centrifugation at 12,000g for 10 minutes at 4°C and the supernatant decanted and pellet discarded. The fusion protein was collected by the addition of 2 ml of a 50% slurry of glutathione sepharose 4B in PBS to the supernatant followed by further gentle mixing for 30 minutes at room temperature. Fusion protein bound to glutathione sepharose beads was collected by centrifugation for 5 minutes at 500g. In total the pellet was washed 3 times with 10 ml of PBS before being finally re-suspended in 2 ml of PBS.

3.3.4 Stimulation of MegCT-GST fusion protein phosphorylation.

Confluent monolayers of PTC were quiesced overnight in serum free media. The media was aspirated and freshly prepared agonists diluted in 1 ml of serum free media were added to each well and incubated for 20 minutes. Stimulation was halted by placing each 6 well plate on ice, the stimulating solution was aspirated and each well washed with ice cold PBS. Cells were lysed in JNK lysis buffer for 10 minutes on a rotator platform.

Insoluble cell debris was removed by centrifugation (10,000g for 10 minutes at 4°C), the supernatant was placed in a sterile eppendorf tube to which was added 75 µl of GST-MegCT complexed to glutathione beads suspended in PBS. Binding of cell proteins within the lysate and the GST-MegCT fusion protein proceeded by incubating the mixture for 60 minutes at 4°C on an end over end rotator. The beads were then washed once in 1 ml of lysis buffer and twice with 1 ml of kinase buffer.

Table 4.1 Summary of agents used in the studies of MegCT phosphorylation alongside rationale for their use.

Agonist	Rationale
1 Human serum albumin (HSA)	<ul style="list-style-type: none"> • A major component of proteinuric urine • An agonist of the megalin-cubilin complex
2 EGF	<ul style="list-style-type: none"> • A megalin ligand • Recognised as a player in proteinuric nephropathy
3 PDBU – a stimulator of PKC	<ul style="list-style-type: none"> • PKC deletion reduces interstitial fibrosis and is renoprotective • PKC activity stimulated by HSA in PTC • PKC activity regulates PTC albumin endocytosis <i>in vitro</i>.
4 Angiotensin-II	<ul style="list-style-type: none"> • An attempt to establish in vitro correlate of clinical trial evidence showing renoprotective effects of ACE inhibition. • Angiotensin II modulates PTC albumin endocytosis.
5 IGF-1	<ul style="list-style-type: none"> • IGF-1 present in proteinuric urine and is a megalin ligand in neuronal cells. • IGF-1 inhibits PTC apoptosis <i>in vitro</i>.
6 Bradykinin	<ul style="list-style-type: none"> • Regulates intracellular calcium and would stimulate calcium dependent protein kinases.

Washed beads were collected by centrifugation at 5000 rpm for 3 minutes. To each washed pellet was added 40 μ l of kinase buffer containing 0.4 μ l of [γ ³²P]ATP and 0.4 μ l of a 2 mM ATP stock solution. Phosphorylation of the fusion protein occurred during a 30 minute incubation at 30°C. The beads were collected as previously and separated by PAGE. Dried gels were exposed to autoradiograph film.

3.4 Results.

3.4.1 A MegCT-GST fusion protein is phosphorylated in vitro.

To test the hypothesis that MegCT is a phospho-acceptor protein, cell lysate stimulated phosphorylation of a MegCT-GST fusion protein complexed to glutathione sepharose beads was examined. There was considerable basal phosphorylation of MegCT-GST seen under all conditions. When incubated with lysates derived from cells pre-stimulated with HSA, bradykinin and PDBU MegCT phosphorylation was augmented. Pre-stimulation with angiotensin II did not increase the phosphorylation of MegCT-GST. No phosphorylation of GST alone was seen (**Fig. 3.2**). Pre-stimulation with HSA, EGF and PDBU augmented phosphorylation by $141.9 \pm 11.4\%$, $148.6 \pm 15.7\%$ and $151.9 \pm 14.1\%$ respectively (**Fig. 3.3**). No phosphorylation of GST alone was observed.

To determine whether the phosphorylation observed *in vitro* was physiologically relevant, a concentration response experiment to EGF was performed (**Fig. 3.4**). Maximal phosphorylation of MegCT-GST fusion protein was stimulated by EGF at a concentration between 500 and 1000 pg/ml, resulting in a 3.42 and 3.02 fold

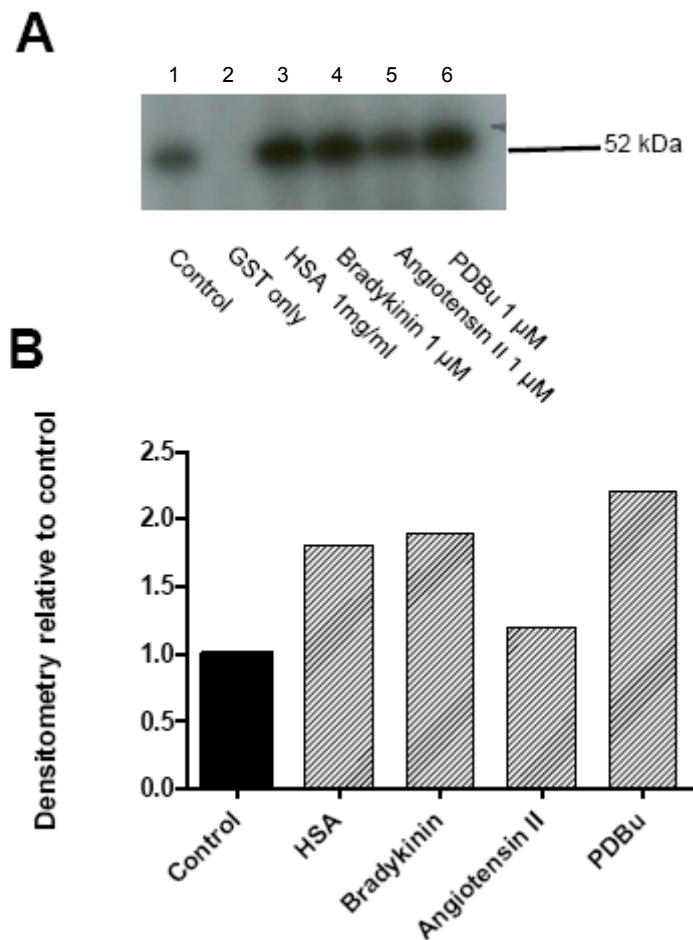


Figure 3.2 Phosphorylation of a meg-CT-GST fusion protein. hPTC were stimulated with the indicated concentrations of agonist. After stimulation cell monolayers were washed and lysed. Cell lysates were incubated with meg-CT-GST complexed to glutathione beads for 60 minutes at 4°C. Collected beads were washed and incubated with kinase buffer in the presence of γ [³²P]-ATP for 30 minutes at 30°C. Beads were washed and applied to polyacrylamide gels and subjected to electrophoresis. Dried gels were exposed to autoradiograph film of which panel **A** is a representative example. Panel **B**. Densitometric analysis of radiolabelled bands. Densitometric values of bands obtained under non-stimulated conditions were normalised to 1 and stimulation expressed relative to that. Pilot data obtained from one experiment.

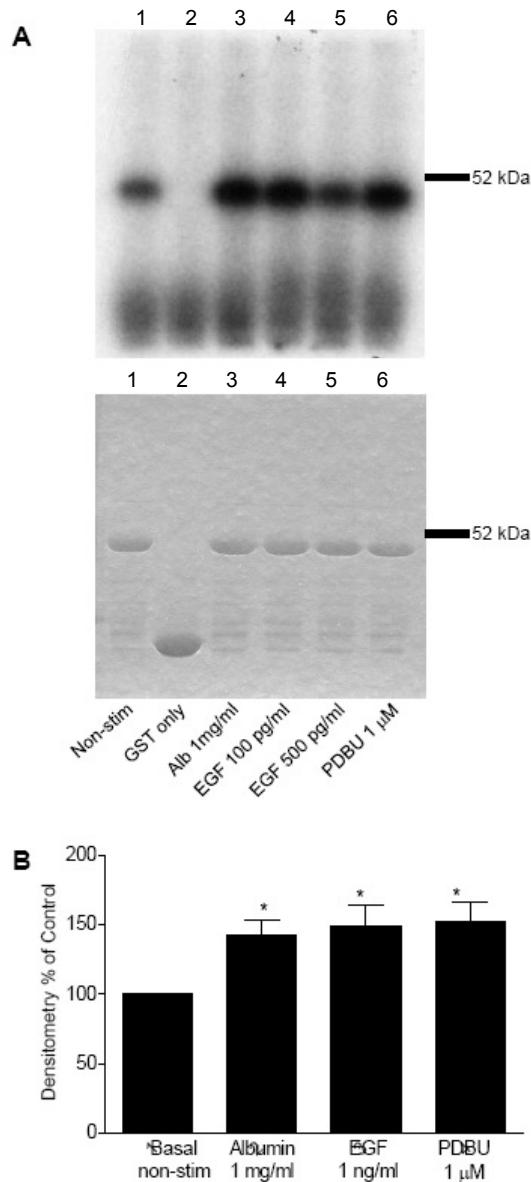


Figure 3.3 Phosphorylation of a meg-CT-GST fusion protein. Monolayers of hPTC were incubated with the indicated concentrations of recombinant human serum albumin (HSA), EGF or PDBu. Stimulated cells were treated exactly as previously. Panel **A** is a representative autoradiograph. Equal loading of protein into each well is shown by a dried Coomassie stained gel is shown. Panel **B**. Densitometric analysis of data obtained from all experiments. Data represents mean \pm SEM of six experiments. * $p \leq 0.01$ compared to non-stimulated controls.

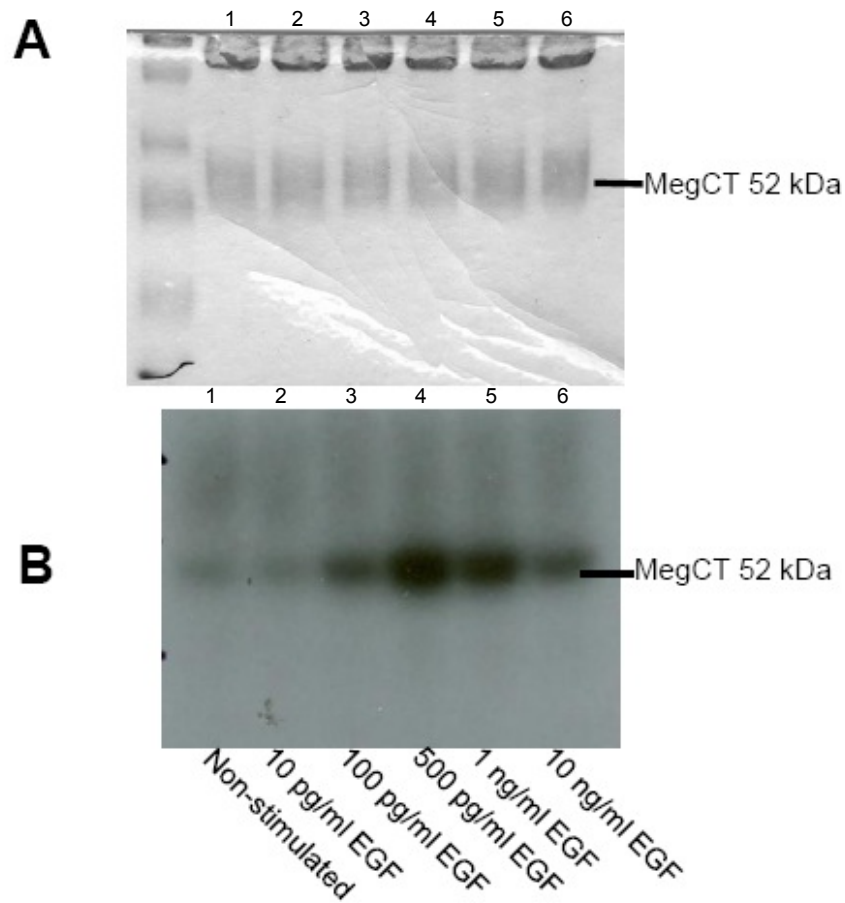


Figure 3.4 EGF concentration response of meg-CT-GST fusion protein phosphorylation. Monolayers of hPTC were incubated with the indicated concentrations of EGF for 20 minutes. The contents of each well was washed and lysed and incubated with megalin cytoplasmic tail fusion protein for 60 minutes. Kinase activity using megalin cytoplasmic tail-GST fusion protein as a substrate proceeded for 30 minutes at 30°C. Beads were washed and subjected to PAGE and the dried gel exposed to autoradiograph film. **A** Dried Coomassie stained gel to demonstrate equal protein loading to each well. **B**. Representative autoradiograph.

graduated increase in the phosphorylation seen under that of unstimulated conditions. At the highest concentration of EGF used (10 ng/ml) there was a reduction in the fold increase in phosphorylation to 1.97 that of unstimulated controls.

Growth factors other than EGF may be relevant to PTC function and alter the phosphorylation status of megalin. To investigate this possibility a time course of IGF-1 stimulated phosphorylation was performed. By inspection, the autoradiograph indicated increased phosphorylation in response to IGF-1 that was maximal after 10-20 minutes of prestimulation (**Fig. 3.5 B**). Evidence of stimulation persisted at the last time point tested of 60 minutes. Changes in the densitometric analysis failed to reach statistical significance (**Fig. 3.5 C**).

Later experiments would investigate OK cell FITC-albumin endocytosis in cells stimulated by agents responsible for MegCT phosphorylation to test if the two were functional associated. To show that agonist stimulated changes to MegCT was not restricted to human primary cell lines the experiments were repeated using OK cells. There was substantial basal phosphorylation of MegCT-GST. Pre-incubation with HSA, EGF (100 pg/ml), EGF (500 pg/ml) and PDBU increased stimulation by $115 \pm 23.6\%$, $143.8 \pm 20.4\%$, $313 \pm 42.8\%$ and $377 \pm 31.5\%$ respectively (**Fig. 3.6**) indicating that human and OK cells were qualitatively and quantitatively similar in terms of MegCT phosphorylation.

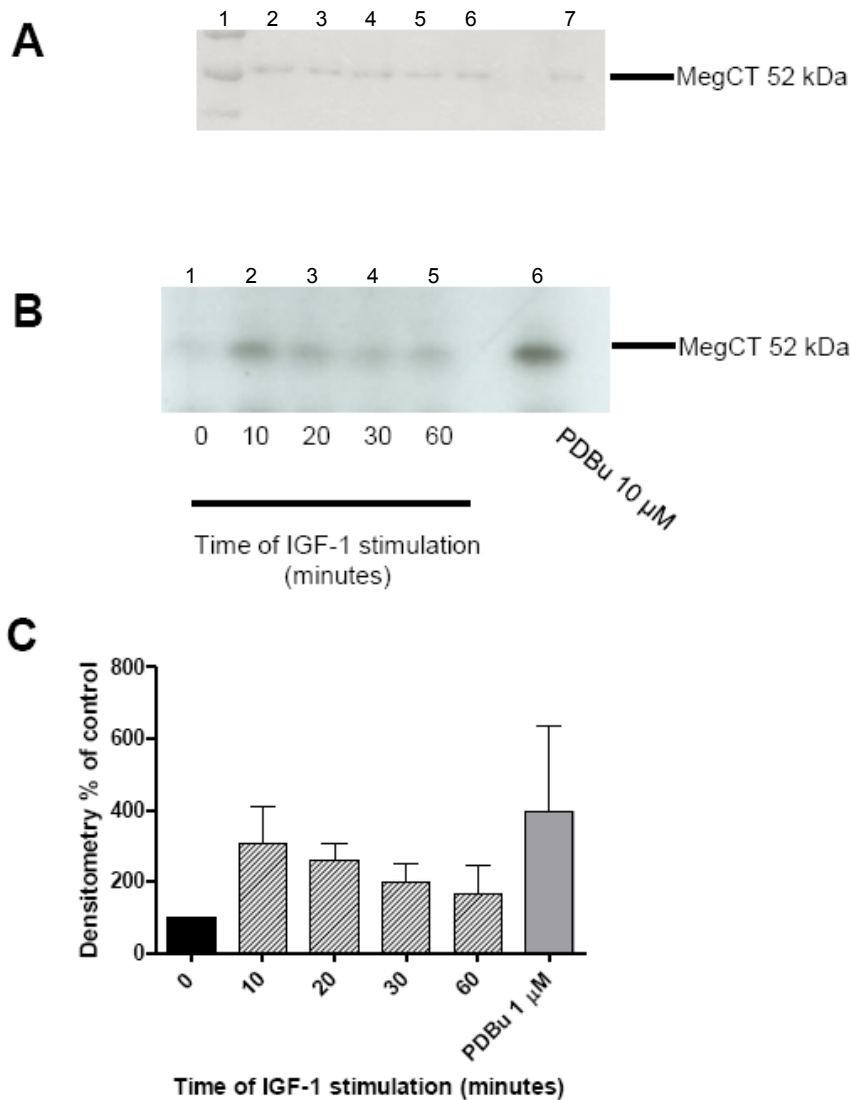


Figure 3.5 Time course of IGF-1 stimulated phosphorylation of meg-CT-GST fusion protein. Monolayers of hPTC were incubated with IGF-1 for the time indicated or PDBU for 20 Kinase activity using megalin cytoplasmic tail-GST fusion protein as a substrate proceeded for 30 minutes at 30°C. Beads were washed and subjected to PAGE and the dried gel exposed to autoradiograph film. **A** Dried Coomassie stained gel to demonstrate equal protein loading to each well. **B**. Representative autoradiograph. **C**. Densitometric analysis of autoradiograph where the unstimulated condition has been normalised to 1 and stimulated lanes expressed as relative to that. Results shown are mean \pm SD of two experiments. There were no statistically significant differences between the conditions

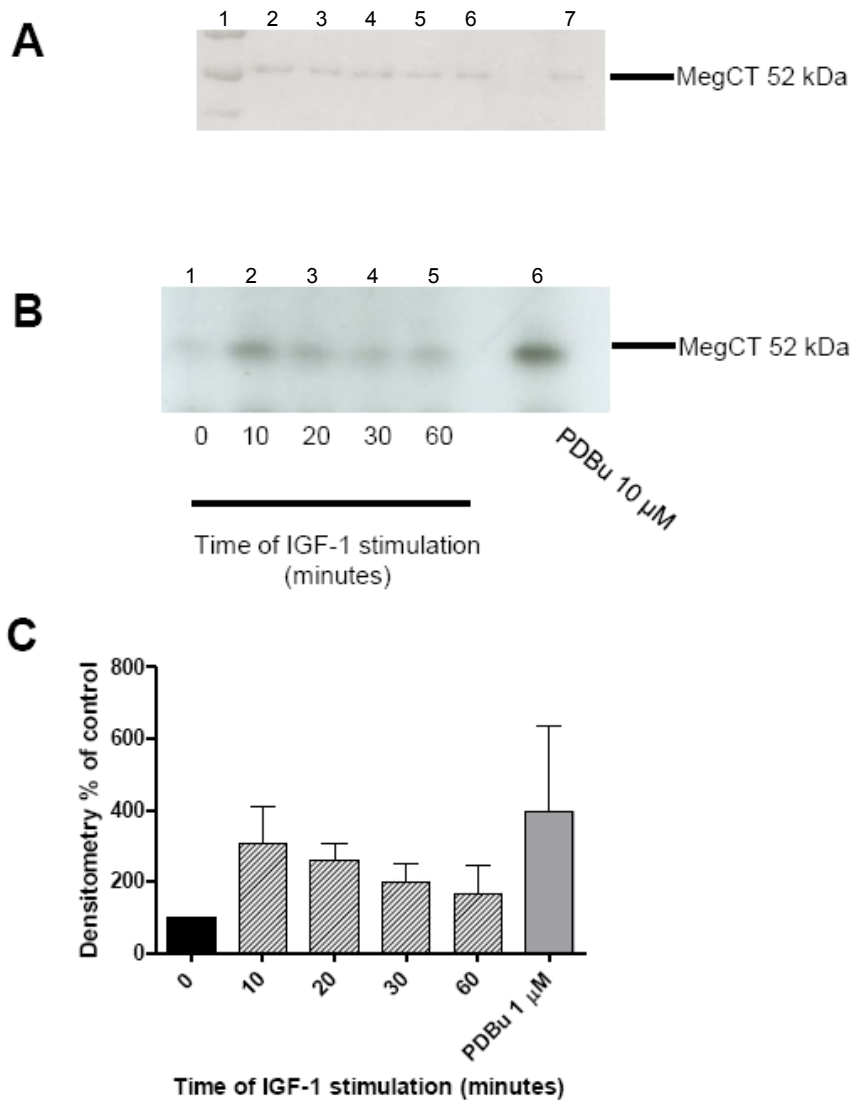


Figure 3.6 Phosphorylation of a meg-CT-GST fusion protein stimulated by OK cell lysate. Monolayers of OK were incubated with the indicated concentrations of recombinant human serum albumin (HSA), EGF or PDBu. Stimulated cells were treated exactly as previously. Panel **A** is a representative autoradiograph with the corresponding Coomassie stained gel shown as evidence of equal protein loading. Panel **B**. Densitometric analysis of data obtained from all experiments. Data represents mean \pm SEM of three experiments. * $p \leq 0.05$ compared to non-stimulated controls.

3.4.2 *Multiple kinases regulate MegCT-GST fusion protein phosphorylation.*

To begin identification of the kinases responsible for MegCT phosphorylation hPTC were treated with a number of protein kinases inhibitors prior to agonist stimulation, cell lysis and lysate application to MegCT-GST-glutathione beads. Two representative blots are shown (**Fig. 3.7 A**).

Key findings of the densitometric analysis are shown in **Fig. 3.7 B**. HSA (1 mg/ml) increased MegCT phosphorylation over basal by $141.9 \pm 4.6\%$. Pre-treatment with wortmannin, Ro 81-3220, PD98059 and AG1478 that inhibit PI 3-kinase, PKC, MEK and EGF-R kinase respectively, reduced the stimulated phosphorylation over basal to $97.7 \pm 2.1\%$, $121.4 \pm 2.1\%$, $120.2 \pm 7.7\%$ and $110.0 \pm 2.6\%$.

Stimulation with 1 ng/ml EGF resulted in an increase in phosphorylation over basal of $148.6 \pm 6.4\%$. Pre-treatment with AG1478 and wortmannin reduced this to $117.1 \pm 5.3\%$ and $118.4 \pm 2.4\%$ respectively. Incubation with PDBu increased phosphorylation by $151.9 \pm 5.7\%$. Pre-treatment with Ro 81-3220 reduced this $111.70 \pm 1.4\%$.

3.5 Discussion.

Current thinking regarding certain members of the LDL-R family favours a role as signal transducers as well as mediating endocytosis. Supporting a hypothesis that megalin has a crucial role beyond endocytosis is the phenotype of the megalin knockout mouse. These animals exhibit a severe forebrain abnormality, respiratory failure and proteinuria, which are incongruent with a simple ligand retrieval function of megalin. Proteinuria is an established prognostic marker of progressive renal

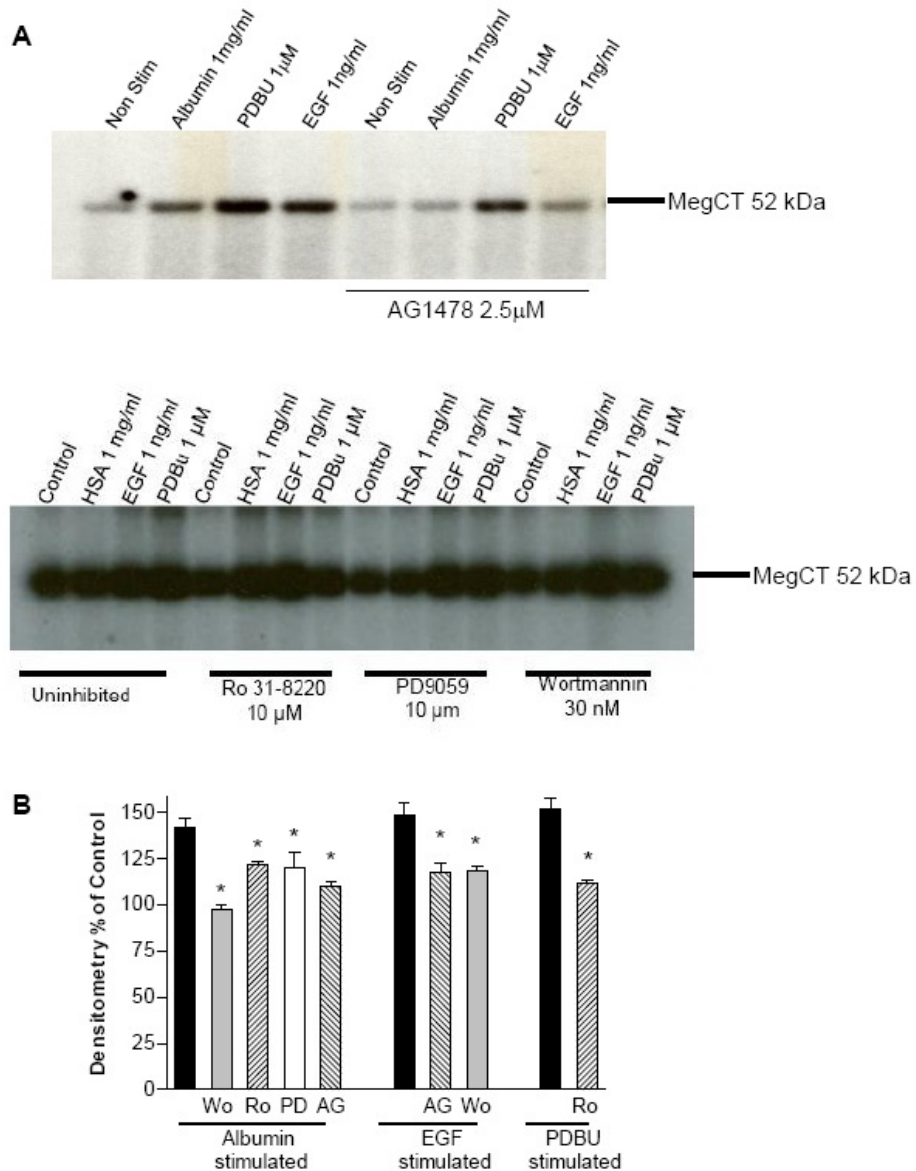


Figure 3.7 Effect of kinase inhibitors on phosphorylation of meg-CT-GST fusion protein phosphorylation. hPTC were incubated with agonists with or without pre-incubation with the indicated kinase inhibitors. Lysed cells were mixed with megalin cytoplasmic tail fusion protein complexed to glutathione sepharose beads. Washed beads were incubated in kinase buffer at 30°C for 30 minutes in the presence of γ [³²P]-ATP. After washing beads were separated by PAGE and exposed to autoradiography. **A.** Representative autoradiographs of the experiments. **B.** Key results following densitometric analysis of phosphorylated megalin cytoplasmic tail GST fusion protein bands. The kinase inhibited stimulation is normalised to that obtained under non-inhibited conditions. Data expressed as mean \pm SEM, $n \geq 3$ individual experiments. * $p \leq 0.05$.

disease and the PTC receptor for a number of filtered proteins megalin is thought to be a significant player in renal patho-physiology. The contribution of megalin to proteinuric nephropathy may be mediated by (i) Retrieval into the PTC of excessive amounts of ligand macromolecules present in the tubular filtrate (ii) Modulating the bio-availability of megalin ligands that may activate signalling pathways in PTC and (iii) Megalin itself transducing extracellular signals.

Mindful of the multiple potential sites for phosphorylation these studies were designed to investigate whether megalin is a phospho-acceptor protein and, if so whether phosphorylation is a regulated process. To ensure biological applicability of these experiments to proteinuric nephropathy human PTC were used. The data in this chapter describe for the first time the agonist regulated phosphorylation of MegCT.

Proteinuric nephropathy occurs as a result of (i) PTC exposure to macromolecules/growth factors (ii) activation of intracellular pathways, such as PKC. Progression can be reduced by agents that interrupt the renin-angiotensin II system. The agents used in the initial studies of MegCT phosphorylation reflected these observations. By pre-incubating glutathione sepharose bound MegCT-GST fusion proteins with hPTC cell lysates and then washing prior to initiating phosphorylation by addition of γ [³²P]-ATP, the aim was to identify activated kinases in stimulated cell lysates that showed some specificity for interaction with MegCT. In this way albumin, IGF-1 and EGF were shown to activate kinases capable of phosphorylating MegCT, as was PKC when activated by PDBU. These findings are congruent with earlier observations of albumin-activated signaling pathways, including PKC in PTC and a key role for EGF in progressive renal disease. The

lack of effect of angiotensin-II, albeit from a single pilot experiment was perhaps surprising given that agents that inhibit its action are reno-protective. Potential MegCT phosphorylation stimulated by angiotensin II may be worth re-visiting as subsequent studies show that, angiotensin-II activates PKB and augments albumin endocytosis (Caruso-Neves et al., 2005) and activated PKB is associated with megalin (Caruso-Neves et al., 2006).

By using specific kinase inhibitors an understanding of the pathways leading to MegCT phosphorylation by albumin, EGF and PDBu can be deduced. That Ro 31-8820 inhibited the PKC induced phosphorylation was unsurprising. Ro-31 8220 pre-incubation partially, but non-significantly reduced albumin stimulated MegCT phosphorylation. The specific EGF-R kinase inhibitor attenuated EGF and albumin induced phosphorylation. Inhibition of PI 3-kinase attenuated EGF and albumin stimulated MegCT phosphorylation. This may have been expected as PI 3-kinase is activated downstream of EGF-R. MEK inhibition differentially inhibited albumin induced MegCT phosphorylation whilst having no significant effect on that stimulated by EGF. This indicates the pathways to increased MegCT phosphorylation activated in response to albumin and EGF are not entirely the same.

These studies are the first to describe agonist regulated phosphorylation of the MegCT in PTC. They are entirely consistent with recent studies that confirm megalin to be phosphorylated constitutively in LLC-PK1 cells (Yuseff et al., 2007) and in response to clusterin in the prostate cancer cell line R3327 MAT LyLu (Ammar and Closset, 2008). Functional effects associated with megalin phosphorylation in these studies are diminished endocytosis (Yuseff et al., 2007)

and protection against TNF α induced apoptosis (Ammar and Closset, 2008). The findings of these studies serve to emphasise the likely multi-functional pathophysiological roles of megalin.

Inhibition of the EGF-R reduces MegCT phosphorylation in response to EGF *in vitro* thus implying EGF induced MegCT phosphorylation is mediated by the EGF-R and not as a consequence of EGF binding to megalin. Studies of the PDGF-R and LRP protein exemplify how growth factor signalling and members of the LDL-R family interact. Phosphorylation of LRP is stimulated by a process involving the PDGF-R, PI 3-kinase and non-receptor associated tyrosine kinase Src (Barnes et al., 2001, Boucher et al., 2002, Loukinova et al., 2002). Furthermore, ligand binding to LRP reduces MAP kinase signalling (Ishigami et al., 1998) and inhibits functional effects of signalling through the PDGF-R (Swertfeger et al., 2002, Boucher et al., 2003). In our studies EGF-R mediates phosphorylation of MegCT but it remains to be determined if the EGF signalling pathway is altered as a result. These studies indicate that EGF is not the only growth factor to regulate MegCT phosphorylation. IGF-1 was associated with a non-significant increase in MegCT phosphorylation. The non-significance of this study was perhaps a reflection of the fact that only two experiments were performed and that repetition might result in a clear stimulation of MegCT phosphorylation by IGF-1. In a number of different PT cell types IGF-1 protects against apoptosis induced by nephrotoxins (Ortiz et al., 2005, Varlam et al., 2001). IGF-1 may be a stimulant of MegCT phosphorylation but unlike EGF is not recognised to be a megalin ligand.

The enzyme PI 3-kinase is implicated in a number of PTC processes and is a regulator of MegCT phosphorylation. PI 3-kinase is both a downstream kinase of

the EGF-R and a regulator of albumin endocytosis in PTC (Brunskill et al., 1998). Wortmannin, an inhibitor of PI 3-kinase inhibits EGF and albumin induced phosphorylation of MegCT. In a rat prostate cell line, PI 3-kinase mediates clusterin stimulated phosphorylation of megalin. Functionally, this phosphorylation event favours further clusterin binding to megalin (Ammar and Closset, 2008). Clusterin is a regulator of apoptosis and protects rat prostate cells from TNF α induced cell death. In PTC too, PI 3-kinase regulates apoptosis by phosphorylating PKB. This results in phosphorylation and inhibition of BAD and thereby inhibits apoptosis (Caruso-Neves et al., 2006). Megalin appears to have a crucial role in binding and locating PKB to the cell membrane. Active PKB is released from megalin by a PI 3-kinase dependent process. What regulates the initial binding and release of PKB from megalin isn't clear but may well be related to a phosphorylation event. The site of PKB binding to megalin is yet to be investigated but the consensus site for phosphorylation by PKB conforms to the sequence RXXS/T. This matches a sequence in the MegCT between residues 4 and 7.

The partial inhibition of HSA stimulated MegCT phosphorylation by the specific EGF-R kinase inhibitor AG1478 is consistent with a model in which some albumin induced effects in PTC are mediated by the EGF-R. For instance, albumin induced ERK activation, IL-8 production and DNA synthesis are downstream of EGF-R activation and dependent on Src kinase activity (Reich et al., 2005, Lee and Han, 2008).

Albumin induced phosphorylation of MegCT is dependent on ERK activity. The MegCT contains two threonine phospho-acceptor sites in a proline rich region that conforms to an ERK 1/2 consensus sequence for phosphorylation. Albumin

stimulates ERK activity in OK cells in a time course compatible with the MegCT phosphorylation observed in this study (Dixon and Brunskill, 2000). In PTC ERK is stimulated by oxidative stress and has an inhibitory influence on PKB (Sinha et al., 2004). The sites and burden of MegCT phosphorylation may be the result of a complex series of interactions between ROS, ERK and PI 3-kinase/PKB activity that potentially reflect the oxidative stress of the cell at the time (**Fig. 3.8**). This concept would dovetail with the observation that albumin's effect on cell viability is concentration dependent. At high concentrations albumin downregulates megalin expression whereas at lower concentrations it is preserved (Caruso-Neves et al., 2006).

In summary, these data provide confirmation of our hypothesis that MegCT is phosphorylated in a regulated fashion. By using cell lysate derived from human PTC the identified kinases stimulating MegCT phosphorylation are physiologically relevant. However, using a cell free system is a limitation of this work as cellular segregation of proteins is lost and this could be important in intact cells. To confirm the observations described in this chapter phosphorylation of MegCT in intact cells was studied.

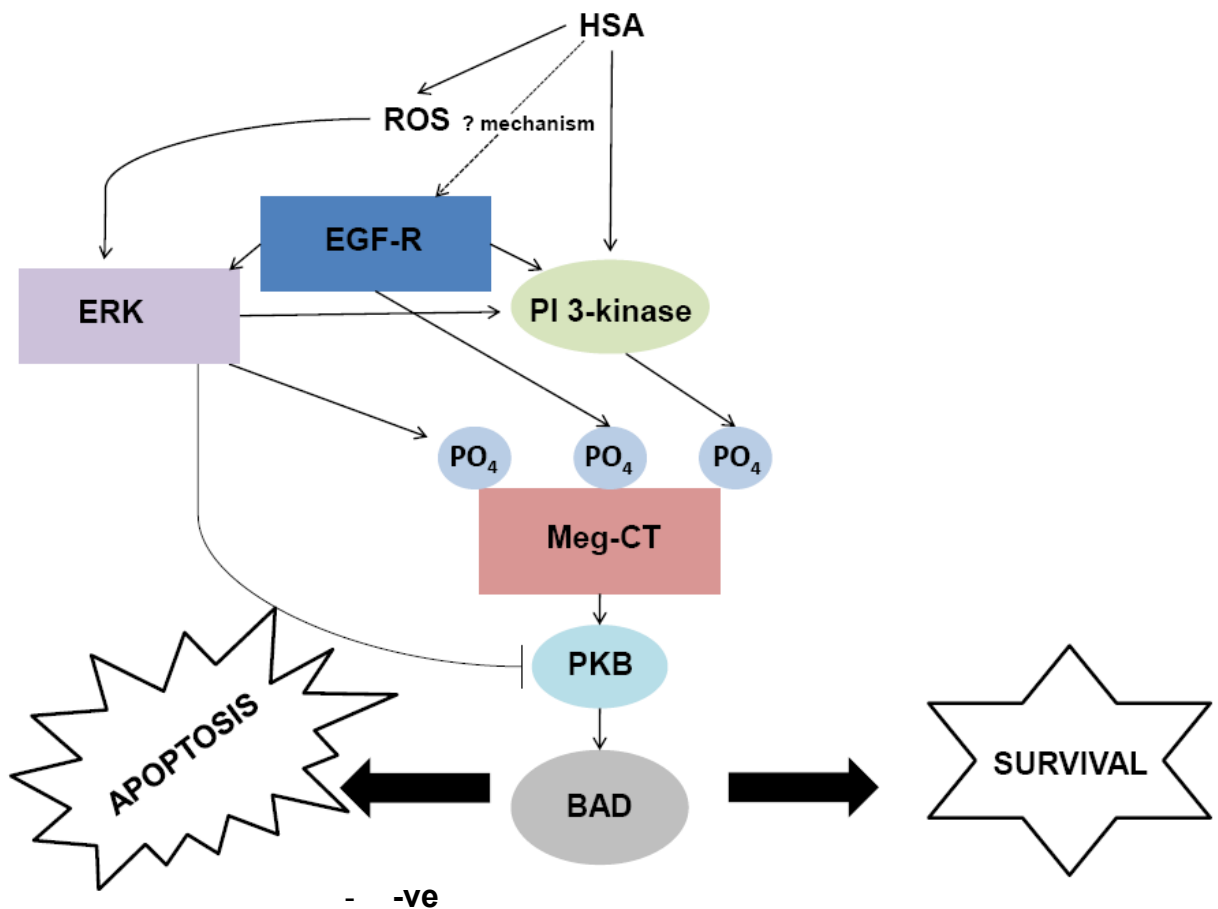


Figure 3.8 Schematic representation demonstrating some of the different kinases that regulate MegCT phosphorylation by albumin. The different kinases stimulating MegCT phosphorylation are shown and the sites of MegCT phosphorylation may reflect the prevailing albumin concentration and/or oxidative stress of the PTC. Under relatively low conditions of oxidative stress the kinases on the left hand side of the diagram may be active. This may stimulate a pattern of MegCT phosphorylation that favours binding and inhibition of PKB by MegCT. Under conditions of high oxidative stress the right hand side of the diagram is favoured by the activation of a different set of kinases and pattern of MegCT phosphorylation. In summary, MegCT phosphorylation status might be the result of a complex series of kinase reactions that could orchestrate cell fate.

4 Characterisation of Polyclonal Rabbit anti-MegCT Antisera.

4.1 Introduction.

It was anticipated that large quantities of anti-MegCT antisera would be required for the experiments outlined in this thesis. The requirements of the anti-sera were that supply should not be limiting and that preferentially the epitopes recognized would not contain any putative phosphorylation sites. At the time of commencing these experiments anti-sera against megalin were not available commercially therefore, CovalAb were commissioned to produce antibodies to MegCT. This is discussed further in chapter 4. The anti-MegCT sera produced was characterised against MegCT-GST fusion protein, HK-2 cell lysate and a homogenate of human renal cortex taken from the unaffected pole of nephrectomy specimens taken from people with renal cell carcinoma.

4.2 Aims.

To produce and characterise polyclonal anti-human MegCT antisera.

4.3 Materials and Methods.

Production of polyclonal anti-MegCT antisera was undertaken by CovalAb (Lyons, France).

4.3.1 Immunisation of rabbits against human MegCT.

Two peptides that were thought to be maximally immunogenic to rabbits were selected from the entire sequence of human MegCT. The peptides selected for immunisation in conjunction with CovalAb were CUK-41A - SLVKPSENGNGVTFR (amino acids 20 – 34) and peptide CUK-41B TVSENVDNKKNYGSP (amino acids 96-110). The TFR sequence in peptide CUK 41A conforms to consensus sequence for phosphorylation by PKC. Their localisation in the entire sequence is shown in **Fig. 3.1**. A BLAST search revealed no protein homology with any other human peptides.

All animal work was carried out by CovalAb. A 5ml pre-bleed of two New Zealand White rabbits coded 215 758 and 215 908 was taken on Day 0 before prior to immunisation with 1 ml of an equal mixture of conjugated antigen and Complete Freund Adjuvant. A second and third vaccination occurred on days 21 and 42 respectively. A test bleed was taken on day 53 before a fourth and final immunisation under the same conditions as previously was performed on day 63. A further bleed was taken on day 74 and the rabbits sacrificed on day 81 and the blood collected.

4.3.2 Determination of antibody titre.

The immunoreactivity of rabbit serum against MegCT was assayed by ELISA by CovalAb. Immunogenic peptide was covalently coupled to the base of a 96 well plate. Applied serum was serially diluted in a range between 1/500 and 1/64,000. Arbitrarily, the titre was expressed as the inverse of the dilution. This was

determined as the dilution giving an optical density ratio of 1 when measured at 450 nm.

4.3.3 Characterisation of rabbit anti-human MegCT antisera.

Antisera was characterised against MegCT present in a MegCT-GST fusion protein, human renal cortex homogenate and HK2 cell lysate.

4.4 Results.

4.4.1 The immunoreactivity of rabbit serum anti-MegCT.

The immunoreactivity of serum derived from two different rabbits against two peptides derived from MegCT was tested and the results shown in **Table 4.1**. At day 74 Rabbit 215 758 demonstrated immunoreactivity to both MegCT peptides with the response against CUK-41B greater than CUK-41A (antibody titre 64,000 vs. 2000). Rabbit 215 908 showed little immunoreactivity against peptide CUK-41A (antibody titre <500) but a good response to CUK-41B (antibody titre 32,000). Informed by these results serum from rabbit 215 758 was used in subsequent studies.

Peptide	Bleeding	Rabbit 215 758	Rabbit 215908
CUK-41A	Day 74	2000	≤500
CUK-41B	Day 74	64,000	32.000

Table 4.1 Antibody titres of rabbits 215 758 and 215 908 to two different epitopes of MegCT. Antibodies were measured by ELISA and titre is expressed as the inverse of the serum dilution that resulted in an optical density reading of 1 at 450 nm. The interpretation of the titres supplied was ≤500 – no immunoreactivity of the serum, 500 ≤ titre ≤ 2000 – low immunoreactivity of the serum and ≥ 2000 – good immunoreactivity of the serum.

4.4.2 Rabbit anti-sera recognised the megalin component of a MegCT-GST fusion protein.

Immunoreactivity of rabbit anti-MegCT sera was tested against samples taken at stages of the purification of MegCT-GST. Samples were subjected to PAGE and western blotting using rabbit anti-MegCT sera as the primary antibody. Sera from both rabbits taken at various days following peptide immunisation behaved in a similar way. Pre-immune sera taken from rabbits prior to peptide immunisation showed no immunoreactivity against MegCT-GST (**Fig. 4.1**). Immunoreactivity against MegCT-GST of sera taken from both rabbits at 53 and 81 days post peptide immunisation is seen (**Fig. 4.1**). The band intensity was greatest against purified MegCT-GST and no reactivity against GST alone demonstrated. The time of exposure of autoradiograph film to the ECL reagents varied and therefore no comment can be made on the relative immunoreactivity of sera derived from the different rabbits.

4.4.3 Intact megalin was detected in human renal cortex homogenate by rabbit anti-sera.

Sera from rabbit 215 758 was used to identify immunoreactivity against intact human megalin derived from a homogenate of renal cortex. As a positive control immunoblots derived using rabbit 215 758 serum were compared with a commercially available goat anti-human megalin antibody that became available

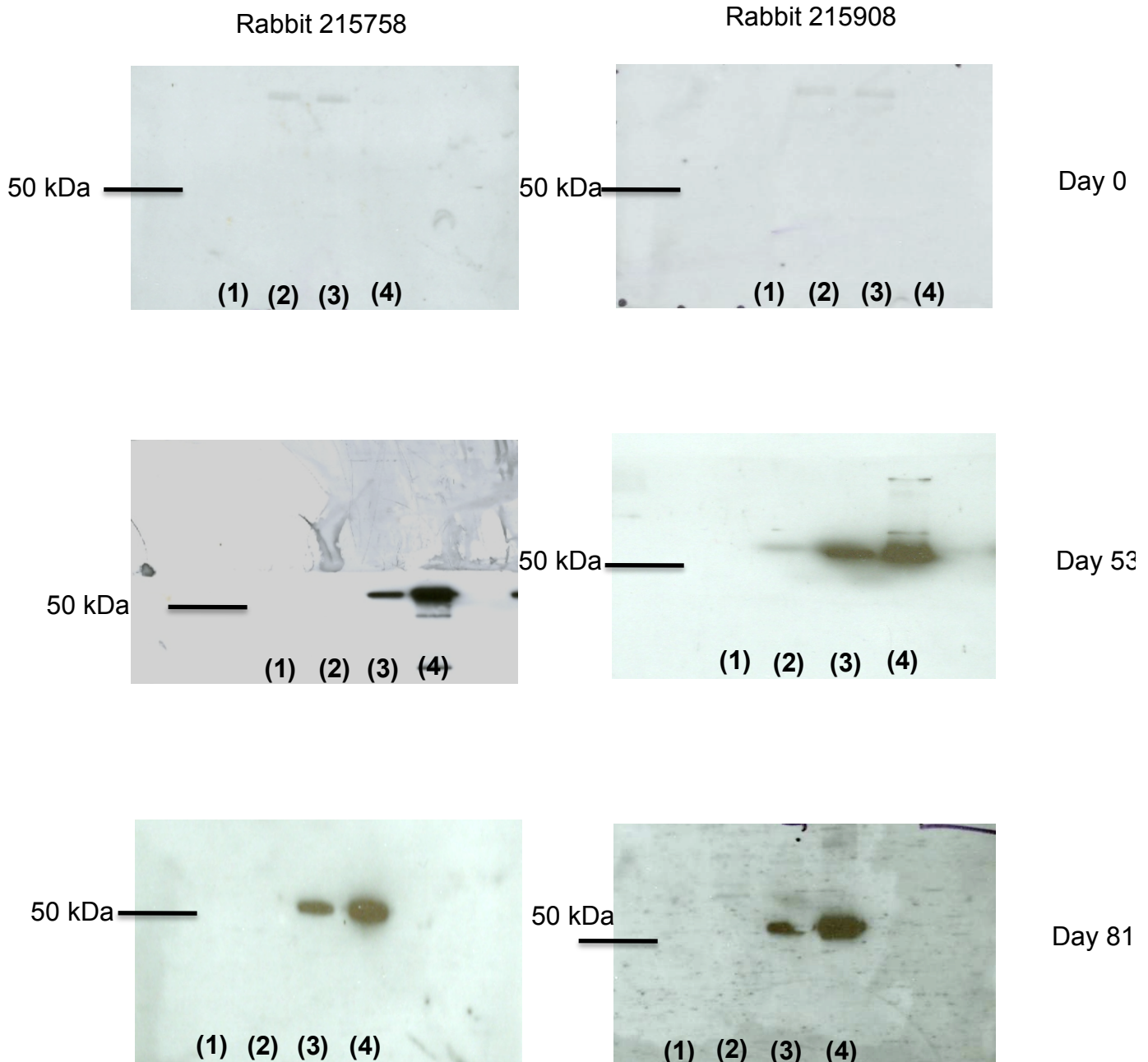


Figure 4.1 Polyclonal rabbit antisera react with the megalin cytoplasmic tail component of MegCT-GST fusion protein. Samples of glutathione sepharose – GST (1), non-induced pGEX-4T1-MegCT transformed bacteria (2), IPTG induced pGEX-4T1-MegCT transformed bacteria (3) and MegCT-GST fusion protein purified on glutathione sepharose beads (4) were subject to PAGE and western blotting performed using anti-MegCT antisera as the primary antibody. Following incubation with an anti-rabbit HRP labelled secondary antibody blots were developed by enhanced chemiluminescence and exposed to X-ray film. One representative blot of at least two is shown. The anticipated mass of MegCT-GST is 52 kDa.

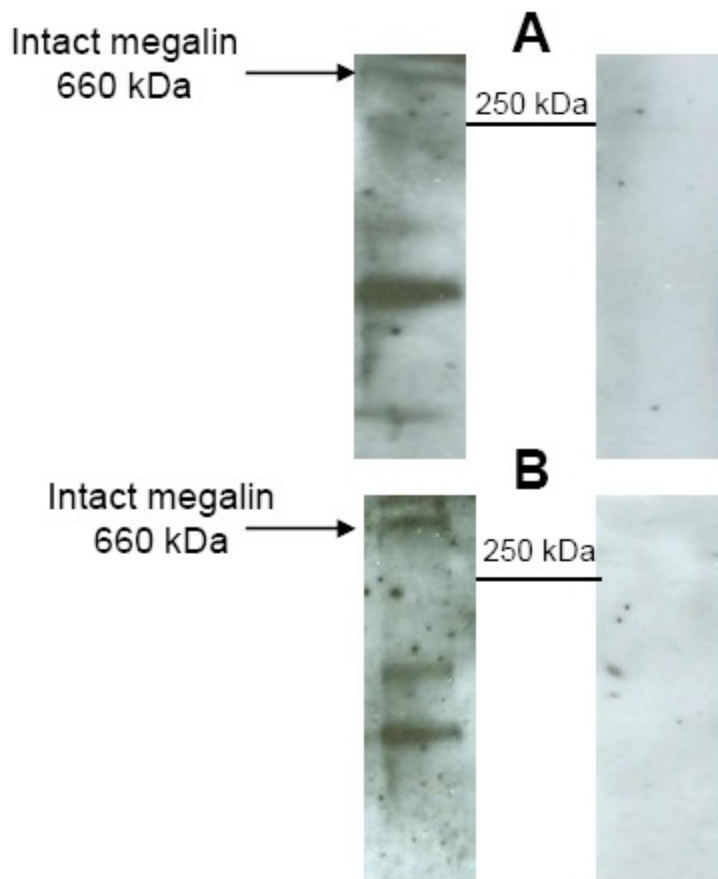


Figure 4.2 Anti-MegCT rabbit sera and a commercially available goat anti-MegCT antibody recognise intact megalin from a human renal cortex homogenate. 20 μ g of cell protein from a human renal cortex preparation were separated on a 4-20% Tris-HCl gradient gel. Nitrocellulose membranes were then probed with either rabbit 715758 sera (A) or goat anti-MegCT antibody (Santa Cruz)(B). The panel on the left was the blot obtained using anti-MegCT antibodies whereas that on the right was the same membrane stripped and re-probed using naive sera from the relevant species. The horizontal arrow indicates intact megalin whereas the horizontal bar marks the position of the 250 kDa protein marker.

during the course of these studies (**Fig. 4.2 A and B**). A number of protein bands were detected including one approximately 600 kDa in mass consistent with intact megalin. Proteins of 150 and 100 kDa in mass were also detected and no bands were detected when sera from human megalin naïve animals was used.

4.4.4 Rabbit antisera is immunoreactive against intact megalin in HK2 cell lysate.

Protease activity during the homogenisation process of human renal cortex may have resulted in megalin fragmentation and the multiple bands detected on the immunoblots. To further investigate the specificity of the interaction between the rabbit sera and MegCT immunoblots of cell lysate derived from HK2 cell lysates were performed. One major immunoreactive peptide of a large molecular mass was detected (**Fig. 4.3B**) that was not present when sera from a human megalin naïve rabbit was used (**Fig. 4.3A**). Faint bands present in **figs 4.3 A and B** may represent non-specific binding of the secondary antibody.

4.5 Discussion.

This chapter describes the production and characterisation of a rabbit anti-human MegCT antibody. Immunoreactivity and specificity of the MegCT antibody for megalin in the form of fusion protein, cultured cells and kidney cortex lysate has been shown. The antisera produced compares favourably with a commercially available antibody. Taken together these data were reassuring that the antibody

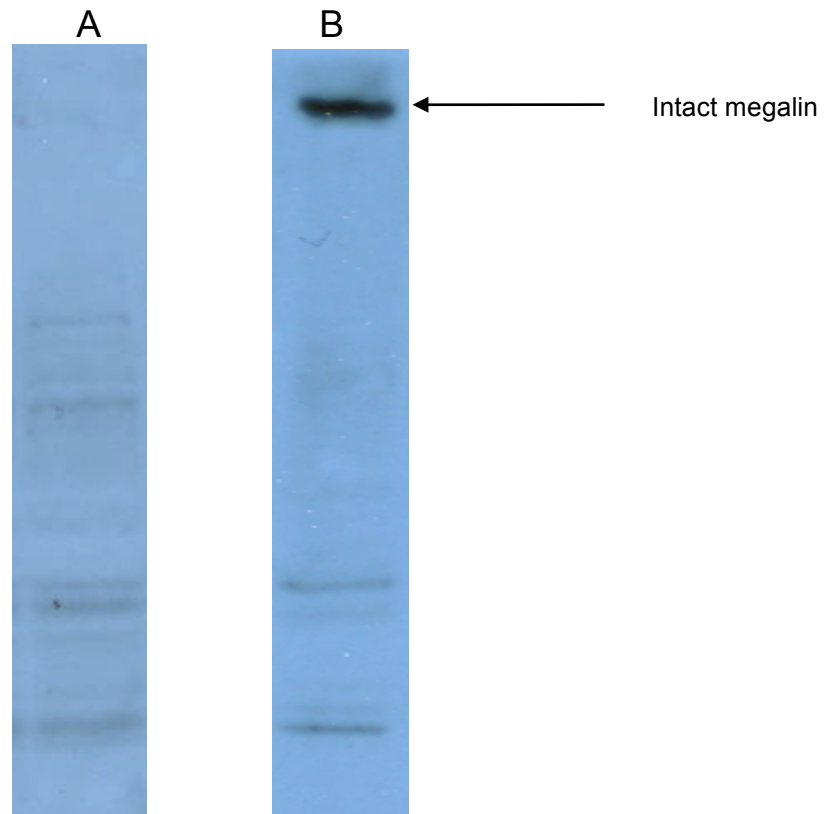


Figure 4.3. Immunoblot demonstrating ability of anti-MegCT antisera to detect intact megalin in HK2 cell lysate. 20 μ g of HK2 cell lysate were loaded onto a 4-15% Tris-HCl gradient gel. Primary antibody incubation was with either naive rabbit sera (A) or sera from rabbit 715758 immunised against MegCT (B). The arrow indicates intact megalin. The panel on the left was exposed to autoradiograph film for four times as long as the panel on the right. The entire length of the gel is shown to demonstrate no immunoreactive peptides of a lower molecular weight.

produced was specific for MegCT and a suitable tool to be used in experiments described later in this thesis.

The initial studies by CovalAb indicated there was differential immunoreactivity to MegCT of sera derived from different rabbits. The anti-sera was used in later studies to immunoprecipitate megalin from lysed cells and in this respect the sera from the two rabbits could not be expected to perform equivalently. In the studies described hereafter, the serum used was from rabbit 215758.

Rabbit anti-MegCT antisera recognised MegCT in the form of MegCT-GST and intact megalin, thus implying maintenance of the tertiary structure of megalin in fusion protein form or that tertiary structure of megalin is not important with regard to recognition by anti-sera.

Rabbit anti-MegCT serum detected a number of protein bands in human renal cortex homogenate. A similar pattern has been described with rabbit renal cortex by Petersen (Petersen et al., 2003) and is indicative of the problems in manipulating such a large protein, even in the presence of protease inhibitors. This degradation pattern of megalin was not seen in HK2 cell lysate and this probably related to rapid denaturation of cellular proteases by reducing lysis buffers.

In summary, this chapter describes the production of an antibody with specificity for MegCT in a variety of different forms. The antibody that was developed performed similarly to antibodies that were available commercially and produced similar patterns to others described in the literature.

5 Studies of Megalin Phosphorylation in Intact Cells.

5.1 Introduction.

The experiments described in chapter three demonstrated phosphorylation of a MegCT-GST fusion protein in a cell free system. To further test the hypothesis that megalin phosphorylation could be important in human proteinuric nephropathy experiments using intact PTC were performed. The large size of native megalin was anticipated to be a considerable hindrance in these experiments and therefore a method was devised to immunoprecipitate only the MegCT. Following stimulation of [³²P]-orthophosphate loaded hPTC the extracellular fragment of megalin was cleaved by light trypsinisation enabling the remaining transmembrane and intracellular fragment to be collected by immunoprecipitation.

5.2 Aims.

To develop the findings that megCT-GST is phosphorylated *in vitro* by examining patterns of megalin in intact cells.

5.3 Methods.

5.3.1 Stimulation of [³²P]-Orthophosphate loaded PTC.

hPTC were grown to confluence in 6 well plates. Prior to stimulation cellular monolayers were quiesced in serum free culture media overnight. Each well was washed twice with phosphate free Krebs solution. To radiolabel the cellular stores of ATP, 50mCi of ³²[P]-orthophosphate were diluted in 1ml of Kreb's phosphate

free buffer and added to each well. Loading proceeded during a 4 hour incubation at 37°C. After loading with [³²P]-orthophosphate, agonists were added directly to each well with stimulation proceeding for the time points indicated.

Following stimulation plates were placed on ice and each well washed once with ice cold Kreb's solution. To cleave the extracellular domain of megalin 1 ml of 0.25% trypsin was added to each well and incubated for 5 minutes at 4°C.

5.3.2 Immunoprecipitation of radiolabelled MegCT.

Each well was washed once with 2ml of ice cold PBS before 1ml of ice cold RIPA buffer containing protease and phosphatase inhibitors. Cell lysis occurred during a 10 minute incubation on ice following which each well was scraped and the contents placed in a pre-chilled 1.5ml eppendorf tube. Insoluble cell debris was collected by centrifugation at 13,000 rpm for 2 minutes in the cold room. The supernatant was removed to a clean eppendorf and the mixture was pre-cleared by the addition of 1µl of megalin naive rabbit serum and 40µl of protein A-agarose. The beads and their associated immune complexes were collected following a 1 hour incubation at 4°C by pulse centrifugation and the supernatant removed to a clean 1.5ml eppendorf tube. To each sample was added 2µl of rabbit anti-MegCT sera. Following mixing at 4°C for 1 hour 50µl of protein A-agarose was added to each sample and mixed for an additional 2 hours. The beads were collected by pulse centrifugation at 2,500 rpm and washed three times with RIPA buffer. After the final wash, 35µl of 2x gel loading buffer was added and heated at 95°C for 5 minutes. The agarose beads were pelleted by centrifugation and the supernatant containing reduced proteins removed for further analysis.

5.3.3 Analysis of immunoprecipitated proteins.

Immunoprecipitates were separated by PAGE on a 12% polyacrylamide gel. Protein bands were stained with Coomassie blue, destained and the gel dried on blotting paper. The dried gel was exposed to autoradiograph film and retained as evidence of equal protein loading.

5.4 Results.

5.4.1 MegCT is phosphorylated in intact cells.

To investigate the physiological relevance of the *in vitro* MegCT-GST fusion protein phosphorylation described, studies were designed to investigate MegCT phosphorylation in intact cells. The size of megalin is a hindrance of the study of the intact molecule. To circumvent this, a method was developed in which the extracellular portion of megalin was cleaved with trypsin and the intracellular MegCT immunoprecipitated from [³²P]-orthophosphate loaded cells.

MegCT immunoprecipitated from hPTC demonstrated increased phosphorylation in response to HSA, EGF and PDBu (**Fig. 5.1**) by $260 \pm 55\%$, $217 \pm 28.8\%$ and $336 \pm 46.6\%$ respectively. The level of basal phosphorylation was much less and no phosphorylated band was detected when pre-immune rabbit sera was used to immunoprecipitate MegCT from PDBu stimulated hPTC. This experiment was performed to exclude non-specific binding of MegCT to the rabbit serum used.

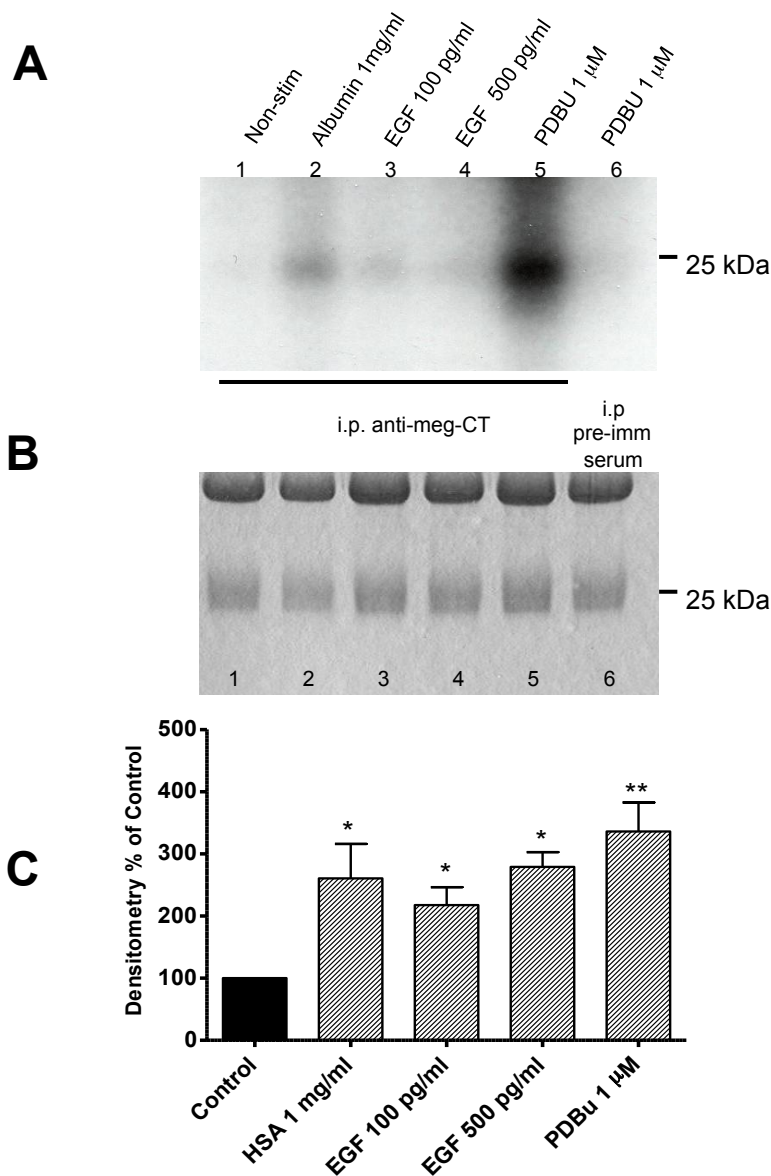


Figure 5.1 Phosphorylation of meg-CT in intact cells. The cytoplasmic tail of megalin was immunoprecipitated from agonist stimulated [32 P]-orthophosphate loaded lysed cells and immunoprecipitates subjected to PAGE. Gels were stained, dried and exposed to autoradiograph film. **A.** Representative autoradiograph. **B.** Dried Coomassie stained gel from the same experiment to demonstrate equal protein loading. **C.** Densitometric analysis of phosphorylated megalin cytoplasmic tail protein bands. Data is expressed as mean \pm SEM, n = 4 experiments. ** p \leq 0.01, * p \leq 0.05.

Overall, the results of MegCT phosphorylation in intact cells were variable. One potential reason for this may have been that the time course varied from the *in vitro* conditions described. A time course of MegCT phosphorylation in response to HSA and EGF was performed that confirmed that maximal phosphorylation was evident after 20 minutes. The phosphorylation was considerably more sustained under conditions of HSA stimulation (**Fig. 5.2**).

5.4.2 Kinase regulation of MegCT in intact cells.

Because of the difficulty in handling large amounts of radioactivity the kinase inhibitors used in studies of MegCT phosphorylation in intact cells was limited to AG1478 and Ro 81-3220. The same pattern of kinase sensitivity was seen. hPTC monolayers were loaded with [³²P]-orthophosphate and pre-incubated under control conditions or with either AG1478 or Ro 81-3220. Cells were stimulated with HSA, EGF and PDBu. Stimulation under non-inhibited conditions was normalised to 100% and the effect of kinase inhibition expressed as relative to that. When pre-incubated with AG1478 MegCT stimulated phosphorylation by HSA and EGF was reduced to $46.13 \pm 6.03\%$ and $41.23 \pm 13.28\%$ that of control condition respectively (**Fig. 5.3**). Pre-incubation with Ro 81-3220 inhibited PDBu induced phosphorylation to $40.06 \pm 15.20\%$ of that seen under control conditions.

5.5 Discussion.

Studies of MegCT phosphorylation in intact cells were hindered by its low endogenous expression levels and enormous size of megalin. The method of cleavage of the extracellular domain of megalin prior to immunoprecipitation of the

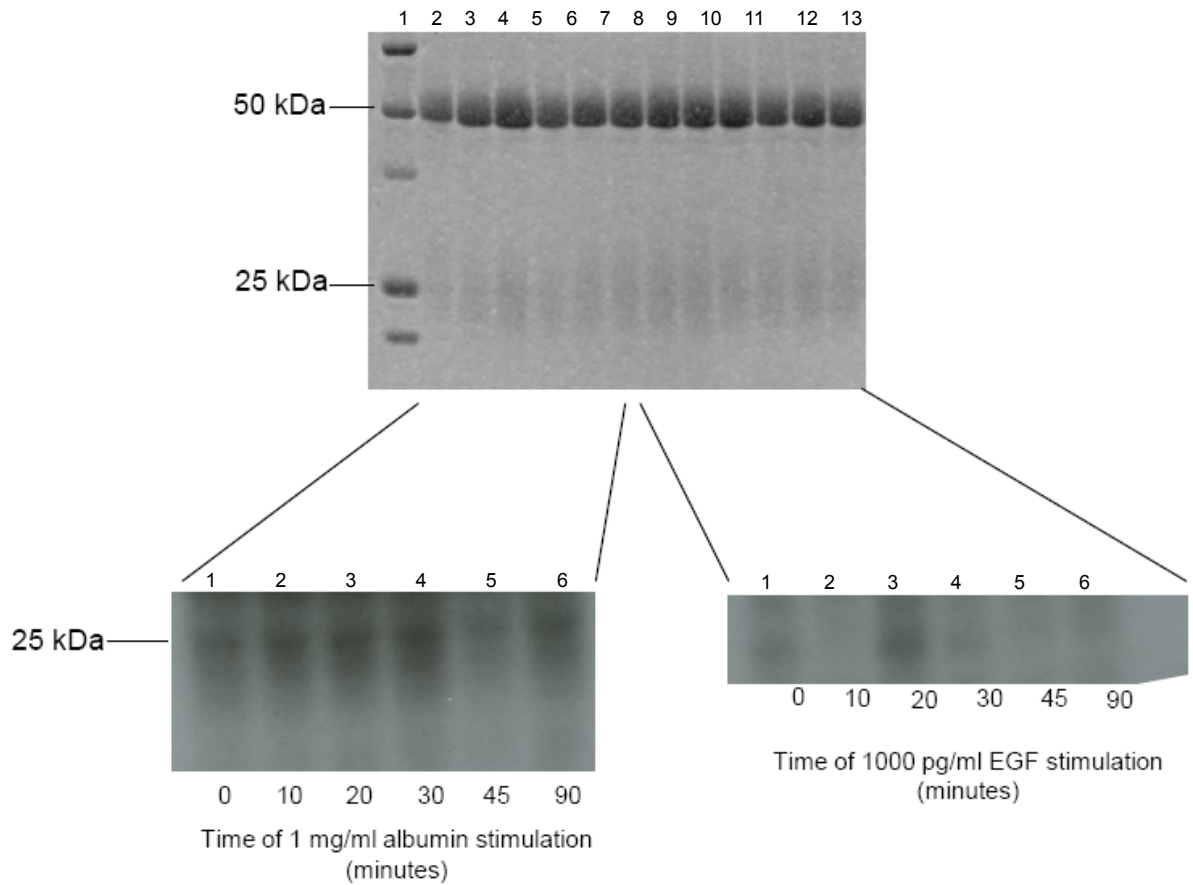


Figure 5.2 Time course of EGF and human serum albumin stimulated phosphorylation of the meg-CT in intact cells. hPTC were loaded with [³²P]-orthophosphate and stimulated for the time points shown. The extracellular portion of megalin was cleaved by light trypsinisation on ice and the cytoplasmic tail of megalin immunoprecipitated. Immunoprecipitates were resolved by PAGE, the gels stained, dried and exposed to autoradiograph film. The experiment was performed once only and the corresponding Coomassie stained gel is shown as evidence of equal protein loading.

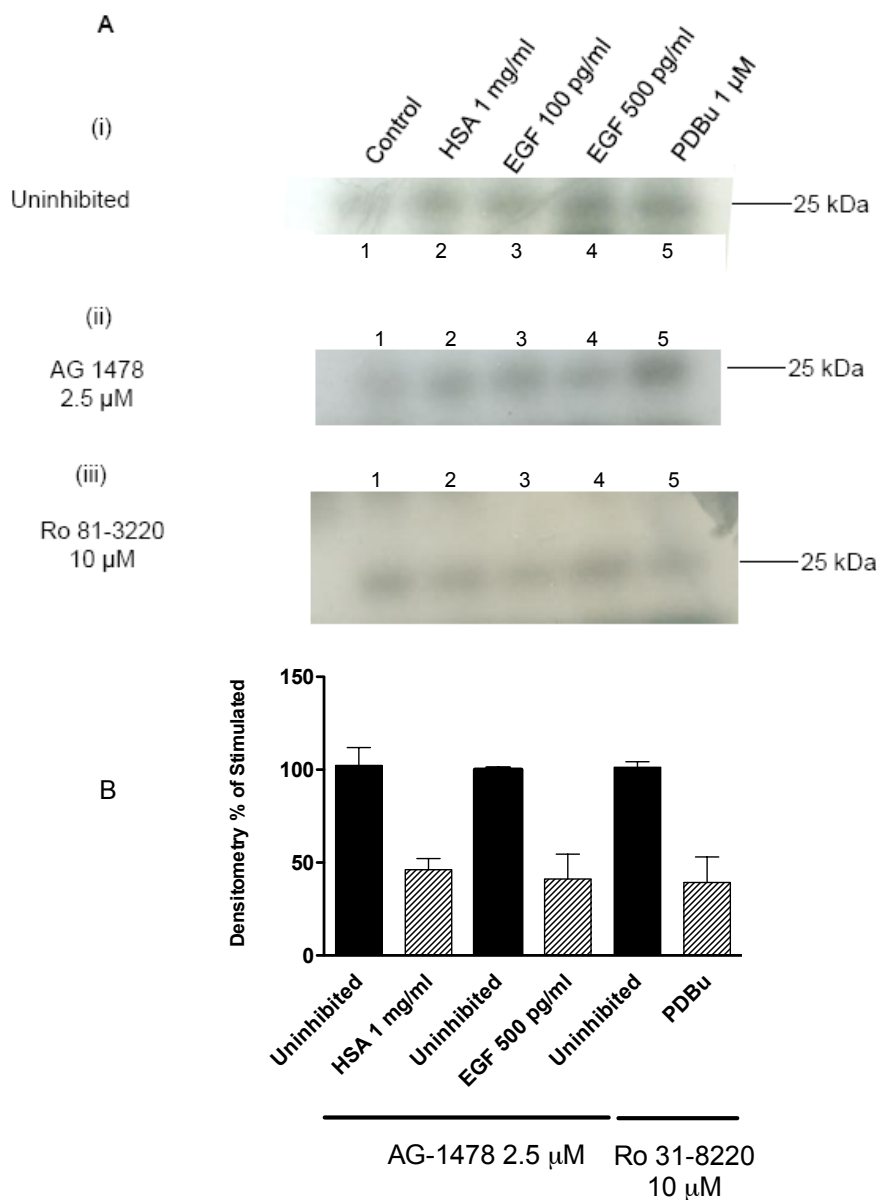


Figure 5.3 Effect of protein kinase inhibitors of meg-CT phosphorylation. hPTC were loaded with [32 P]-orthophosphate and pre-incubated with or without protein kinase inhibitors. **A (i-iii).** Autoradiographs showing agonist stimulated phosphorylation under uninhibited and inhibited conditions. **B.** Densitometric analysis in which uninhibited stimulation is normalised to 100% and inhibited stimulation expressed as a percentage of that. Data shown mean \pm SEM, n =3. *p \leq 0.05.

MegCT introduced a delay which despite the presence of phosphatase inhibitors could have altered the phosphorylation status of MegCT. In combination, these problems along with the large amount of radioactivity needed rendered the experiments technically challenging.

Despite these caveats, in comparison with the data obtained using the MegCT-GST fusion protein an identical pattern of megalin phosphorylation in response to albumin, EGF and PDBu was seen with the same susceptibility to kinase inhibition. The MegCT phosphorylation in response to EGF was variable between experiments when using intact cells. This may reflect either less phosphorylation or variable expression of megalin. Another explanation may be the technical problems associated with immunoprecipitation resulting in rapid dephosphorylation. A further consideration may be that in PTC the EGF-R is largely restricted to the basolateral surface of the PTC with only 10% expressed at the apical surface (Gesualdo et al., 1996) although this ratio is increased under proteinuric conditions. Megalin is largely apically restricted and therefore the two receptors are in distinct subcellular locations. Stimulation *in vitro* will not be affected by this as much as megalin phosphorylation in intact cells and the kinase activity will appear more robust.

The studies demonstrating basolateral restriction of the EGF-R were performed by immunohistochemistry of biopsy specimens (Gesualdo et al., 1996). Therefore, it remains unknown how dynamic the process of redistribution of EGF-R from the basolateral to apical surface may be under proteinuric conditions. This is important in considering the dependence of albumin stimulated MegCT phosphorylation to on the EGF-R.

The possibilities are that albumin signals through the 10% of EGF-R that is apically restricted and/or stimulates a rapid redistribution from the basolateral to the apical cell surface. Potentially this could be investigated by real time imaging of live cells transfected with a fluorescently labeled EGF-R. Transcytosis of intact albumin across the cell from the apical surface has never been demonstrated and this would seem to be an unlikely mechanism by which albumin could stimulate the basolateral EGF-R.

The published literature does not indicate the mechanism by which albumin stimulates the EGF-R (Reich et al., 2005, Lee and Han, 2008). In these studies the functional effects of albumin on PTC were not only dependent on the EGF-R but also the cellular kinase Src. Whether the dependence on Src is up- or downstream of the EGF-R is not established. Bearing in mind that a number of tissues expressing the EGF-R that are exposed to albumin with no published reports of a signaling effect, it seems unlikely that there is a straightforward ligand-receptor interaction between the albumin and the EGF-R.

Perhaps the likeliest mechanism leading to EGF-R activation is that albumin exposure increases production of ROS which could diffuse from intracellular compartments to the basolaterally restricted EGF-R. Albumin stimulated EGF-R activation and downstream MegCT phosphorylation warrants further investigation as a pathway that may be susceptible to pharmacological intervention.

In summary, this chapter indicates concordant findings between constitutive and stimulated phosphorylation of MegCT in intact cells and the previously discussed Meg-CT-GST fusion protein. The technical challenges of studying MegCT phosphorylation in intact cells were considerable. A chimaeric protein that enabled

overexpression of MegCT was developed to overcome these problems, and these studies are described in the following chapter.

6 Development and Phosphorylation of a MegCT-CD8 Chimaeric Protein.

6.1 Introduction.

Studies of megalin in intact cells were hampered by the low native expression of megalin and difficulties in experimentally manipulating such a large molecule. To circumvent these twin problems an alternative approach was sought that would enable overexpression of the MegCT. Other groups faced with these problems have developed truncated forms of megalin (by removing portions of the extracellular domain) and used such mini-megalin receptors to investigate megalin's cellular trafficking and to introduce specific point mutations (Marzolo et al., 2003, Yuseff et al., 2007). The investigations described later in this thesis specifically related to MegCT and in order to exclude phosphorylation occurring at sites on the extracellular domain of megalin a chimaeric protein containing MegCT and CD8 was developed. CD8 was used as the extracellular and transmembrane vehicle for MegCT as when used previously as part of chimaeric proteins it has not affected protein trafficking of its attached moiety i.e. it acts as a neutral reporter (Ihrke et al., 2000). The ability of CD8 to act as a neutral reporter was important as the correct cellular trafficking and physiological function of megalin are crucially related.

6.2 Strategy for the development of a MegCT-CD8 chimaeric protein.

The strategy for the development of a MegCT-CD8 chimaeric protein is outlined in **Fig. 6.1**. Oligonucleotide primers were designed so that MegCT and CD8 cDNA could be amplified from appropriate expression vectors whilst introducing recognition sequences for digestion by restriction endonucleases that would not digest at sites other than the termini of the cDNA. Following digestion with appropriate restriction endonucleases cohesive ended DNA would be created that would ligate with a complementary sequence of cDNA (**Fig. 6.2**). It was anticipated that during a reaction catalysed by DNA T4 ligase the DNA fragments would assemble as in **Fig 6.1** to form a circularised piece of DNA.

Many variations on the above strategy were developed which are described in the results section below and summarised in **Table 6.1**. Details regarding the PCR primers used are given in **Table 6.2**.

6.3 Aims.

The aims of this work were to:

- Develop a megCT-CD8 chimaeric protein that could be overexpressed in OK cells.
- To study the subcellular distribution of a MegCT-CD8 chimaeric protein.
- Determine whether a MegCT-CD8 chimaeric protein is phosphorylated.

6.4 Methods.

6.4.1 Primer design and conditions for the PCR.

Primers were synthesised by Invitrogen (Paisley, UK) and were designed to introduce restriction endonuclease sites within the cDNA whilst providing sufficient bases at the ends of the generated cDNA to enable each restriction enzyme to function efficiently. Primers were designed using Oligo Perfect™ Designer software provided by Invitrogen.

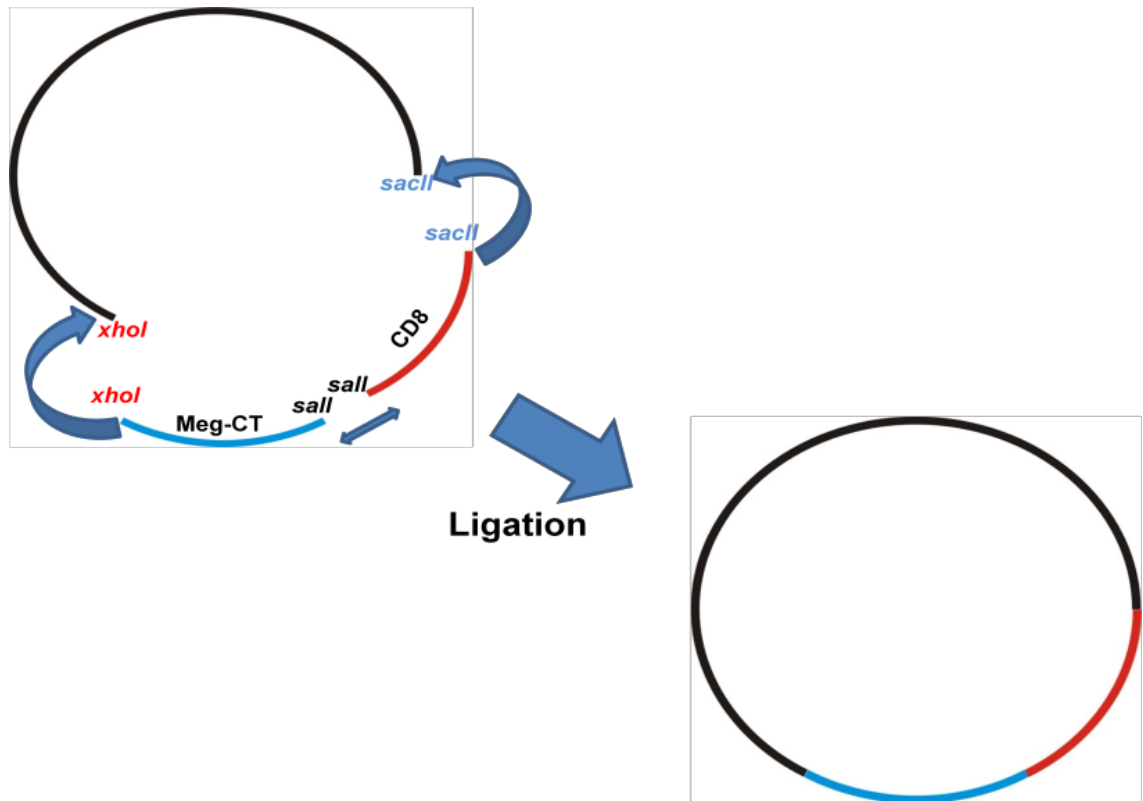


Figure 6.1. Scheme for generating a circular plasmid containing the cDNA that will encode a MegCT-CD8 chimeric protein. A circular plasmid capable of bacterial transfection is generated by a series of ligation reactions between cohesive ended cDNA. The approaches used to achieve this are detailed within the text.

5' GGGGTCGACCACTATAGAAGGACC....GAAGACTCT....
 3' CCCCAGCTGGTGATATCTTCCTGG....CTTCTGAGA....

...GAAGTATAGCTCGAGAAA3'
 ...CTTCATATCGAGCTCTTT5'



SacII

5' GGGG TCGACCACTATAGAAGGACC....GAAGACTCT....
 3' CCCCAGCT GGTGATATCTTCCTGG....CTTCTGAGA....

...GAAGTATAGC TCGAGAAA3'
 ...CTTCATATCGAGCT CTTT5'

Figure 6.2. Generation of cohesive ended DNA following a *SacII* and *XhoI* digestion of MegCT cDNA. The 5' and 3' overhang of the MegCT cDNA produced by PCR is shown in black, the introduced restriction endonuclease sites in red and the coding region in blue. Following restriction endonuclease digestion a four base pair overhang is created at both ends of the MegCT cDNA. In a reaction catalysed by DNA T4 ligase this will join with complementary appropriately digested DNA – either a pre-digested vector or linear segment of DNA. The efficiency of the restriction endonuclease digestion is dependent on the region shown in black to be of a sufficient length to act as a platform for enzyme activity.

Table 6.1. A summary of strategies used for the development of a MegCT-CD8 chimaeric protein.

<u>Vector</u>	<u>Pre-existing insert.</u>	<u>Cloning or expression vector.</u>	<u>Insert(s) for ligation.</u>	<u>Source of DNA fragment for ligation.</u>	<u>RE sites ligated between.</u>	<u>Rationale of method.</u>	<u>Successful/Unsuccessful</u>
<u>pCMV-script</u>	Nil	Expression	CD8 and MegCT	PCR amplification from BSII SK-CD8 and pGEX-4T1-MegCT	<i>sacII/xhoI</i>	Anticipated to be the most straightforward method	Unsuccessful
<u>pCMV-script</u>	Nil	Expression	CD8 and MegCT pre-ligated at <i>sacII</i> site	As above. DNA fragments purified, <i>sacII</i> digested and ligated	<i>sacII/xhoI</i>	Less risk of concatamer formation	Unsuccessful
<u>BSII SKI-CD8</u>	CD8	Cloning	MegCT	PCR amplification from pGEX-4T1-MegCT	<i>afIII/notI</i>	Partial digest of MegCT (<i>afIII</i> is a MegCT cutter) would result in a product that could be subcloned into an expression vector	Unsuccessful
<u>pCRII-TOPO</u>	Nil	Cloning	MegCT	PCR amplification (using Taq polymerase) from pGEX-4T1-MegCT	Cloning vector	Digestion and purification would result in a DNA fragment with guaranteed cohesive ends	Successful
<u>pCRII-TOPO</u>	Nil	Cloning	CD8	PCR amplification (using Taq polymerase) from BSII SK-CD8	Cloning vector	Digestion and purification would result in a DNA fragment with guaranteed cohesive ends	Successful
<u>pCMV-script</u>	Nil	Expression	CD8	<i>sacII/sacII</i> digestion of pCRII-TOPO-CD8	<i>sacII/sacII</i>	Start of stepwise approach	Successful
<u>pCMV-script-CD8</u>	CD8	Expression	MegCT	<i>sacII/xhoI</i> digestion of pCRII-TOPO-MegCT	<i>sacII/xhoI</i>	Continuation of stepwise approach	Unsuccessful
<u>pCMV-script-CD8</u>	CD8	Expression	MegCT	<i>sacII/apal</i> digestion of pCRII-TOPO-MegCT	<i>sacII/apal</i>	More base pairs separate the <i>sacII/apal</i> (cf. <i>sacII/xhoI</i>) sites within the MCS of pCMV-script-CD8 resulting in a more efficient digestion	Successful
<u>pEGFP-N1</u>	Nil	Expression	CD8-MegCT	PCR amplification from pCMV-script-CD8-MegCT	<i>xhoI/sacII</i>	Transfection into mammalian cells results in a GFP tagged CD8-MegCT chimaeric protein	Successful

Target	Name of primer	Restriction endonuclease site introduced	Sequence (5' to 3')	Modification introduced by primer	Orientation	T_m (°C)
MegCT	MEG2F	<i>sall</i>	GGGGTCGACCACTATAGAAGGACCGGCTCC	Nil	F	63
MegCT	MEG2R	<i>xhoI</i>	CGGCTCGAGCTATACTTCAGAGTCTTCTTT	Nil	R	57
CD8	CD8F	<i>sacII</i>	GGGCCGCGGGAATTCGGCGGCTCCCGCGCGCCT	Nil	F	73
CD8	CD8R	<i>sall</i>	GGGGTCGACCCGCTTGCACTAAAGGGTGAT	Nil	R	62
MegCT	MEG3F	<i>afIII</i>	GGGCTTAAGCACTATAGAAGGACCGGCTCC	<i>afIII</i> site introduced	F	61
MegCT	MEG3R	<i>notI</i>	GGGGGGGGCGGCCGCGATACTTCAGAGTCTTCTTTAAC	<i>notI</i> site introduced	R	68
CD8	CD82F	<i>sacII</i>	GCGGCGCGGCCGCGGGCCACCATGGCCTTACCAGTGACCGCC	Increased 5' overhang	F	76
CD8	CD82R	<i>sall</i>	GCGGGGCGGGTTCGACCCGCTTGCACTAAAGGGTGAT	Increased 5' overhang	R	68
MegCT	MEG4F	<i>sall</i>	GCGGGGCGGGTTCGACCACTATAGAAGGACCGGCTCC	Increased 5' overhang	F	70
MegCT	MEG4R	<i>xhoI</i>	GCGGGGCGGCTCAGCTATACTTCAGAGTCTTCTTT	Increased 5' overhang	R	63
MegCT	MEGAPAR	<i>apaI</i>	GCGGCGCGGGGCCCTATACTTCAGAGTCTTCTTT	<i>apaI</i> site introduced	R	66
MegCT	MEGGFPR	<i>sacII</i>	GGGGCGGGGGCGGCCGCGTACTTCAGAGTCTTCTTT	Termination signal removed, change of RE	R	68
CD8	CD8GFPF	<i>xhoI</i>	GCGGCGGGCTCGAGGCCACCATGGCCTTA	Change of RE	F	67

Table 6.2. Sequences and properties of primers used for PCR for these studies.

PCR was performed in a total volume of 50 μ l. The components of each reaction were 45 μ l of PCR supermix, forward and reverse primers diluted to a final concentration of 200 nM, 10 pg-1 ng template DNA and made up to a final volume of 50 μ l with DNAase free water. Two different forms of supermix were purchased (Invitrogen, Paisely, UK) and used depending on whether a proof or non-proof reading form of DNA polymerase was required. AccuprimeTM Pfx supermix contains the proof reading Thermococcus species KOD thermostable polymerase (22 U/ml) along with 66 mM Tris-SO₄ (pH 8.4), 30.8 mM (NH₄)₂SO₄, KCl, 1.1mM MgSO₄, 330 μ M dNTP's and AccuprimeTM proteins. Non-proof reading polymerases generate a 5' overhang of the cDNA that was required for ligation into the cloning vector TOPO 2.1. For these reactions PCR Supermix was used. This was comprised of 22 U/ml recombinant Taq DNA polymerase, 22 mM Tris-HCl (pH 8.4), 55 mM KCl, 1.6 mM MgCl₂ and 220 μ M each of dGTP, dATP, dTTP and dCTP.

An MJ Research PTS-200 Peltier Thermal Cycler with a heated lid was used for all reactions. Amplification of samples was performed using an initial denaturation step at 95°C (5 minutes) followed by 30 cycles consisting of denaturing at 95°C for one minute, one minute of primer annealing at 55°C and one minute of nucleotide extension at 72°C. A final elongation step at 72°C for seven minutes was included in all PCR amplifications. Negative controls were performed by replacing template DNA with DNAase free water. If the conditions had previously been ascertained to result in a single PCR product it was purified using a Qiagen PCR purification kit by exactly following the manufacturers instructions. If multiple products were

obtained the band of appropriate size was extracted from an agarose gel and purified.

6.4.2 Separation and Visualisation of DNA products.

DNA was separated using a 1% agarose gel containing 0.5 µg/ml ethidium bromide alongside a DNA ladder. The gel was submerged under TAE buffer containing 0.5 µg/ml ethidium bromide. Bands were visualised and photographed over ultraviolet illumination.

6.4.3 Gel Extraction of DNA bands.

Relevant DNA bands were excised from the agarose gel and purified using a Qiagen Gel Extraction kit following precisely the manufacturers instructions. Purified DNA was collected and suspended in DNAase free water. The approximate concentration of purified DNA was estimated by comparison with known amount of DNA ladder separated on a 1% agarose gel containing 0.5 µg/ml ethidium bromide or by spectrometry.

6.4.4 Restriction endonuclease digestion of DNA.

DNA digestion by restriction endonucleases was performed in a final volume of 10 µl or 20 µl. The temperature, duration and buffer of each digestion varied depending on the enzymes used and these are charted below. Digested DNA was purified using a QIAgen Reaction cleanup kit. This kit salvages all DNA that is greater than 70 base pairs in length. So, following plasmid digestion when the unwanted fragment was larger than that, the reaction products were purified by

agarose gel electrophoresis and subsequent gel extraction. Purified DNA was collected into DNAase free water.

<u>Restriction enzyme</u>	<u>Buffer</u>	<u>BSA added</u>	<u>Temp. of incubation (°C)</u>	<u>Time of incubation. (mins)</u>
SacII	NEB4	Yes	37	60
Sall	Sall specific buffer	Yes	37	60
XhoI	NEB3	Yes	37	60
Sall/XhoI	NEB3	Yes	37	60
AflII/HindIII	NEB2	Yes	37	60
AflII/NotI	NEB4	Yes	37	60
AflII	NEB2	Yes	37	30
NotI	NEB5	Yes	37	60
EcoRI/XhoI	NEB4	Yes	37	60
SacII/XhoI	NEB2	Yes	37	120
ApaI	NEB2	Yes	25	60
SacII/Sall		Performed sequentially		
Sall/ApaI		Performed sequentially		

6.4.5 Ligation of DNA fragments.

Three different methods were used to successfully ligate DNA fragments into expression or cloning vectors. Common details are outlined below, and the precise conditions described in the results section.

6.4.5.1.1 The 16 hour duration T4 DNA ligation.

Ligation reactions took place in a total volume of 20 µl. The components of which were assembled on ice and consisted of varying volumes of vector and insert, 2 µl of T4 ligase buffer (New England Biolabs). The concentration of the DNA

fragments was estimated by comparison to a known standard on an agarose gel containing ethidium bromide. The amount in ng of each component to be used was calculated using the formula below. In general the molar ratio of insert to vector was three.

$$ng\ of\ insert = \frac{ng\ of\ vector \times kb\ size\ of\ insert}{kb\ size\ of\ vector} \times molar\ ratio\ \frac{insert}{vector}$$

The reaction was catalysed by the addition of 400 units of T4 DNA ligase and proceeded at 16°C for 14 hours. A proportion of the ligation mixture was used directly for the transfection of DH5α *E. Coli* as described previously in this chapter.

6.4.5.1.2 *The five minute T4 DNA ligation.*

Due to suspected problems with the T4 DNA ligase used in the reactions described above an alternative supplier and method was sought. In a reaction volume of 20 μl were mixed vector and DNA, the concentrations of which had been estimated using the approach described previously. To 30 fmoles of vector were added 90 fmoles of insert, the mass of DNA required was calculated from the formula;

$$\mu g\ DNA = f mol. DNA \times \frac{1\ \mu g}{3000\ f mol.} \times \frac{size\ of\ DNA\ in\ bp}{1000\ bp}$$

The reaction was catalysed by the addition of 1 unit of T4 DNA ligase and the reaction allowed to proceed at room temperature for five minutes in T4 ligase buffer (Invitrogen). Two μl of the ligation reaction was used to transfect competent DH5α *E. Coli*. as described previously.

6.4.5.1.3 *The TOPO TA cloning kit.*

The TOPO TA cloning kit enables the ligation of freshly produced PCR products into the cloning vector TOPO 2.1 (Appendix B. **Fig. 10.5**). Propagation of the freshly prepared PCR product – flanked by the introduced restriction enzyme sites - in a cloning vector had one major advantage. Following appropriate restriction endonuclease digestion and subsequent purification there was a high probability of producing cohesive ended DNA.

Taq polymerase adds a single deoxyadenosine residue to the 3' end of PCR products. The linearised vector supplied in the TOPO TA cloning kit has a overhanging 3' deoxythymidine residue. In the presence of topoisomerase the PCR product is ligated efficiently within the cloning vector.

The TOPO cloning reaction was performed following the manufacturer's instructions. Each reaction took place in a final volume of 6 µl and consisted of 1 µl each of fresh PCR product, salt solution (1M NaCl, 0.06M MgCl₂) and plasmid, along with 3 µl of sterile water. Each reaction proceeded for 5 minutes at room temperature.

Circular plasmid DNA was propagated by transfecting Mach1-T1 *E. Coli* and ultimately plasmid DNA isolated as described previously.

6.4.6 *DNA sequencing.*

DNA sequencing was performed by the Protein and Nucleic Acid Laboratory at the University of Leicester.

6.4.7 *Transfection MegCT-CD8 Chimaeric construct into OK cells.*

6.4.7.1 Transient transfection.

Transient expression of the CD8-MegCT chimaera within OK cells was achieved using the polyanionic transfection reagent Fugene 6. On the day prior to transfection OK cells were plated out at a density of 150,000 cells/well of a 6 well plate in culture media devoid of antibiotics. On the day of transfection exponentially growing OK cells were between 50 and 60% confluent. Fugene 6 was used exactly as per manufacturer's protocol. To each well was added 1µg of chimaeric cDNA and 3µl of fugene 6 transfection reagent which had been diluted with 97µl of serum free/antibiotic free DMEM F12. To achieve uniform transfection across each well the transfection mixture was added dropwise.

Cells were grown to confluence without a change in media. Typically this was achieved within 24 hours. Following which the cells were incubated in serum free DMEM F12 prior to experimentation.

6.4.7.2 Stable transfection.

To establish cell lines stably expressing the CD8-MegCT chimaeric construct the same procedure as described in the above section was followed. 48 hours after transfection cells were harvested using trypsin/EDTA, diluted 1 in 10 and grown in DMEM F12 culture media supplemented with 300µg/ml G418. Individual colonies of G418 resistant cells were amplified separately and screened for expression of the chimearic protein.

6.4.8 Visualisation of OK cells transiently transfected with MegCT-CD8 chimaeric protein.

To determine whether transiently expressed MegCT-CD8 was associated with the plasma membrane indirect immunohistochemistry and confocal microscopy was performed. OK cells were grown on glass coverslips and transiently transfected as described previously. Cells were allowed to grow to about 50% confluence with the anticipation that single cells would be visible on the coverslip. Monolayers of cells were fixed in 2% paraformaldehyde in PBS, pH 7.4 for 2 minutes followed by two 10 minutes washes with PBS pH 7.4. Fixed cells were permeabilised by incubating with PBS, pH 7.4 containing 0.05% Triton-100. Non-specific protein binding was blocked by a one hour incubation at room temperature with PBS-0.05% Triton 100, pH 7.4 containing 10% goat serum. Cells were labelled by incubating with a polyclonal goat anti-CD8 antibody diluted 1:100 in PBS-0.05% Triton 100, pH 7.4 at 4°C overnight. Non-bound antibody was removed by three 10 minute washes with PBS pH 7.4. A FITC labelled rabbit anti-goat secondary antibody was diluted 1 in 200 in PBS pH 7.4, containing 10% goat serum and added for one hour at room temperature. Following two final washes with PBS pH 7.4 labelled cells on coverslips were mounted on glass slides with citifluor AF1 mountant.

Images were collected using a Laser Scanning Confocal Microscope (Olympus Fluoview 300) with either the x40 or the x60 oil immersion objective at a scan resolution of 1024 x 1024 pixels. Three dimensional reconstructions were obtained by collecting a series of 12-29 images in a z-series with a slice thickness of 0.5-1.0 microns. Using Olympus Fluoview software the images were reconstructed from

each z-series, rotated around a closed axis and saved in AVI format for simple visualisation.

6.4.9 Phosphorylation of MegCT-CD8 Transiently expressed in OK Cells.

OK cells transiently expressing MegCT-CD8 were loaded with [³²P]-orthophosphate and stimulated with agonists exactly as described in section **5.2.1**. Following cell monolayer lysis the MegCT-CD8 chimaeric protein was immunoprecipitated using antisera directed against an epitope in the extracellular region of CD8. Immunoprecipitates were treated exactly as described previously.

6.5 Results.

6.5.1 Propagation of pGEX-4T1-MegCT.

To confirm the vector pGEX-4T1-MegCT still contained MegCT cDNA between the *EcoRI* and *XhoI* sites of the MCS a test digest was performed. A 2 µg aliquot of plasmid DNA was subjected to digestion with 10 units each of *EcoRI* and *XhoI*. The products of the reaction were separated on an ethidium bromide stained agarose gel and the results shown in **Fig 6.3**. Two products were obtained. A larger band that runs alongside the 5 kb DNA marker is consistent with the linearised pGEX-4T1, whereas the 600 bp fragment represents the excised MegCT cDNA. This confirmed that the pGEX-4T1-MegCT was a suitable template from which to expand the MegCT cDNA using PCR.

6.5.2 Propagation of pBS SKII-CD8.

The plasmid DNA supplied to us contained wild type CD8 cDNA ligated between the *HindIII* and *AflIII* sites of the MCS of pBS-SKII. To confirm the continued presence of the insert in the harvested plasmid DNA a test digest was performed. A 2 µg aliquot of plasmid DNA was subject to digestion with 10 units of *AflIII* and *HindIII*. The products of the reaction were separated on an ethidium bromide stained agarose gel and the results shown in **Fig 6.4**. Lanes 2 and 4 represents a test digest on the plasmid DNA as supplied or following a maxi-prep respectively. In both digests a 800 bp DNA fragment of the CD8 cDNA is liberated by the reaction.

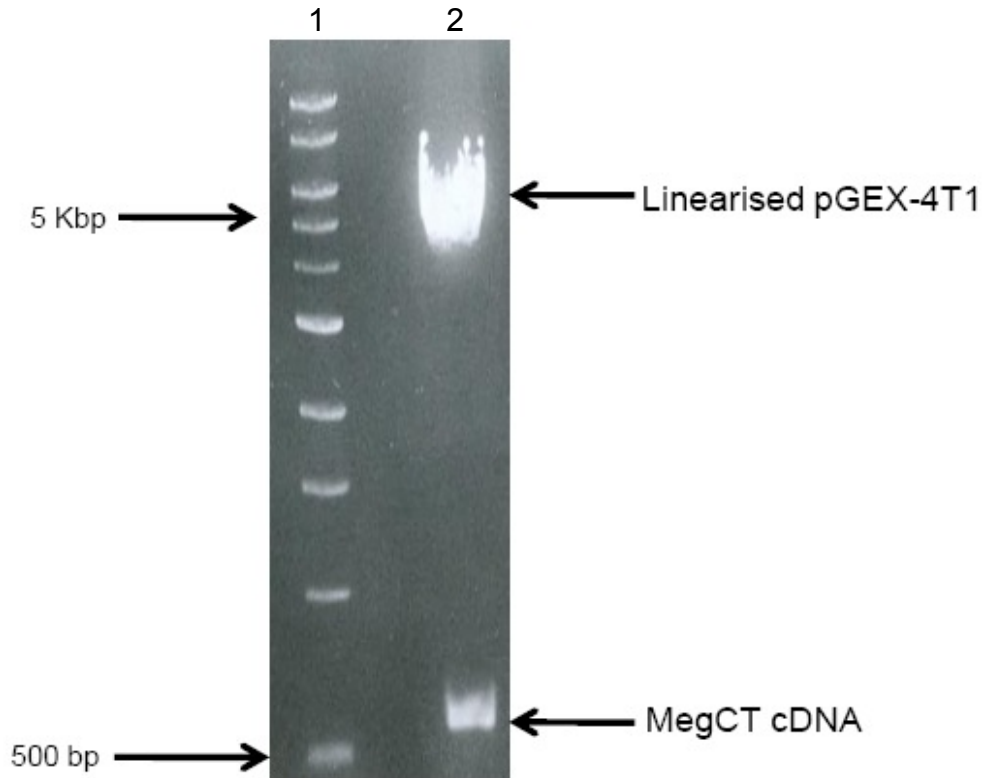


Figure 6.3 MegCT insert is present in pGEX-4T1-MegCT. pGEX-4T1-MegCT was digested with *EcoRI* and *XhoI*. Digest products were applied to a 1% agarose gel containing 0.5 $\mu\text{g/ml}$ ethidium bromide and separated by electrophoresis. Bands were visualised and photographed over UV light. Two products of the enzyme digestion are seen; the upper band at 4.9 kbp is the linearised pGEX-4T1 whilst the lower 600 bp fragment represents the MegCT cDNA.

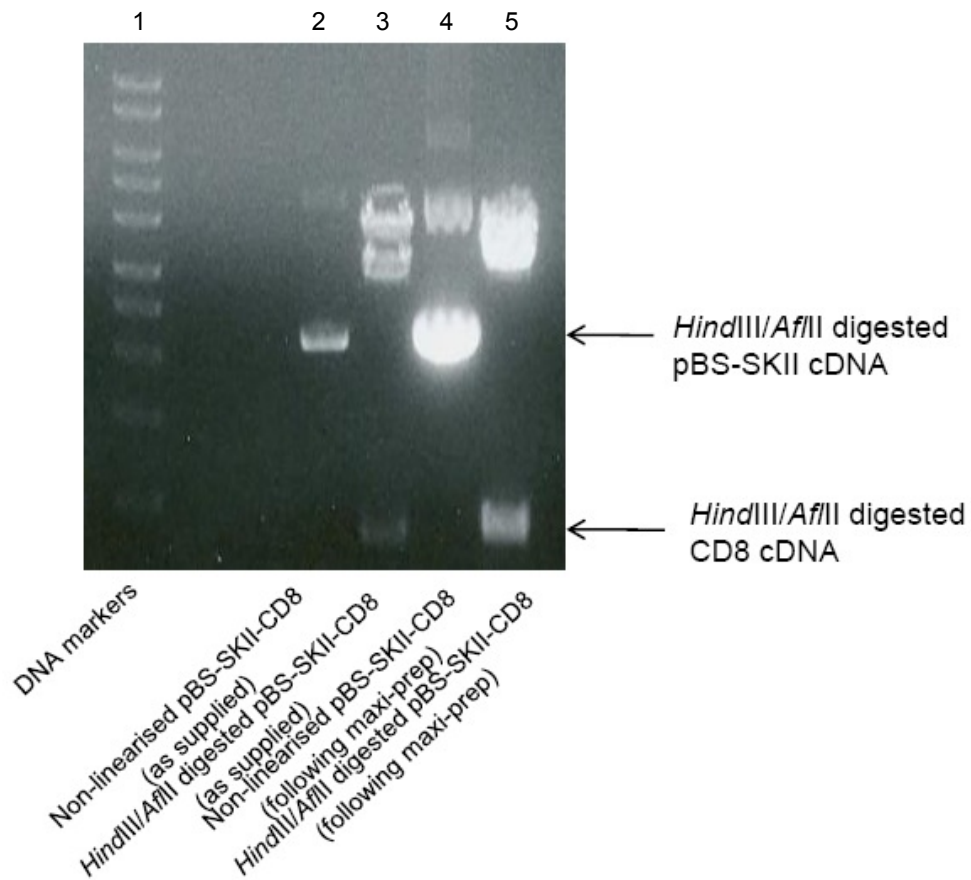


Figure 6.4 A *HindIII/AflIII* digest of BS-SKII-CD8 verifies presence of CD8 cDNA. Restriction enzyme digests were performed on BS-SKII-CD8 as supplied or following a large scale plasmid production. Plasmid DNA were digested with *HindIII* and *AflIII*. Also shown are the products of the same reaction without either restriction enzyme. Non-digestion has resulted in multiple bands consistent with the presence of supercoiled plasmid whereas digestion liberates a 800 bp fragment consistent with CD8 cDNA.

In lane 3 multiple bands are present of around 4 kb in size, whereas in lane 5 a single band is present. In lanes 2 and 4 no restriction enzymes were included in the reaction and as a result the plasmid DNA was non-linearised and no insert DNA was seen. Having confirmed the presence of the DNA insert the plasmid was used as a template for PCR leading to the expansion of CD8 cDNA.

6.5.3 Amplification of MegCT cDNA by PCR from pGEX-4T1-MegCT.

The initial strategy to develop the chimaeric CD8-MegCT protein is depicted in **Fig 6.1**. Therefore, MegCT cDNA was expanded from pGEX-4T1-MegCT using primers that incorporated *Sall* and *XhoI* restriction enzyme recognition sequences at the 5' and 3' termini respectively.

The results of amplification of MegCT cDNA using primers at a concentration of 0.1, 1 and 10 μ M are seen in **Fig 6.5**. All three conditions resulted in a broadly equivalent amount of MegCT cDNA being generated. There is a single band visible that indicated that the reaction conditions were optimal (**Fig 6.5**).

In all PCR experiments henceforth an appropriate negative control of exactly the same PCR conditions without the plasmid DNA being added. In all experiments no PCR product was formed under these conditions.

6.5.4 Amplification of CD8 cDNA from BS-SKII-CD8 using PCR.

Primers were designed to introduce *SacII* and *Sall* restriction endonuclease recognition sequences into the CD8 cDNA PCR product. **Figure 6.6 (panel A)** shows the products of a PCR reaction. Despite optimising conditions multiple bands were seen representing multiple PCR products.

To produce a single product a different PCR mix was used – Accuprime Supermix. A single PCR product was seen which is consistent with the estimated size of CD8 cDNA of approximately 800 bp (**Fig. 6.6 (panel B)**).

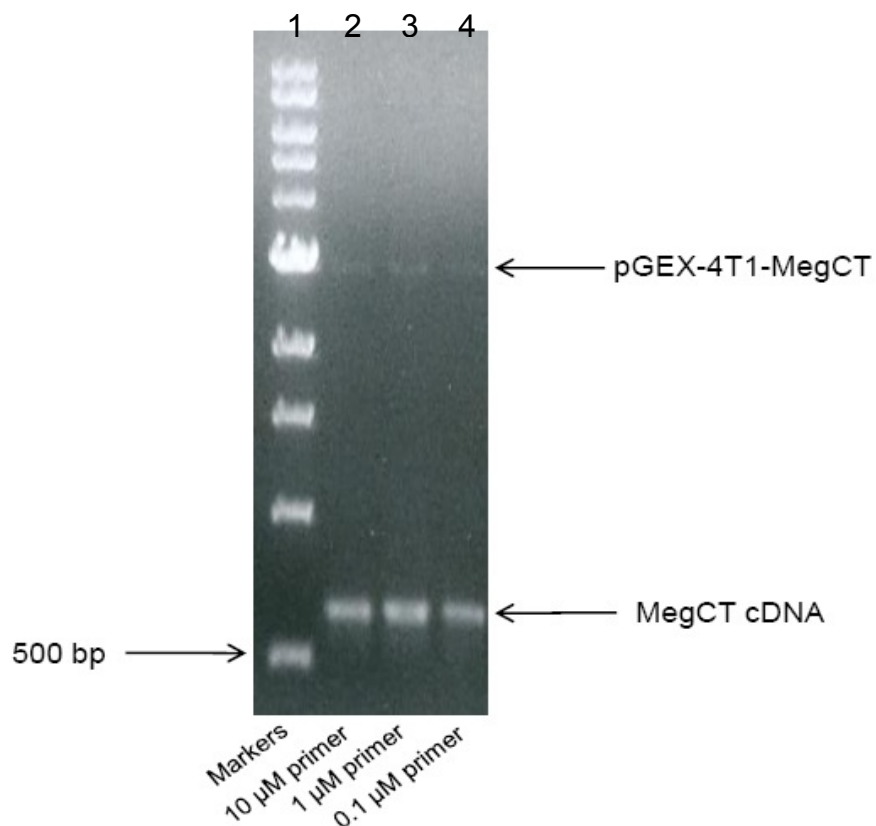


Figure 6.5. Amplification of MegCT cDNA from pGEX-4T1-MegCT by PCR. PCR reactions were performed using primer (MEG2F and MEG2R) at concentrations of 10, 1 and 0.1 μ M. Each condition resulted in a good yield of PCR product that is running just above the 500 bp marker. Each band was excised from the agarose gel, purified and the product of all three reactions combined.

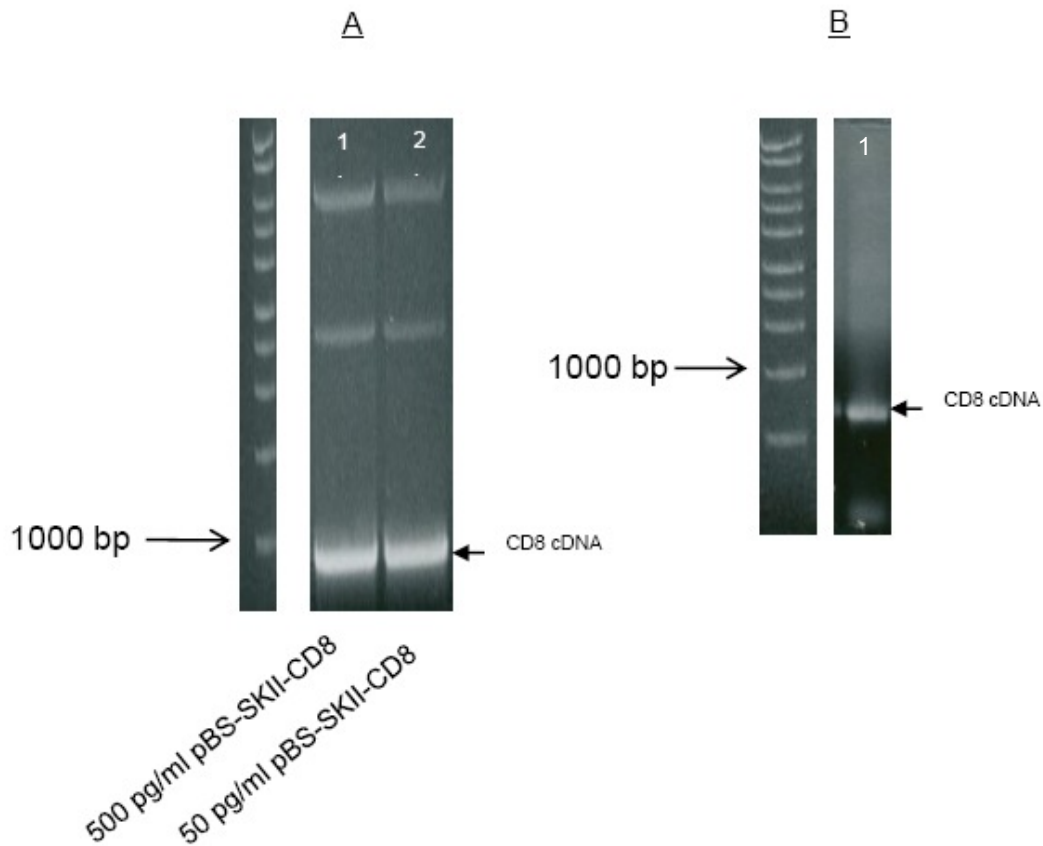


Figure 6.6. CD8 cDNA is amplified by PCR from BS-SKII-CD8 and optimisation of conditions results in a single PCR product. PCR reactions were performed using PCR Supermix™ with *Taq* polymerase (A) or Accuprime™ supermix with *Pfx* polymerase (B). Multiple non-specific bands are seen in panel A. In contrast, the greater affinity offered by the Accuprime™ supermix results in a greater yield of a single PCR product. The faint band at the bottom is created by free nucleotides.

6.5.5 Subcloning of CD8 and MegCT cDNA into *SacII/XhoI* digested pCMV-Script.

A 5 μ l aliquot of pCMV-Script (1mg/ml) was digested with *SacII* and *XhoI* to produce cohesive ended DNA that was anticipated to ligate with appropriately digested CD8 and MegCT cDNA. DNA fragments were separated by agarose gel electrophoresis (**Fig. 6.7**). Two fragments were obtained. A heavier 4.3 kb fragment consistent with linearised *SacII/XhoI* digested pCMV-Script and a small 60 bp region removed from the MCS of pCMV-Script. The heavier fragment was excised from the gel, purified and resuspended in 30 μ l of sterile water. To prove complete digestion of the vector had occurred a 5 μ l aliquot of purified *SacII/XhoI* digested pCMV-Script was incubated with T4 DNA ligase as described in 6.4.5.1 and the products used to transfect DH5 α as described in 2.2.7. No colonies were formed indicating that linearised vector failed to recircularise and confer ampicillin resistance on the bacteria. In all ligation reactions described in this chapter an identical reaction to that described above was used as a negative control.

DNA fragments were estimated by comparison with a known mass of DNA marker (**Fig 6.8**). A DNA ladder was diluted such that each marker contained 100 ng of DNA. By comparison it was estimated that the approximate amounts of cDNA were 100 ng/5 μ l of purified *SacII/XhoI* digested pCMV-Script, 50 ng/5 μ l *SacII/SalI* digested CD8 and 25 ng/5 μ l *SalI/XhoI* digested MegCT. Four different ligation reactions were setup in which the molar ratios of vector:insert DNA varied between 1 and 4. The volume of each purified DNA fragment added to each reaction was as shown below.



Figure 6.7. A *SacII* and *XhoI* digest of pCMV-Script results in a 4.3 kb linearised DNA fragment. pCMV-Script was digested with *SacII* and *XhoI*. Reaction products were separated by agarose gel electrophoresis and the gel photographed. Two products of the restriction endonuclease digest are seen. The upper band is the c.4.3 kb linearised pCMV-Script whilst the lower bands size is difficult to estimate, it lies below the lowest 200 bp marker and is compatible with the 60 bp fragment anticipated from the digest. The upper band was excised from the gel and purified. A small aliquot of purified DNA was subject to a ligation reaction, the products of which failed to transform competent DH5 α *E.Coli* . This confirmed complete digestion had occurred and that the two ends of the digested DNA were non-cohesive

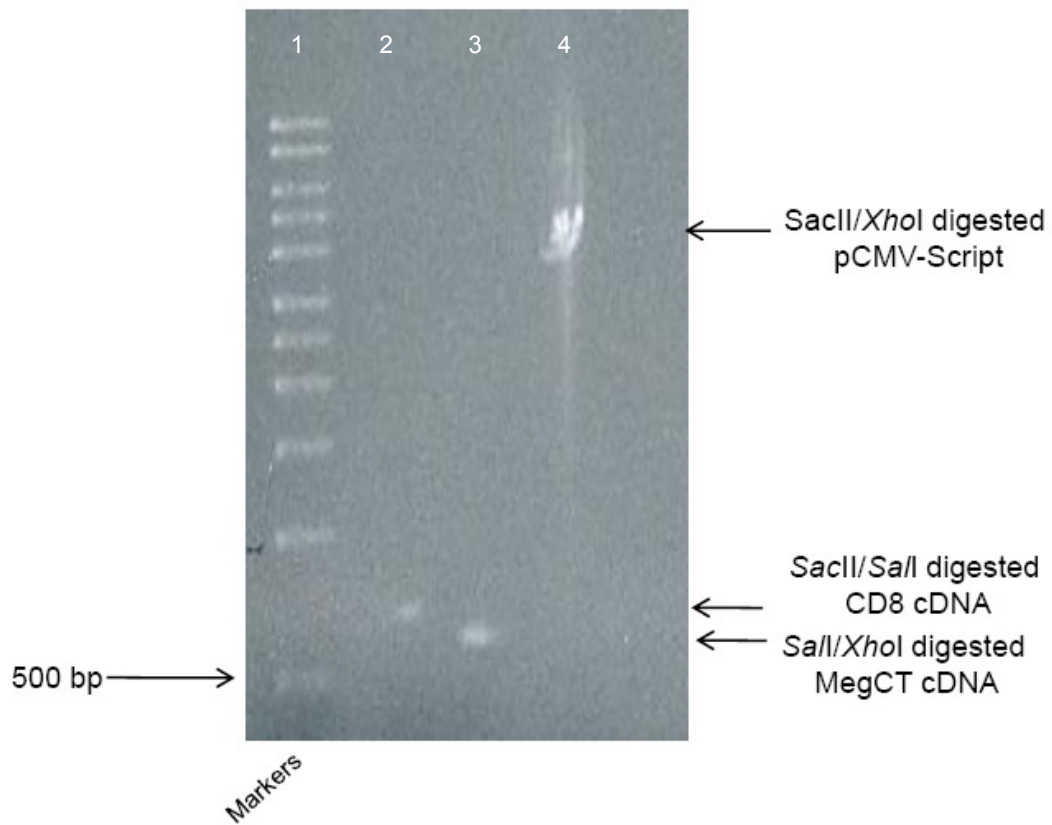


Figure 6.8. Pre-ligation quantification of DNA fragments by comparison with DNA ladder standard. Each DNA band of the ladder shown contains 100 ng of DNA. By visual comparison it was estimated that 25 ng/5 μ l of MegCT cDNA, 50 ng/5 μ l of CD8 cDNA and 100 ng/5 μ l of linearised pCMV-Script were present. A number of ligation reactions were performed with the components informed by this estimation.

<u>Molar ratio of insert:vector in ligation reaction</u>	<u>pCMV-Script (μl)</u>	<u>CD8 (μl)</u>	<u>MegCT (μl)</u>
1:1	1	0.6	0.4
2:1	1	1.1	0.7
3:1	1	1.7	1.1
4:1	1	2.2	1.5

Following a 16 hour ligation reaction the products of which were used for a bacterial transformation, the failure of individual colonies of DH5α cells to grow indicated that the vector had not re-circularised and bacteria remained ampicillin sensitive. As a control pCMV-script was singularly digested with *SaII*, purified and re-ligated under the same conditions as above. T4 ligase was active as colonies of ampicillin resistant bacteria grew after transfection. In all future ligations this reaction was used as the positive control for T4 activity.

6.5.6 *SaII* digestion of MegCT and CD8 and ligation.

For the approach described in the section above three separate successful ligation reactions were required for the formation of circularised plasmid. There was the potential for concatamer formation, where, for example two *SacII* digested CD8 cDNA fragments may ligate thereby reducing the probability of successful ligation with *SacII* digested pCMV. Therefore, a second approach was used in which CD8 and MegCT cDNA were ligated at the *SaII* site. It was anticipated that a second ligation reaction would then be set up to subclone the entire CD8-MegCT cDNA fragment into *SacII/XhoI* digested pCMV-script.

SaII digested CD8 and MegCT cDNA were ligated using a 16 hour ligation reaction. The products were visualised on an ethidium bromide stained agarose

gel (**Fig 6.9 A**). A 1.4 kb DNA fragment was seen which was consistent with the expected size of the CD8-MegCT cDNA fragment. This was excised and purified from the agarose gel.

A 5 µl aliquot of *SacII/XhoI* digested pCMV and *SacII/XhoI* digested CD8-MegCT were compared on an ethidium bromide stained agarose gel (**Fig.6.9 B**). By comparison with a known amount of marker it was estimated that 50 ng/5 µl of *SacII/XhoI* digested pCMV and 10 ng/5 µl of *SacII/XhoI* digested CD8-MegCT were present.

Ligation reactions were setup to differ in the molar ratio of insert to vector and the components of each reaction were as follows.

<u>Molar ratio of insert to vector</u>	<u>pCMV (µl)</u>	<u>CD8-MegCT (µl)</u>	<u>T4 ligase (µl)</u>	<u>T4 buffer (µl)</u>	<u>DNAase free water (µl)</u>
1:1	0.5	1.6	1	1	5.9
2:1	0.5	3.2	1	1	4.2
3:1	0.5	4.8	1	1	2.7
4:1	0.5	6.5	1	1	1

Of each ligation reaction 2 µl were taken to transfect chemically competent DH5α bacteria as described previously. No colonies were formed indicating a failure of circularised plasmid to form.

6.5.7 Attempted ligation of NotI/AflII digested MegCT cDNA into NotI/AflII digested BS-SKII-CD8.

A strategy was developed that would enable ligation of *NotI/AflII* digested MegCT into BS-SKII-CD8 as it had been supplied. An anticipated pitfall to this approach was that the MegCT cDNA contained an *AflII* restriction endonuclease recognition site

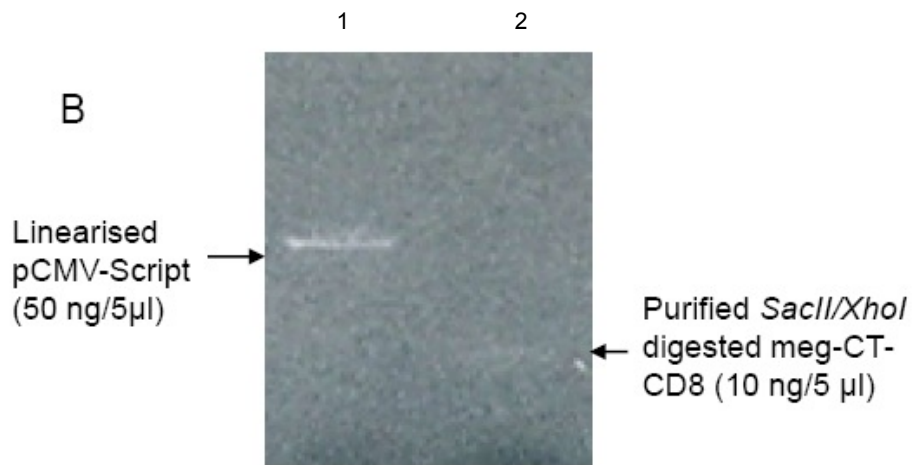
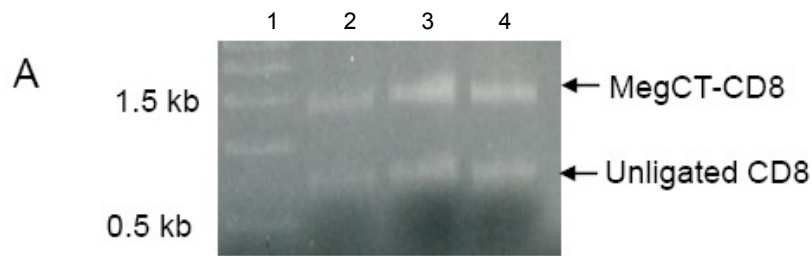


Figure 6.9. Formation of ligated MegCT-CD8 cDNA and pre-ligation quantification of *SacII/XhoI* MegCT-CD8 cDNA and pCMV. CD8 and MegCT cDNA was amplified and purified as described previously. Purified DNA was digested with *SacII*. Digested DNA was purified and 1 μ g of CD8 cDNA and 1.3 μ g of MegCT cDNA were ligated.. Panel **A** shows the results of the ligation reaction with a visible band consistent with the expected size of the CD8-MegCT cDNA of 1.4 kb.

(**Fig. 6.10 A**). *Afl*III digestion of MegCT would produce a mixture of full and partial length MegCT and if this approach was successful plasmid DNA isolated from individual bacterial colonies would be sequenced to ensure the full MegCT cDNA was present.

The PCR products were visualised on an ethidium bromide stained agarose gel and a single band of 600 bp consistent with MegCT cDNA seen (**Fig 6.10 B**). The band was excised from the agarose gel and the DNA purified and quantified by spectrometry. Five μ l aliquots of *Afl*III/*Not*I digested BS-SKII-CD8 and *Afl*III/*Not*I digested MegCT were compared on an ethidium bromide stained agarose gel with a DNA ladder (**Fig. 6.10 C**). It was estimated that 80 ng/ μ l of *Afl*III/*Not*I digested BS-SKII-CD8 and 16 ng/ μ l of *Afl*III/*Not*I digested MegCT were present. A number of ligation reactions were performed that differed in the molar ratio of vector and insert and the components are shown below.

<u>Molar ratio of insert:vector</u>	<u>BS-SKII-CD8 (μl)</u>	<u>MegCT (μl)</u>	<u>T4 ligase (μl)</u>	<u>T4 ligase buffer (μl)</u>	<u>DNAase free water (μl)</u>
1:1	1	1.1	1	1	5.9
2:1	1	2.2	1	1	4.8
3:1	1	3.3	1	1	3.7
4:1	1	4.4	1	1	2.6

Two μ l of each ligation reaction were used to transform chemically competent DH5 α bacteria. No ampicillin resistant bacterial colonies grew.

6.5.8 Introduction of greater 5' and 3' overhang into CD8 and MegCT cDNA.

The digestion efficiency of restriction endonucleases is dependent on the number of base pairs present either side of the recognition sequence. For instance increasing the number of base pairs 5' to a recognition sequence from 1 to 3

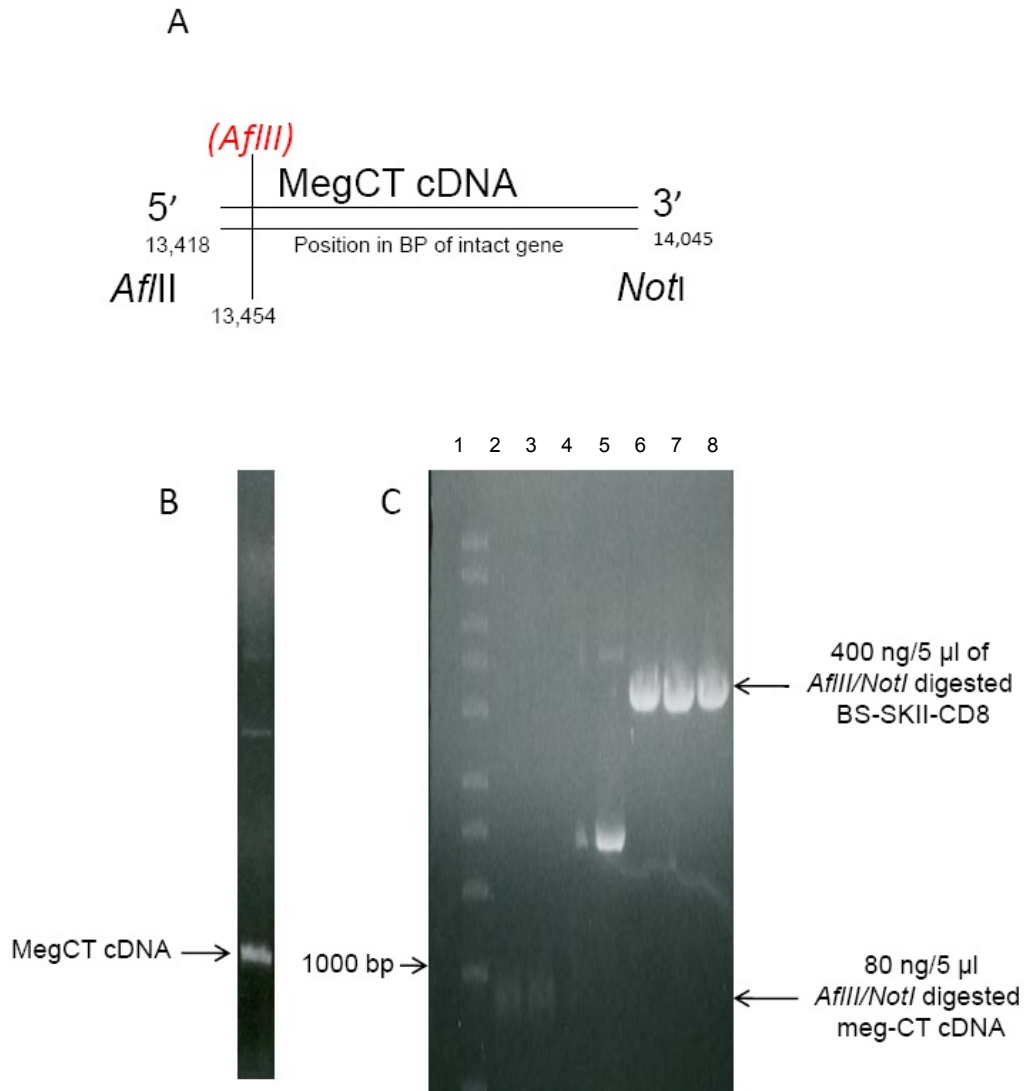


Figure 6.10. An *AfIII/NotI* partial digest of MegCT cDNA as a strategy to subclone that DNA fragment into BS-SKII-CD8. CD8 cDNA was supplied in BS-SKII with an *AfIII* site introduced at the end of the cDNA encoding the transmembrane domain. Primers were designed to introduce a 5' *AfIII* and 3' *NotI* site within MegCT cDNA. MegCT cDNA would then be directly ligated into pBS-SKII-CD8. An *AfIII* site is present in MegCT cDNA at the site shown (panel A). Following an *AfIII* digestion in sub-optimal conditions it was anticipated that a proportion of the molecule would remain intact. Panel B demonstrates the product of a PCR reaction using MEG3F and MEG3R to amplify MegCT cDNA. The MegCT cDNA was gel purified and *AfIII* digested and following purification was *NotI* digested.

increases the cleavage efficiency of *Sac*II from 0 to 50%. One possibility for the failed approaches was that there was incomplete digestion and lack of cohesive ended DNA. CD8 and MegCT cDNA with increased overhang were amplified by PCR and the products of both PCR reactions were visualised on an ethidium bromide stained agarose gel. Single PCR products of CD8 cDNA (**Fig. 6.11 A** lane 1) and MegCT (**Fig. 6.11 A** lane 2) are seen. DNA bands were excised and purified using an agarose gel extraction kit and quantified by spectrometry.

6.5.8.1 Ligation of CD8 and MegCT cDNA fragments produced with an increased overhang.

Five μ l aliquots of appropriately digested pCMV-Script, CD8 cDNA and MegCT cDNA that were produced to have an increased 5' and 3' overhang were separated on an ethidium bromide stained agarose gel and the results shown in **Fig. 6.11 B**. By comparison with known markers (not shown) it was estimated that 100 ng/5 μ l MegCT cDNA, 300 ng/5 μ l pCMV-Script and 100 ng/5 μ l CD8 cDNA were present.

Ligation reactions were setup as shown below.

Molar ratio insert:vector	pCMV (μ l)	MegCT cDNA (μ l)	CD8 cDNA (μ l)	T4 ligase buffer (μ l)	T4 ligase (μ l)	DNAase free water (μ l)
1:1	1	0.24	0.25	1	1	6.5
2:1	1	0.48	0.5	1	1	6.0
3:1	1	0.72	0.75	1	1	5.5
4:1	1	0.96	1.0	1	1	5.0

Two μ l of each ligation reaction was used to transform chemically competent bacteria. There were no colonies of bacterial growth.

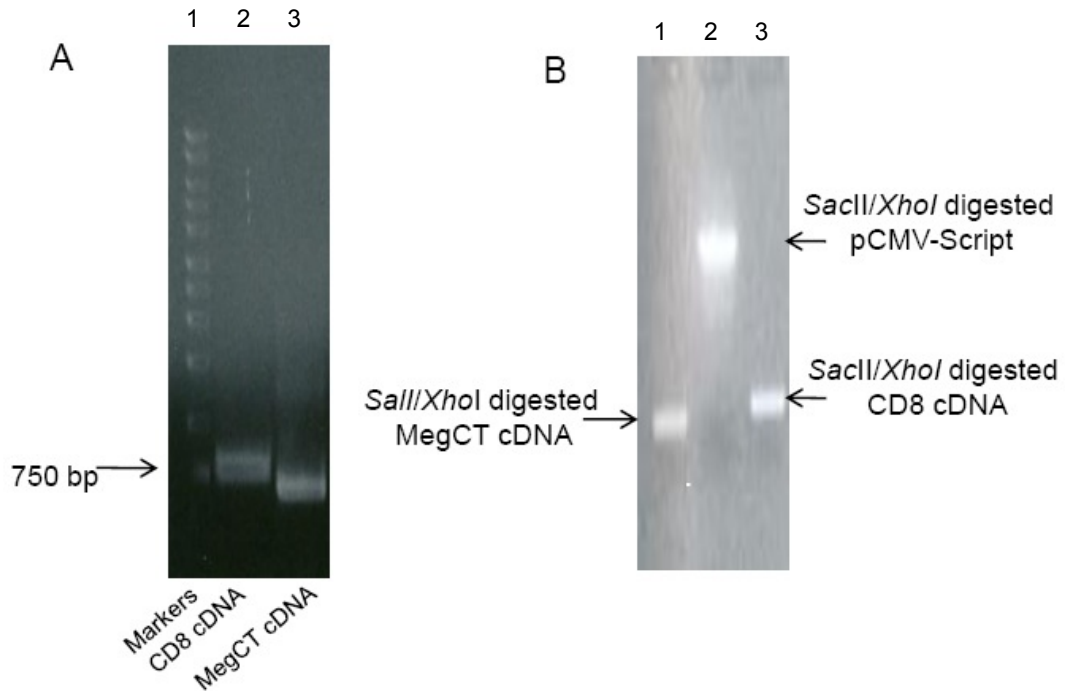


Figure 6.11. PCR primers designed to introduce a greater 5' and 3' overhang into CD8 and MegCT cDNA results in a significant yield of PCR product. To potentially increase the digestion efficiency of restriction endonucleases a greater 5' and 3' overhang of CD8 and MegCT cDNA were introduced by increasing G or C residues 5' to the restriction enzyme recognition sequence. **A** MegCT cDNA (lane 1) and CD8 cDNA (lane 2) were amplified by PCR using the primers MEG4F/MEG4R and CD82F/CD82R respectively. **B** Pre-ligation quantification of *Sall/XhoI* digested MegCT cDNA, *Sall/XhoI* digested pCMV-Script and *SaclI/Sall* digested CD8 cDNA. It was estimated that the concentrations of DNA were 100 ng/5 μ l MegCT cDNA, 300 ng/5 μ l pCMV-Script and 100 ng/5 μ l CD8 cDNA.

6.5.9 Cloning of CD8 cDNA and MegCT cDNA into pCRII-TOPO.

Separate cloning of CD8 and MegCT into the cloning vector pCRII-TOPO had two benefits. Extraction of the inserted DNA from circularised plasmid guaranteed that the fragment had cohesive ends and offered a ready supply of the relevant cDNA without repeating PCR. PCR products were cloned into pCRII-TOPO using the TOPO TA cloning kit. The multiple cloning site (MCS) of the vector supplied with this kit has a single 3'-thymidine overhang with topoisomerase non-covalently linked to it. PCR products generated using *Taq* polymerase have a single deoxyadenosine residue added to the 3' end which enables ligation between the MCS termini.

CD8 and MegCT PCR products were generated using *Taq* polymerase and gel purified. (**Fig 6.12 A**). Separate ligation reactions were set up using CD8 and MegCT cDNA and performed as instructed by the manufacturers of the TOPO TA cloning kit. The ligation mixture was used to transform DH5 α *E.Coli*. Six colonies from the MegCT plate and seven from the CD8 plate were expanded and used for plasmid mini-preparations. Ten μ l each pCRII-TOPO-CD8 were digested with *SacII* and *SaII* (**Fig 6.12 B lanes 7-13**). A 10 μ l aliquot of the plasmid pCRII-TOPO-MegCT was digested with *SaII* and *XhoI* (**Fig 6.12 B lanes 1-6**). As can be seen there was differential carriage of the CD8 and MegCT cDNA and as a result colonies 1 and 7 were selected for further expansion and plasmid DNA isolated using a maxi prep kit.

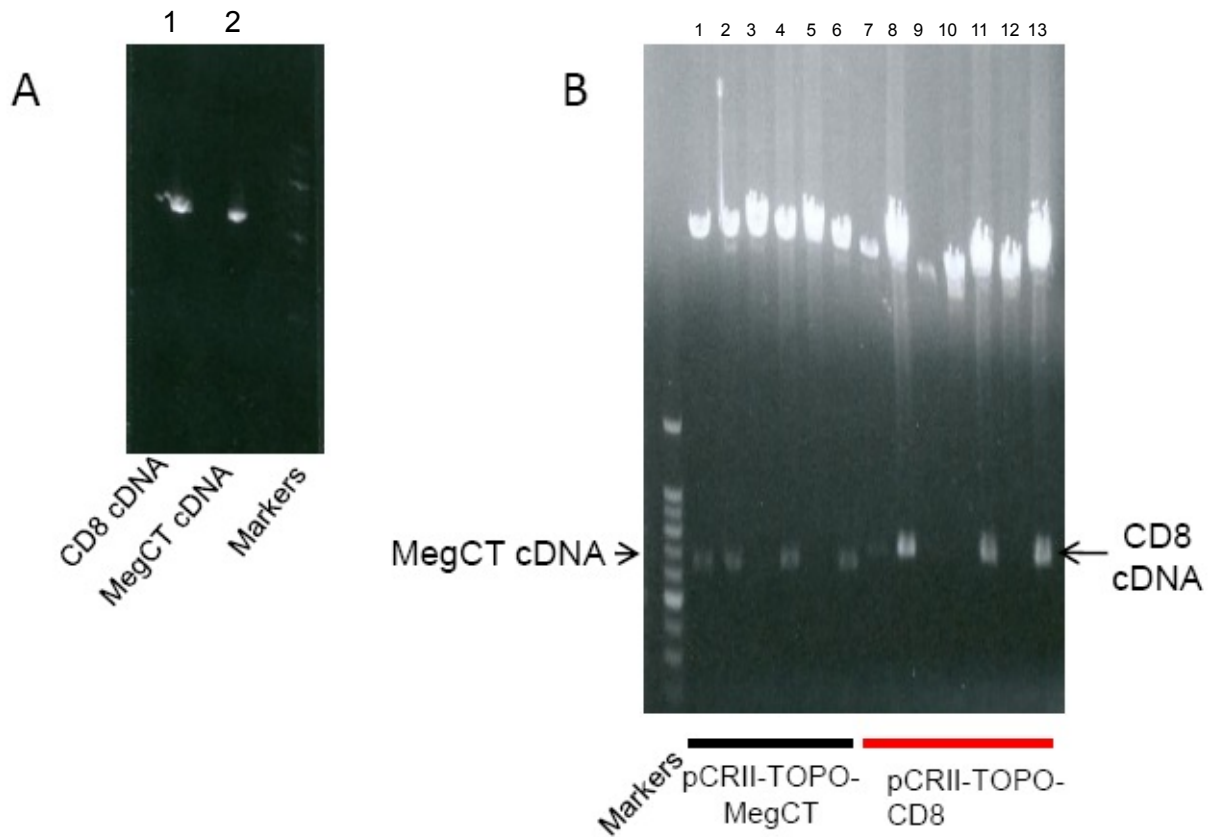


Figure 6.12 Sub-cloning of CD8 and MegCT cDNA into the non-expression vector pCRII TOPO. MegCT and CD8 cDNA were subcloned into separate pCRII TOPO from which they could later be excised. Depending on the restriction enzymes used this yields cDNA with cohesive ends for ligation into an expression vector. **Panel A.** MegCT and CD8 cDNA is produced as previously. One μl of fresh PCR product was into pCRII-TOPO and used to transform DH5 α *E. Coli*. Six colonies from the MegCT and 7 from the CD8 plate were amplified separately and the plasmid DNA purified. **Panel B.** TOPO-MegCT was subject to a *SalI/XhoI* digest and TOPO-CD8 to a *SacII/SalI* digest. The lower band represents successfully ligated DNA product.

6.5.10 Subcloning of CD8 cDNA into pCMV-Script.

To progress the CD8 cDNA was subcloned from pCRII-TOPO-CD8 into the eukaryotic transcription vector pCMV-Script. To achieve this 5 µg of pCRII-TOPO-CD8 was digested with *SacII* and *SalI* to generate the fragment annotated in **Fig.6.13 A** lane 1. The 800 bp fragment was excised from the agarose gel and purified. A 1 µg aliquot of pCMV-Script was digested with *SacII* and *SalI* to give the band shown in **Fig. 6.13 A** lane 2. A ligation reaction was performed and the products used to transform DH5α *E.Coli*. Multiple kanamycin resistant colonies grew and one colony was expanded and plasmid DNA isolated. Of this DNA a 1 µl aliquot was digested with *SacII* and *SalI* to prove the presence of the CD8 cDNA (**Fig. 6.13 B**). As shown digestion has liberated a 800 bp fragment from the vector pCMV-Script-CD8 confirming carriage of the inserted DNA.

6.5.11 Subcloning of MegCT cDNA into pCMV-Script-CD8.

A 5 µg aliquot of pCRII-TOPO-MegCT was digested with *SalI* and *XhoI* to generate the 600 bp band seen in **Fig. 6.13 A** lane 3 which was then gel purified. A 5 µg aliquot of pCMV-Script-CD8 was digested with *SalI* and *XhoI*. Aliquots of MegCT cDNA and pCMV-Script-CD8 were separated on an agarose gel to quantify them. (**Fig. 6.14**). Multiple ligation reactions were set up with conditions ranging between 3 and 30 fmol of *SalI/XhoI* digested pCMV-Script- CD8 and 9 and 90 fmol of

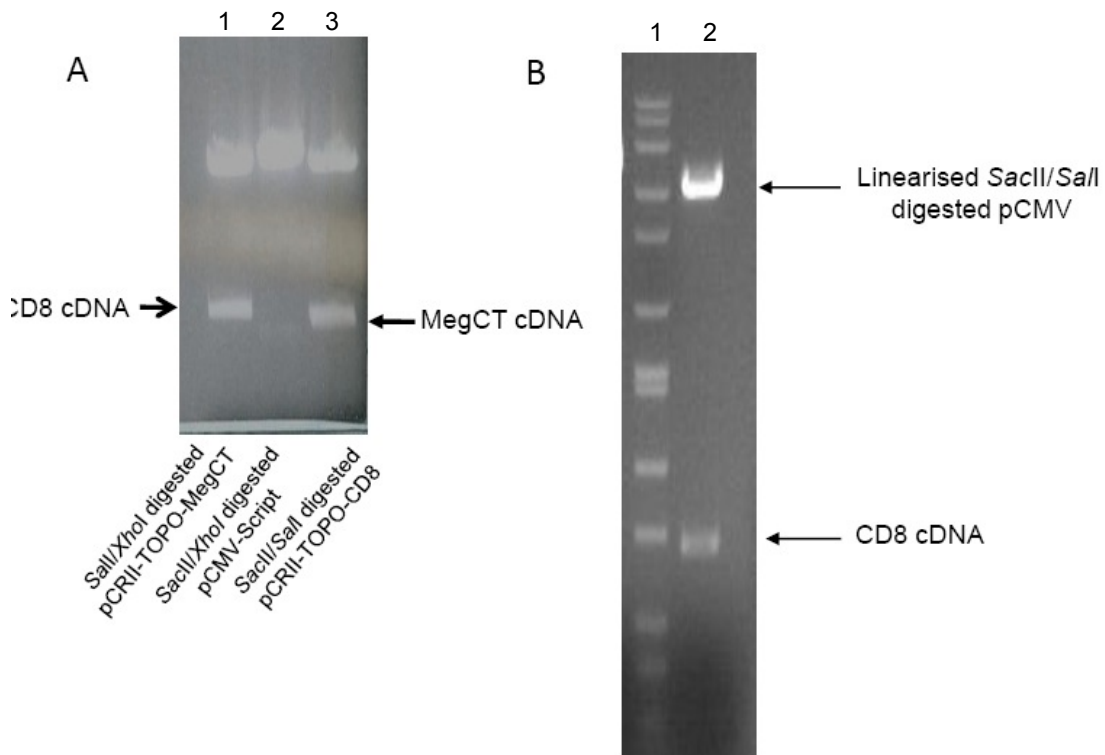


Figure 6.13 Subcloning of *SaclI/SalI* digested CD8 cDNA into pCMV-script. TOPO-CD8 and pCMV was digested with *SaclI/SalI*. After purification, the amount of DNA was quantified (**panel A**). It was estimated that 500 ng/5 μ l of CD8 cDNA and 1000 ng of pCMV script (lane 2) were present. Ligation reactions were performed and the products used to transform competent DH5 α *E. Coli*. Colonies of bacteria containing circular plasmid was present on all plates and 1 colony was expanded and the plasmid DNA purified. To confirm the purified plasmid DNA contained the CD8 insert 1 μ l of DNA was digested with *SaclI* and *SalI* in sequential digestion reactions. The products of the reaction were separated on a 1% agarose gel containing 0.5 μ g of ethidium bromide and photographed (**panel B**). The two bands confirm the successful ligation of CD8 into pCMV. This plasmid was labelled pCMV-CD8.

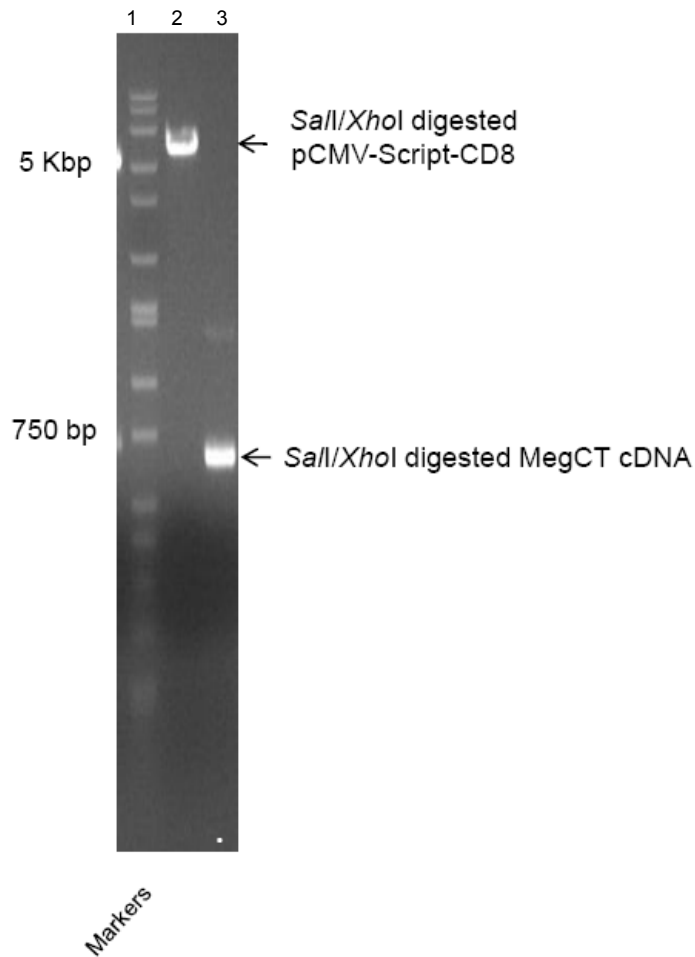


Figure 6.14 Attempted sub-cloning of *SalI/XhoI* digested MegCT cDNA into *SalI/XhoI* digested pCMV-CD8. Following the successful ligation of CD8 cDNA into pCMV script the second part of the strategy was to insert MegCT cDNA. The cDNA encoding MegCT was excised from pCRII TOPO by digesting with *SalI* and *SacII*. pCMV Script-CD8 was digested under the same conditions and the products separated on a 1% agarose gel containing ethidium bromide. By comparison it was estimated that 300 ng/5 μ l of plasmid and insert was present. Multiple ligation reactions were set up but aliquots of each ligation reaction failed to transform competent DH5 α *E. Coli*.

Sall/XhoI digested MegCT cDNA. The products of the ligation reaction failed to transfect DH5 α *E.Coli*.

On inspection of the DNA sequence of pCMV-Script it was apparent the *Sall* and *XhoI* sites were separated by only 3 base pairs (**Fig. 6.15 A**). This reduced the restriction endonuclease efficiency and resulted in incomplete digestion of pCMV-Script-CD8 and hence the failed ligations. **Figures 6.15 B and C** informed the strategy that followed. The vector pCRII-TOPO-MegCT contained a *Sall* recognition site by virtue of the MegCT PCR product and there is a 3' *Apal* site in the MCS. Similarly pCMV-Script-CD8 contains both 5' *Sall* and 3' *Apal* sites.

6.5.12 Preparation of Sall/Apal MegCT cDNA and Sall/Apal pCMV-Script-CD8 for ligation.

Aliquots of *Sall/Apal* pCMV-Script-CD8 and *Sall/Apal* MegCT cDNA were separated on an agarose gel and the relative amount of each estimated at 100 ng/ μ l and 40 ng/ μ l respectively (**Fig. 6.16**).

Ligation reactions were performed that contained between 10 and 30 fmol of pCMV-Script-CD8 and 30 and 90 fmol MegCT cDNA. A 1 μ l of each ligation reaction was used to transfect DH5 α *E.Coli*. The ligation mixture that contained the highest concentration of DNA resulted in the growth of kanamycin resistant colonies of bacteria.

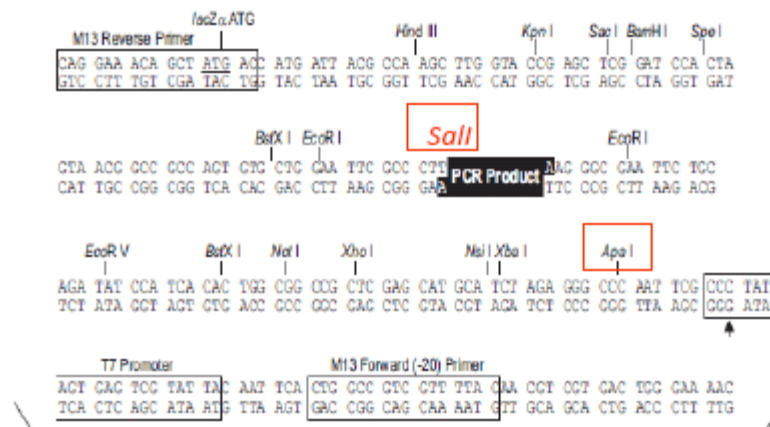
Nine colonies were amplified and plasmid DNA isolated using a mini-prep kit. A 5 μ l aliquot of DNA was subject to digestion with *SacII* and *XhoI* and the products separated on an agarose gel (**Fig. 6.17**). As can be seen *SacII/XhoI* digestion of isolated plasmid resulted in a 1.4 kb fragment consistent with CD8-MegCT cDNA

along with a 4.3 kb linearised pCMV-Script. Two colonies, the DNA from which was visualised in lanes 2 and 9 (**Fig. 6.17**) were further expanded and plasmid DNA isolated using a maxi-prep kit.

A

...TATCAAGCTTATCGATACC

GTCGACCTCGAGGGGGGGCC...

B**C**

pCMV-Script Multiple Cloning Site Region
(sequence shown 620-799)

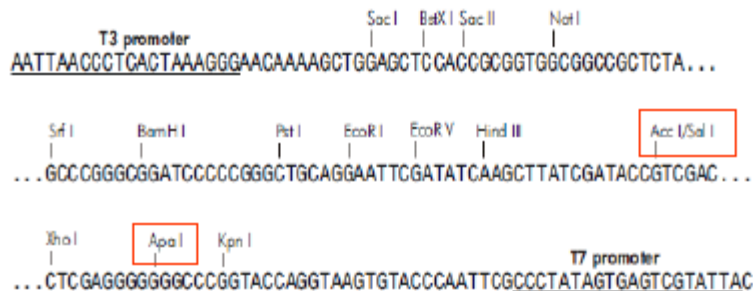


Figure 6.15 The *Sal*I and *Xho*I sites are contiguous within pCMV-script. A. The *Sal*I (red) and *Xho*I (blue) sites lie contiguously within pCMV-script reducing the probability of a successful restriction endonuclease digestion at both sites. The *Apa*I site (green) is separated by 9 bp from the *Sal*I site so the chances of an adequate digestion are greater. *Apa*I is an appropriate choice as it lies 3' in the MCS of pCRII-TOPO (**B**) and pCMV-Script, of which the full region is shown (**C**).

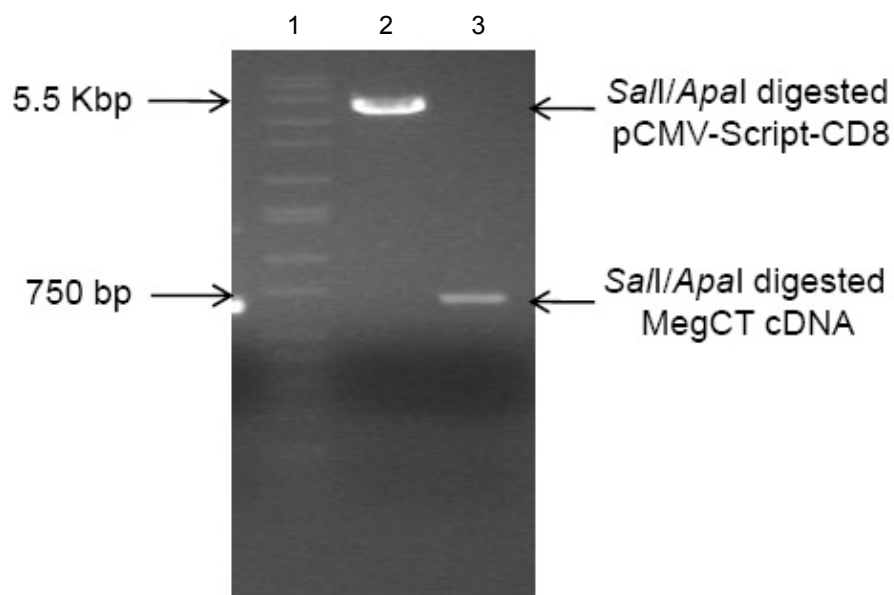


Figure 6.16 Pre-ligation quantification of *Sall* and *ApaI* digested meg-CT and pCMV-Script-CD8. pCRII-TOPO-meg-CT and pCMV-Script-CD8 were digested sequentially with *Sall* at Reaction products were separated on a 1% agarose gel with ethidium bromide, the bands of interest excised and the DNA purified. Aliquots of the purified DNA were separated on an agarose gel and compared to the DNA markers. It was estimated that 500 ng/5 μ l of *Sall/ApaI* digested pCMV-Script-CD8 and 200 ng/5 μ l of *Sall/ApaI* meg-CT were present. Ligation reactions were performed and an aliquot of each reaction was used to transform chemically competent DH5 α *E. Coli*. The products of the ligation reaction involving the highest concentrations of DNA successfully transformed the competent bacteria.

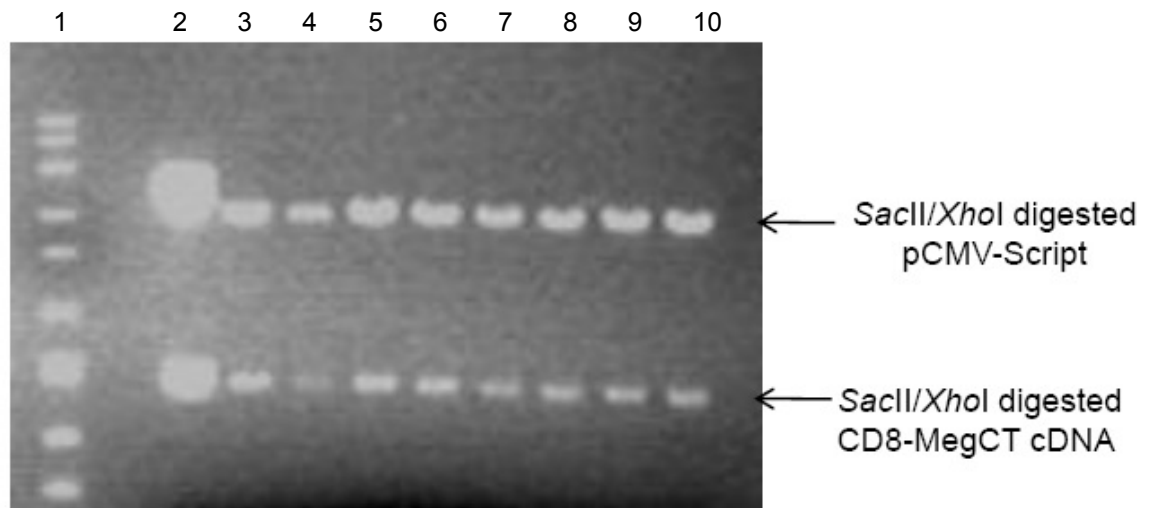


Figure 6.17. A *SacII/XhoI* digest of plasmid DNA isolated from nine colonies of transformed DH5 α *E.Coli* results in the release of a 1.4 kb DNA fragment consistent with the size of MegCT-CD8 cDNA. Plasmid DNA was isolated from each colony and subjected to a *SacII/XhoI* digestion and the products applied to an agarose gel and subjected to electrophoresis. The bands were visualised and photographed. A 1.4 kb DNA fragment was present in all samples and was of a size consistent with MegCT-CD8 cDNA.

6.5.13 Introduction of a full Kozak initiation sequence into the CD8-MegCT cDNA.

Using a variety of conditions there was a consistent failure to achieve expression of the CD8-MegCT chimaeric protein following transient transfection of OK cells. Transcription is under the control of the immediate early gene of the human cytomegalovirus which had achieved excellent levels of protein expression in OK cells previously. To improve transcription efficiency the basic ATG initiation sequence was supplemented with a 5' GC rich region by re-designing a forward primer (CD8KOZ).

The vector pCMV-Script-CD8-MegCT at a concentration of 1 ng was used as a template in a PCR that utilised CD8KOZ and MEG4R (forward and reverse primers respectively) at a final concentration of 1 μ M in Accuprime supermix. The reaction resulted in a single c. 1.4 kb PCR product (**Fig. 6.18 A**). After purification, CD8-MegCT cDNA was subject to a *SacII/XhoI* digestion. The vector was prepared for ligation by a *SacII/XhoI* digestion of 0.5 μ g of pCMV-Script. The products of both digestions were separated on an agarose gel (**Fig. 6.18 B**) and complete linearization of the vector was seen to have occurred. The estimated concentrations of DNA were 20 ng/ μ l of pCMV-Script and 10 ng/ μ l CD8-MegCT cDNA. A ligation reaction was set up to include 10 fmol pCMV-Script (0.7 μ l) and 30 fmol CD8-MegCT cDNA (1 μ l). After a 5 minute ligation reaction 2 μ l of the ligation mixture were used to transfect DH5 α *E. Coli* and following an overnight incubation multiple kanamycin resistant bacterial colonies were present.

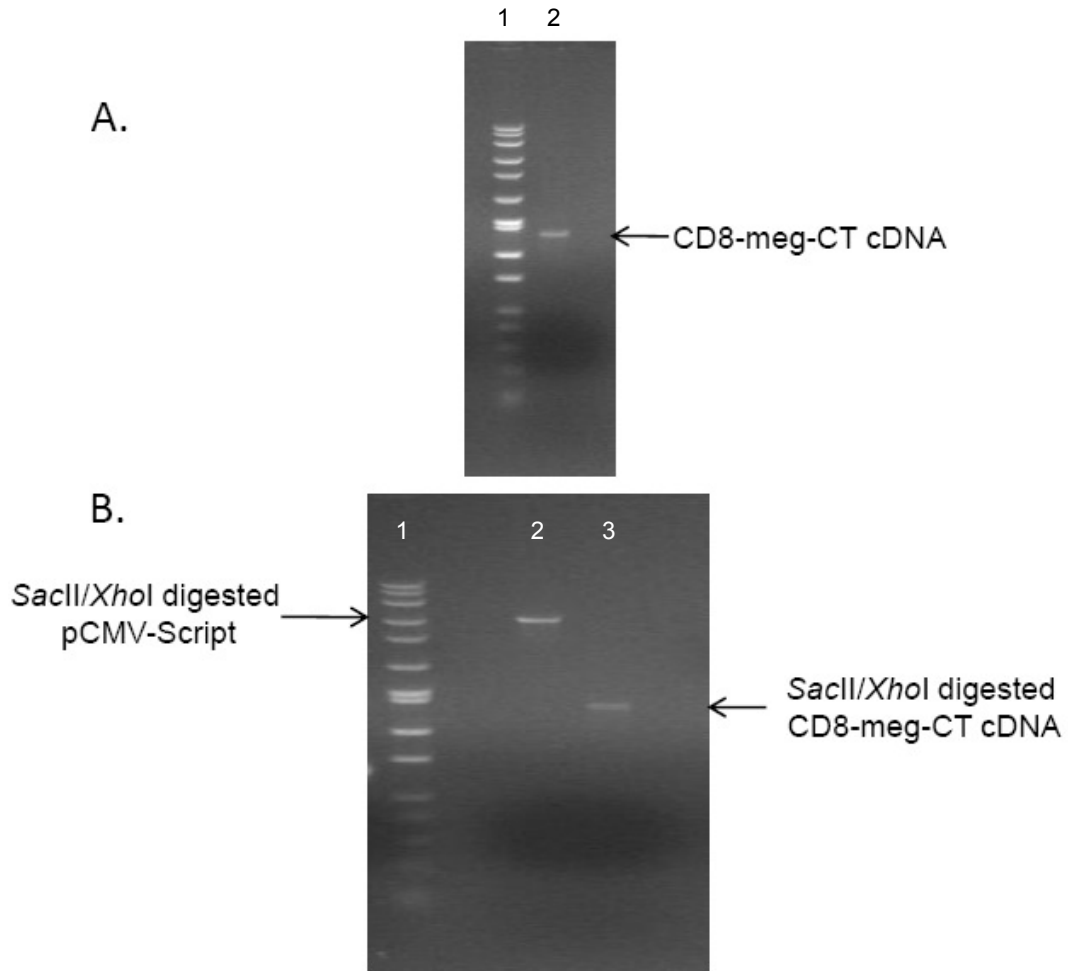


Figure 6.18 Introduction of complete Kozak sequence into the CD8-MegCT cDNA to achieve optimal translation. **A.** PCR primers were designed to introduce a full Kozak sequence 5' to the *SacII* restriction enzyme recognition sequence. CD8-MegCT was expanded from pCMV-Script-CD8-MegCT using the forward primer CD8KOZ and the reverse primer MEG4R. The PCR products applied to a 1% agarose gel supplemented with 0.5 $\mu\text{g/ml}$ ethidium bromide. A single product of c. 1400 bp is seen. **B** The remainder (45 μl) of the PCR product and 0.5 μg of pCMV-Script were digested with *SacII* and *XhoI*. Purified DNA fragments were collected and aliquots applied to an agarose gel for quantification prior to a ligation reaction. The estimated concentration of pCMV-Script was 100 ng/5 μl and CD8-MegCT 50 ng/5 μl .

Seven colonies were expanded and plasmid DNA isolated using a mini-prep kit. A 5 µl aliquot of plasmid DNA was subject to a *SacII* /*XhoI* restriction endonuclease digestion and the products separated on an agarose gel (**Fig. 6.19**). Plasmid digestion resulted in the release of a 1.4 kb fragment in at least 5 of the lanes indicating successful ligation. Large scale plasmid production was achieved using bacterial reference culture corresponding to plasmid preparations 1 and 7 (marked by an asterisk).

6.5.14 Sequencing of pCMV-Script-CD8-MegCT.

Sequencing of pCMV-Script-CD8-MegCT was performed on a commercial basis by the Protein and Nucleic Acid Laboratory (PNACL) at the University of Leicester. Three mis-matches were identified. TGC was replaced by TAC at position 335, GGG by GGA at position 582 and GTG by GCG at position 723 (**Fig. 6.20**). The latter mutation resulted in an amino acid change from valine to alanine. The other mutations were non-coding changes.

6.5.15 Transient expression of MegCT-CD8 chimaeric protein in OK cells.

OK cells were transiently transfected with pCMV-MegCT-CD8 using the Fugene-6 transfection reagent. Control cells were transfected with pCMV-script alone.

Monolayers of cells at 50% confluence were transfected for 48 hours using ratios of plasmid DNA to transfection reagent that varied between 0.5 to 2 µg plasmid DNA to 3 µl of fugene-6. Immunoblotting using anti-MegCT antisera of transiently transfected cell lysate confirms expression of a 47 kDa protein consistent with the anticipated mass of the MegCT-CD8 chimaeric protein (**Fig. 6.21 A**). Optimal

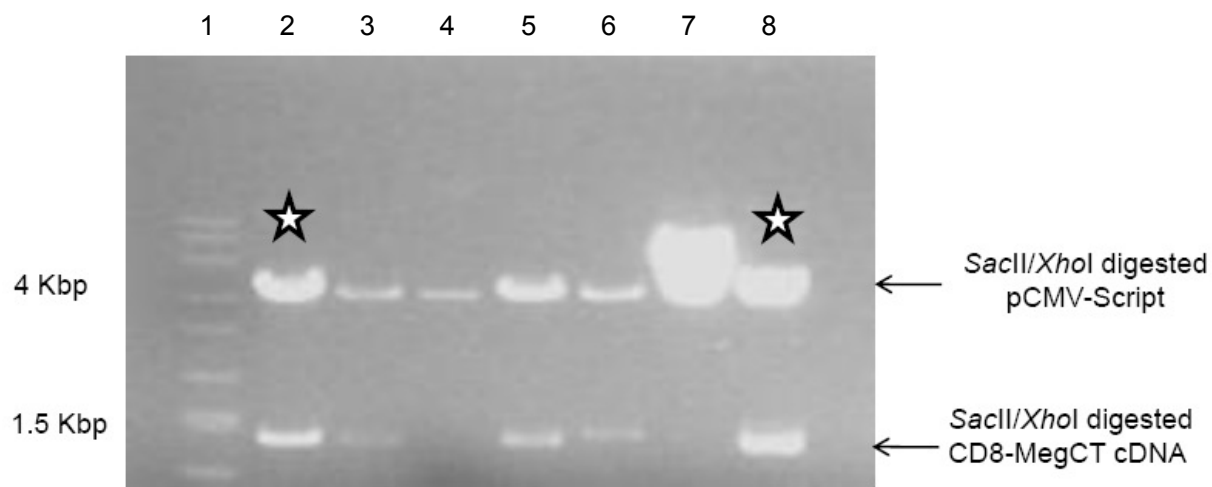


Figure 6.19. A *SacII/XhoI* digest of plasmid DNA isolated from nine colonies of transformed DH5 α *E.Coli* results in the release of a 1.4 kb DNA fragment consistent with the size of MegCT-CD8 cDNA. Plasmid DNA from 7 separate bacterial colonies was isolated and subjected to a *SacII/XhoI* digest. The entire reaction was applied to an agarose gel and subjected to electrophoresis. The bands were visualised and photographed. A 1.4 kb DNA fragment was present in five of the seven samples and was of a size consistent with MegCT-CD8 cDNA. Two colonies (indicated with a asterisk) known to contain the insert from the patched plate were used to separately inoculate fresh media and plasmid DNA isolated using a maxi-prep kit. Plasmid DNA derived from those two colonies was submitted for sequencing and also used to transiently and stably transfect OK cells.

ATGGCCTTACCAGTGACCGCCTTGCTCCTGCCGCTGGCCTTGCTGCTCCACGCCGCCAGGC
CGAGCCAGTTCCGGGTGTCGCCGCTGGATCGGACCTGGAACCTGGGCGAGACAGTGGAGCT
GAAGTGCCAGGTGCTGCTGTCCAACCCGACGTCGGGCTGCTCGTGGCTCTTCCAGCCGCGC
GGCGCCGCCAGTCCCACCTTCTCCTATACCTCTCCAAAACAAGCCCAAGGCGGCCG
AGGGGCTGGACACCCAGCGGTTCTCGGGCAAGAGGTTGGGGGACACCTTCGTCTCACCC
GAGCGACTTCCGCCGAGAGAACGAGGGCTACTATTTCTGCTCGGCCCTGAGCAACTCCATC
ATGTACTTCAGCCACTTCGTGCCGGTCTTCCCTGCCAGCGAAGCCCACCACGACGCCAGCGC
CGCGACCACCAACACCGGCGCCCACCATCGCGTCGCAGCCCCTGTCCCTGCGCCCAGAGGC
GTGCCGGCCAGCGGCGGGGGCGCAGTGCACACGAGGGGGCTGGACTTCGCCTGTGATATC
TACATCTGGGCGCCCTTGGCCGGGACTTGTGGAGTCTTCTCCTGTCACTGGTTATCACCC
TTTACTGCAAGCGGGTCGACCACTATAGAAGGACCGGCTCCCTTTTGCCTGCTCTGCCCAA
GCTGCCAAGCTTAAGCAGTCTCGTCAAGCCCTCTGAAAATGGGAATGGGGCGACCTTCAGA
TCAGGGGCAGATCTTAACATGGATATTGGAGTGTCTGGTTTTGGACCTGAGACTGCTATTG
ACAGGTCAATGGCAATGAGTGAAGACTTTGTGATGAAAATGGGGAAGCAGCCCATAATATT
TGAAAACCCAATGTACTCAGCCAGAGACAGTGTGTCAAAGTGGTTCAGCCAATCCAGGTG
ACTGTATCTGAAAATGTGGATAATAAGAATTATGGAAGTCCATAAACCCTTCTGAGATAG
TTCCAGAGACAAACCCAACTTCACCAGCTGCTGATGGAACCTCAGGTGACAAAATGGAATCT
CTTCAAACGAAAATCTAAACAAACTACCAACTTTGAAAATCCAATCTATGCACAGATGGAG
AACGAGCAAAGGAAAGTGTGCTGCGACACCACCTCCATCACCTTCGCTCCCTGCTAAGC
CTAAGCCTCCTTCGAGAAGAGACCCAACCTCAACCTATTCTGCAACAGAAGACACTTTTAA
AGACACCGCAAATCTTGTTAAAGAAGACTCTGAAGTA

Figure 6.20 Schematic representation of the nucleotide sequence of the cDNA encoding the MegCT-CD8 chimaeric protein. The full sequence is as shown. The residues highlighted in are mismatched nucleotides only one of which results in an amino acid sequence change.

expression was achieved using 1 µg/well of plasmid DNA and 3 µl of fugene-6 transfection reagent. Two discrete bands are present indicating that under these conditions the chimaeric protein was present as a dimer. To confirm the protein band detected in **6.21 A** as the MegCT-CD8 chimaeric protein immunoblotting of the OK cell lysate using anti-CD8 antibody was performed. A representative immunoblot is shown in **Fig. 6.21 B** and confirms expression of a 47 kDa CD8 containing protein in transiently transfected cells. Optimal expression was achieved using 1 µg of pCMV-MegCT-CD8 cDNA and 3 µl of fugene-6. At higher concentrations of DNA expression of the chimaeric protein declined, and immunoblotting against CD8 detected a single discrete protein band. Control transfections using pCMV-script did not result in expression of CD8.

6.5.16 Stable transfection of MegCT-CD8 and CD8.

In an estimation of transfection efficiency it was estimated to be only about 20%. In order to investigate the role of over-expression of MegCT on albumin endocytosis the expression of the MegCT-CD8 chimaeric protein had to be more generalised. Therefore, cell lines stably expressing MegCT-CD8 and CD8 were generated.

OK cells were transiently transfected with either pCMV-MegCT-CD8 or pCMV-CD8 and selected for resistance to G418. Individual cells were clonally expanded over a period of weeks. Different clones were screened for expression of MegCT-CD8 or CD8. **Figure 6.22 A** depicts an immunoblot using an anti-MegCT primary antibody. There are differential levels of expression of the MegCT-CD8 chimaeric protein with expression being greatest in colonies 3 and 4. Colonies of G418 resistant cells were screened for CD8 expression. Immunodetection using anti-

CD8 antibody of CD8 protein was greatest in colony 3, with lesser amounts in colonies 1 and 2 and none in colony 4 (**Fig. 6.22 B**).

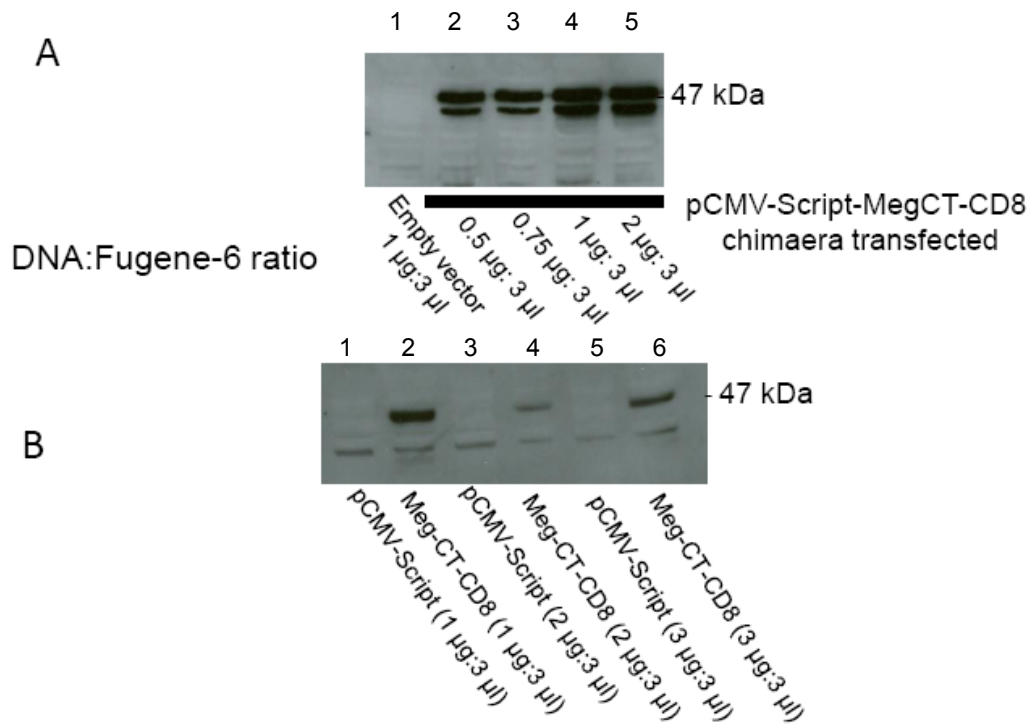
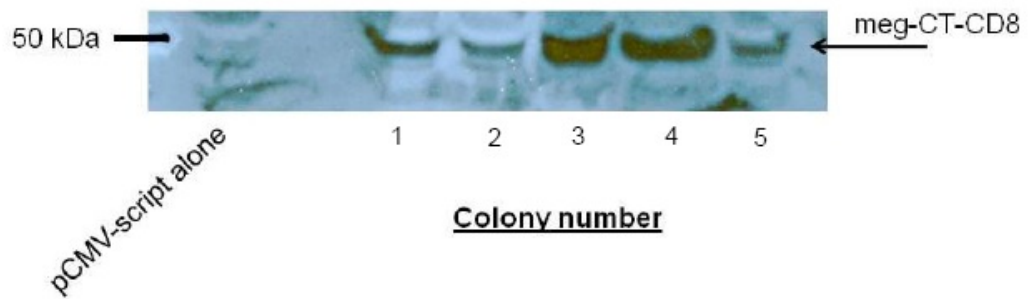


Figure 6.21 Optimisation of conditions for transient transfection of OK cells with MegCT-CD8 chimaeric protein. **(A)** Monolayers of OK cells at 50% confluence grown in 6-well plates were transiently transfected pCMV-CD8-MegCT. Cell protein was harvested and applied to a 10% polyacrylamide gel, subjected to PAGE and immunoblotted using a rabbit anti-MegCT primary antibody. A band is seen that represents a protein of around 43 kDa which is consistent with the expected mass of the chimaeric protein. Consistently, the protein travels as a dimer when detected by anti-MegCT antisera. Optimal transfection was seen when a ratio of 3 μ l Fugene-6: 1 μ g of pCMV-CD8-MegCT was used. No band is seen when monolayers are transfected with pCMV-Script. **(B)** In a repeat of the experiment described in **(A)** transient expression of CD8-MegCT chimaeric protein was detected using a goat anti-CD8 primary antibody.

A



B

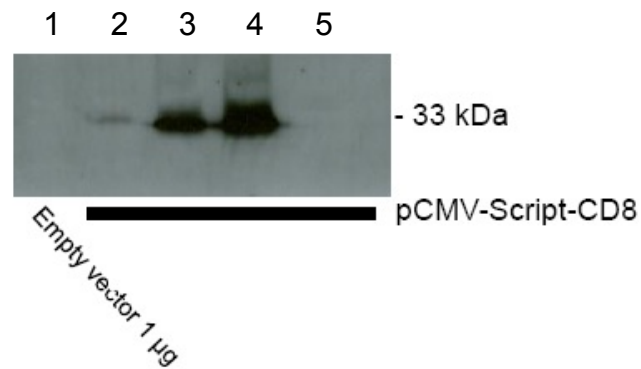


Figure 6.22 Immunoblot depicting screening of OK cells stably transfected with MegCT-CD8. OK cells were stably transfected with pCMV-MegCT-CD8 were selected by incubation with media containing G418. Individual cells were selected and clonally expanded over weeks before being screened for the expression of MegCT-CD8 chimaeric protein by western blotting using anti-CD8 antibody. There was differential expression of MegCT-CD8 between clones and no protein was detected when cells were transfected with pCMV-script alone (panel A.). Panel B. **Immunoblot depicting screening of OK cells stably transfected with CD8.** OK cells were stably transfected with pCMV-CD8 and treated as above. Colonies were screened for the expression of CD8 by western blotting using anti-CD8 antibody. Cellular protein levels were measured prior to PAGE and equal amounts added to each well. There was differential expression of CD8 (33 kDa) between clones and no protein was detected when cells were transfected with pCMV-script alone.

6.5.17 A MegCT-CD8 chimaeric protein transiently expressed in OK cells was associated with the cell membrane.

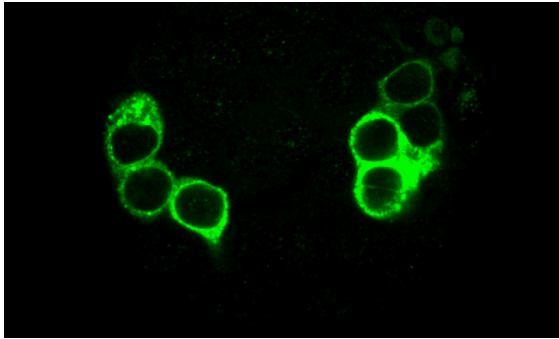
For the MegCT-CD8 chimaeric protein to be an adequate mimic of native megalin an association with the cell membrane of OK cells had to be shown. The confocal photomicrographs shown in **Figs. 6.23 A-B** demonstrate fluorescence associated with the cell membrane. The primary antibody was directed against an epitope in the extracellular domain of CD8 and the cells used were permeabilised. A 3-dimensional reconstruction of the z-series of photomicrographs (Supplementary movie 1.) demonstrates that the distribution of the chimaeric protein is non-polarised and that in areas the fluorescence clumps consistent with an aggregation of MegCT-CD8 either with itself or as part of a multi-molecular complex. Similar findings were observed using a GFP tagged MegCT-CD8 which is reassuring as it implies membrane association of the entire chimaeric protein (data not shown).

6.5.18 MegCT-CD8 chimeric proteins transiently transfected into OK cells are phosphorylated.

To support our observations of MegCT phosphorylation in intact cells studies of phosphorylation of the chimeric MegCT-CD8 protein were undertaken. This method was developed so that there was no delay to immunoprecipitation of MegCT while trypsinisation of the megalin extracellular domain proceeded. Furthermore, it overcame the problems associated with a low cellular abundance of megalin. Cells transiently transfected with MegCT-CD8 chimeric receptor were loaded with [³²P]-orthophosphate. Following which, stimulation with HSA (1 mg/ml),

EGF (500 pg/ml) and PDBu (1 μ M) increased phosphorylation of MegCT-CD8 by $142 \pm 13.2\%$, 177.3 ± 33.5 and $174 \pm 36\%$ that of control respectively (**Fig. 6.24**).

1



2

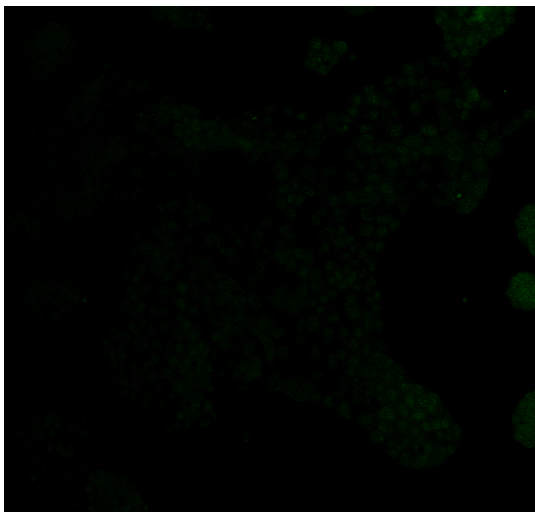
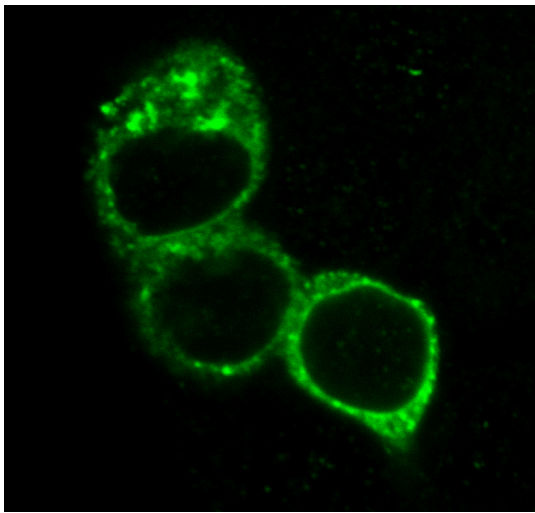


Figure 6.23 Indirect immunofluorescence and confocal microscopy confirm expression and membrane association of MegCT-CD8 chimaeric protein. OK cells were grown on coverslips and monolayers at 50% confluence were transiently transfected with pCMV-CD8-MegCT. Cells were grown for a further 24 hours before being fixed with paraformaldehyde. Indirect immunohistochemistry was performed on permeabilised cells using goat anti-sera directed against CD8 as the primary antibody and FITC-labelled anti-goat F(ab) secondary that was raised in rabbits. Fluorescence was visualised by confocal microscopy at x400 (panel **A**) and x800 (panel **B**) magnification. After treatment under identical conditions OK cells transfected with pCMV alone were visualised (panel **C**).

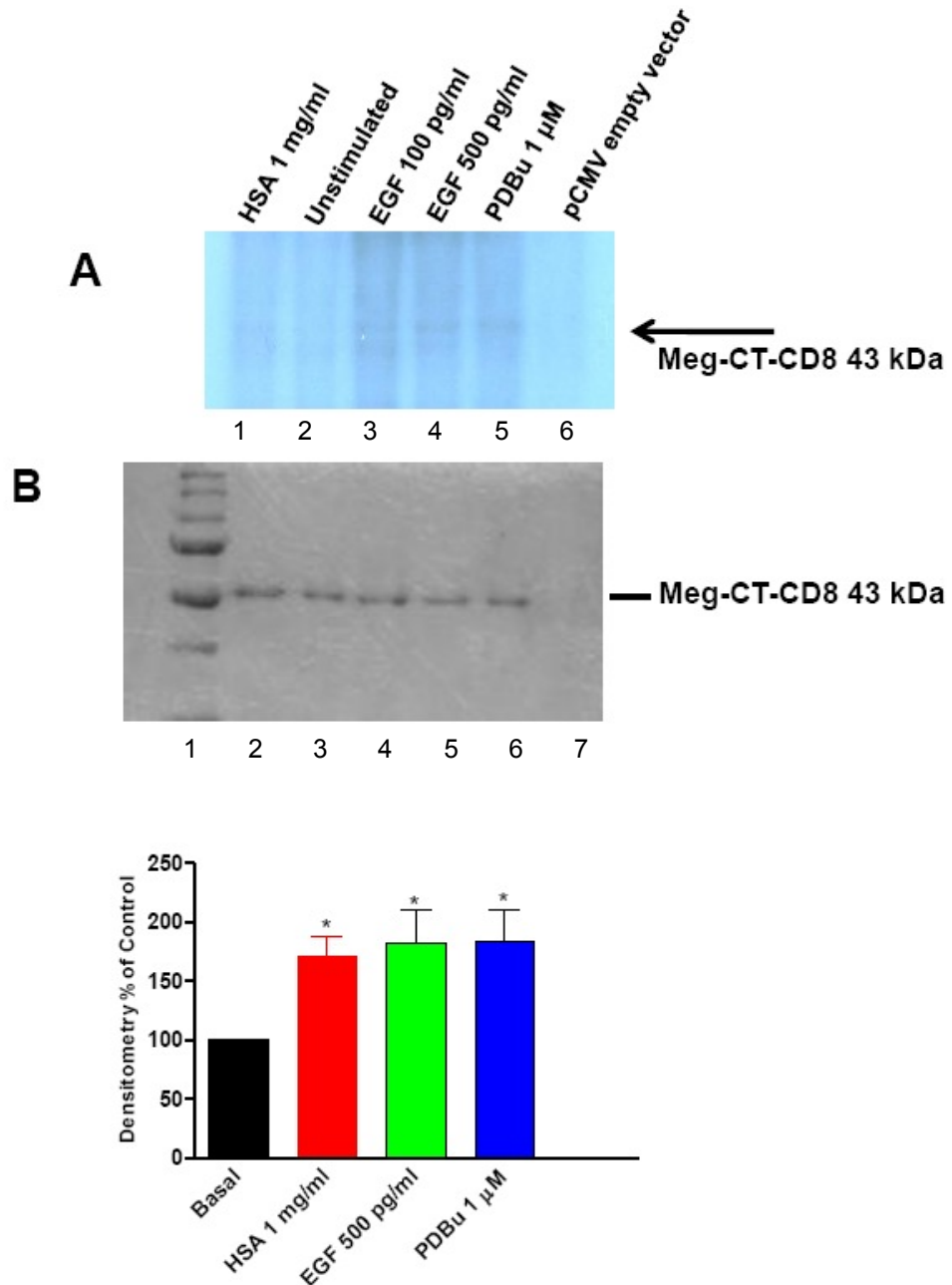


Figure 6.26 Phosphorylation of a CD8/meg-CT chimeric protein in transiently transfected OK cells. Transiently transfected OK cells were loaded with [32 P]-orthophosphate and stimulated with the indicated agonists. CD8/meg-CT was immunoprecipitated using anti-CD8 antisera. Immunoprecipitates were subjected to PAGE, the gels dried and exposed to autoradiograph film. A representative autoradiograph is shown (A). The corresponding Coomassie stained dried gel is shown (B). Densitometric analysis of phosphorylated CD8/meg-CT from a number of experiments is shown (C). Data shown is mean \pm SEM, $n \geq 3$.

6.6 Discussion.

To investigate possible MegCT phosphorylation in intact cells a chimaeric MegCT-CD8 protein was developed. This chapter describes (i) several strategies that were used to develop a MegCT-CD8 chimaeric protein (ii) the transient expression of MegCT-CD8 in OK cells (iii) the investigation of the cellular localisation of the MegCT-CD8 chimaeric protein and (IV) the phosphorylation of a MegCT-CD8 protein. This is the first description of the production of a chimaeric protein containing MegCT as published studies to date have used truncated versions of megalin.

The production of circularised pCMV-MegCT-CD8 capable of transiently transfecting OK cells was not straightforward. The discussion of how this was achieved will be used to question why other strategies failed. The conditions needed for the generation of antibiotic resistant bacterial colonies can be summarised as;

1. Production of a clean, high fidelity PCR product by amplification from an appropriate vector.
2. Adequate restriction enzyme digestion of the 5' and 3' termini of DNA components of the T4 ligation reaction.
3. Successful ligation and the avoidance of concatemar formation. Concatamars are formed when cohesive DNA termini assemble to form a long DNA sequence of repeating oligonucleotides.
4. Sufficient, though not excessive circularised plasmid DNA concentrations to result in bacterial transfection.

The vectors containing the cDNA encoding MegCT and CD8 were both confirmed to carry the appropriate insert. The conditions for cDNA amplification by PCR were optimised although single reaction products were difficult to achieve. By extracting and purifying a single DNA band excised from an agarose gel it was ensured that appropriately sized and pure DNA fragments were used in further reactions.

Successful restriction endonuclease digestion of oligonucleotide and plasmid DNA is dependent on appropriate concentrations of BSA and glycerol (Sambrook et al., 1989). Both were appropriate in the experiments outlined above. The efficiency of restriction endonuclease digestion is also dependent on the number of base pairs flanking the recognition site. This was accounted for in the initial design of the primers, and further extended when primers were re-designed. A possibility to increase the number of cohesive ended DNA was to increase the stringency of the digestion conditions by either increasing either the enzyme concentration or the duration of the reaction. The propensity of restriction endonucleases to exhibit star activity, in which the fidelity of the enzyme for its recognition sequence is diminished limited this as a method.

To counter continuing concern that DNA ligation was not occurring because of incomplete digestion PCR products were cloned into a non-expression vector. After appropriate digestion and purification there was a high probability of both termini of the cDNA having cohesive ends. Sub-cloning CD8 cDNA into pCMV produced in such a way was straightforward but attempted ligation of MegCT cDNA into pCMV-CD8 failed. Inspection of the sequence of the multiple cloning sequence of pCMV established that there were no intervening DNA base pairs between the *Sa*I and *Xho*I recognition sites. The number of base pairs flanking the

*Xho*I recognition site was three, which practically resulted in no activity of the enzyme and a non-cohesive end of the plasmid. Circularised plasmid was produced when an alternative restriction enzyme was selected as a larger number of base pairs flanked its recognition sequence and digestion at 5' and 3' termini was achieved.

The initial approach used in these studies was to attempt to ligate cDNA encoding CD8 and MegCT in broadly equivalent concentrations into appropriately digested pCMV. It was anticipated that after a series of ligation reactions between the cohesive ends of the DNA fragments circularised plasmid would be produced. On reflection this approach encouraged the formation of concatamers in which oligonucleotides and/or plasmid DNA form stretches of multimers. In principle this may have been visible when the products of a ligation reaction were visualised on an ethidium bromide stained gel. No discrete bands were seen (data not shown) perhaps because of a low starting concentration of DNA or that the ligation reaction resulted in numerous DNA fragments of different masses that would appear as a faint smear on the gel. To reduce concatamer formation sequential ligation reactions were attempted. After each ligation reaction the formed DNA components were gel purified before being used for the next reaction. With each step the recovered amount of DNA diminished which limited this as an approach. The solution to this was cloning CD8 cDNA into pCMV and transfecting competent bacteria and purifying large amounts of pCMV-CD8 DNA. This was the vehicle into which MegCT cDNA could be cloned in a separate reaction.

The introduction of a full Kozak sequence resulted in successful transient transfection of OK cells with MegCT-CD8. The ATG sequence is sufficient to

initiate translation in some circumstances. However, in these experiments a 5' GC rich region needed to be added which is recognised to optimise translation efficiency (Kozak, 1991b, Kozak, 1991a).

Transient transfection of OK cells was assessed by western blotting against the MegCT and CD8 portions of the chimaeric protein. When using MegCT anti-serum the chimera was detected as a dimer, although using anti-CD8 antibodies a single protein band was detected. Although not investigated further this may reflect a post-translational modification of the CD8 portion of the molecule that altered the molecular weight of the entire chimera and shielded it from recognition by the CD8 antibody.

Confocal microscopy of OK cells transiently transfected with the MegCT-CD8 chimaeric protein confirmed a substantial portion of the molecule was associated with the cell membrane. There was also evidence of involvement with sub-cellular structures consistent with mimicry of trafficking of native megalin, a process attributed to peptide sequences in the MegCT (Marzolo et al., 2003, Takeda et al., 2003). A z-series of confocal micrographs was reconstructed to give a 3D representation of the distribution of MegCT-CD8 in OK cells. The primary aim of this study was to demonstrate membrane association of the MegCT-CD8 chimera. Whilst a clear view of the basolateral surface of the cells was not possible the distribution of MegCT-CD8 on the apical surface appeared to be in a punctate distribution. In different cell types membrane associated native megalin clusters in microvillar spaces (Niemeier et al., 1999, Birn et al., 2000b) and binding of megalin ligands to the PTC membrane occurs in a similar distribution (Kozyraki et al., 2001, Olson et al., 2008). Furthermore, in PTC megalin and some binding

partners of its cytosolic domain co-localise in large aggregates (Akhter et al., 2002, Nagai et al., 2005). Overall, these studies fulfil the primary aim of confirming membrane association of the MegCT-CD8 chimaeric protein and suggest that in terms of MegCT it traffics and should function as native megalin.

It is self-evident that the MegCT-CD8 chimaera and native megalin will not have equivalent extracellular binding partners. In at least one other respect it can be anticipated that the two molecules will not behave similarly. γ -Secretase activity at the intracellular juxta-membrane region of megalin releases the cytosolic fragment of the molecule during regulated intramembrane proteolysis (RIP) (Biemesderfer, 2006). As the MegCT-CD8 chimaera has been developed to include the transmembrane domain of CD8 it may not be subject to RIP. Conceivably this made MegCT-CD8 a more useful tool in phosphorylation studies as it was located to the region of kinase activity for longer than if a cytosolic fragment were released. The pattern of constitutive and agonist mediated phosphorylation of the MegCT but not CD8 portion of the chimera was identical to that seen with the GST-MegCT fusion protein in human and opossum cells. As with the study of EGF induced MegCT phosphorylation in intact cells, the phosphorylation of the chimeric protein was weaker than seen in the fusion protein. This may reflect the largely basolateral restriction of the EGF-R and apical distribution of MegCT-CD8 that was referred to in a previous chapter. Alternatively, the diminished EGF response may reflect the effect of recombinant human EGF used on opossum cells.

The mechanism of albumin induced phosphorylation of MegCT is unclear. The MegCT-CD8 chimaeric protein developed in this chapter is a unique tool as the extracellular portion of CD8 would not be expected to bind albumin.

Phosphorylation of the MegCT-CD8 chimeric receptor as observed indicates that stimulation is not the result of a straightforward ligand-receptor interaction between albumin and megalin. Native megalin is still present so theoretically neighbouring molecules in multi-molecular complexes could phosphorylate each other. However, megalin is not recognised to have intrinsic kinase activity of its own but there is some evidence that albumin binding to megalin could activate Src family kinases.

Albumin endocytosis and megalin mediated PTC immunoglobulin light chain uptake both generate H_2O_2 (Morigi et al., 2002, Tang et al., 2003, Nakajima et al., 2004) that activate Src family kinases (Basnayake et al., 2010). Src kinase activity appears to be crucial in signalling by other LDL-R family members. Ligand binding to LRP1 in PC12 cells transactivates the neurotrophic Trk receptor by Src family kinase dependent mechanism (Shi et al., 2009).

Albumin endocytosis may not be a pre-requisite for superoxide generation. Under some circumstances interaction between cognate ligand and receptor generates hydrogen peroxide and activates the EGF-R (DeYulia et al., 2005). Taken together superoxide generation and Src activation could be an important mechanism by whereby albumin binding to megalin may phosphorylate neighbouring MegCT domains via a mechanism that could involve the activated EGF-R.

In summary this chapter describes the successful production of a MegCT-CD8 chimaeric protein and the strategies used to reach that point. Robust expression of the chimaeric protein is demonstrated in appropriately treated cells with some evidence that the chimaera adequately mimics native megalin. In these studies the pattern of constitutive and agonist stimulated MegCT-CD8 phosphorylation were very similar to the studies described in previous chapters.

7 PTC functional associations of MegCT phosphorylation.

7.1 Introduction.

Proteinuria is a hallmark of progressive renal disease and arises as a result of altered glomerular permselectivity and/or PTC handling of filtered proteins. A retrieval system of filtered proteins is mediated by the megalin/cubilin complex (Gekle, 2005). A number of cellular kinases regulate PTC albumin endocytosis *in vitro* including PKA, PKC (Gekle et al., 1997) and PI 3-kinase (Brunskill et al., 1998). The mechanism of inhibition or stimulation of each is not known but efficient endocytosis of albumin is dependent on the coordinated activity of a multimolecular complex that includes megalin/cubilin, CIC5, NHE-3 and the V-type H⁺ ATPase (Gekle, 2005). Kinases potentially could act on a number of these components with functional effects on albumin endocytosis. However, a number of the kinases that regulate endocytosis also mediate MegCT phosphorylation, and it may be that the two phenomena are functionally associated.

Albumin stimulates MegCT phosphorylation and also negatively regulates endocytic capacity of the PTC by reducing the number of albumin binding sites (Gekle et al., 1998). Furthermore, albumin has a differential effect on megalin expression *in vitro* dependent on its prevailing concentration (Caruso-Neves et al., 2006). At high concentrations of albumin, megalin is downregulated with the converse being true at low concentrations. The effect of albumin in inhibiting endocytosis is pleiotropic and involves inhibition of CIC-5 (Hryciw et al., 2003) and NHE-3 (Drumm et al., 2003, Lee et al., 2003). The net result is that a negative

feedback loop of albumin on its own endocytosis is well described but not fully mechanistically understood.

The endocytic function of megalin is likely to be significantly affected as a result of RIP. Whilst the precise cellular location where RIP occurs is unknown it is thought to be at the plasma membrane or early endosome (Biemesderfer, 2006). Conceivably, RIP at either sub-cellular location may inhibit the capacitance of the megalin mediated retrieval pathway by reducing intact apical megalin expression. The extracellular cleavage of megalin is the result of PKC stimulated MMP activity and thus altered activity of either enzyme could potentially affect albumin endocytosis.

Binding site number, and hence endocytic capacity is also regulated by receptor degradation. Endocytosed receptors can be targeted to the endosome and recycled back to the cell membrane or they can be degraded by the ubiquitin-proteasome pathway (Herschko and Ciechanover, 1998). Proteins destined for degradation are modified by a polyubiquitin tag attached to a lysine residue by a reaction catalysed by three types of ubiquitin ligase (E1, E2 and E3). This identifies proteins for proteolytic degradation in the barrel like core of the 20S complex of the proteasome (Herschko and Ciechanover, 1998). The proteosomal and endosomal/lysosomal pathways do not operate independently and there is flux between the two (Rocca et al., 2001). Moreover, ubiquitinylation does not always target proteins for degradation. Monoubiquitinylation can target proteins to the endosomal pathway and subsequently the lysosome (Melman et al., 2002, Longva et al., 2002). Ubiquitinylation is also a mechanism by which some transcriptional factors are activated (Kodadek, 2010).

7.2 Aim.

One of the best characterised features of the PTC is albumin endocytosis. The aim of these studies was to assess whether agents under the same conditions that stimulate MegCT phosphorylation, are functionally associated with a change in albumin uptake. A caveat is that these experiments also reflect that endocytosis is a product of the number of binding/uptake sites associated with the cell membrane. A further aim of these studies was to determine the effect of inhibiting the proteosomal degradative pathway on albumin endocytosis.

7.3 Methods.

7.3.1 The assay of endocytosis.

To investigate whether agents that were associated with a stimulation of MegCT phosphorylation were associated with any functional change within the cell, albumin endocytosis was examined. OK cells were selected for these experiments as they have previously been demonstrated to exhibit an avid endocytic capacity (Brunskill et al., 1996).

Cells were seeded at a density of 1.5×10^4 into 24 well plates such that a fully confluent monolayer was formed after 48 hours. For the 24 hours prior to experimentation cells were incubated in serum free media. Prior to stimulation cells were washed three times with an acidic Ringer's solution (pH 6.0) to strip cell monolayers of bound proteins. Cells were stimulated with relevant agents diluted in Ringer's solution at pH 7.4. The stimulating solution was then removed, the contents of the well washed once with Ringer's solution (pH 7.4) before being

incubated with FITC labelled BSA. In order to assess uptake, incubation proceeded at 37°C for 15 minutes whereas binding was measured by pre-chilling each plate to 4°C and then exposing to FITC-BSA at 4°C for 15 minutes. Unbound FITC was removed by washing each well 6 times with ice cold Ringer's (pH 7.4). Cell monolayers were lysed by the addition of 150µl of MOPS buffer. Cell associated fluorescence was measured using a Beckman spectrophotometer and each measurement corrected for cellular protein content.

7.4 Results.

7.4.1 Effect of agents that stimulate MegCT phosphorylation on albumin endocytosis.

Both EGF and PDBu significantly inhibited FITC-BSA endocytosis to 77 ± 1.4 and $48.1 \pm 3.5\%$ of control respectively (mean \pm SEM, n=3) (**Fig. 7.1**).

7.4.2 Effect of inhibitors of megalin RIP on endocytosis.

The extracellular cleavage of megalin mediated by PKC and MMP activity is likely to significantly impact on the endocytic function of megalin. Experiments were performed to investigate the effect of an MMP inhibitor on basal and phorbol ester mediated inhibition of FITC-BSA endocytosis.

Pre-incubation with 20 µM MMP13 inhibitor resulted in a small but significant increase in FITC-BSA uptake to $108.8 \pm 0.99\%$ that of control ($p \leq 0.05$). PMA (1 nM) reduced FITC-BSA uptake to $89.33 \pm 2.33\%$ of control whilst co-incubation

with MMP and PMA resulted in a non-significant reduction in FITC-BSA uptake to $93.67 \pm 1.76\%$ that of control (mean \pm SEM, n=3, one representative experiment of three) (**Fig. 7.2 A**). FITC-BSA binding at 4°C was not affected by pre-incubation with MMP-III inhibitor. When exposed to 100 $\mu\text{g/ml}$ FITC-BSA control cell associated fluorescence was 6.34 ± 0.36 RFU/ μg cell protein and in cells pre-incubated with MMP-III inhibitor it was 6.84 ± 0.36 RFU/ μg cell protein (mean \pm SEM, n=3, one representative experiment of three) (**Fig. 7.2 B**).

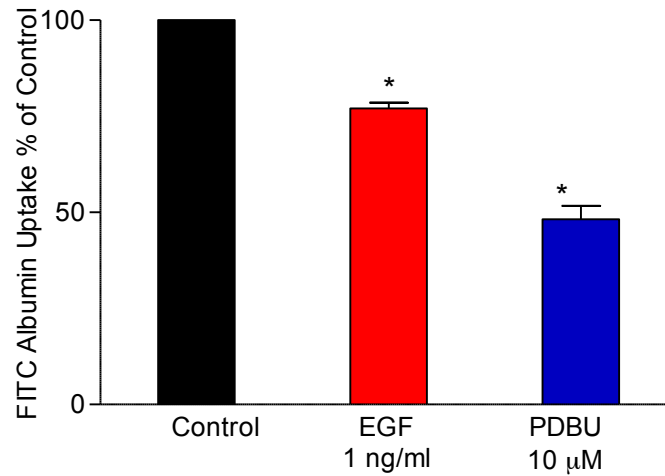


Figure 7.1 Effect of EGF and PDBU on FITC-BSA endocytosis. Monolayers of OK cells were incubated with 1 ng/ml EGF or 10 μM PDBU for 20 minutes. Stimulating solutions were replaced with 1 mg/ml FITC-BSA and uptake assessed after 15 minutes. In all experiments binding was measured by performing an identical experiment at 4°C and subtracting these values from uptake. Pre-incubation with EGF and PDBU significantly attenuated FITC-BSA uptake. (Means ± SEM, n=3. Data shown as percentage of control, mean ± SEM, n = 3, from one representative experiment of four. *= $p \leq 0.05$)

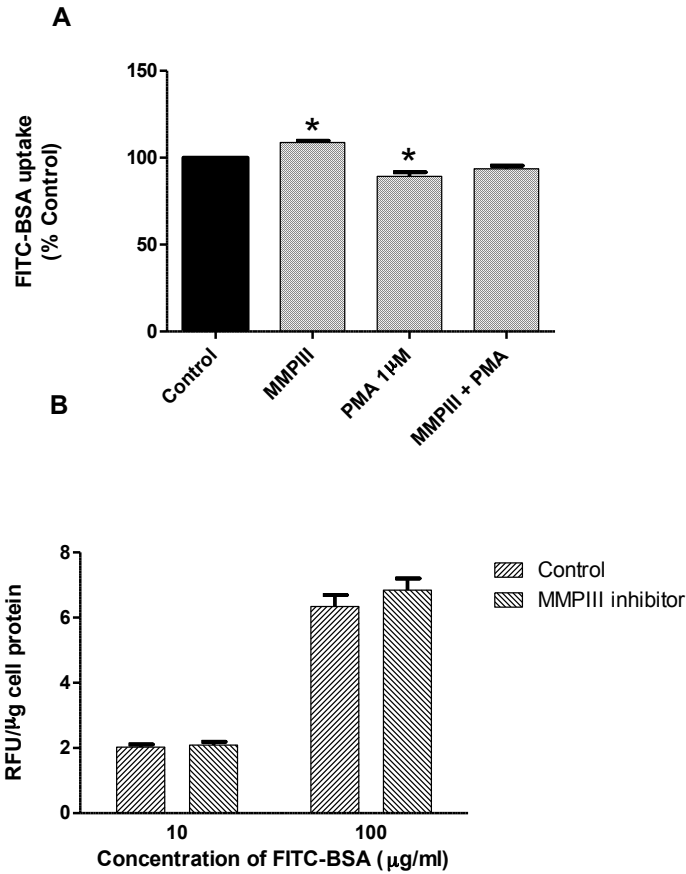


Figure 7.2 Pre-incubation of OK cells with MMPiII inhibitor, PMA and MMPiII + PMA. OK cell monolayers were pre-incubated for 60 minutes with MMPiII inhibitor or 20 minutes with PMA before stimulating solutions were replaced with 1 mg/ml of FITC-BSA. (i) FITC-BSA uptake MMPiII inhibitor augmented FITC-BSA whereas PMA had the opposite effect. In combination there was no significant difference from control (**A**). (ii) Binding. Pre-incubation with MMPiII inhibitor had no significant effect on FITC-BSA binding. Data shown as percentage of control, mean \pm SEM, n = 3, one representative experiment of three. *p \leq 0.05.

7.4.3 The effect of transient overexpression of MegCT-CD8 on albumin endocytosis.

As the agents used to stimulate MegCT phosphorylation may regulate a number of pathways relating to endocytosis the effect of specifically over-expressing MegCT was investigated.

At all concentrations of FITC-BSA tested there were no significant differences between the albumin uptake of cells transiently transfected with pCMV-Script, pCMV-CD8 or pCMV-MegCT-CD8 (**Fig. 7.3**). At a concentration of FITC-BSA of 100 µg/ml measured RFU values for pCMV-Script, pCMV-CD8 and pCMV-MegCT-CD8 expressing cells were 1301 ± 8.0 , 1469 ± 89.50 and 1377 ± 8.0 respectively (mean \pm SEM, n=3, one representative experiment of 2).

7.4.4 Investigations on OK cells stably expressing MegCT-CD8.

The transfection efficiency obtained when transiently expressing CD8-MegCT was low, and this may explain the lack of effect on FITC-albumin endocytosis of overexpressing MegCT. One strategy to counter this was the development of stably expressing MegCT-CD8 OK cell lines.

Cells stably expressing MegCT-CD8 demonstrated a statistically significant augmentation of albumin uptake compared to cells transfected with pCMV-Script alone or pCMV-CD8. Cells overexpressing MegCT-CD8 had an albumin uptake of $130.67 \pm 3.93\%$ ($p \leq 0.05$), compared to a value of $88.03 \pm 4.58\%$ (NS) in the CD8 overexpressing cell lines (mean \pm SEM, n=3, one experiment representative of three). To determine if this difference was the result of a change in FITC-BSA

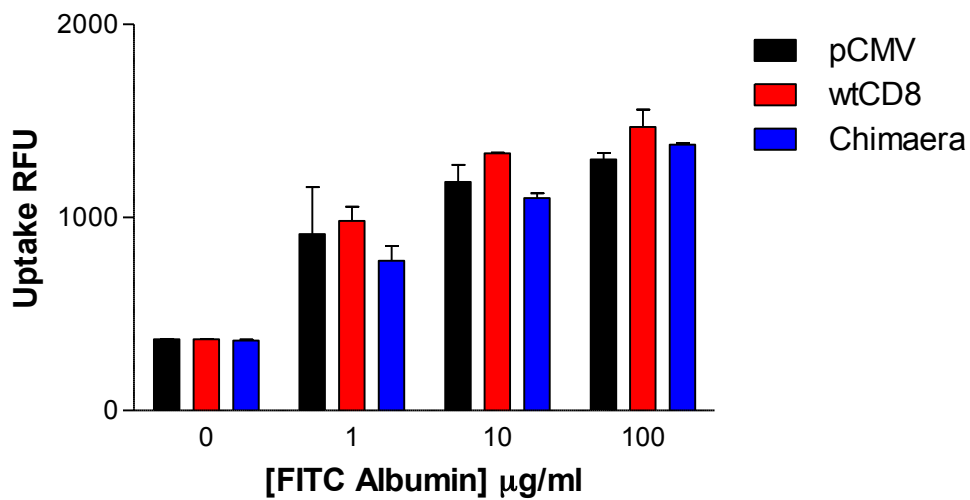
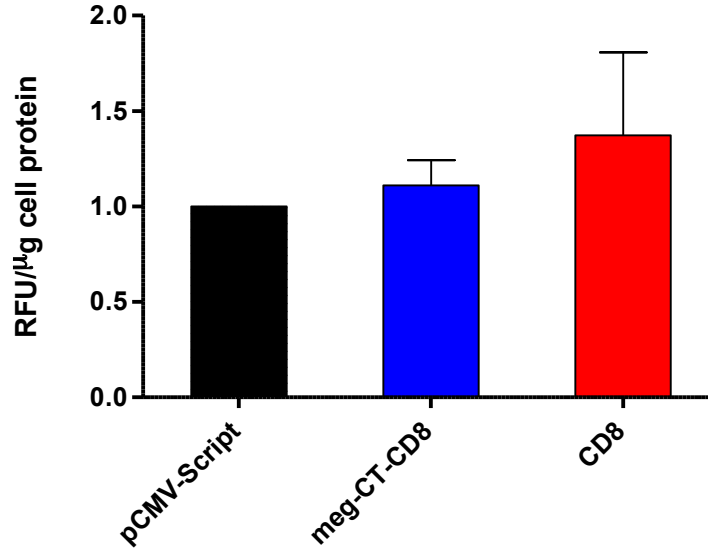


Figure 7.3 Transient transfection pCMV-Script, pCMV-CD8 and pCMV-MegCT-CD8 on FITC-BSA uptake. Transiently transfected OK cells were incubated with varying concentrations of FITC-BSA and uptake measured after 15 minutes. There was no significant difference between the three conditions across the range of FITC-BSA concentrations. Data shown mean \pm SEM, n=3. One representative experiment of two.

4



5

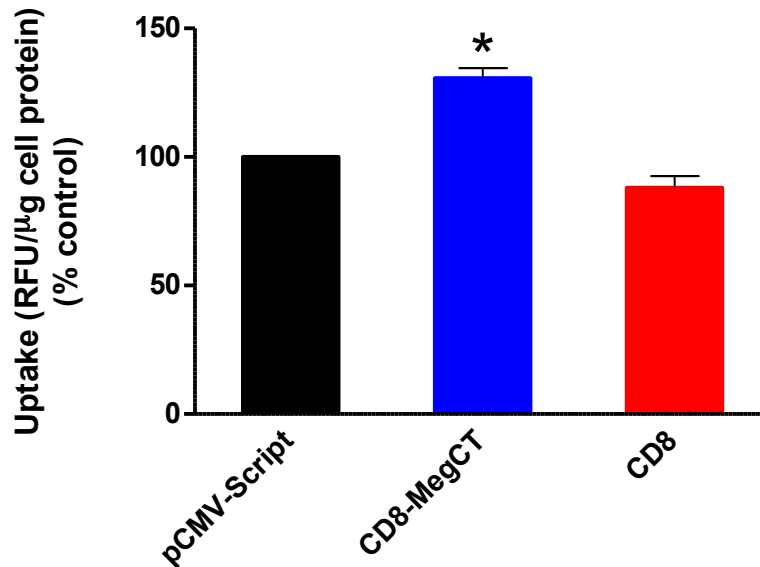


Figure 7.4 Effect of stable overexpression of MegCT-CD8 and CD8 on FITC-BSA binding and uptake. Confluent monolayers of stably transfected OK cells were incubated with 100 μg/ml FITC-BSA for 15 minutes. Binding. There were no significant differences in either condition relative to control (A). Uptake. Stable expression of MegCT-CD8 was associated with a significant augmentation of FITC-BSA uptake whereas CD8 was not significantly different from control (B). Data shown as percentage of control mean ± SEM, n = 3, one representative experiment of three. *p ≤ 0.05.

binding the data acquired at 4°C is shown (**Fig. 7.4 B**). This data is normally subtracted from total uptake to give a measure of FITC-BSA endocytosed. There were no significant differences in FITC-BSA bound to each cell line at 4°C. The binding of the empty vector transfected, MegCT-CD8 overexpressing and CD8 overexpressing cell lines were 0.98 ± 0.12 , 1.11 ± 0.13 and 1.37 ± 0.43 RFU/ μ g cell protein respectively (**Fig. 7.4 A**).

7.4.5 The role of the proteasome in albumin endocytosis.

The proteasome may have potentially significant effects on albumin endocytosis by regulating degradation of megalin and other members of the albumin endocytic complex. To investigate this cells were pre-incubated with the proteasomal inhibitor MG-132 prior to an assessment of FITC-BSA endocytosis.

Pre-incubation of OK cells with 6 μ M MG-132 significantly inhibited albumin endocytosis. This effect was apparent at all concentrations of MG-132 tested. At a concentration of 0.1 μ M FITC-BSA uptake was reduced to 0.37 ± 0.01 fold that of control. Of the concentrations of MG-132 tested a maximal effect was achieved at 10 μ M which reduced FITC-BSA uptake to 0.16 ± 0.02 fold that of control (**Fig. 7.5A**).

The effect of MG-132 on FITC-BSA binding was also assessed. There were no significant changes on FITC-BSA binding associated with pre-incubation with MG-132 (**Fig. 7.5B**).

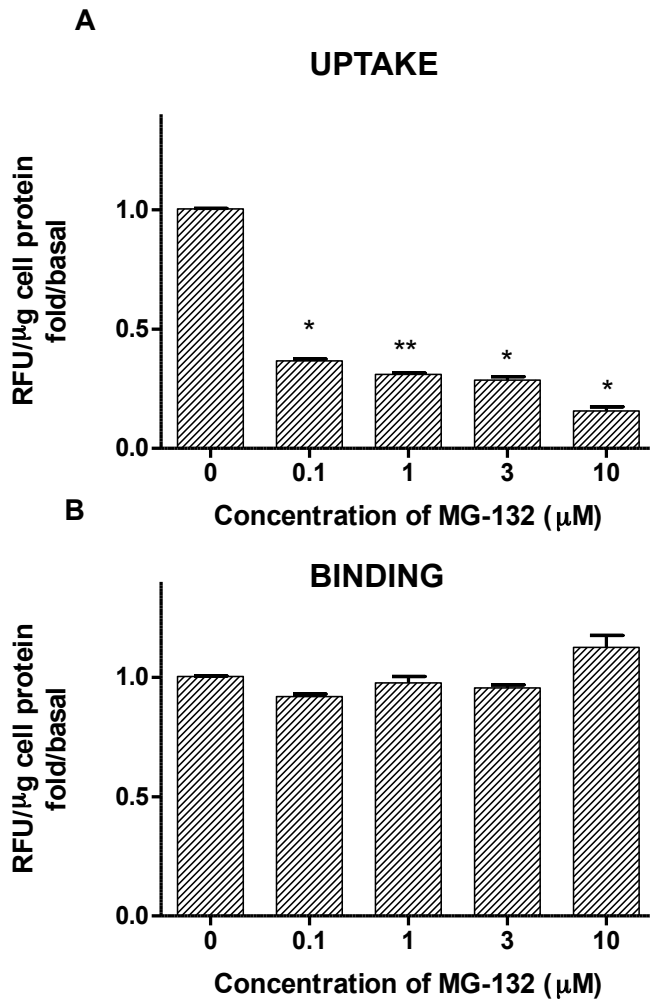


Figure 7.5 Proteosomal regulation of FITC-BSA endocytosis. Monolayers of OK cells were pre-incubated with varying concentrations of the proteasome inhibitor MG-132 for 90 minutes. The inhibitor was removed and an assay of FITC-BSA endocytosis or binding performed. **(A)** Uptake. At all concentrations of MG-132 tested there was a significant reduction in FITC-BSA uptake. **(B)** Binding. Pre-incubation with MG-132 had no effect on binding at any concentration tested. Data shown as fold/basal. Mean \pm SEM, $n = 3$, one representative experiment of three. * $p \leq 0.005$, ** $p \leq 0.001$.

7.5 Discussion.

This chapter describes experiments that suggest that agents that stimulate MegCT phosphorylation are associated with attenuated albumin endocytosis. At least in part the PKC mediated inhibition is a result of MMP mediated cleavage of the extracellular domain. Proteosomal activity is important in maintaining a fully functional endocytic apparatus, and this may regulate many components of the uptake process. There are inherent weaknesses in much of the study design that only enables associations to be made between observations. However, many of the findings are consistent with the published literature and are suggestive of useful future studies.

These studies use the OK cells which is a well characterised PTC line in which polarised cells form a confluent monolayer with tight junctions and display avid albumin endocytosis (Brunskill et al., 1997, Brunskill et al., 1998, Gekle et al., 1997). As always, caution must be applied when extrapolating the results of cell culture studies to whole animals. This is particularly as albumin uptake by PTC is ATP dependent which in the OK cell line is provided by glycolysis whereas anaerobic conditions predominate *in vivo* (Hall et al., 2010).

Constitutive phosphorylation mediated by GSK3 of MegCT of the serine in the PPPSP negatively regulates recycling of megalin by inhibiting traffic to the plasma membrane from recycling endosomes (Yuseff et al., 2007). The introduction of a point mutation changing PPPSP to PPPAP augments membrane association of truncated forms of megalin. This clearly suggests that megalin phosphorylation affects function and the studies described in this chapter indicate that

phosphorylation is an agonist mediated process. As MegCT might be phosphorylated at a number of other sites it would be interesting to develop mini-megalin receptors with point mutations at each site to observe the effect on receptor recycling.

These experiments were limited to establishing associations between agents that stimulate MegCT phosphorylation and endocytosis rather than developing mechanistic insights as to how the two phenomena are related. It is well described that PKC activity modulates albumin endocytosis (Gekle et al., 1997). PKC disassembles the actin cytoskeleton and depolymerises microtubules thereby inhibiting endocytosis. More sophisticated techniques indicate the effect of that PKC to be isoform dependent as PKC α augments endocytosis in PTC (Hryciw et al., 2005). The data presented here suggests that PKC is stimulating RIP of megalin via MMP activity and potentially reducing intact megalin at the cell surface. As pravastatin is another inhibitor of MMP this may be another mechanism by which HMG CoA reductase inhibitors reduce albumin endocytosis (Sidaway et al., 2004). An ELISA for the extracellular domain of megalin has been developed (Thraill et al., 2009). Using a similar technique it would be interesting to determine the effect of MMPIII inhibitors on release of the extracellular fragment of megalin.

The effect of EGF emphasises the role of multiple kinase activity on albumin endocytosis. Activated EGF-R stimulates PI 3-kinase (Hu et al., 1992) and PKB/Akt both of which stimulate albumin endocytosis (Brunskill et al., 1998, Caruso-Neves et al., 2005). The PI 3-kinase/Akt pathway phosphorylates and downregulates GSK3, an anticipated consequence of which is reduced constitutive

phosphorylation of megalin and augmented albumin endocytosis (Yuseff et al., 2007). NHE-3 activity is stimulated by EGF-R and PI 3-kinase activation (Khurana et al., 1996). Yet, the overall effect of EGF over the time course studied in these experiments is to diminish albumin endocytosis indicating that other, inhibitory pathways are also activated. Evidence supporting the existence of multiple pathways arises from the time courses of the different effects. The phosphorylation of MegCT stimulated by EGF is manifest after 20 minutes and hence this was the time point chosen to assay albumin endocytosis. In contrast the PKB mediated augmentation of albumin uptake peaks between 3 and 4 hours after stimulation (Caruso-Neves et al., 2005). Changes in the local concentrations of phosphoinositides modulate endocytosis (Carvou et al., 2007) and activation of phospholipase C- γ by EGF-R could result in such a change. Megalin and NHE-3 associate by an interaction that is likely to involve their cytoplasmic domains and megalin bound NHE-3 is inactive (Biemesderfer et al., 1999, Biemesderfer et al., 2001). In the short time course investigated in these experiments megalin may affect NHE-3 activity and endocytosis by changes to its phosphorylation status but in the longer term experiments described above down-regulation of megalin by albumin could increase NHE-3 activity. The distinction is acute regulation of megalin's function by phosphorylation is relatively transient but the long term effects are more relevant in the pathology of proteinuric nephrology.

Transient over-expression of MegCT in the form of a MegCT-CD8 chimeric protein had no effect on basal albumin endocytosis. The transfection efficiency was poor and if MegCT was having an effect the signal was lost in the noise of the non-transfected cells. Stably expressing MegCT-CD8 cell lines were developed that

demonstrated a small enhancement in albumin uptake. The mechanism of this is unclear from this data but it is possible to hypothesise that membrane associated MegCT-CD8 is acting as a decoy for kinase activity rendering native megalin relatively unphosphorylated and the endocytosis pathway more active. MegCT overexpression does not change the number of albumin binding sites and therefore, it is perhaps affecting traffic through the recycling endosomes. An interesting experiment would be to relate augmentation of albumin uptake to degree of MegCT overexpression across the different colonies of stably expressing cells.

Megalín recycling is dependent on the relative flux through the endosomal/lysosomal pathway versus the proteosomal pathway. The proteosomal inhibitor MG132 reduces albumin endocytosis in a concentration dependent fashion. One explanation would be that MG-132 is cytotoxic. This has been previously investigated in the host laboratory and cell viability is maintained at all concentrations tested in these experiments (Al-Rasheed et al., 2006). Reassuringly, the same observation has been made by another group who describe a 50% reduction in albumin uptake when OK cells are preincubated with MG-132 (Hryciw et al., 2004). Not only is albumin endocytosis dependent on proteosomal activity it is also stimulatory to it. Albumin stimulates proteosomal activity with a maximal effect at the physiological concentration of 10 µg/ml and falls off to baseline at higher concentrations. In OK cells MG-132 is associated with an accumulation of ubiquitin tagged CIC-5, proteosomal degradation of which is associated with an increase in total CIC-5 (Hryciw et al., 2004). Clearly this is very likely to be an operating mechanism in our studies too. Studies of MG-132 on

megalin trafficking and membrane expression in OK cells are hampered by the the lack of immunoreactivity between opossum native megalin and anti-human megalin sera. However, there is some evidence to suggest that the proteasome regulates megalin and NHE-3 cell surface expression as well. Over-expression of the intramembrane and cytoplasmic domain of megalin is not itself associated with a rise in concentration of the cytosolic tail of the protein (Li et al., 2008). This is only apparent when γ -secretase activity is stimulated and proteosomal activity is inhibited and therefore the proteasome is implicated in MegCT degradation. As one effect of MegCT is to negatively regulate megalin and NHE-3 expression, at least *in vitro*, this may be contributing to the diminished rate of albumin endocytosis in response to MG-132. However, as this effect would depend on reduced gene transcription and translation exposure of OK cells to MG-132 for 90 minutes makes this less plausible.

The rapid endocytosis and degradation of LRP1 is blocked by proteasome inhibitors and as a result cell surface expression increased (Melman et al., 2002). Mechanistically, this wasn't investigated further but the proteasome is an important regulator of activated EGF-R degradation. Proteosomal inhibition results in increased recycling of activated EGF-R via recycling endosomes (Longva et al., 2002). Megalin phosphorylation is associated with attenuated endocytosis and it may be that proteosomal inhibition increases phosphorylated megalin cell surface association by increasing both membrane bound megalin and EGF-R.

In summary, in the short time courses investigated in these experiments MegCT phosphorylation was functionally associated with reduced albumin endocytosis. Effort has been made not to over-interpret these findings as the potential sites for

kinase activity to regulate endocytosis are many and may, or may not involve megalin. Nevertheless, megalin phosphorylation may be an important point at which the short and long term effects of kinase activity on endocytosis diverge.

8 Determination of phosphorylation sites in MegCT.

8.1 Introduction.

The studies of MegCT phosphorylation to this point have essentially been descriptive with the kinase inhibitor data providing some mechanistic insights. To strengthen the findings by developing knowledge of the mechanistic and functional processes associated with MegCT phosphorylation we sought to produce a phosphopeptide map of the region.

8.2 Aim.

To determine the sites on which MegCT is phosphorylated and from that infer potential kinases that mediate phosphorylation and potential protein binding partners of megalin.

8.3 Methods

8.3.1 Phosphorylation of MegCT-GST by HK-2 cell lysate.

Phosphorylation of MegCT is mediated by kinases and potentially has functional consequences on protein/protein interaction. To investigate these further a phosphopeptide map of MegCT was produced. To ensure biological applicability the HK-2 immortalised human derived PTC line was used. HK-2 cells were grown to confluence in 6-well plates and quiesced overnight. Control or stimulated cell lysate was applied to MegCT-GST and treated exactly as in 3.1.3.5. Kinase activity was stimulated with kinase buffer containing 1mM of unlabelled ATP. Glutathione

beads were washed and collected as previously. MegCT-GST fusion proteins were separated by PAGE on a 10% gel and protein bands stained with coomassie blue. After destaining protein bands were excised from the gel and subjected to further analysis by the Protein and Nucleic Acid Laboratory (PNAACL) at the University of Leicester.

Protein bands excised from the gel were blocked with 0.5% polyvinylpyrrolidone in 0.6% acetic acid for 30 min at 37 °C before digestion with trypsin (1 µg) in 50 mM ammonium bicarbonate, overnight at 37 °C. Tryptic peptides were collected, dried in a rotary evaporator, and resuspended in 50% acetonitrile, 0.1% formic acid. Enrichment of phosphopeptides was carried out using titanium dioxide contained in a MonoTip according to the manufacturer's instructions, and the phosphopeptides were eluted in a solution of 5% ammonium hydroxide containing 20% acetonitrile. Where indicated, the enriched phosphopeptides were dried and resuspended in 10 mM Tris, pH 7.4, 10 mM CaCl₂ and subjected to further proteolytic digestion by the addition of 1 µg of chymotrypsin for 2 h at 25 °C.

8.3.2 LC-MS/MS.

LC-MS/MS was carried out upon each sample using a 4000 Q-Trap mass spectrometer. Peptides resulting from proteolytic digestion were loaded at high flow rate onto a reverse phase trapping column (0.3 mm inner diameter × 1 mm), containing 5 µM C18 300 Å Acclaim PepMap media and eluted through a reverse phase capillary column (75 µm inner diameter × 150 mm) containing Jupiter Proteo 4 µM 90 Å media (that was self-packed using a high pressure packing device. The output from the column was sprayed directly into the nanospray ion source of the

4000 Q-Trap mass spectrometer. The analysis was carried out in positive ion mode using data-dependent switching.

Fragment ion spectra generated by LC-MS/MS were searched using the MASCOT search tool against an updated copy of the SwissProt protein data base using appropriate parameters. The criteria for protein identification were based on the manufacturer's definitions (Perkins et al., 1999). Candidate peptides with probability-based Mowse scores exceeding threshold ($p < 0.05$), thus indicating a significant or extensive homology, were referred to as "hits." Protein scores were derived from peptide ion scores as a non-probability basis for ranking proteins.

For the phosphopeptides elucidated by MASCOT, individual MS/MS spectra were interrogated manually to validate both the peptide identity and position of assignment. In each case it was clear as to the identity of the peptide (and that the peptide was indeed phosphorylated), but for some MS/MS spectra it was not possible to validate the MASCOT assignment of the residue position for phosphorylation, because of low abundance of the required fragment ions. In these cases (because the sample amount was not limiting), the samples were repeated using multiple reaction monitoring inclusion lists comprising ion pairs consisting of the precursor ion $[M+2H]^{2+}$ and that of the neutral ion loss $[M+2H-H_3PO_4]^{2+}$, such that the MS/MS data were obtained over a longer time period (5.86 s), which resulted in significantly improved data quality. This allowed unambiguous assignment of the position of phosphorylation.

8.4 Results.

8.4.1 Identification of phospho-acceptor sites in MegCT.

To determine the sites of phosphorylation in MegCT mass spectrometry of a tryptic digest of MegCT-GST fusion protein was performed. MegCT-GST was phosphorylated *in vitro* by cell lysate derived from HK-2 cells from basal conditions or after stimulation with either HSA (1 mg/ml) or EGF(500 pg/ml). All serine/threonine containing peptides with allowance for up to two phosphorylation sites were scanned and Selected Reaction Monitoring (SRM) performed.

Four phosphorylated peptides were identified;

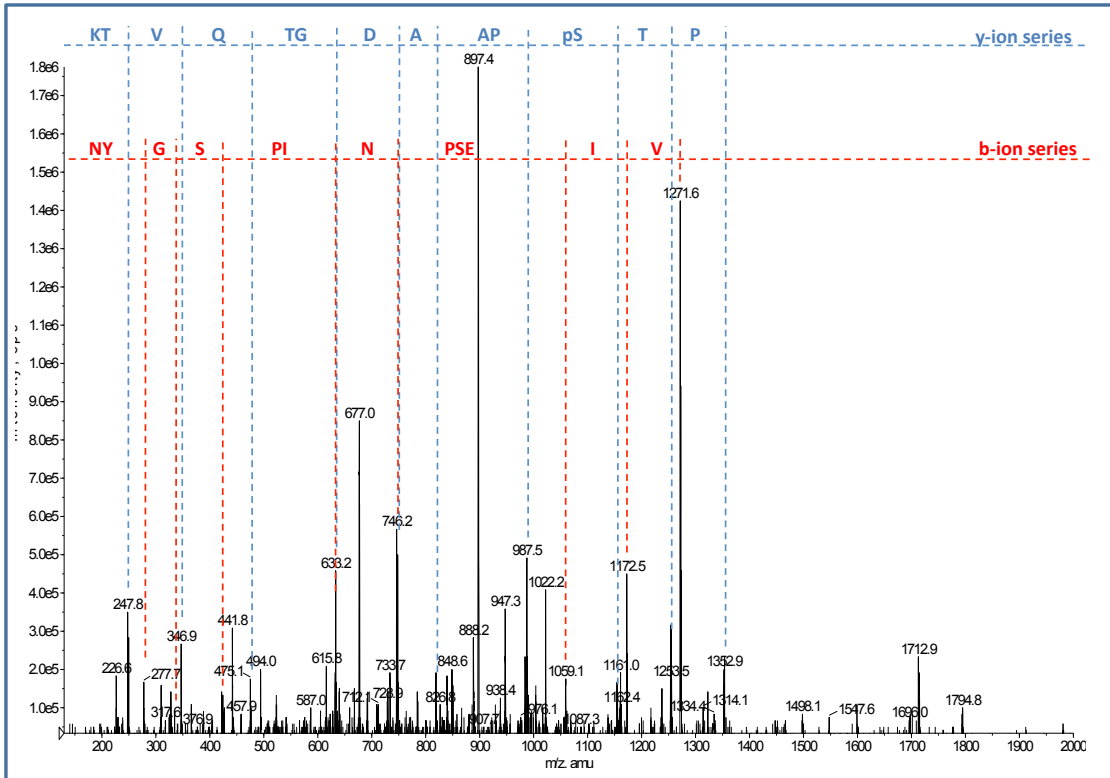
TG**S**LLPALPK - phosphorylated at the indicated position

DP**T****T**YSATEDTFK - phosphorylated at both of the two indicated positions

SGADLNMDIGV**S**GFGPETAIDR - phosphorylated at the indicated position

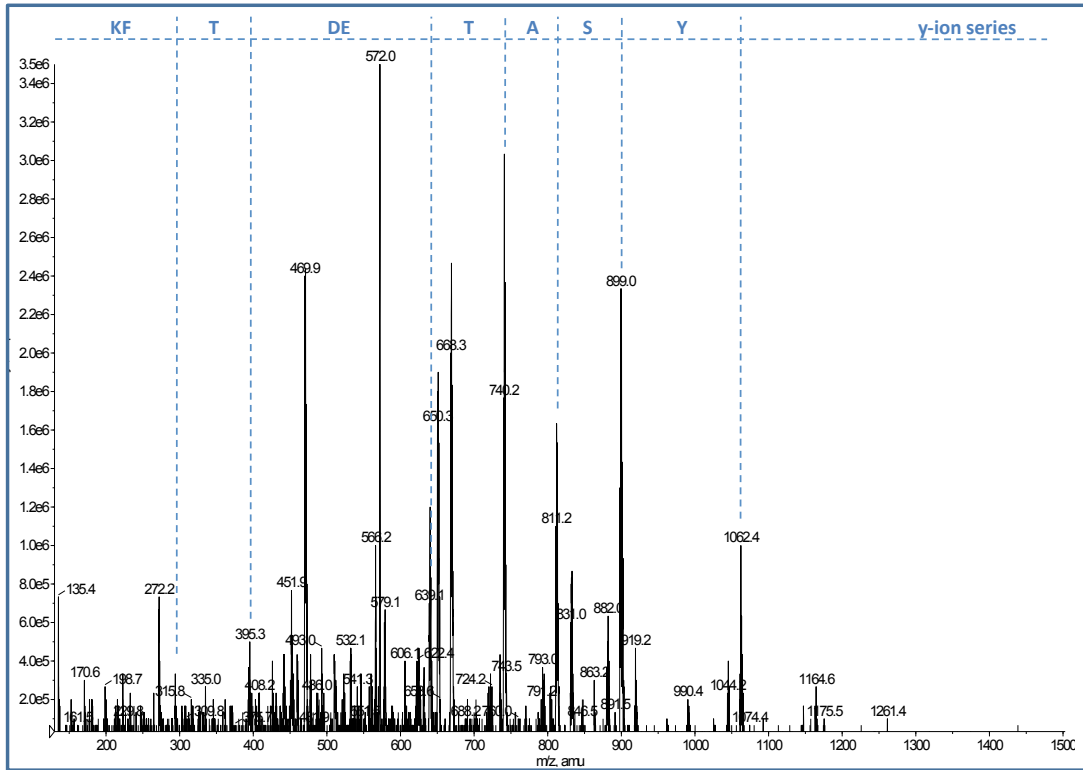
NYGSPINPSEIVPETNPT**S**PAADGTQVTK - phosphorylated at the indicated position

NYGSPINPSEIVPETNPTSPAADGTQVTK

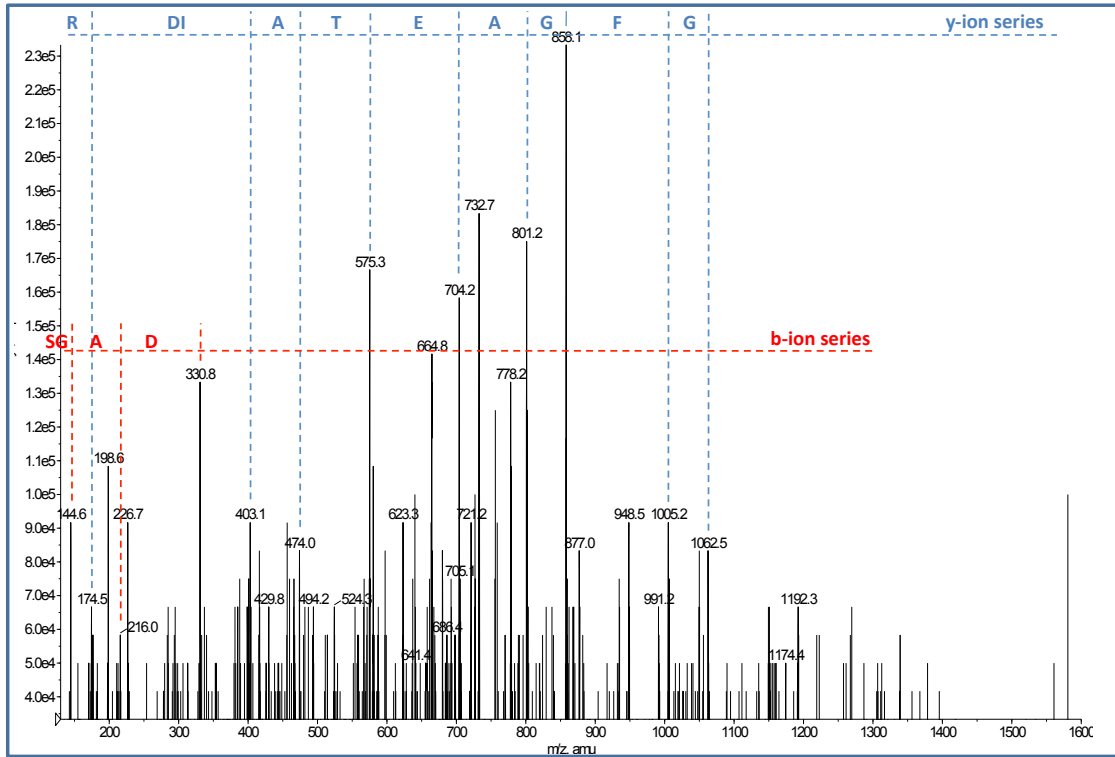


Figures 8.1-8.4. LC-MS/MS peptide sequencing identifies five phosphorylated residues in MegCT. Shown are three LC-MS/MS traces that identify the residue highlighted in red at the top of the trace as a site of phosphorylation.

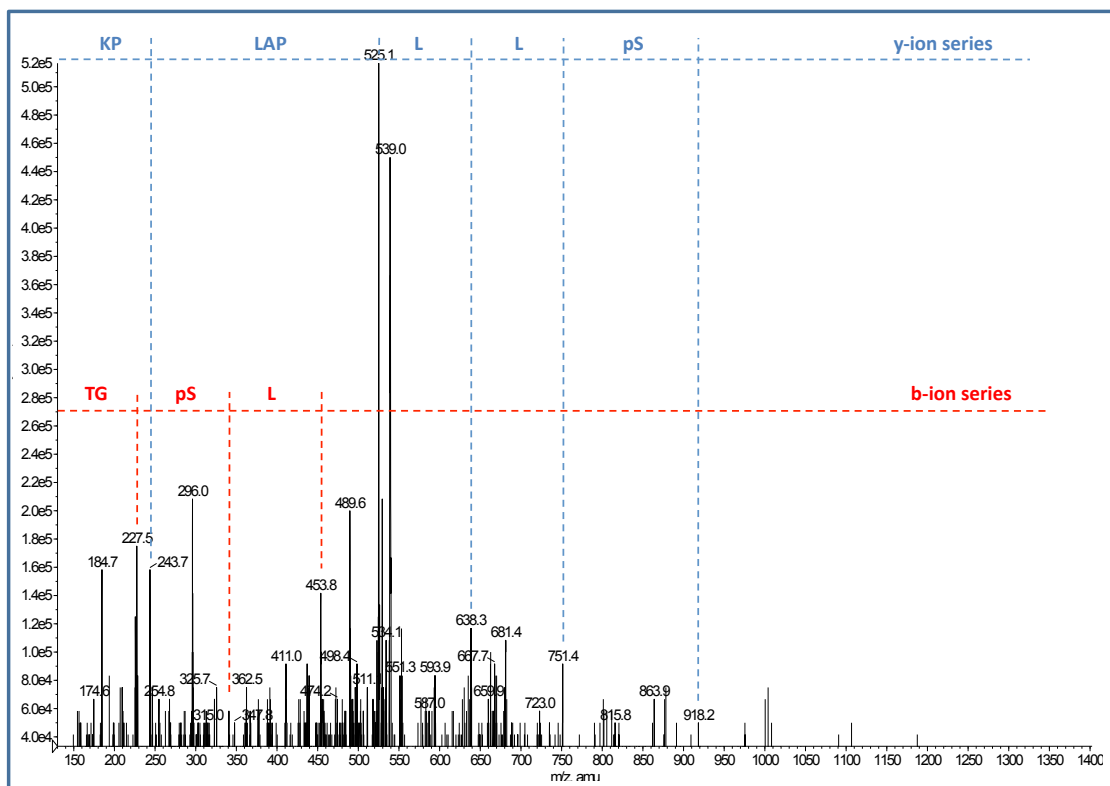
DPTPTYSATEDTFK



SGADLNMDIGVSGFGPETAIDR



TG**S**LLPALPK



HYRRTG**S**LLPALPKLPSLSSLVKPSENGNGVTFRSGADL
 NMDIGV**S**GFPGPETAIDRSMAMSEDFVMEMGKQPIIFENP
 MYSARDSAVKVVQPIQVTVSENVDNKNYGSPINPSEIVP
 ETNPT**S**PAADGTQVTKWNLFKRKSQTTNFENPIYAQME
 NEQKESVAATPPPSLPAKPKPPSRRD**P****T****P****T**YSATEDT
 FKDTANLVKEDSEV

Figure 8.5 Identified sites of phosphorylation in meg-CT. A composite of each individual phosphopeptide was constructed to demonstrate the phosphorylation sites identified in the megalin cytoplasmic tail. In total six sites of phosphorylation were identified which were Ser⁷, Ser⁴⁶, Ser¹²³, Ser¹⁷⁰, Thr¹⁸⁶ and Thr¹⁸⁸.

MS/MS spectra for each is shown (**Fig. 8.1 – 8.4**). Thus, phosphorylation was identified at residues Ser⁷, Ser⁴⁶, Ser¹²³, Ser¹⁷⁰, Thr¹⁸⁶ and Thr¹⁸⁸. These are shown in a composite figure of the 209 amino acids of MegCT in **Fig.8.5**.

8.5 Discussion.

Specific phosphorylation sites in MegCT are indicative of the responsible kinase and suggestive of potential binding partners regulated by the post-translational modification. To interrogate phosphorylation sites of MegCT MS/MS analysis of a tryptic digest of agonist stimulated MegCT-GST was performed. Seven sites of phosphorylation were identified, but, at present the technology does not extend to determining agonist dependent changes at each specific site. The tryptic digest inevitably leads to some very small peptides being generated that are lost for further analysis. Therefore, a full coverage of the peptide is not achievable and in these studies about 78% of the peptide was covered. In time, confirming the identified phosphorylation sites with phospho-specific antisera will need to be performed.

Constitutive phosphorylation of megalin at the PPPSP motif in the MDCK cell line occurs mainly as the result of GSK3 activity with a small contribution from PKC (Yuseff et al., 2007). Using a human derived-cell line our studies confirm this as a site of phosphorylation in human MegCT. The studies described in this thesis differ with respect to the number of phosphorylation sites in MegCT and the degree of phosphorylation that can be attributed to GSK3 at the PPPSP motif. In mini-megaline receptors transfected into CHO cells mutation of PPPSP to PPPAP virtually abolishes all phosphorylation. In contrast, our studies indicate at least five

other phosphorylation sites that may reflect the greater sensitivity of our approach using mass spectrometry. Mass spectrometry does not quantify phosphorylation at each site, however, it seems unlikely that having identified a number of phospho-acceptor sites the burden of phosphorylation will fall on one residue. In MDCK and CHO cells a mini-megalin receptor was almost exclusively phosphorylated by GSK3 at the sequence PPPSP. Taken together, the studies described in this thesis indicate a number of kinases acting at a number of sites are important in mediating MegCT phosphorylation. The differences between the studies may reflect the repertoire of kinases in hPTC, MDCK and CHO cells. It is difficult to reconcile the results of the two studies and overall, given their specificity of activity it seems unlikely that multiple kinases either all phosphorylate the same site or in unison, act through GSK3. Indeed, if this were the case it could be anticipated that the kinase inhibitors would have a more uniform inhibition of MegCT phosphorylation.

GSK3 is important in regulating cell fate and exerts a tonic inhibitory effect on pro-growth pathways (Kerkela et al., 2007). In PTC inhibition of GSK3 up-regulates PI 3-kinase, PKB and promotes cell survival (Sinha et al., 2005). As both GSK3 and PI 3-kinases mediate MegCT phosphorylation this reciprocal activity may be crucial to megalin's functional effects in PTC. This highlights a developing theme of competing pathways which determine cell fate and contain kinases that use MegCT as a substrate (as outlined in **Fig. 3.8**). The pattern of sites of MegCT phosphorylation is likely to be critical as it may be in a unique position to orchestrate the overall cellular response to competing influences. This argument is enhanced by the data provided from the phosphopeptide map of MegCT. The

phosphoserine residue at position 7 conforms to the sequence RXXpS/T that is a consensus sequence for phosphorylation by PKB. In addition two threonine residues in the sequence DPpTPpTY are sited in a consensus sequence for phosphorylation by ERK 1/2. Therefore, it could be that enhanced phosphorylation at RXXpS/T and diminished phosphorylation at DPpTPpTY favours cell survival with the converse leading to apoptosis. Much more work is needed to clarify the agonist specific phosphorylation sites of MegCT, and, whether these are dose dependent. Phospho-specific antibodies to different regions of MegCT may be very useful tools in performing such studies.

The overall aim of this study was to determine whether MegCT is a phospho-acceptor protein. None of the studies described confirm protein-protein interaction. However, the phosphopeptide map is suggestive of a number of potential binding partners. Furthermore, the phosphorylation sites identified in these studies suggests how interaction with existing binding partners may be regulated. These are clearly relevant to a consideration of megalin's function and are discussed below.

The response to MegCT phosphorylation is mediated by the protein-protein interactions that are initiated or terminated as a result of post-translational modification.

14-3-3 proteins have important roles in diverse cellular processes including protein trafficking, signal transduction, apoptosis and cell cycle regulation (Morrison, 2009). Phosphorylation of 14-3-3 proteins results in their dislodgement from binding partners and can allow other protein complexes to assemble. MegCT is phosphorylated at a serine residue in the sequence RRTGpSLL that conforms to

the sequence RXXXpSXP that is recognised by 14-3-3 proteins. Not all phosphorylation sites strictly conform to these motifs and the requirement of 14-3-3 protein binding for phosphorylation is variable but kinases involved in phosphorylation at these sites include PKA and PKB (Brunet et al., 1999). BAD binds 14-3-3 proteins and as a consequence its cytoplasmic release and pro-apoptotic activities are inhibited. In this respect 14-3-3 proteins could bridge MegCT and BAD in a PKB dependent fashion and anchor the latter to the cell membrane inhibiting apoptosis.

The JNK kinase pathway is activated in proteinuric nephropathy (de Borst et al., 2009). A consequence may be the phosphorylation of 14-3-3 proteins which releases BAD to the cytoplasm and promotes apoptosis (Sunayama et al., 2005). This could be part of a coordinated pathway as the JNK kinase interacting proteins (JIP) 1 and JIP-2 that promote JNK activity bind and could be sequestered by MegCT (Yasuda et al., 1999). The literature contains no reports of megalin binding 14-3-3 proteins, therefore the reality and functional significance of this potential interaction remains to be determined.

Megalin binding protein (MegBP) is a protein containing two tetratricopeptide repeats (TPR). These form an amphipathic helical structure that acts as a docking site in protein-protein interactions (Petersen et al., 2003, D'Andrea and Regan, 2003). MegBP is widely expressed including in the proximal tubule and overexpression results in a similar phenotype as that seen in megalin deficiency. Yet, overexpression does not alter the endocytic function of megalin (Petersen et al., 2003), and provides a point of divergence between an endocytic and cell regulating function of MegCT. The nature of that function may be gene

transcription regulation as an interacting partner of megBP is SKI-interacting partner (SKIP) which is a co-transcription activator of the vitamin D receptor (Zhang et al., 2001). Renal specific megalin deficiency is associated with a vitamin D deficiency phenotype and osteodystrophy suggesting the interaction between megalin, MegBP and SKIP is potentially biologically significant (Lehste et al., 2003). Whether by assembling complexes for transcriptional regulation following RIP of intact megalin or the controlled release of megBP/SKIP MegCT may have an important role in the process. By developing a series of truncation mutants a proline rich region of MegCT has been identified as the crucial area for megBP binding. The studies described in this chapter indicate a serine phospho-acceptor site is positioned -2 residues to the start of this region. Modulated binding at this site could compete with megBP/MegCT binding nearby or the phospho-serine could itself provide steric hinderance to megBP binding. Alternatively, the binding region of megBP was not mapped precisely and may involve the region including the (phospho-)serine residue.

This proline rich region is the site at which another binding partner of MegCT, ANKRA interacts. ANKRA contains ankyrin and in a murine T-cell line homodimerisation of an ANKRA-homologue RFXANK regulates Raf-1 kinase stimulated by EGF (Lin et al., 1999). ANKRA dimerisation could facilitate Raf-1 localisation to the MegCT and provide a link between the EGF signalling pathway and megalin. The ankyrin-3 protein is a novel binding partner for the p85 subunit of PI 3-kinase. Binding of ankyrin-3 to p85 results in enhanced PDGF-R degradation, and thus attenuates PDGF stimulated signalling (Ignatiuk et al., 2006). As a

potential link between EGF-R and Raf-1 kinase activity MegCT phosphorylation dependent ANKRA binding is clearly worthy of further investigation.

Serine⁷ occurs in the middle of a sequence that is important in sorting and regulation through the trans-golgi network. Phosphorylation at this site may regulate interaction with adapter proteins.(ELM, 2010). The regulation of binding to adapter proteins for endocytosis at this site could switch megalin from a signalling role to an endocytic function. This is a hypothetical observation based on a database search of protein like motifs with no experimental evidence to support such a function.

The regulation of RIP is also likely to be a mechanism by which megalin is switched from an endocytic function to a cell signalling role. In this respect there is uncertainty as to the region where gamma-secretase acts to release the cytosolic fragment of megalin during RIP. As the cytosolic fragment is almost an identical size to the anticipated mass of the terminal 209 amino acids of megalin cleavage must occur very close to the cell membrane at a region that might include the RXXpS/T region. Regulation of gamma-secretase activity in PTC is not well understood but potentially it may be initiated by a straightforward conformational change of megalin as a consequence extracellular domain cleavage. An additional regulator may be post-translational modification at the site of gamma-secretase activity.

The phosphorylation sites have been discussed in the context of known kinases or binding partners. However, a number of the described phosphorylation sites are in regions where the stimulating kinases cannot be inferred or binding partners suggested. In a number of systems it is recognised that basal phosphorylation

primes subsequent agonist driven kinase activity. Such priming phosphorylation events are important in the GSK-3 stimulated phosphorylation of beta-catenin (Liu et al., 2002).

To summarise, the phosphopeptide map generated enables associations to be made between sites of MegCT phosphorylation, kinases such as PKB that are recognised to be crucial to PTC function and a number of potential and recognised binding partners of megalin. As it stands, these associations are hypothetical but provides a rich source of hypothesis driven future investigation.

9 Final discussion, summary and indications for future work.

Albumin signals within PTC to stimulate a secretory and pro-inflammatory phenotype which dovetails with the histological changes that are characteristic of proteinuric nephropathy (Brunskill, 2004). The impetus to these studies was to link albumin's signalling effects to a novel cell regulatory function for one PTC receptor, megalin. Such a function has been postulated for megalin based on unique sequence motifs within its cytoplasmic tail (Saito et al., 1994, Hjalms et al., 1996) and the severe phenotype associated with megalin deficiency in humans and mice (Willnow et al., 1996a, Kantarci et al., 2007).

This thesis describes for the first time, clear evidence that megalin is phosphorylated in an agonist driven manner by agents implicated in proteinuric renal disease. Three different methods have been used, and whilst each alone has methodological inadequacies, mutually they are convincing. Preliminary studies indicate sites of phosphorylation and some of these sites are relevant to known binding partners of MegCT and relate to some of the described albumin stimulated effects in PTC.

Agonist stimulated and significant basal phosphorylation of MegCT has been shown of a MegCT-GST fusion protein, in immunoprecipitates of megalin from intact cells and of a MegCT-CD8 chimaeric protein. Phosphorylation of megalin is likely to be fundamental to the regulation of intracellular signalling cascades and

Table 9.1 Summary of major findings described in this thesis and indications for future work.

Finding	Future work
<p>Agonist regulated phosphorylation of:</p> <ul style="list-style-type: none"> • MegCT-GST fusion protein • MegCT in intact cells • A MegCT-CD8 chimaeric protein <p>Phosphorylation is mediated by multiple protein kinases including some activated by HSA in PTC.</p>	<p>Develop anti-phospho-MegCT antisera to:</p> <ul style="list-style-type: none"> • Demonstrate agonist specific sites of MegCT phosphorylation • Investigate relevance to human disease by examining megalin phosphorylation in human renal biopsy specimens <p>Examine megalin distribution in human renal biopsy specimens. Compare different proteinuric conditions to healthy kidney</p>
<p>EGF-R mediates phosphorylation of MegCT by:</p> <ul style="list-style-type: none"> • EGF • HSA 	<p>Examine effects of proteinuria on PTC EGF-R distribution. What is the effect of MegCT and phospho-MegCT overexpression on EGF-R derived signals? Is cleavage of the extracellular domain of megalin needed to elicit HSA mediated activation of EGF-R? Are ROS necessary for HSA stimulated MegCT phosphorylation and EGF-R activation?</p>
<p>Site specific phosphorylation of MegCT</p>	<p>Determine effect of site specific MegCT phosphorylation on binding partner interaction. Potentially use a combination of co-immunoprecipitation studies and proteomic analysis. What is the effect of site specific phosphorylation on RIP?</p>
<p>MegCT phosphorylation functionally associated with reduced albumin endocytosis</p>	<p>Introduce point specific mutations to MegCT to investigate the effect of each on megalin mediated endocytosis.</p>

studies performed entirely contemporaneously with the experiments described in this thesis confirm megalin to be phosphorylated on residues of its cytoplasmic tail. (Yuseff et al., 2007, Ammar and Closset, 2008).

The role of the basal phosphorylation has not been elucidated in these studies but one possibility is that constitutive phosphorylation functions to tonically activate intracellular signalling pathways that are beneficial to the cell. Under proteinuric conditions over-stimulation of these pathways or activation of antagonistic pathways results in cell damage. Alternatively, what isn't clear from these experiments, but will be investigated in the future is whether basal and agonist stimulated MegCT phosphorylation occur at the same sites. It could be that basal phosphorylation facilitates agonist stimulated MegCT modification as is the case for casein kinase I stimulated β -catenin phosphorylation (Liu et al., 2002). A contrary possibility is that basal phosphorylation inhibits further agonist stimulated change to prevent downstream activation of signalling pathways. Using mass spectrometry it may be possible to quantify phosphorylation of the four phosphopeptides derived from MegCT and quantify each relative to the other three. This approach does not enable quantification of phosphorylation of a phosphopeptide between for example HSA and EGF stimulated conditions but would be useful to address the above questions.

The studies presented in this thesis need to be extended to demonstrate relevance to human disease. Phosphorylated residues of megalin have been identified and phospho-specific antibodies could be produced to these regions of MegCT. One

utility of such antibodies would be in detecting if there were changes in the pattern of basal and agonist stimulated phosphorylation of MegCT-GST fusion protein and MegCT-CD8 chimeric receptor that were alluded to above. The same antibodies could also be used to examine patterns of megalin phosphorylation in renal biopsy specimens taken from individuals with proteinuric nephropathies versus healthy controls (i.e. tissue taken from the unaffected pole of renal cell carcinoma nephrectomy specimens). Phosphorylated MegCT would have to be related to total MegCT as megalin is also likely to be modulated in proteinuric renal disease based on *ex vivo* studies. The pattern of megalin distribution in renal biopsy samples from individuals with proteinuric nephropathies would itself, make an interesting study.

More mechanistic insight of MegCT phosphorylation and in particular the role of the EGF-R needs to be developed. The data presented in this thesis suggests a significant role for the EGF-R in stimulating megalin phosphorylation. This could be viewed as analogous to the PDGF-R stimulated phosphorylation of LRP-1 which is a mutually regulating process that dampens the PDGF derived signal in vascular smooth muscle cells (Boucher et al., 2003). If a parallel role were extended to the megalin/EGF-R partnership albumin induced megalin downregulation and EGF-R redistribution to the apical PTC surface seen under proteinuric conditions in cell culture studies could result in a significant augmentation of EGF stimulated signalling. The corollary of this would be to measure EGF-R derived signals in MegCT over-expressing cells. Based on the observation that LRP1 dampens PDGF signalling the hypothesis for such studies would be that MegCT overexpression will attenuate EGF-R derived signals. Loss of function of the EGF-

R is renoprotective (Terzi et al., 2000) and as EGF mediated MegCT phosphorylation is mediated via its receptor it could be concluded that megalin phosphorylation is deleterious to PTC. What is far from clear on the available evidence is whether megalin phosphorylation is part of a negative feedback loop that itself attenuates EGF (and other growth factor) stimulated pathways and clearly this needs to be understood. Overall, the interaction between megalin and the EGF-R may be a mechanism of pharmacologically regulating albumin endocytosis, megalin and EGF-R signalling which requires further investigation with the potential to develop novel pharmacological agents.

Functioning of the EGF-R is, in part responsible for the albumin induced phosphorylation of MegCT. Activation of the EGF-R by members of the EGF like family members often requires cleavage of membrane bound pre-cursors (Carpenter, 2000). In this respect the EGF type repeats within the megalin extracellular domain could be viewed as a membrane bound precursor and may be critical (Christensen et al., 2009). The RIP of megalin results in extracellular release of EGF-like repeats that in theory would be free to interact and activate the EGF-R. Whilst this theory is entirely speculative at the current time it could be investigated by a number of approaches including inhibiting cleavage of megalin, investigating albumin's effects in megalin deficient PTC, or inhibiting albumin binding to megalin by coincubating with the megalin antagonist RAP.

EGF-R is activated by ROS either as a result of EGF-R-ligand interaction or as the result of a cognate ligand interacting with other receptors such as members of the

haematopoietin receptor family (DeYulia et al., 2005). It may be that albumin-EGF-R or albumin-megalin interaction stimulates ROS production which activates the EGF-R. The dependence of EGF/albumin stimulated MegCT phosphorylation on superoxide generation could be relatively easily studied in the presence of extracellular catalase or using hydrogen peroxide.

The data presented in this thesis suggests that albumin stimulated effects are only partly dependent on the EGF-R. It would be interesting to perform comparative studies of the signalling actions of albumin in EGF-R expressing versus non-expressing cells. Albumin stimulated MegCT phosphorylation is also partly dependent on the MEK signalling pathway. The magnitude of the effects of AG1478 and PD98059 on albumin stimulated MegCT phosphorylation are different indicating that at least in part albumin activates MEK1 in an EGF-R independent way. This might be further investigated in EGF-R deficient but megalin expressing cells as the balance between albumin stimulated EGF-R dependent and independent pathways may be critical and could be altered under proteinuric conditions. In particular, albumin dose dependently affects the levels of membrane associated megalin and rates of PTC apoptosis (Caruso-Neves et al., 2006).

The role of megalin phosphorylation in regulating RIP is yet to be determined but an attractive hypothesis is that specific agents such as albumin may stimulate megalin phosphorylation and RIP which could govern the balance between an endocytic and cell regulatory function of megalin. Clearly, megalin's endocytic function is very important and ligand binding does not stimulate RIP following all, or even a majority of ligand binding events. It could be that regulated interaction of

other binding partners of MegCT governs whether RIP of megalin occurs, raising the possibility that MegCT could regulate the extracellular function of megalin.

Whilst a number of binding partners for MegCT have been identified in the literature the site and regulation of protein-MegCT interaction in many cases has not been studied. Furthermore, the list of MegCT binding partners constructed from the literature is unlikely to be complete. In particular, a potential regulated interaction between MegCT, 14-3-3 domain containing proteins and BAD warrants further study. Commercial antisera are available to conserved regions of 14-3-3 proteins and these could be used to confirm 14-3-3-MegCT interaction by GST fusion protein pulldown or chimeric MegCT-CD8 co-immunoprecipitation assays. Proteomic analysis could then be used to identify the 14-3-3 domain containing protein which would be a significant step in understanding the megalin regulated control of PTC apoptosis. Specific point mutations could be introduced to determine the importance of phosphorylated residues and the same approach could be used to investigate other hypothesis driven MegCT-protein interactions.

Functionally, megalin phosphorylation is associated with reduced albumin endocytosis which is consistent with the results of another study in a different cell type (Yuseff et al., 2007). This study examined the role of constitutive megalin phosphorylation compared with the agonist regulated association that this thesis describes. It would be intuitive, though unproven that inhibiting albumin endocytosis would be reno-protective. Uptake mediated by megalin may predispose the PTC to injury induced by the activation of intracellular signalling

pathways. Alternatively, limiting uptake by megalin/cubilin may increase flux through other pathways such as CD36 or the EGF-R with unpredictable consequences in terms of stimulating tubulointerstitial fibrosis. Currently, urinary protein loss is used as a measure of efficacy of ACE inhibitors or ARBs. A reduction in glomerular filtration of macromolecules reduces proteinuria and PTC exposure to injurious agents. If manipulation of megalin phosphorylation status and endocytic capacity is used as a therapeutic strategy proteinuria may increase and therefore treatment would need to be based on more nuanced biomarkers of PTC injury.

These studies were conducted at a time when the most clearly recognised function of megalin was to mediate cargo retrieval. It is still true that albumin endocytosis is a straightforward functional association to measure. However, the literature has developed and associations between MegCT phosphorylation and control of gene transcription, predominantly of megalin itself, and control of apoptotic rates of PTC are putative functions of MegCT that should fuel future studies. Phospho-site specific mutations could be introduced to determine which, if any, phosphorylation sites of MegCT are important in regulating megalin's endocytic function. Careful thought would need to be given as to how the experiments are to be conducted as over expression of megalin risks a 'dominant negative' effect over native megalin's function. This was suggested by the described studies of the effect on albumin endocytosis of stably over-expressing the MegCT-CD8 chimeric protein. Furthermore, there is emerging evidence that the control of forebrain development is dependent on the extra- and intracellular domains of megalin and that

overexpression of the latter is in itself, insufficient to rescue the holoprosencephalic phenotype of megalin deficient mice (Christ et al., 2010). This doesn't negate the signalling function of megalin but may reflect a delicate balance between MegCT phosphorylation and protein binding that could be disrupted by MegCT/transmembrane domain overexpression. Also, there is no *in vivo* evidence that MegCT/transmembrane domain over-expression is cleaved to release MegCT in the same way that native megalin is.

To summarise, these studies are the first description of constitutive and regulated MegCT phosphorylation on multiple sites in PTC. A number of kinases critical to this process have been identified, and functionally MegCT phosphorylation is associated with reduced albumin endocytosis and hence could impact on the progression of proteinuric nephropathy. Future studies should focus on the interaction between megalin and other PTC receptors, the regulation of MegCT-binding partner interaction and develop systems such that functional correlations of MegCT phosphorylation can be studied.

10 Appendices.

10.1 Appendix A – Buffers used in these studies.

PBS:

10 mM phosphate buffer
2.7 mM KCl
137 mM NaCl

Ringer's solution:

122.5 mM NaCl
5.4 mM KCl
1.2 mM CaCl₂
0.8 mM MgCl₂
0.8 mM Na₂HPO₄
0.2 mM NaH₂PO₄
5.5 mM glucose
10 mM HEPES

Gel loading buffer:

50 mM Tris (pH 6.8)
10 % glycerol
2 % sodium-dodecyl-sulphate (SDS)
200 mM dithiothreitol (DTT)

Electrophoresis running buffer:

25 mM Tris-base
250 mM glycine
10% SDS (w/v)

Transfer buffer:

48 mM Tris base
39 mM glycine
0.037 % SDS (w/v)
20% methanol
(pH not adjusted)

TBS buffer:

20 mM Tris base
500 mM NaCl

TBST buffer:

20 mM Tris base
500 mM NaCl
0.05 % Tween 20

Homogenisation buffer:

Mannitol 280 mM
HEPES 10 mM
KCl 10 mM
MgCl₂ 1 mM
pH 7.0 supplemented with 200 µl of Protease inhibitor cocktail III

Coomassie staining solution:

90% Methanol:distilled water 1:1
10% glacial acetic acid
0.2% brilliant colloidal blue

Coomassie destaining solution:

90% Methanol:distilled water 1:1
10% glacial acetic acid

SOC media

20 g bacto-tryptone
5 g yeast extract
0.5 g NaCl
Were added to a litre of a solution containing:
10 mM MgCl₂
2.5 mM KCl
20 mM glucose,
(pH 7.0)

2X YTA media (1L):

Tryptone 16 g/l
yeast extract 10 g/l
NaCl 5g/l
(pH 7.0)
100 µg/ml ampicillin

Alkaline copper sulphate reagent:

25 ml 2 % (w/v) Na₂CO₃/0.4 % (w/v) NaOH
250 µl 1 % (w/v) CuSO₄
250 µl K/Na Tartrate

JNK lysis buffer:

Tris-HCl pH 8.0
20mM, NP-40
0.5%, NaCl 250 mM
EDTA 3 mM
EGTA 3 mM:
Supplemented with;
PMSF 1 mM
Na₃VO₄ 2 mM
Protease Inhibitor Cocktail III diluted 1:25
DTT 1mM

TAE buffer:

40 mM Tris-acetate
1mM EDTA, pH 8.0

T4 ligase buffer (New England Biolabs):

50mM Tris-HCl (pH 7.5),
10 mM MgCl₂,
10 mM DTT
1 mM ATP
25 µg/ml BSA

T4 ligase buffer (Invitrogen):

250 mM Tris-HCl (pH 7.6),
50 mM MgCl₂
5 mM ATP
5 mM DTT
25% (v/w) polyethylene glycol 8000.

Krebs solution:

HEPES 10 mM,
NaCl 118 mM
KCl 4.3 mM

MgSO₄ 1.17 mM
CaCl₂ 1.3 mM
NaHCO₃ 0.34 mM
glucose 5.5 mM
pH 7.4

RIPA buffer:

1 x PBS
1% NP-40
0.5% sodium deoxycholate
0.1% SDS
PMSF 100 µg/ml
aprotinin 5 µg/ml
Na₃VO₄ 1 mM

MOPS buffer:

20 mM MOPS, pH 7.4
0.01% Triton X100)

Kinase Buffer:

HEPES, pH 7.2
20 mM, β-glycerophosphate, pH 7.2
MgCl₂ 10 mM
DTT 1 mM
Na₃VO₄ 50 µM

10.2 Appendix B. Vector maps of plasmids used in these studies.

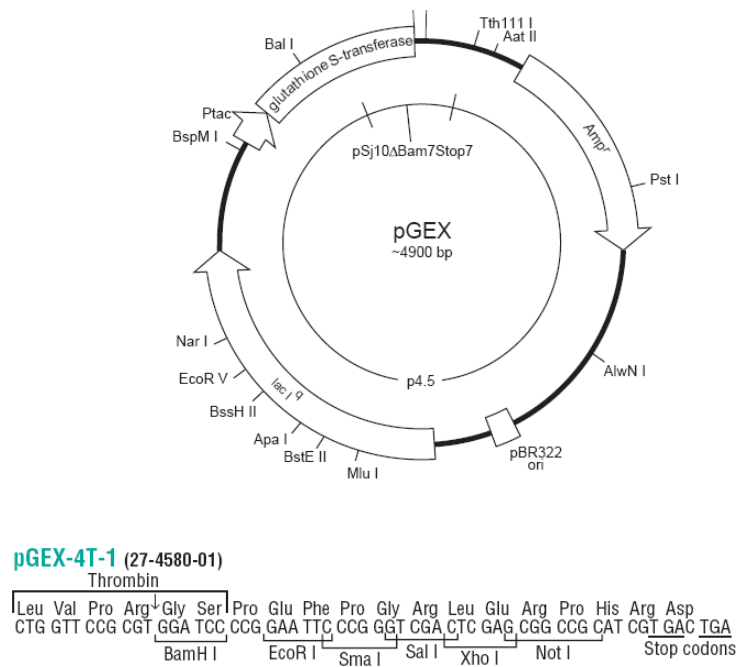
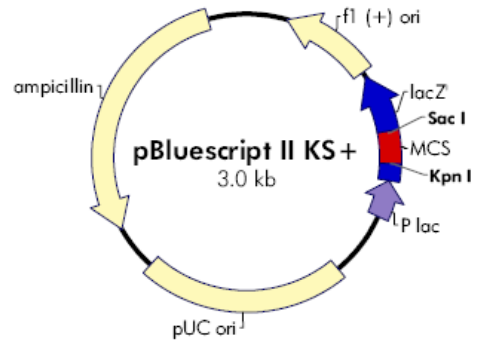


Figure 10.1 Map of the vector pGEX-4T1 showing the multiple cloning site (MCS). The meg-CT cDNA as supplied was ligated between the *EcoRI* and *XhoI* sites of the MCS. Successful bacterial transfection with pGEX-4T1 confers ampicillin resistance to competent bacteria.

f1 (+) origin 135–441
 β -galactosidase α -fragment 460–816
multiple cloning site 653–760
lac promoter 817–938
pUC origin 1158–1825
ampicillin resistance (*bla*) ORF 1976–2833



pBluescript II KS (+/-) Multiple Cloning Site Region (sequence shown 598–826)

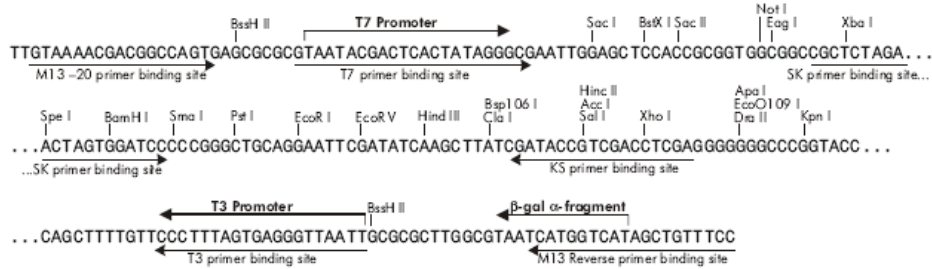
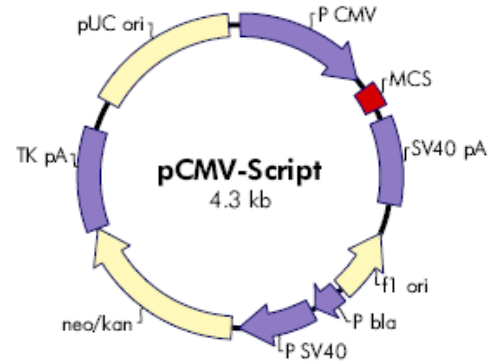


Figure 10.2 Vector map of the plasmid pBluescript II KS showing the multiple cloning site in more detail. BS-SKII-CD8 as supplied contained CD8 cDNA ligated between the *Hind*III and *Afl*III sites in the MCS. Successful bacterial transfection was manifested as ampicillin resistance of competent bacteria.

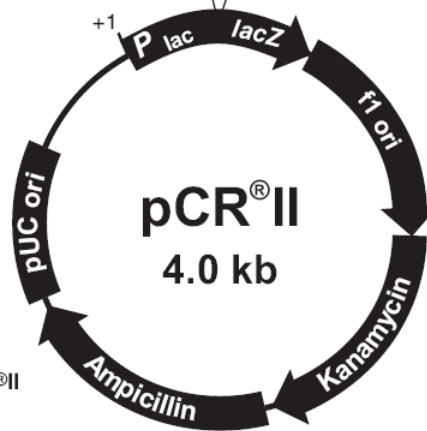
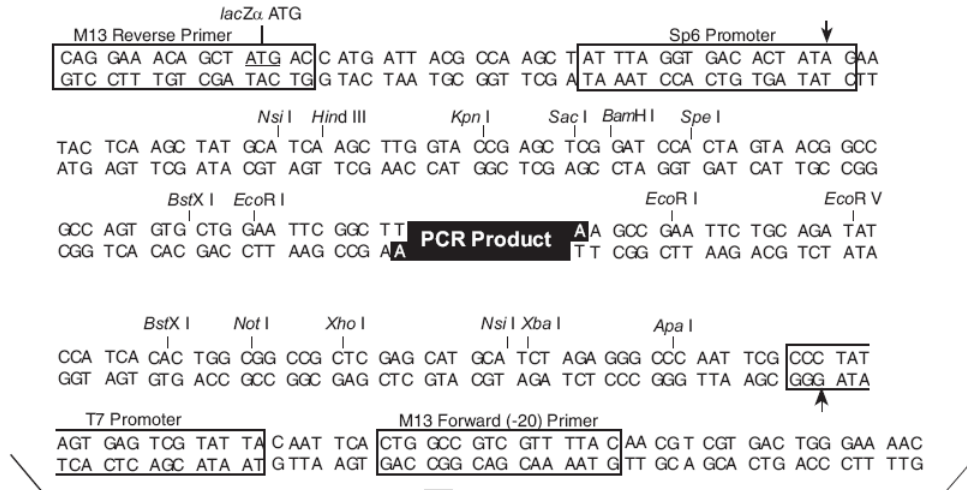
CMV promoter 1–602
 multiple cloning site 651–758
 SV40 polyA 811–1194
 f1 origin 1332–1638
 bla promoter 1663–1787
 SV40 promoter 1807–2145
 neomycin/kanamycin resistance ORF 2180–2971
 HSV-TK polyA 2972–3421
 pUC origin 3559–4226



pCMV-Script Multiple Cloning Site Region
(sequence shown 620–799)

T3 promoter
 AATTAACCCCTCACTAAAGGGAACAAAAGCTGGAGCTCCACC GCGGTGGCGGC CGCTCTA . . .
 Sac I BstX I Sac II Not I
 Srf I BamH I Pst I EcoR I EcoR V Hind III Acc I/Sal I
 . . . GCCCGGGCGGATCCCGGGCTGCA GGAATTCGATATCAAGCTTATCGATACCGTCGAC . . .
 Xho I Apa I Kpn I
 . . . CTCGAGGGGGGGCCCGGTACCAGGT AAGTGTACCCAATTCGCCCTATAGTGAGTCGTATTAC
 T7 promoter

Figure 10.3 Vector map of the plasmid pCMV-Script showing the multiple cloning site. The aim was to excise the fragment of DNA between the SacII and XhoI sites of the MCS. To create a re-circularised plasmid complementary ended CD8 and meg-CT cDNA would be ligated into the plasmid. Circular plasmid would confer kanamycin resistance to competent bacteria.



Comments for pCR®II
3971 nucleotides

LacZα gene: bases 1-587
M13 Reverse priming site: bases 205-221
Sp6 promoter: bases 239-256
T7 promoter: bases 404-423
M13 (-20) Forward priming site: bases 431-446
f1 origin: bases 588-1025
Kanamycin resistance ORF: bases 1359-2153
Ampicillin resistance ORF: bases 2171-3031
pUC origin: bases 3176-3849

Figure 10.4 Vector map of the sub-cloning vector pCRII showing the MCS. The vector is prepared such that topoisomerase is non-covalently linked to both termini of the MCS. *Taq* polymerase creates a PCR product with a 3' overhang that is complementary to the overhang of the vector. The topoisomerase catalyses the ligation of the PCR product into the vector. Bacterial transfection is manifested by ampicillin or kanamycin resistance.

11 References.

ABBATE, M., ZOJA, C., MORIGI, M., ROTTOLI, D., ANGIOLETTI, S., TOMASONI, S., ZANCHI, C., LONGARETTI, L., DONADELLI, R. & REMUZZI, G. (2002) Transforming growth factor-beta1 is up-regulated by podocytes in response to excess intraglomerular passage of proteins: a central pathway in progressive glomerulosclerosis. *Am J Pathol*, 161, 2179-93.

ABRAHAMSON, D. R. (1987) Structure and development of the glomerular capillary wall and basement membrane. *Am J Physiol*, 253, F783-94.

ADLER, A. I., STEVENS, R. J., MANLEY, S. E., BILOUS, R. W., CULL, C. A. & HOLMAN, R. R. (2003) Development and progression of nephropathy in type 2 diabetes: the United Kingdom Prospective Diabetes Study (UKPDS 64). *Kidney Int*, 63, 225-32.

AITKEN, A. (2006) 14-3-3 proteins: a historic overview. *Semin Cancer Biol*, 16, 162-72.

AKHTER, S., KOVBASNJUK, O., LI, X., CAVET, M., NOEL, J., ARPIN, M., HUBBARD, A. L. & DONOWITZ, M. (2002) Na(+)/H(+) exchanger 3 is in large complexes in the center of the apical surface of proximal tubule-derived OK cells. *Am J Physiol Cell Physiol*, 283, C927-40.

AL-RASHEED, N. M., WILLARS, G. B. & BRUNSKILL, N. J. (2006) C-peptide signals via Galpha i to protect against TNF-alpha-mediated apoptosis of opossum kidney proximal tubular cells. *J Am Soc Nephrol*, 17, 986-95.

ALBERTS, B. (2008) *Molecular biology of the cell*, New York, Garland Science.

ALEXOPOULOS, E., SERON, D., HARTLEY, R. B. & CAMERON, J. S. (1990) Lupus nephritis: correlation of interstitial cells with glomerular function. *Kidney Int*, 37, 100-9.

AMINOFF, M., CARTER, J. E., CHADWICK, R. B., JOHNSON, C., GRASBECK, R., ABDELAAL, M. A., BROCH, H., JENNER, L. B., VERROUST, P. J., MOESTRUP, S. K., DE LA CHAPELLE, A. & KRAHE, R. (1999) Mutations in CUBN, encoding the intrinsic factor-vitamin B12 receptor, cubilin, cause hereditary megaloblastic anaemia 1. *Nat Genet*, 21, 309-13.

AMMAR, H. & CLOSSET, J. L. (2008) Clusterin activates survival through the phosphatidylinositol 3-kinase/Akt pathway. *J Biol Chem*, 283, 12851-61.

ANDERSON, S., MEYER, T. W. & BRENNER, B. M. (1985a) The role of hemodynamic factors in the initiation and progression of renal disease. *J Urol*, 133, 363-8.

ANDERSON, S., MEYER, T. W., RENNKE, H. G. & BRENNER, B. M. (1985b) Control of glomerular hypertension limits glomerular injury in rats with reduced renal mass. *J Clin Invest*, 76, 612-9.

ANDERSON, S., RENNKE, H. G. & BRENNER, B. M. (1986) Therapeutic advantage of converting enzyme inhibitors in arresting progressive renal disease associated with systemic hypertension in the rat. *J Clin Invest*, 77, 1993-2000.

ANDREWS, P. M. (1977) A scanning and transmission electron microscopic comparison of puromycin aminonucleoside-induced nephrosis to hyperalbuminemia-induced proteinuria with emphasis on kidney podocyte pedicel loss. *Lab Invest*, 36, 183-97.

ANSELL, D., RODERICK, P., STEENKAMP, R. & TOMSON, C. R. (2010) UK Renal Registry 12th Annual Report (December 2009): Chapter 7: Survival and causes of death of UK adult patients on renal replacement therapy in 2008: national and centre-specific analyses. *Nephron Clin Pract*, 115 Suppl 1, c117-44.

ARAKI, S., HANEDA, M., KOYA, D., HIDAKA, H., SUGIMOTO, T., ISONO, M., ISSHIKI, K., CHIN-KANASAKI, M., UZU, T. & KASHIWAGI, A. (2007) Reduction in microalbuminuria as an integrated indicator for renal and cardiovascular risk reduction in patients with type 2 diabetes. *Diabetes*, 56, 1727-30.

ASCHENBRENNER, J. K., SOLLINGER, H. W., BECKER, B. N. & HULLETT, D. A. (2001) 1,25-(OH₂)D₃ alters the transforming growth factor beta signaling pathway in renal tissue. *J Surg Res*, 100, 171-5.

ASHWORTH, S. L., SOUTHGATE, E. L., SANDOVAL, R. M., MEBERG, P. J., BAMBURG, J. R. & MOLITORIS, B. A. (2003) ADF/cofilin mediates actin cytoskeletal alterations in LLC-PK cells during ATP depletion. *Am J Physiol Renal Physiol*, 284, F852-62.

ATKINS, R. C., BRIGANTI, E. M., LEWIS, J. B., HUNSICKER, L. G., BRADEN, G., CHAMPION DE CRESPIGNY, P. J., DEFERRARI, G., DRURY, P., LOCATELLI, F., WIEGMANN, T. B. & LEWIS, E. J. (2005) Proteinuria reduction and progression to renal failure in patients with type 2 diabetes mellitus and overt nephropathy. *Am J Kidney Dis*, 45, 281-7.

BABOOLAL, K., MCEWAN, P., SONDHI, S., SPIEWANOWSKI, P., WECHOWSKI, J. & WILSON, K. (2008) The cost of renal dialysis in a UK setting--a multicentre study. *Nephrol Dial Transplant*, 23, 1982-9.

BARNES, H., ACKERMANN, E. J. & VAN DER GEER, P. (2003) v-Src induces Shc binding to tyrosine 63 in the cytoplasmic domain of the LDL receptor-related protein 1. *Oncogene*, 22, 3589-97.

BARNES, H., LARSEN, B., TYERS, M. & VAN DER GEER, P. (2001) Tyrosine-phosphorylated low density lipoprotein receptor-related protein 1 (Lrp1) associates with the adaptor protein SHC in SRC-transformed cells. *J Biol Chem*, 276, 19119-25.

BASNAYAKE, K., YING, W. Z., WANG, P. X. & SANDERS, P. W. (2010) Immunoglobulin Light Chains Activate Tubular Epithelial Cells through Redox Signaling. *J Am Soc Nephrol*, 21, 1165-73.

BAZZI, C., PETRINI, C., RIZZA, V., ARRIGO, G., NAPODANO, P., PAPARELLA, M. & D'AMICO, G. (2002) Urinary N-acetyl-beta-glucosaminidase excretion is a marker of tubular cell dysfunction and a predictor of outcome in primary glomerulonephritis. *Nephrol Dial Transplant*, 17, 1890-6.

BEDARD, K. & KRAUSE, K. H. (2007) The NOX family of ROS-generating NADPH oxidases: physiology and pathophysiology. *Physiol Rev*, 87, 245-313.

BIEMESDERFER, D. (2006) Regulated intramembrane proteolysis of megalin: linking urinary protein and gene regulation in proximal tubule? *Kidney Int*, 69, 1717-21.

BIEMESDERFER, D., DEGRAY, B. & ARONSON, P. S. (2001) Active (9.6 s) and inactive (21 s) oligomers of NHE3 in microdomains of the renal brush border. *J Biol Chem*, 276, 10161-7.

BIEMESDERFER, D., NAGY, T., DEGRAY, B. & ARONSON, P. S. (1999) Specific association of megalin and the Na⁺/H⁺ exchanger isoform NHE3 in the proximal tubule. *J Biol Chem*, 274, 17518-24.

BIRN, H., FYFE, J. C., JACOBSEN, C., MOUNIER, F., VERROUST, P. J., ORSKOV, H., WILLNOW, T. E., MOESTRUP, S. K. & CHRISTENSEN, E. I. (2000a) Cubilin is an albumin binding protein important for renal tubular albumin reabsorption. *J Clin Invest*, 105, 1353-61.

BIRN, H., VORUM, H., VERRONST, P. J., MOESTRUP, S. K. & CHRISTENSEN, E. I. (2000b) Receptor-associated protein is important for normal processing of megalin in kidney proximal tubules. *J Am Soc Nephrol*, 11, 191-202.

BOHLE, A., CHRIST, H., GRUND, K. E. & MACKENSEN, S. (1979) The role of the interstitium of the renal cortex in renal disease. *Contrib Nephrol*, 16, 109-14.

BOHLE, A., MACKENSEN-HAEN, S., GISE, H. V., GRUND, K. E. & WEHRMANN, M. (1991) *The consequences of the tubulointerstitial changes for renal function in glomerulopathies: a morphometric and cytological analysis*, Kluwer Press, Boston.

BOTTINGER, E. P. & BITZER, M. (2002) TGF-beta signaling in renal disease. *J Am Soc Nephrol*, 13, 2600-10.

BOUCHER, P., GOTTHARDT, M., LI, W. P., ANDERSON, R. G. & HERZ, J. (2003) LRP: role in vascular wall integrity and protection from atherosclerosis. *Science*, 300, 329-32.

BOUCHER, P., LIU, P., GOTTHARDT, M., HIESBERGER, T., ANDERSON, R. G. & HERZ, J. (2002) Platelet-derived growth factor mediates tyrosine phosphorylation of the cytoplasmic domain of the low Density lipoprotein receptor-related protein in caveolae. *J Biol Chem*, 277, 15507-13.

BOURDEAU, J. E., CARONE, F. A. & GANOTE, C. E. (1972) Serum albumin uptake in isolated perfused renal tubules. Quantitative and electron microscope radioautographic studies in three anatomical segments of the rabbit nephron. *J Cell Biol*, 54, 382-98.

BRENNER, B. M., COOPER, M. E., DE ZEEUW, D., KEANE, W. F., MITCH, W. E., PARVING, H. H., REMUZZI, G., SNAPINN, S. M., ZHANG, Z. & SHAHINFAR, S. (2001) Effects of losartan on renal and cardiovascular outcomes in patients with type 2 diabetes and nephropathy. *N Engl J Med*, 345, 861-9.

BRENNER, B. M. & ZAGROBELNY, J. (2003) Clinical renoprotection trials involving angiotensin II-receptor antagonists and angiotensin-converting-enzyme inhibitors. *Kidney Int Suppl*, S77-85.

BREYER, J. A., BAIN, R. P., EVANS, J. K., NAHMAN, N. S., JR., LEWIS, E. J., COOPER, M., MCGILL, J. & BERL, T. (1996) Predictors of the progression of renal insufficiency in patients with insulin-dependent diabetes and overt diabetic nephropathy. The Collaborative Study Group. *Kidney Int*, 50, 1651-8.

BRUNET, A., BONNI, A., ZIGMOND, M. J., LIN, M. Z., JUO, P., HU, L. S., ANDERSON, M. J., ARDEN, K. C., BLENIS, J. & GREENBERG, M. E. (1999) Akt promotes cell survival by phosphorylating and inhibiting a Forkhead transcription factor. *Cell*, 96, 857-68.

BRUNSKILL, N., BASTANI, B., HAYES, C., MORRISSEY, J. & KLAHR, S. (1991) Localization and polar distribution of several G-protein subunits along nephron segments. *Kidney Int*, 40, 997-1006.

BRUNSKILL, N. J. (2004) Albumin signals the coming of age of proteinuric nephropathy. *J Am Soc Nephrol*, 15, 504-5.

BRUNSKILL, N. J., COCKCROFT, N., NAHORSKI, S. & WALLS, J. (1996) Albumin endocytosis is regulated by heterotrimeric GTP-binding protein G alpha i-3 in opossum kidney cells. *Am J Physiol*, 271, F356-64.

BRUNSKILL, N. J., NAHORSKI, S. & WALLS, J. (1997) Characteristics of albumin binding to opossum kidney cells and identification of potential receptors. *Pflugers Arch*, 433, 497-504.

BRUNSKILL, N. J., STUART, J., TOBIN, A. B., WALLS, J. & NAHORSKI, S. (1998) Receptor-mediated endocytosis of albumin by kidney proximal tubule cells is regulated by phosphatidylinositide 3-kinase. *J Clin Invest*, 101, 2140-50.

BULGER, S. C. H. A. R. E. (1988) *Structural-functional relationships in the kidney*, Little, Brown and Co. Boston.

BURTON, C. J., COMBE, C., WALLS, J. & HARRIS, K. P. (1996) Fibronectin production by human tubular cells: the effect of apical protein. *Kidney Int*, 50, 760-7.

BYRNE, C., FORD, D., GILG, J., ANSELL, D. & FEEHALLY, J. (2010a) UK Renal Registry 12th Annual Report (December 2009): Chapter 3: UK ESRD incident rates in 2008: national and centre-specific analyses. *Nephron Clin Pract*, 115 Suppl 1, c9-39.

BYRNE, C., STEENKAMP, R., CASTLEDINE, C., ANSELL, D. & FEEHALLY, J. (2010b) UK Renal Registry 12th Annual Report (December 2009): Chapter 4: UK ESRD prevalent rates in 2008: national and centre-specific analyses. *Nephron Clin Pract*, 115 Suppl 1, c41-67.

CAMERON, J. S. (1989) Immunologically mediated interstitial nephritis: primary and secondary. *Adv Nephrol Necker Hosp*, 18, 207-48.

CANTLEY, L. C. (2002) The phosphoinositide 3-kinase pathway. *Science*, 296, 1655-7.

CARPENTER, G. (2000) EGF receptor transactivation mediated by the proteolytic production of EGF-like agonists. *Sci STKE*, 2000, pe1.

CARUSO-NEVES, C., KWON, S. H. & GUGGINO, W. B. (2005) Albumin endocytosis in proximal tubule cells is modulated by angiotensin II through an AT2 receptor-mediated protein kinase B activation. *Proc Natl Acad Sci U S A*, 102, 17513-8.

CARUSO-NEVES, C., PINHEIRO, A. A., CAI, H., SOUZA-MENEZES, J. & GUGGINO, W. B. (2006) PKB and megalin determine the survival or death of renal proximal tubule cells. *Proc Natl Acad Sci U S A*, 103, 18810-5.

CARVOU, N., NORDEN, A. G., UNWIN, R. J. & COCKCROFT, S. (2007) Signalling through phospholipase C interferes with clathrin-mediated endocytosis. *Cell Signal*, 19, 42-51.

CESSAC-GUILLEMET, A. L., MOUNIER, F., BOROT, C., BAKALA, H., PERICHON, M., SCHAEVERBEKE, M. & SCHAEVERBEKE, J. (1996) Characterization and distribution of albumin binding protein in normal rat kidney. *Am J Physiol*, 271, F101-7.

CHANA, R. S., SIDAWAY, J. E. & BRUNSKILL, N. J. (2008) Statins but not thiazolidinediones attenuate albumin-mediated chemokine production by proximal tubular cells independently of endocytosis. *Am J Nephrol*, 28, 823-30.

CHANUTIN A, F. E. (1932) Experimental renal insufficiency produced by partial nephrectomy. *Archives of Internal Medicine*, 49, 767-787.

CHEN, W. J., GOLDSTEIN, J. L. & BROWN, M. S. (1990) NPXY, a sequence often found in cytoplasmic tails, is required for coated pit-mediated internalization of the low density lipoprotein receptor. *J Biol Chem*, 265, 3116-23.

CHRIST, A., TERRY, S., SCHMIDT, V., CHRISTENSEN, E. I., HUSKA, M. R., ANDRADE-NAVARRO, M. A., HUBNER, N., DEVUYST, O., HAMMES, A. & WILLNOW, T. E. (2010) The soluble intracellular domain of megalin does not affect renal proximal tubular function *in vivo*. *Kidney Int*, epub.

CHRISTENSEN, E. I. & BIRN, H. (2002) Megalin and cubilin: multifunctional endocytic receptors. *Nat Rev Mol Cell Biol*, 3, 256-66.

CHRISTENSEN, E. I., BIRN, H., VERRAUST, P. & MOESTRUP, S. K. (1998) Membrane receptors for endocytosis in the renal proximal tubule. *Int Rev Cytol*, 180, 237-84.

CHRISTENSEN, E. I., DEVUYST, O., DOM, G., NIELSEN, R., VAN DER SMISSEN, P., VERRAUST, P., LERUTH, M., GUGGINO, W. B. & COURTOY, P. J. (2003) Loss of chloride channel CIC-5 impairs endocytosis by defective trafficking of megalin and cubilin in kidney proximal tubules. *Proc Natl Acad Sci U S A*, 100, 8472-7.

CHRISTENSEN, E. I. & MAUNSBACH, A. B. (1974) Intralysosomal digestion of lysozyme in renal proximal tubule cells. *Kidney Int*, 6, 396-407.

CHRISTENSEN, E. I. & NIELSEN, S. (1991) Structural and functional features of protein handling in the kidney proximal tubule. *Semin Nephrol*, 11, 414-39.

CHRISTENSEN, E. I., NIELSEN, S., MOESTRUP, S. K., BORRE, C., MAUNSBACH, A. B., DE HEER, E., RONCO, P., HAMMOND, T. G. & VERRAUST, P. (1995) Segmental distribution of the endocytosis receptor gp330 in renal proximal tubules. *Eur J Cell Biol*, 66, 349-64.

CHRISTENSEN, E. I., VERRAUST, P. J. & NIELSEN, R. (2009) Receptor-mediated endocytosis in renal proximal tubule. *Pflugers Arch*, 458, 1039-48.

CLAPP, W. L., PARK, C. H., MADSEN, K. M. & TISHER, C. C. (1988) Axial heterogeneity in the handling of albumin by the rabbit proximal tubule. *Lab Invest*, 58, 549-58.

COBB, M. H., HEPLER, J. E., CHENG, M. & ROBBINS, D. (1994) The mitogen-activated protein kinases, ERK1 and ERK2. *Semin Cancer Biol*, 5, 261-8.

COLLINS, B. M., MCCOY, A. J., KENT, H. M., EVANS, P. R. & OWEN, D. J. (2002) Molecular architecture and functional model of the endocytic AP2 complex. *Cell*, 109, 523-35.

COMPER, W. D., HARALDSSON, B. & DEEN, W. M. (2008a) Resolved: normal glomeruli filter nephrotic levels of albumin. *J Am Soc Nephrol*, 19, 427-32.

COMPER, W. D., HILLIARD, L. M., NIKOLIC-PATERSON, D. J. & RUSSO, L. M. (2008b) Disease-dependent mechanisms of albuminuria. *Am J Physiol Renal Physiol*, 295, F1589-600.

COMPER, W. D. & RUSSO, L. M. (2009) The glomerular filter: an imperfect barrier is required for perfect renal function. *Curr Opin Nephrol Hypertens*, 18, 336-42.

CONNER, S. D. & SCHMID, S. L. (2003) Regulated portals of entry into the cell. *Nature*, 422, 37-44.

COSPEDAL, R., ABEDI, H. & ZACHARY, I. (1999) Platelet-derived growth factor-BB (PDGF-BB) regulation of migration and focal adhesion kinase phosphorylation in rabbit aortic vascular smooth muscle cells: roles of phosphatidylinositol 3-kinase and mitogen-activated protein kinases. *Cardiovasc Res*, 41, 708-21.

COUDROY, G., GBUREK, J., KOZYRAKI, R., MADSEN, M., TRUGNAN, G., MOESTRUP, S. K., VERROUST, P. J. & MAURICE, M. (2005) Contribution of cubilin and amnionless to processing and membrane targeting of cubilin-amnionless complex. *J Am Soc Nephrol*, 16, 2330-7.

CUI, S., GUERRIERO, C. J., SZALINSKI, C. M., KINLOUGH, C. L., HUGHEY, R. P. & WEISZ, O. A. (2010) OCRL1 function in renal epithelial membrane traffic. *Am J Physiol Renal Physiol*, 298, F335-45.

CUI, S., VERROUST, P. J., MOESTRUP, S. K. & CHRISTENSEN, E. I. (1996) Megalin/gp330 mediates uptake of albumin in renal proximal tubule. *Am J Physiol*, 271, F900-7.

CUTILLAS, P. R., CHALKLEY, R. J., HANSEN, K. C., CRAMER, R., NORDEN, A. G., WATERFIELD, M. D., BURLINGAME, A. L. & UNWIN, R. J. (2004) The urinary proteome in Fanconi syndrome implies specificity in the reabsorption of proteins by renal proximal tubule cells. *Am J Physiol Renal Physiol*, 287, F353-64.

D'AMICO, G. & BAZZI, C. (2003) Pathophysiology of proteinuria. *Kidney Int*, 63, 809-25.

D'ANDREA, L. D. & REGAN, L. (2003) TPR proteins: the versatile helix. *Trends Biochem Sci*, 28, 655-62.

D'SOUZA, S., GARCIA-CABADO, A., YU, F., TETER, K., LUKACS, G., SKORECKI, K., MOORE, H. P., ORLOWSKI, J. & GRINSTEIN, S. (1998) The epithelial sodium-hydrogen antiporter Na⁺/H⁺ exchanger 3 accumulates and is functional in recycling endosomes. *J Biol Chem*, 273, 2035-43.

DAVIES, D. J., BREWER, D. B. & HARDWICKE, J. (1978) Urinary proteins and glomerular morphometry in protein overload proteinuria. *Lab Invest*, 38, 232-43.

DAVIS, C. G., GOLDSTEIN, J. L., SUDHOF, T. C., ANDERSON, R. G., RUSSELL, D. W. & BROWN, M. S. (1987) Acid-dependent ligand dissociation and recycling of LDL receptor mediated by growth factor homology region. *Nature*, 326, 760-5.

DCCT (1993) *N Engl J Med*, 329, 977-986.

DCCT (2003) Sustained Effect of Intensive Treatment of Type 1 Diabetes Mellitus on Development and Progression of Diabetic Nephropathy: The Epidemiology of Diabetes Interventions and Complications (EDIC) Study. *JAMA*, 290, 2159-2167.

DE BORST, M. H., PRAKASH, J., SANDOVICI, M., KLOK, P. A., HAMMING, I., KOK, R. J., NAVIS, G. & VAN GOOR, H. (2009) c-Jun NH2-terminal kinase is crucially involved in renal tubulointerstitial inflammation. *J Pharmacol Exp Ther*, 331, 896-905.

DE ZEEUW, D., REMUZZI, G., PARVING, H. H., KEANE, W. F., ZHANG, Z., SHAHINFAR, S., SNAPINN, S., COOPER, M. E., MITCH, W. E. & BRENNER, B. M. (2004) Proteinuria, a target for renoprotection in patients with type 2 diabetic nephropathy: lessons from RENAAL. *Kidney Int*, 65, 2309-20.

DETRISAC, C. J., SENS, M. A., GARVIN, A. J., SPICER, S. S. & SENS, D. A. (1984) Tissue culture of human kidney epithelial cells of proximal tubule origin. *Kidney Int*, 25, 383-90.

DEYULIA, G. J., JR., CARCAMO, J. M., BORQUEZ-OJEDA, O., SHELTON, C. C. & GOLDE, D. W. (2005) Hydrogen peroxide generated extracellularly by receptor-ligand interaction facilitates cell signaling. *Proc Natl Acad Sci U S A*, 102, 5044-9.

DI FIORE, P. P. & DE CAMILLI, P. (2001) Endocytosis and signaling. an inseparable partnership. *Cell*, 106, 1-4.

DIAMANDOPOULOS, A., GOUDAS, P. & OREOPOULOS, D. (2009) Thirty-six Hippocratic aphorisms of nephrologic interest. *Am J Kidney Dis*, 54, 143-53.

DIWAKAR, R., PEARSON, A. L., COLVILLE-NASH, P., BRUNSKILL, N. J. & DOCKRELL, M. E. (2007) The role played by endocytosis in albumin-induced secretion of TGF-beta1 by proximal tubular epithelial cells. *Am J Physiol Renal Physiol*, 292, F1464-70.

DIXON, R. & BRUNSKILL, N. J. (1999) Activation of mitogenic pathways by albumin in kidney proximal tubule epithelial cells: implications for the pathophysiology of proteinuric states. *J Am Soc Nephrol*, 10, 1487-97.

DIXON, R. & BRUNSKILL, N. J. (2000) Albumin stimulates p44/p42 extracellular-signal-regulated mitogen-activated protein kinase in opossum kidney proximal tubular cells. *Clin Sci (Lond)*, 98, 295-301.

DONADELLI, R., ZANCHI, C., MORIGI, M., BUELLI, S., BATANI, C., TOMASONI, S., CORNA, D., ROTTOLI, D., BENIGNI, A., ABBATE, M., REMUZZI, G. & ZOJA, C. (2003) Protein overload induces fractalkine upregulation in proximal tubular cells through nuclear factor kappaB- and p38 mitogen-activated protein kinase-dependent pathways. *J Am Soc Nephrol*, 14, 2436-46.

DRUMM, K., LEE, E., STANNERS, S., GASSNER, B., GEKLE, M., PORONNIK, P. & POLLOCK, C. (2003) Albumin and glucose effects on cell growth parameters, albumin uptake and Na(+)/H(+)-exchanger Isoform 3 in OK cells. *Cell Physiol Biochem*, 13, 199-206.

EDDY, A. A. (1989) Interstitial nephritis induced by protein-overload proteinuria. *Am J Pathol*, 135, 719-33.

EDDY, A. A. (1994) Protein restriction reduces transforming growth factor-beta and interstitial fibrosis in nephrotic syndrome. *Am J Physiol*, 266, F884-93.

EDDY, A. A. & GIACHELLI, C. M. (1995) Renal expression of genes that promote interstitial inflammation and fibrosis in rats with protein-overload proteinuria. *Kidney Int*, 47, 1546-57.

EDDY, A. A., MCCULLOCH, L., LIU, E. & ADAMS, J. (1991) A relationship between proteinuria and acute tubulointerstitial disease in rats with experimental nephrotic syndrome. *Am J Pathol*, 138, 1111-23.

EIJKELKAMP, W. B., ZHANG, Z., REMUZZI, G., PARVING, H. H., COOPER, M. E., KEANE, W. F., SHAHINFAR, S., GLEIM, G. W., WEIR, M. R., BRENNER, B. M. & DE ZEEUW, D. (2007) Albuminuria is a target for renoprotective therapy independent from blood pressure in patients with type 2 diabetic nephropathy: post hoc analysis from the Reduction of Endpoints in NIDDM with the Angiotensin II Antagonist Losartan (RENAAL) trial. *J Am Soc Nephrol*, 18, 1540-6.

EL-NAHAS, A. M., PARASKEVAKOU, H., ZOOB, S., REES, A. J. & EVANS, D. J. (1983) Effect of dietary protein restriction on the development of renal failure after subtotal nephrectomy in rats. *Clin Sci (Lond)*, 65, 399-406.

EL NAHAS, A. M., MASTERS-THOMAS, A., BRADY, S. A., FARRINGTON, K., WILKINSON, V., HILSON, A. J., VARGHESE, Z. & MOORHEAD, J. F. (1984) Selective effect of low protein diets in chronic renal diseases. *Br Med J (Clin Res Ed)*, 289, 1337-41.

ELM (2010).

EYRE, J., IOANNOU, K., GRUBB, B. D., SALEEM, M. A., MATHIESON, P. W., BRUNSKILL, N. J., CHRISTENSEN, E. I. & TOPHAM, P. S. (2007) Statin-sensitive endocytosis of albumin by glomerular podocytes. *Am J Physiol Renal Physiol*, 292, F674-81.

FARESE, R. V., JR. & HERZ, J. (1998) Cholesterol metabolism and embryogenesis. *Trends Genet*, 14, 115-20.

FEBBRAIO, M., ABUMRAD, N. A., HAJJAR, D. P., SHARMA, K., CHENG, W., PEARCE, S. F. & SILVERSTEIN, R. L. (1999) A null mutation in murine CD36 reveals an important role in fatty acid and lipoprotein metabolism. *J Biol Chem*, 274, 19055-62.

FYFE, J. C., GIGER, U., HALL, C. A., JEZYK, P. F., KLUMPP, S. A., LEVINE, J. S. & PATTERSON, D. F. (1991) Inherited selective intestinal cobalamin malabsorption and cobalamin deficiency in dogs. *Pediatr Res*, 29, 24-31.

FYFE, J. C., MADSEN, M., HOJRUP, P., CHRISTENSEN, E. I., TANNER, S. M., DE LA CHAPELLE, A., HE, Q. & MOESTRUP, S. K. (2004) The functional cobalamin (vitamin B12)-intrinsic factor receptor is a novel complex of cubilin and amnionless. *Blood*, 103, 1573-9.

GARDAI, S. J., XIAO, Y. Q., DICKINSON, M., NICK, J. A., VOELKER, D. R., GREENE, K. E. & HENSON, P. M. (2003) By binding SIRPalpha or calreticulin/CD91, lung collectins act as dual function surveillance molecules to suppress or enhance inflammation. *Cell*, 115, 13-23.

GEKLE, M. (2005) Renal tubule albumin transport. *Annu Rev Physiol*, 67, 573-94.

GEKLE, M., FREUDINGER, R. & MILDENBERGER, S. (2001) Inhibition of Na⁺-H⁺ exchanger-3 interferes with apical receptor-mediated endocytosis via vesicle fusion. *J Physiol*, 531, 619-29.

GEKLE, M., MILDENBERGER, S., FREUDINGER, R., SCHWERDT, G. & SILBERNAGL, S. (1997) Albumin endocytosis in OK cells: dependence on actin and microtubules and regulation by protein kinases. *Am J Physiol*, 272, F668-77.

GEKLE, M., MILDENBERGER, S., FREUDINGER, R. & SILBERNAGL, S. (1995) Kinetics of receptor-mediated endocytosis of albumin in cells derived from the proximal tubule of the kidney (opossum kidney cells): influence of Ca²⁺ and cAMP. *Pflugers Arch*, 430, 374-80.

GEKLE, M., MILDENBERGER, S., FREUDINGER, R. & SILBERNAGL, S. (1996) Functional characterization of albumin binding to the apical membrane of OK cells. *Am J Physiol*, 271, F286-91.

GEKLE, M., MILDENBERGER, S., FREUDINGER, R. & SILBERNAGL, S. (1998) Long-term protein exposure reduces albumin binding and uptake in proximal tubule-derived opossum kidney cells. *J Am Soc Nephrol*, 9, 960-8.

GEKLE, M., SERRANO, O. K., DRUMM, K., MILDENBERGER, S., FREUDINGER, R., GASSNER, B., JANSEN, H. W. & CHRISTENSEN, E. I. (2002) NHE3 serves as a molecular tool for cAMP-mediated regulation of receptor-mediated endocytosis. *Am J Physiol Renal Physiol*, 283, F549-58.

GEKLE, M., VOLKER, K., MILDENBERGER, S., FREUDINGER, R., SHULL, G. E. & WIEMANN, M. (2004) NHE3 Na⁺/H⁺ exchanger supports proximal tubular protein reabsorption in vivo. *Am J Physiol Renal Physiol*, 287, F469-73.

GELLMAN, D. D., PIRANI, C. L., SOOTHILL, J. F., MUEHRCKE, R. C. & KARK, R. M. (1959) Diabetic nephropathy: a clinical and pathologic study based on renal biopsies. *Medicine (Baltimore)*, 38, 321-67.

GESUALDO, L., DI PAOLO, S., CALABRO, A., MILANI, S., MAIORANO, E., RANIERI, E., PANNARALE, G. & SCHENA, F. P. (1996) Expression of epidermal growth factor and its receptor in normal and diseased human kidney: an immunohistochemical and in situ hybridization study. *Kidney Int*, 49, 656-65.

GIANNONI, E., BURICCHI, F., RAUGEI, G., RAMPONI, G. & CHIARUGI, P. (2005) Intracellular reactive oxygen species activate Src tyrosine kinase during cell adhesion and anchorage-dependent cell growth. *Mol Cell Biol*, 25, 6391-403.

GOTTHARDT, M., TROMMSDORFF, M., NEVITT, M. F., SHELTON, J., RICHARDSON, J. A., STOCKINGER, W., NIMPF, J. & HERZ, J. (2000) Interactions of the low density lipoprotein receptor gene family with cytosolic adaptor and scaffold proteins suggest diverse biological functions in cellular communication and signal transduction. *J Biol Chem*, 275, 25616-24.

GRAHAM, R. C., JR. & KARNOVSKY, M. J. (1966) The early stages of absorption of injected horseradish peroxidase in the proximal tubules of mouse kidney: ultrastructural cytochemistry by a new technique. *J Histochem Cytochem*, 14, 291-302.

GRASBECK, R., GORDIN, R., KANTERO, I. & KUHBACK, B. (1960) Selective vitamin B12 malabsorption and proteinuria in young people. *Acta Paediatr Scand*, 167, 289-296.

GROSS, M. L., HANKE, W., KOCH, A., ZIEBART, H., AMANN, K. & RITZ, E. (2002) Intraperitoneal protein injection in the axolotl: the amphibian kidney as a novel model to study tubulointerstitial activation. *Kidney Int*, 62, 51-9.

GUDER, W. G. & HOFMANN, W. (1992) Markers for the diagnosis and monitoring of renal tubular lesions. *Clin Nephrol*, 38 Suppl 1, S3-7.

GUNTHER, W., LUCHOW, A., CLUZEAUD, F., VANDEWALLE, A. & JENTSCH, T. J. (1998) CIC-5, the chloride channel mutated in Dent's disease, colocalizes with the proton pump in endocytotically active kidney cells. *Proc Natl Acad Sci U S A*, 95, 8075-80.

GUNTHER, W., PIWON, N. & JENTSCH, T. J. (2003) The CIC-5 chloride channel knock-out mouse - an animal model for Dent's disease. *Pflugers Arch*, 445, 456-62.

HALL, A. M., CAMPANELLA, M., LOESCH, A., DUCHEN, M. R. & UNWIN, R. J. (2010) Albumin uptake in OK cells exposed to rotenone: a model for studying the effects of mitochondrial dysfunction on endocytosis in the proximal tubule? *Nephron Physiol*, 115, p9-p19.

HARALDSSON, B., NYSTROM, J. & DEEN, W. M. (2008) Properties of the glomerular barrier and mechanisms of proteinuria. *Physiol Rev*, 88, 451-87.

HAYMANN, J. P., LEVRAUD, J. P., BOUET, S., KAPPES, V., HAGEGE, J., NGUYEN, G., XU, Y., RONDEAU, E. & SRAER, J. D. (2000) Characterization and localization of the neonatal Fc receptor in adult human kidney. *J Am Soc Nephrol*, 11, 632-9.

HEBERT, L. A., BAIN, R. P., VERME, D., CATTRAN, D., WHITTIER, F. C., TOLCHIN, N., ROHDE, R. D. & LEWIS, E. J. (1994) Remission of nephrotic range proteinuria in type I diabetes. Collaborative Study Group. *Kidney Int*, 46, 1688-93.

HEPTINSTALL, R. H. (1983) *Pathology of the kidney*.

HERSCHKO, A. & CHIECHANOVER, A. (1998) *Annu Rev Biochem*, 67, 425-479.

HERZ, J. (2003) LRP: a bright beacon at the blood-brain barrier. *J Clin Invest*, 112, 1483-5.

HERZ, J., GOTTHARDT, M. & WILLNOW, T. E. (2000) Cellular signalling by lipoprotein receptors. *Curr Opin Lipidol*, 11, 161-6.

HERZ, J., HAMANN, U., ROGNE, S., MYKLEBOST, O., GAUSEPOHL, H. & STANLEY, K. K. (1988) Surface location and high affinity for calcium of a 500-kd liver membrane protein closely related to the LDL-receptor suggest a physiological role as lipoprotein receptor. *EMBO J*, 7, 4119-27.

HILPERT, J., WOGENSEN, L., THYKJAER, T., WELLNER, M., SCHLICHTING, U., ORNTOFT, T. F., BACHMANN, S., NYKJAER, A. & WILLNOW, T. E. (2002) Expression profiling confirms the role of endocytic receptor megalin in renal vitamin D3 metabolism. *Kidney Int*, 62, 1672-81.

HJALM, G., MURRAY, E., CRUMLEY, G., HARAZIM, W., LUNDGREN, S., ONYANGO, I., EK, B., LARSSON, M., JUHLIN, C., HELLMAN, P., DAVIS, H., AKERSTROM, G., RASK, L. & MORSE, B. (1996) Cloning and sequencing of human gp330, a Ca(2+)-binding receptor with potential intracellular signaling properties. *Eur J Biochem*, 239, 132-7.

HOCEVAR, B. A., SMINE, A., XU, X. X. & HOWE, P. H. (2001) The adaptor molecule Disabled-2 links the transforming growth factor beta receptors to the Smad pathway. *EMBO J*, 20, 2789-801.

HOOKE, D. H., GEE, D. C. & ATKINS, R. C. (1987) Leukocyte analysis using monoclonal antibodies in human glomerulonephritis. *Kidney Int*, 31, 964-72.

HOPE (2000) Effects of ramipril on cardiovascular and microvascular outcomes in people with diabetes mellitus: results of the HOPE study and MICRO-HOPE substudy. Heart Outcomes Prevention Evaluation Study Investigators. *Lancet*, 355, 253-9.

HORTIN, G. L. & MEILINGER, B. (2005) Cross-reactivity of amino acids and other compounds in the biuret reaction: interference with urinary peptide measurements. *Clin Chem*, 51, 1411-9.

HOSTETTER, T. H., OLSON, J. L., RENNKE, H. G., VENKATACHALAM, M. A. & BRENNER, B. M. (1981) Hyperfiltration in remnant nephrons: a potentially adverse response to renal ablation. *Am J Physiol*, 241, F85-93.

HOSTETTER, T. H., RENNKE, H. G. & BRENNER, B. M. (1982) The case for intrarenal hypertension in the initiation and progression of diabetic and other glomerulopathies. *Am J Med*, 72, 375-80.

HOU, F. F., XIE, D., ZHANG, X., CHEN, P. Y., ZHANG, W. R., LIANG, M., GUO, Z. J. & JIANG, J. P. (2007) Renoprotection of Optimal Antiproteinuric Doses (ROAD) Study: a randomized controlled study of benazepril and losartan in chronic renal insufficiency. *J Am Soc Nephrol*, 18, 1889-98.

HRYCIW, D. H., EKBERG, J., LEE, A., LENSINK, I. L., KUMAR, S., GUGGINO, W. B., COOK, D. I., POLLOCK, C. A. & PORONNIK, P. (2004) Nedd4-2 functionally interacts with CIC-5: involvement in constitutive albumin endocytosis in proximal tubule cells. *J Biol Chem*, 279, 54996-5007.

HRYCIW, D. H., POLLOCK, C. A. & PORONNIK, P. (2005) PKC-alpha-mediated remodeling of the actin cytoskeleton is involved in constitutive albumin uptake by proximal tubule cells. *Am J Physiol Renal Physiol*, 288, F1227-35.

HRYCIW, D. H., WANG, Y., DEVUYST, O., POLLOCK, C. A., PORONNIK, P. & GUGGINO, W. B. (2003) Cofilin interacts with CIC-5 and regulates albumin uptake in proximal tubule cell lines. *J Biol Chem*, 278, 40169-76.

HSU, S. I. & COUSER, W. G. (2003) Chronic progression of tubulointerstitial damage in proteinuric renal disease is mediated by complement activation: a therapeutic role for complement inhibitors? *J Am Soc Nephrol*, 14, S186-91.

HU, P., MARGOLIS, B., SKOLNIK, E. Y., LAMMERS, R., ULLRICH, A. & SCHLESSINGER, J. (1992) Interaction of phosphatidylinositol 3-kinase-associated p85 with epidermal growth factor and platelet-derived growth factor receptors. *Mol Cell Biol*, 12, 981-90.

HUNSICKER, L. G., ADLER, S., CAGGIULA, A., ENGLAND, B. K., GREENE, T., KUSEK, J. W., ROGERS, N. L. & TESCHAN, P. E. (1997) Predictors of the progression of renal disease in the Modification of Diet in Renal Disease Study. *Kidney Int*, 51, 1908-19.

ICHIMURA, T., BONVENTRE, J. V., BAILLY, V., WEI, H., HESSION, C. A., CATE, R. L. & SANICOLA, M. (1998) Kidney injury molecule-1 (KIM-1), a putative epithelial cell adhesion molecule containing a novel immunoglobulin domain, is up-regulated in renal cells after injury. *J Biol Chem*, 273, 4135-42.

ICHIMURA, T., HUNG, C. C., YANG, S. A., STEVENS, J. L. & BONVENTRE, J. V. (2004) Kidney injury molecule-1: a tissue and urinary biomarker for nephrotoxicant-induced renal injury. *Am J Physiol Renal Physiol*, 286, F552-63.

IGNATIUK, A., QUICKFALL, J. P., HAWRYSH, A. D., CHAMBERLAIN, M. D. & ANDERSON, D. H. (2006) The smaller isoforms of ankyrin 3 bind to the p85 subunit of phosphatidylinositol 3'-kinase and enhance platelet-derived growth factor receptor down-regulation. *J Biol Chem*, 281, 5956-64.

IHRKE, G., GRAY, S. R. & LUZIO, J. P. (2000) Endolyn is a mucin-like type I membrane protein targeted to lysosomes by its cytoplasmic tail. *Biochem J*, 345 Pt 2, 287-96.

IMAI, E., NAKAJIMA, H. & KAIMORI, J. Y. (2004) Albumin turns on a vicious spiral of oxidative stress in renal proximal tubules. *Kidney Int*, 66, 2085-7.

IMERSLUND, O. (1960) Idiopathic chronic megaloblastic anaemia in children. *Acta Paediatr Scand*, 49, 1-115.

ISHIGAMI, M., SWERTFEGER, D. K., GRANHOLM, N. A. & HUI, D. Y. (1998) Apolipoprotein E inhibits platelet-derived growth factor-induced vascular smooth muscle cell migration and proliferation by suppressing signal transduction and preventing cell entry to G1 phase. *J Biol Chem*, 273, 20156-61.

ISHOLA, D. A., JR., POST, J. A., VAN TIMMEREN, M. M., BAKKER, S. J., GOLDSCHMEDING, R., KOOMANS, H. A., BRAAM, B. & JONES, J. A. (2006) Albumin-bound fatty acids induce mitochondrial oxidant stress and impair antioxidant responses in proximal tubular cells. *Kidney Int*, 70, 724-31.

IWAO, Y., NAKAJOU, K., NAGAI, R., KITAMURA, K., ANRAKU, M., MARUYAMA, T. & OTAGIRI, M. (2008) CD36 is one of important receptors promoting renal tubular injury by advanced oxidation protein products. *Am J Physiol Renal Physiol*, 295, F1871-80.

JEANSSON, M., BJORCK, K., TENSTAD, O. & HARALDSSON, B. (2009) Adriamycin alters glomerular endothelium to induce proteinuria. *J Am Soc Nephrol*, 20, 114-22.

JEANSSON, M. & HARALDSSON, B. (2003) Glomerular size and charge selectivity in the mouse after exposure to glucosaminoglycan-degrading enzymes. *J Am Soc Nephrol*, 14, 1756-65.

JEANSSON, M. & HARALDSSON, B. (2006) Morphological and functional evidence for an important role of the endothelial cell glycocalyx in the glomerular barrier. *Am J Physiol Renal Physiol*, 290, F111-6.

JERNIGAN, S. M. & EDDY, A. A. (2000) *Experimental insights into the mechanisms of tubulointerstitial scarring.*, Oxford University Press.

JORGENSEN, F. (1966) *The ultrastructure of the normal human glomerulus.*, Ejnar Munksgaard, Copenhagen.

KANG, D. H., KANELIS, J., HUGO, C., TRUONG, L., ANDERSON, S., KERJASCHKI, D., SCHREINER, G. F. & JOHNSON, R. J. (2002) Role of the microvascular endothelium in progressive renal disease. *J Am Soc Nephrol*, 13, 806-16.

KANTARCI, S., AL-GAZALI, L., HILL, R. S., DONNAI, D., BLACK, G. C., BIETH, E., CHASSAING, N., LACOMBE, D., DEVRIENDT, K., TEEBI, A., LOSCERTALES, M., ROBSON, C., LIU, T., MACLAUGHLIN, D. T., NOONAN, K. M., RUSSELL, M. K., WALSH, C. A., DONAHOE, P. K. & POBER, B. R. (2007) Mutations in LRP2, which encodes the multiligand receptor megalin, cause Donnai-Barrow and facio-oculo-acoustico-renal syndromes. *Nat Genet*, 39, 957-9.

KEBACHE, S., ASH, J., ANNIS, M. G., HAGAN, J., HUBER, M., HASSARD, J., STEWART, C. L., WHITEWAY, M. & NANTEL, A. (2007) Grb10 and active Raf-1 kinase promote Bad-dependent cell survival. *J Biol Chem*, 282, 21873-83.

KENT, D. M., JAFAR, T. H., HAYWARD, R. A., TIGHIOUART, H., LANDA, M., DE JONG, P., DE ZEEUW, D., REMUZZI, G., KAMPER, A. L. & LEVEY, A. S. (2007) Progression risk, urinary protein excretion, and treatment effects of angiotensin-converting enzyme inhibitors in nondiabetic kidney disease. *J Am Soc Nephrol*, 18, 1959-65.

KERJASCHKI, D. & FARQUHAR, M. G. (1982) The pathogenic antigen of Heymann nephritis is a membrane glycoprotein of the renal proximal tubule brush border. *Proc Natl Acad Sci U S A*, 79, 5557-61.

KERKELA, R., WOULFE, K. & FORCE, T. (2007) Glycogen synthase kinase-3beta -- actively inhibiting hypertrophy. *Trends Cardiovasc Med*, 17, 91-6.

KHURANA, S., NATH, S. K., LEVINE, S. A., BOWSER, J. M., TSE, C. M., COHEN, M. E. & DONOWITZ, M. (1996) Brush border phosphatidylinositol 3-kinase mediates epidermal growth factor stimulation of intestinal NaCl absorption and Na⁺/H⁺ exchange. *J Biol Chem*, 271, 9919-27.

KIM, K. H., KIM, Y., GUBLER, M. C., STEFFES, M. W., LANE, P. H., KASHTAN, C. E., CROSSON, J. T. & MAUER, S. M. (1995) Structural-functional relationships in Alport syndrome. *J Am Soc Nephrol*, 5, 1659-68.

KLAHR, S. (2003) The bone morphogenetic proteins (BMPs). Their role in renal fibrosis and renal function. *J Nephrol*, 16, 179-85.

KODADEK, T. (2010) No Splicing, no dicing: non-proteolytic roles of the ubiquitin-proteasome system in transcription. *J Biol Chem*, 285, 2221-6.

KORENBERG, J. R., ARGRAVES, K. M., CHEN, X. N., TRAN, H., STRICKLAND, D. K. & ARGRAVES, W. S. (1994) Chromosomal localization of human genes for the LDL receptor family member glycoprotein 330 (LRP2) and its associated protein RAP (LRPAP1). *Genomics*, 22, 88-93.

KOZAK, M. (1991a) Effects of long 5' leader sequences on initiation by eukaryotic ribosomes in vitro. *Gene Expr*, 1, 117-25.

KOZAK, M. (1991b) Structural features in eukaryotic mRNAs that modulate the initiation of translation. *J Biol Chem*, 266, 19867-70.

KOZYRAKI, R., FYFE, J., VERROUST, P. J., JACOBSEN, C., DAUTRY-VARSAT, A., GBUREK, J., WILLNOW, T. E., CHRISTENSEN, E. I. & MOESTRUP, S. K. (2001) Megalin-dependent cubilin-mediated endocytosis is a major pathway for the apical uptake of transferrin in polarized epithelia. *Proc Natl Acad Sci U S A*, 98, 12491-6.

KRAMER, A. B., VAN TIMMEREN, M. M., SCHUURS, T. A., VAIDYA, V. S., BONVENTRE, J. V., VAN GOOR, H. & NAVIS, G. (2009) Reduction of proteinuria in adriamycin-induced nephropathy is associated with reduction of renal kidney injury molecule (Kim-1) over time. *Am J Physiol Renal Physiol*, 296, F1136-45.

KRIZ, W., HARTMANN, I., HOSSER, H., HAHNEL, B., KRANZLIN, B., PROVOOST, A. & GRETZ, N. (2001) Tracer studies in the rat demonstrate misdirected filtration and peritubular filtrate spreading in nephrons with segmental glomerulosclerosis. *J Am Soc Nephrol*, 12, 496-506.

KRIZ, W. & LEHIR, M. (2005) Pathways to nephron loss starting from glomerular diseases-insights from animal models. *Kidney Int*, 67, 404-19.

LAEMMLI, U. K. (1970) Cleavage of structural proteins during the assembly of the head of bacteriophage T4. *Nature*, 227, 680-5.

LAMBERT, P. (1932) Sur les potentialites de resorption du tube contourne chez les urodeles. *Compt. Rend. Soc. Biol.*, 110, 114-116.

LARSSON, L. & MAUNSBACH, A. B. (1980) The ultrastructural development of the glomerular filtration barrier in the rat kidney: a morphometric analysis. *J Ultrastruct Res*, 72, 392-406.

LARSSON, M., HJALM, G., SAKWE, A. M., ENGSTROM, A., HOGLUND, A. S., LARSSON, E., ROBINSON, R. C., SUNDBERG, C. & RASK, L. (2003) Selective interaction of megalin with postsynaptic density-95 (PSD-95)-like membrane-associated guanylate kinase (MAGUK) proteins. *Biochem J*, 373, 381-91.

LE HIR, M. & BESSE-ESCHMANN, V. (2003) A novel mechanism of nephron loss in a murine model of crescentic glomerulonephritis. *Kidney Int*, 63, 591-9.

LEBOVITZ, H. E., WIEGMANN, T. B., CNAAN, A., SHAHINFAR, S., SICA, D. A., BROADSTONE, V., SCHWARTZ, S. L., MENGEL, M. C., SEGAL, R., VERSAGGI, J. A. & ET AL. (1994) Renal protective effects of enalapril in hypertensive NIDDM: role of baseline albuminuria. *Kidney Int Suppl*, 45, S150-5.

LEE, E. M., POLLOCK, C. A., DRUMM, K., BARDEN, J. A. & PORONNIK, P. (2003) Effects of pathophysiological concentrations of albumin on NHE3 activity and cell proliferation in primary cultures of human proximal tubule cells. *Am J Physiol Renal Physiol*, 285, F748-57.

LEE, Y. J. & HAN, H. J. (2008) Albumin-stimulated DNA synthesis is mediated by Ca²⁺/PKC as well as EGF receptor-dependent p44/42 MAPK and NF-kappaB signal pathways in renal proximal tubule cells. *Am J Physiol Renal Physiol*, 294, F534-41.

LEHESTE, J. R., MELSEN, F., WELLNER, M., JANSEN, P., SCHLICHTING, U., RENNER-MULLER, I., ANDREASSEN, T. T., WOLF, E., BACHMANN, S., NYKJAER, A. & WILLNOW, T. E. (2003) Hypocalcemia and osteopathy in mice with kidney-specific megalin gene defect. *FASEB J*, 17, 247-9.

LEHESTE, J. R., ROLINSKI, B., VORUM, H., HILPERT, J., NYKJAER, A., JACOBSEN, C., AUCOUTURIER, P., MOSKAUG, J. O., OTTO, A., CHRISTENSEN, E. I. & WILLNOW, T. E. (1999) Megalin knockout mice as an animal model of low molecular weight proteinuria. *Am J Pathol*, 155, 1361-70.

LEVINE, T. P. & MUNRO, S. (2002) Targeting of Golgi-specific pleckstrin homology domains involves both PtdIns 4-kinase-dependent and -independent components. *Curr Biol*, 12, 695-704.

LEWIS, E. J., HUNSICKER, L. G., CLARKE, W. R., BERL, T., POHL, M. A., LEWIS, J. B., RITZ, E., ATKINS, R. C., ROHDE, R. & RAZ, I. (2001) Renoprotective effect of the angiotensin-receptor antagonist irbesartan in patients with nephropathy due to type 2 diabetes. *N Engl J Med*, 345, 851-60.

LI, X., PABLA, N., WEI, Q., DONG, G., MESSING, R. O., WANG, C. Y. & DONG, Z. (2010) PKC- δ Promotes Renal Tubular Cell Apoptosis Associated with Proteinuria. *J Am Soc Nephrol*, 21, 1115-24.

LI, Y., CONG, R. & BIEMESDERFER, D. (2008) The COOH terminus of megalin regulates gene expression in opossum kidney proximal tubule cells. *Am J Physiol Cell Physiol*, 295, C529-37.

LI, Y., MARZOLO, M. P., VAN KERKHOF, P., STROUS, G. J. & BU, G. (2000) The YXXL motif, but not the two NPXY motifs, serves as the dominant endocytosis

signal for low density lipoprotein receptor-related protein. *J Biol Chem*, 275, 17187-94.

LI, Y., VAN KERKHOFF, P., MARZOLO, M. P., STROUS, G. J. & BU, G. (2001) Identification of a major cyclic AMP-dependent protein kinase A phosphorylation site within the cytoplasmic tail of the low-density lipoprotein receptor-related protein: implication for receptor-mediated endocytosis. *Mol Cell Biol*, 21, 1185-95.

LILLIS, A. P., VAN DUYN, L. B., MURPHY-ULLRICH, J. E. & STRICKLAND, D. K. (2008) LDL receptor-related protein 1: unique tissue-specific functions revealed by selective gene knockout studies. *Physiol Rev*, 88, 887-918.

LIM, H. H. & PARK, C. S. (2005) Identification and functional characterization of ankyrin-repeat family protein ANKRA as a protein interacting with BKCa channel. *Mol Biol Cell*, 16, 1013-25.

LIN, J. H., MAKRIS, A., MCMAHON, C., BEAR, S. E., PATRIOTIS, C., PRASAD, V. R., BRENT, R., GOLEMIS, E. A. & TSICHLIS, P. N. (1999) The ankyrin repeat-containing adaptor protein Tvl-1 is a novel substrate and regulator of Raf-1. *J Biol Chem*, 274, 14706-15.

LIU, C., LI, Y., SEMENOV, M., HAN, C., BAEG, G. H., TAN, Y., ZHANG, Z., LIN, X. & HE, X. (2002) Control of beta-catenin phosphorylation/degradation by a dual-kinase mechanism. *Cell*, 108, 837-47.

LONGVA, K. E., BLYSTAD, F. D., STANG, E., LARSEN, A. M., JOHANNESSEN, L. E. & MADSHUS, I. H. (2002) Ubiquitination and proteasomal activity is required for transport of the EGF receptor to inner membranes of multivesicular bodies. *J Cell Biol*, 156, 843-54.

LOUKINOVA, E., RANGANATHAN, S., KUZNETSOV, S., GORLATOVA, N., MIGLIORINI, M. M., LOUKINOV, D., ULERY, P. G., MIKHAILENKO, I., LAWRENCE, D. A. & STRICKLAND, D. K. (2002) Platelet-derived growth factor (PDGF)-induced tyrosine phosphorylation of the low density lipoprotein receptor-related protein (LRP). Evidence for integrated co-receptor function between LRP and the PDGF. *J Biol Chem*, 277, 15499-506.

LOWE, M. (2005) Structure and function of the Lowe syndrome protein OCRL1. *Traffic*, 6, 711-9.

LUND, U., RIPPE, A., VENTUROLI, D., TENSTAD, O., GRUBB, A. & RIPPE, B. (2003) Glomerular filtration rate dependence of sieving of albumin and some neutral proteins in rat kidneys. *Am J Physiol Renal Physiol*, 284, F1226-34.

LUTZ, C., NIMPF, J., JENNY, M., BOECKLINGER, K., ENZINGER, C., UTERMANN, G., BAIER-BITTERLICH, G. & BAIER, G. (2002) Evidence of functional modulation of the MEKK/JNK/cJun signaling cascade by the low density lipoprotein receptor-related protein (LRP). *J Biol Chem*, 277, 43143-51.

MA, F. Y., FLANC, R. S., TESCH, G. H., HAN, Y., ATKINS, R. C., BENNETT, B. L., FRIEDMAN, G. C., FAN, J. H. & NIKOLIC-PATERSON, D. J. (2007) A pathogenic role for c-Jun amino-terminal kinase signaling in renal fibrosis and tubular cell apoptosis. *J Am Soc Nephrol*, 18, 472-84.

MAACK, T., PARK, C. H. & CAMARGO, M. J. F. (1992) *Renal filtration, transport and metabolism of proteins.*, New York, Raven.

MALLICK, N. P., SHORT, C. D. & HUNT, L. P. (1987) How far since Ellis? The Manchester Study of glomerular disease. *Nephron*, 46, 113-24.

MALSTROM, K., STANGE, G. & MURER, H. (1987) Identification of proximal tubular transport functions in the established kidney cell line, OK. *Biochim Biophys Acta*, 902, 269-77.

MANN, J. F., SCHMIEDER, R. E., MCQUEEN, M., DYAL, L., SCHUMACHER, H., POGUE, J., WANG, X., MAGGIONI, A., BUDAJ, A., CHAITHIRAPHAN, S., DICKSTEIN, K., KELTAI, M., METSARINNE, K., OTO, A., PARKHOMENKO, A., PIEGAS, L. S., SVENDSEN, T. L., TEO, K. K. & YUSUF, S. (2008) Renal outcomes with telmisartan, ramipril, or both, in people at high vascular risk (the ONTARGET study): a multicentre, randomised, double-blind, controlled trial. *Lancet*, 372, 547-53.

MARZOLO, M. P., YUSEFF, M. I., RETAMAL, C., DONOSO, M., EZQUER, F., FARFAN, P., LI, Y. & BU, G. (2003) Differential distribution of low-density lipoprotein-receptor-related protein (LRP) and megalin in polarized epithelial cells is determined by their cytoplasmic domains. *Traffic*, 4, 273-88.

MAUNSBACH, A. B. (1966) Absorption of I-125-labeled homologous albumin by rat kidney proximal tubule cells. A study of microperfused single proximal tubules by electron microscopic autoradiography and histochemistry. *J Ultrastruct Res*, 15, 197-241.

MAUNSBACH, A. B. (1970) *Ultrastructure and digestive activity of lysosomes from proximal tubule cells.*, Karger, Basel.

MAURER, M. E. & COOPER, J. A. (2005) Endocytosis of megalin by visceral endoderm cells requires the Dab2 adaptor protein. *J Cell Sci*, 118, 5345-55.

MAY, P., WOLDT, E., MATZ, R. L. & BOUCHER, P. (2007) The LDL receptor-related protein (LRP) family: an old family of proteins with new physiological functions. *Ann Med*, 39, 219-28.

MCCARTHY, R. A., BARTH, J. L., CHINTALAPUDI, M. R., KNAAK, C. & ARGRAVES, W. S. (2002) Megalin functions as an endocytic sonic hedgehog receptor. *J Biol Chem*, 277, 25660-7.

MEIER, M., MENNE, J., PARK, J. K., HOLTZ, M., GUELER, F., KIRSCH, T., SCHIFFER, M., MENGEL, M., LINDSCHAU, C., LEITGES, M. & HALLER, H. (2007) Deletion of protein kinase C-epsilon signaling pathway induces glomerulosclerosis and tubulointerstitial fibrosis in vivo. *J Am Soc Nephrol*, 18, 1190-8.

MELMAN, L., GEUZE, H. J., LI, Y., MCCORMICK, L. M., VAN KERKHOFF, P., STROUS, G. J., SCHWARTZ, A. L. & BU, G. (2002) Proteasome regulates the delivery of LDL receptor-related protein into the degradation pathway. *Mol Biol Cell*, 13, 3325-35.

MILLER, F. (1960) Hemoglobin absorption by the cells of the proximal convoluted tubule in mouse kidney. *J Biophys Biochem Cytol*, 8, 689-718.

MOESTRUP, S. K., CUI, S., VORUM, H., BREGENGARD, C., BJORN, S. E., NORRIS, K., GLIEMANN, J. & CHRISTENSEN, E. I. (1995) Evidence that epithelial glycoprotein 330/megalin mediates uptake of polybasic drugs. *J Clin Invest*, 96, 1404-13.

MOESTRUP, S. K., KOZYRAKI, R., KRISTIANSEN, M., KAYSEN, J. H., RASMUSSEN, H. H., BRAULT, D., PONTILLON, F., GODA, F. O., CHRISTENSEN, E. I., HAMMOND, T. G. & VERROUST, P. J. (1998) The intrinsic factor-vitamin B12 receptor and target of teratogenic antibodies is a megalin-binding peripheral membrane protein with homology to developmental proteins. *J Biol Chem*, 273, 5235-42.

MOGENSEN (2000) Diabetic nephropathy: natural history and management. IN EL NAHAS, A. M. (Ed.) *Mechanisms and Clinical Management of Chronic Renal Failure*. Oxford University Press.

MOHAN, P. S. & SPIRO, R. G. (1986) Macromolecular organization of basement membranes. Characterization and comparison of glomerular basement membrane and lens capsule components by immunochemical and lectin affinity procedures. *J Biol Chem*, 261, 4328-36.

MORIGI, M., MACCONI, D., ZOJA, C., DONADELLI, R., BUELLI, S., ZANCHI, C., GHILARDI, M. & REMUZZI, G. (2002) Protein overload-induced NF-kappaB activation in proximal tubular cells requires H₂O₂ through a PKC-dependent pathway. *J Am Soc Nephrol*, 13, 1179-89.

MORRIS, S. M., TALLQUIST, M. D., ROCK, C. O. & COOPER, J. A. (2002) Dual roles for the Dab2 adaptor protein in embryonic development and kidney transport. *EMBO J*, 21, 1555-64.

MORRISON, D. K. (2009) The 14-3-3 proteins: integrators of diverse signaling cues that impact cell fate and cancer development. *Trends Cell Biol*, 19, 16-23.

MOTOYOSHI, Y., MATSUSAKA, T., SAITO, A., PASTAN, I., WILLNOW, T. E., MIZUTANI, S. & ICHIKAWA, I. (2008) Megalin contributes to the early injury of proximal tubule cells during nonselective proteinuria. *Kidney Int*, 74, 1262-9.

NAGAI, J., CHRISTENSEN, E. I., MORRIS, S. M., WILLNOW, T. E., COOPER, J. A. & NIELSEN, R. (2005) Mutually dependent localization of megalin and Dab2 in the renal proximal tubule. *Am J Physiol Renal Physiol*, 289, F569-76.

NAGAI, M., MEERLOO, T., TAKEDA, T. & FARQUHAR, M. G. (2003) The adaptor protein ARH escorts megalin to and through endosomes. *Mol Biol Cell*, 14, 4984-96.

NAKAI, M., KINOSHITA, Y., FUKASE, M. & FUJITA, T. (1987) Phorbol esters inhibit phosphate uptake in opossum kidney cells: a model of proximal renal tubular cells. *Biochem Biophys Res Commun*, 145, 303-8.

NAKAJIMA, H., TAKENAKA, M., KAIMORI, J. Y., HAMANO, T., IWATANI, H., SUGAYA, T., ITO, T., HORI, M. & IMAI, E. (2004) Activation of the signal transducer and activator of transcription signaling pathway in renal proximal tubular cells by albumin. *J Am Soc Nephrol*, 15, 276-85.

NASSAR, T., AKKAWI, S., SHINA, A., HAJ-YEHIA, A., BDEIR, K., TARSHIS, M., HEYMAN, S. N. & HIGAZI, A. A. (2004) In vitro and in vivo effects of tPA and PAI-1 on blood vessel tone. *Blood*, 103, 897-902.

NATH, K. A., HOSTETTER, M. K. & HOSTETTER, T. H. (1985) Pathophysiology of chronic tubulointerstitial disease in rats. Interactions of dietary acid load, ammonia, and complement component C3. *J Clin Invest*, 76, 667-75.

NICHOLSON, T. & RODERICK, P. (2007) International Study of Health Care Organization and Financing of renal services in England and Wales. *Int J Health Care Finance Econ*, 7, 283-99.

NIELSEN, R., COURTOY, P. J., JACOBSEN, C., DOM, G., LIMA, W. R., JADOT, M., WILLNOW, T. E., DEVUYST, O. & CHRISTENSEN, E. I. (2007) Endocytosis provides a major alternative pathway for lysosomal biogenesis in kidney proximal tubular cells. *Proc Natl Acad Sci U S A*, 104, 5407-12.

NIEMEIER, A., WILLNOW, T., DIEPLINGER, H., JACOBSEN, C., MEYER, N., HILPERT, J. & BEISIEGEL, U. (1999) Identification of megalin/gp330 as a receptor for lipoprotein(a) in vitro. *Arterioscler Thromb Vasc Biol*, 19, 552-61.

NORDEN, A. G., LAPSLEY, M., IGARASHI, T., KELLEHER, C. L., LEE, P. J., MATSUYAMA, T., SCHEINMAN, S. J., SHIRAGA, H., SUNDIN, D. P., THAKKER, R. V., UNWIN, R. J., VERROUST, P. & MOESTRUP, S. K. (2002) Urinary megalin deficiency implicates abnormal tubular endocytic function in Fanconi syndrome. *J Am Soc Nephrol*, 13, 125-33.

NORDEN, A. G., LAPSLEY, M., LEE, P. J., PUSEY, C. D., SCHEINMAN, S. J., TAM, F. W., THAKKER, R. V., UNWIN, R. J. & WRONG, O. (2001) Glomerular protein sieving and implications for renal failure in Fanconi syndrome. *Kidney Int*, 60, 1885-92.

NORDEN, A. G., SHARRATT, P., CUTILLAS, P. R., CRAMER, R., GARDNER, S. C. & UNWIN, R. J. (2004) Quantitative amino acid and proteomic analysis: very low excretion of polypeptides >750 Da in normal urine. *Kidney Int*, 66, 1994-2003.

OKAMURA, D. M., PENNATHUR, S., PASICHNYK, K., LOPEZ-GUISA, J. M., COLLINS, S., FEBBRAIO, M., HEINECKE, J. & EDDY, A. A. (2009) CD36 regulates oxidative stress and inflammation in hypercholesterolemic CKD. *J Am Soc Nephrol*, 20, 495-505.

OLEINIKOV, A. V., ZHAO, J. & MAKKER, S. P. (2000) Cytosolic adaptor protein Dab2 is an intracellular ligand of endocytic receptor gp600/megalyn. *Biochem J*, 347 Pt 3, 613-21.

OLIVER, J., MACDOWELL, M. & LEE, Y. C. (1954) Cellular mechanisms of protein metabolism in the nephron. I. The structural aspects of proteinuria; tubular absorption, droplet formation, and the disposal of proteins. *J Exp Med*, 99, 589-604.

OLIVOS-GLANDER, I. M., JANNE, P. A. & NUSSBAUM, R. L. (1995) The oculocerebrorenal syndrome gene product is a 105-kD protein localized to the Golgi complex. *Am J Hum Genet*, 57, 817-23.

OLSON, G. E., WINFREY, V. P., HILL, K. E. & BURK, R. F. (2008) Megalin mediates selenoprotein P uptake by kidney proximal tubule epithelial cells. *J Biol Chem*, 283, 6854-60.

ORLANDO, R. A., EXNER, M., CZEKAY, R. P., YAMAZAKI, H., SAITO, A., ULLRICH, R., KERJASCHKI, D. & FARQUHAR, M. G. (1997) Identification of the second cluster of ligand-binding repeats in megalin as a site for receptor-ligand interactions. *Proc Natl Acad Sci U S A*, 94, 2368-73.

ORTIZ, A., JUSTO, P., SANZ, A., MELERO, R., CAMELO, C., GUERRERO, M. F., STRUTZ, F., MULLER, G., BARAT, A. & EGIDO, J. (2005) Tubular cell apoptosis and cidofovir-induced acute renal failure. *Antivir Ther*, 10, 185-90.

PANZER, U., STEINMETZ, O. M., TURNER, J. E., MEYER-SCHWESINGER, C., VON RUFFER, C., MEYER, T. N., ZAHNER, G., GOMEZ-GUERRERO, C., SCHMID, R. M., HELMCHEN, U., MOECKEL, G. W., WOLF, G., STAHL, R. A. & THAISS, F. (2009) Resolution of renal inflammation: a new role for NF-kappaB1 (p50) in inflammatory kidney diseases. *Am J Physiol Renal Physiol*, 297, F429-39.

PARK, C. H. & MAACK, T. (1984) Albumin absorption and catabolism by isolated perfused proximal convoluted tubules of the rabbit. *J Clin Invest*, 73, 767-77.

PARK, M. H., D'AGATI, V., APPEL, G. B. & PIRANI, C. L. (1986) Tubulointerstitial disease in lupus nephritis: relationship to immune deposits, interstitial inflammation, glomerular changes, renal function, and prognosis. *Nephron*, 44, 309-19.

PERGANDE, M., JUNG, K., PRECHT, S., FELS, L. M., HERBORT, C. & STOLTE, H. (1994) Changed excretion of urinary proteins and enzymes by chronic exposure to lead. *Nephrol Dial Transplant*, 9, 613-8.

PERKINS, D. N., PAPPIN, D. J., CREASY, D. M. & COTTRELL, J. S. (1999) Probability-based protein identification by searching sequence databases using mass spectrometry data. *Electrophoresis*, 20, 3551-67.

PETERSEN, H. H., HILPERT, J., MILITZ, D., ZANDLER, V., JACOBSEN, C., ROEBROEK, A. J. & WILLNOW, T. E. (2003) Functional interaction of megalin with the megalinbinding protein (MegBP), a novel tetratricopeptide repeat-containing adaptor molecule. *J Cell Sci*, 116, 453-61.

PETI-PETERDI, J. (2009) Independent two-photon measurements of albumin GSC give low values. *Am J Physiol Renal Physiol*, 296, F1255-7.

PETI-PETERDI, J., TOMA, I., SIPOS, A. & VARGAS, S. L. (2009) Multiphoton imaging of renal regulatory mechanisms. *Physiology (Bethesda)*, 24, 88-96.

POOK, M. A., WRONG, O., WOODING, C., NORDEN, A. G., FEEST, T. G. & THAKKER, R. V. (1993) Dent's disease, a renal Fanconi syndrome with nephrocalcinosis and kidney stones, is associated with a microdeletion involving DXS255 and maps to Xp11.22. *Hum Mol Genet*, 2, 2129-34.

PRICE, R. G. (1992) The role of NAG (N-acetyl-beta-D-glucosaminidase) in the diagnosis of kidney disease including the monitoring of nephrotoxicity. *Clin Nephrol*, 38 Suppl 1, S14-9.

RADER, K., ORLANDO, R. A., LOU, X. & FARQUHAR, M. G. (2000) Characterization of ANKRA, a novel ankyrin repeat protein that interacts with the cytoplasmic domain of megalin. *J Am Soc Nephrol*, 11, 2167-78.

RANGANATHAN, S., LIU, C. X., MIGLIORINI, M. M., VON ARNIM, C. A., PELTAN, I. D., MIKHAILENKO, I., HYMAN, B. T. & STRICKLAND, D. K. (2004) Serine and threonine phosphorylation of the low density lipoprotein receptor-related protein by protein kinase Calpha regulates endocytosis and association with adaptor molecules. *J Biol Chem*, 279, 40536-44.

RAYCHOWDHURY, R., NILES, J. L., MCCLUSKEY, R. T. & SMITH, J. A. (1989) Autoimmune target in Heymann nephritis is a glycoprotein with homology to the LDL receptor. *Science*, 244, 1163-5.

REICH, H., TRITCHLER, D., HERZENBERG, A. M., KASSIRI, Z., ZHOU, X., GAO, W. & SCHOLEY, J. W. (2005) Albumin activates ERK via EGF receptor in human renal epithelial cells. *J Am Soc Nephrol*, 16, 1266-78.

RHEE, S. G. (2006) Cell signaling. H₂O₂, a necessary evil for cell signaling. *Science*, 312, 1882-3.

RISDON, R. A., SLOPER, J. C. & DE WARDENER, H. E. (1968) Relationship between renal function and histological changes found in renal-biopsy specimens from patients with persistent glomerular nephritis. *Lancet*, 2, 363-6.

ROCCA, A., LAMAZE, C., SUBTIL, A. & DAUTRY-VARSAT, A. (2001) Involvement of the ubiquitin/proteasome system in sorting of the interleukin 2 receptor beta chain to late endocytic compartments. *Mol Biol Cell*, 12, 1293-301.

RODERICK, P., NICHOLSON, T., ARMITAGE, A., MEHTA, R., MULLEE, M., GERARD, K., DREY, N., FEEST, T., GREENWOOD, R., LAMPING, D. & TOWNSEND, J. (2005) An evaluation of the costs, effectiveness and quality of renal replacement therapy provision in renal satellite units in England and Wales. *Health Technol Assess*, 9, 1-178.

RODEWALD, R. & KARNOVSKY, M. J. (1974) Porous substructure of the glomerular slit diaphragm in the rat and mouse. *J Cell Biol*, 60, 423-33.

ROOPENIAN, D. C. & AKILESH, S. (2007) FcRn: the neonatal Fc receptor comes of age. *Nat Rev Immunol*, 7, 715-25.

ROTHWARF, D. M. & KARIN, M. (1999) The NF-kappa B activation pathway: a paradigm in information transfer from membrane to nucleus. *Sci STKE*, 1999, RE1.

RUDNICKI, M., EDER, S., PERCO, P., ENRICH, J., SCHEIBER, K., KOPPELSTATTER, C., SCHRATZBERGER, G., MAYER, B., OBERBAUER, R., MEYER, T. W. & MAYER, G. (2007) Gene expression profiles of human proximal tubular epithelial cells in proteinuric nephropathies. *Kidney Int*, 71, 325-35.

RUGGENENTI, P., MOSCONI, L., SANGALLI, F., CASIRAGHI, F., GAMBARA, V., REMUZZI, G. & REMUZZI, A. (1999a) Glomerular size-selective dysfunction in NIDDM is not ameliorated by ACE inhibition or by calcium channel blockade. *Kidney Int*, 55, 984-94.

RUGGENENTI, P., PERNA, A., GHERARDI, G., GARINI, G., ZOCCALI, C., SALVADORI, M., SCOLARI, F., SCHENA, F. P. & REMUZZI, G. (1999b) Renoprotective properties of ACE-inhibition in non-diabetic nephropathies with non-nephrotic proteinuria. *Lancet*, 354, 359-64.

RUGGENENTI, P., PERNA, A., GHERARDI, G., GASPARI, F., BENINI, R. & REMUZZI, G. (1998) Renal function and requirement for dialysis in chronic nephropathy patients on long-term ramipril: REIN follow-up trial. Gruppo Italiano di Studi Epidemiologici in Nefrologia (GISEN). Ramipril Efficacy in Nephropathy. *Lancet*, 352, 1252-6.

RUSSO, L. M., BAKRIS, G. L. & COMPER, W. D. (2002) Renal handling of albumin: a critical review of basic concepts and perspective. *Am J Kidney Dis*, 39, 899-919.

RUSSO, L. M., SANDOVAL, R. M., MCKEE, M., OSICKA, T. M., COLLINS, A. B., BROWN, D., MOLITORIS, B. A. & COMPER, W. D. (2007) The normal kidney filters nephrotic levels of albumin retrieved by proximal tubule cells: retrieval is disrupted in nephrotic states. *Kidney Int*, 71, 504-13.

RUSTOM, R., COSTIGAN, M., SHENKIN, A. & BONE, J. M. (1998) Proteinuria and renal tubular damage: urinary N-acetyl-beta-D-glucosaminidase and isoenzymes in dissimilar renal disease. *Am J Nephrol*, 18, 179-85.

SAITO, A., PIETROMONACO, S., LOO, A. K. & FARQUHAR, M. G. (1994) Complete cloning and sequencing of rat gp330/"megalin," a distinctive member of the low density lipoprotein receptor gene family. *Proc Natl Acad Sci U S A*, 91, 9725-9.

SALMON, A. H., TOMA, I., SIPOS, A., MUSTON, P. R., HARPER, S. J., BATES, D. O., NEAL, C. R. & PETI-PETERDI, J. (2007) Evidence for restriction of fluid and solute movement across the glomerular capillary wall by the subpodocyte space. *Am J Physiol Renal Physiol*, 293, F1777-86.

SAMBROOK, J., FRITSCH, E. F. & MANIATIS, T. (1989) *Molecular cloning : a laboratory manual*, Cold Spring Harbor, N.Y., Cold Spring Harbor Laboratory.

SARAV, M., WANG, Y., HACK, B. K., CHANG, A., JENSEN, M., BAO, L. & QUIGG, R. J. (2009) Renal FcRn reclaims albumin but facilitates elimination of IgG. *J Am Soc Nephrol*, 20, 1941-52.

SCHAINUCK, L. I., STRIKER, G. E., CUTLER, R. E. & BENDITT, E. P. (1970) Structural-functional correlations in renal disease. II. The correlations. *Hum Pathol*, 1, 631-41.

SCHWEGLER, J. S., HEPPELMANN, B., MILDENBERGER, S. & SILBERNAGL, S. (1991) Receptor-mediated endocytosis of albumin in cultured opossum kidney cells: a model for proximal tubular protein reabsorption. *Pflugers Arch*, 418, 383-92.

SEDGWICK, S. G. & SMERDON, S. J. (1999) The ankyrin repeat: a diversity of interactions on a common structural framework. *Trends Biochem Sci*, 24, 311-6.

SEETHARAM, B., CHRISTENSEN, E. I., MOESTRUP, S. K., HAMMOND, T. G. & VERROUST, P. J. (1997) Identification of rat yolk sac target protein of teratogenic antibodies, gp280, as intrinsic factor-cobalamin receptor. *J Clin Invest*, 99, 2317-22.

SETO, E. S., BELLEN, H. J. & LLOYD, T. E. (2002) When cell biology meets development: endocytic regulation of signaling pathways. *Genes Dev*, 16, 1314-36.

SHAHEEN, I. S., FINLAY, E., PRESCOTT, K., RUSSELL, M., LONGONI, M. & JOSS, S. (2010) Focal segmental glomerulosclerosis in a female patient with Donnai-Barrow syndrome. *Clin Dysmorphol*, 19, 35-7.

SHI, Y., MANTUANO, E., INOUE, G., CAMPANA, W. M. & GONIAS, S. L. (2009) Ligand binding to LRP1 transactivates Trk receptors by a Src family kinase-dependent pathway. *Sci Signal*, 2, ra18.

SHIUE, H., MUSCH, M. W., WANG, Y., CHANG, E. B. & TURNER, J. R. (2005) Akt2 phosphorylates ezrin to trigger NHE3 translocation and activation. *J Biol Chem*, 280, 1688-95.

SIDAWAY, J. E., DAVIDSON, R. G., MCTAGGART, F., ORTON, T. C., SCOTT, R. C., SMITH, G. J. & BRUNSKILL, N. J. (2004) Inhibitors of 3-hydroxy-3-methylglutaryl-CoA reductase reduce receptor-mediated endocytosis in opossum kidney cells. *J Am Soc Nephrol*, 15, 2258-65.

SINHA, D., BANNERGEE, S., SCHWARTZ, J. H., LIEBERTHAL, W. & LEVINE, J. S. (2004) Inhibition of ligand-independent ERK1/2 activity in kidney proximal tubular cells deprived of soluble survival factors up-regulates Akt and prevents apoptosis. *J Biol Chem*, 279, 10962-72.

SINHA, D., WANG, Z., RUCHALSKI, K. L., LEVINE, J. S., KRISHNAN, S., LIEBERTHAL, W., SCHWARTZ, J. H. & BORKAN, S. C. (2005) Lithium activates the Wnt and phosphatidylinositol 3-kinase Akt signaling pathways to promote cell survival in the absence of soluble survival factors. *Am J Physiol Renal Physiol*, 288, F703-13.

SLEPNEV, V. I. & DE CAMILLI, P. (2000) Accessory factors in clathrin-dependent synaptic vesicle endocytosis. *Nat Rev Neurosci*, 1, 161-72.

SMITH, D. B. & JOHNSON, K. S. (1988) Single-step purification of polypeptides expressed in *Escherichia coli* as fusions with glutathione S-transferase. *Gene*, 67, 31-40.

SONGYANG, Z., GISH, G., MBAMALU, G., PAWSON, T. & CANTLEY, L. C. (1995a) A single point mutation switches the specificity of group III Src homology (SH) 2 domains to that of group I SH2 domains. *J Biol Chem*, 270, 26029-32.

SONGYANG, Z., MARGOLIS, B., CHAUDHURI, M., SHOELSON, S. E. & CANTLEY, L. C. (1995b) The phosphotyrosine interaction domain of SHC recognizes tyrosine-phosphorylated NPXY motif. *J Biol Chem*, 270, 14863-6.

SONGYANG, Z., SHOELSON, S. E., CHAUDHURI, M., GISH, G., PAWSON, T., HASER, W. G., KING, F., ROBERTS, T., RATNOFSKY, S., LECHLEIDER, R. J. & ET AL. (1993) SH2 domains recognize specific phosphopeptide sequences. *Cell*, 72, 767-78.

SPOELGEN, R., HAMMES, A., ANZENBERGER, U., ZECHNER, D., ANDERSEN, O. M., JERCHOW, B. & WILLNOW, T. E. (2005) LRP2/megalin is required for patterning of the ventral telencephalon. *Development*, 132, 405-14.

STEINBERG, S. F. (2008) Structural basis of protein kinase C isoform function. *Physiol Rev*, 88, 1341-78.

STORA, S., CONTE, M., CHOUERY, E., RICHA, S., JALKH, N., GILLART, A. C., JOANNIS, A. L. & MEGARBANE, A. (2009) A 56-year-old female patient with facio-oculo-acoustico-renal syndrome (FOAR) syndrome. Report on the natural history and of a novel mutation. *Eur J Med Genet*, 52, 341-3.

SUNAYAMA, J., TSURUTA, F., MASUYAMA, N. & GOTOH, Y. (2005) JNK antagonizes Akt-mediated survival signals by phosphorylating 14-3-3. *J Cell Biol*, 170, 295-304.

SUNDIN, D. P., COHEN, M., DAHL, R., FALK, S. & MOLITORIS, B. A. (1994) Characterization of the beta 2-microglobulin endocytic pathway in rat proximal tubule cells. *Am J Physiol*, 267, F380-9.

SUSZTAK, K., CICCONE, E., MCCUE, P., SHARMA, K. & BOTTINGER, E. P. (2005) Multiple metabolic hits converge on CD36 as novel mediator of tubular epithelial apoptosis in diabetic nephropathy. *PLoS Med*, 2, e45.

SWERTFEGER, D. K., BU, G. & HUI, D. Y. (2002) Low density lipoprotein receptor-related protein mediates apolipoprotein E inhibition of smooth muscle cell migration. *J Biol Chem*, 277, 4141-6.

TAKASE, O., MINTO, A. W., PURI, T. S., CUNNINGHAM, P. N., JACOB, A., HAYASHI, M. & QUIGG, R. J. (2008) Inhibition of NF-kappaB-dependent Bcl-xL expression by clusterin promotes albumin-induced tubular cell apoptosis. *Kidney Int*, 73, 567-77.

TAKEDA, T., YAMAZAKI, H. & FARQUHAR, M. G. (2003) Identification of an apical sorting determinant in the cytoplasmic tail of megalin. *Am J Physiol Cell Physiol*, 284, C1105-13.

TANG, S., LEUNG, J. C., ABE, K., CHAN, K. W., CHAN, L. Y., CHAN, T. M. & LAI, K. N. (2003) Albumin stimulates interleukin-8 expression in proximal tubular epithelial cells in vitro and in vivo. *J Clin Invest*, 111, 515-27.

TANNER, G. A. (2009) Glomerular sieving coefficient of serum albumin in the rat: a two-photon microscopy study. *Am J Physiol Renal Physiol*, 296, F1258-65.

TANNER, S. M., AMINOFF, M., WRIGHT, F. A., LIYANARACHCHI, S., KURONEN, M., SAARINEN, A., MASSIKA, O., MANDEL, H., BROCH, H. & DE LA CHAPELLE, A. (2003) Amnionless, essential for mouse gastrulation, is mutated in recessive hereditary megaloblastic anemia. *Nat Genet*, 33, 426-9.

TERZI, F., BURTIN, M., HEKMATI, M., FEDERICI, P., GRIMBER, G., BRIAND, P. & FRIEDLANDER, G. (2000) Targeted expression of a dominant-negative EGF-R in the kidney reduces tubulointerstitial lesions after renal injury. *J Clin Invest*, 106, 225-34.

THEILIG, F., KRIZ, W., JERICHOW, T., SCHRADE, P., HAHNEL, B., WILLNOW, T., LE HIR, M. & BACHMANN, S. (2007) Abrogation of protein uptake through megalin-deficient proximal tubules does not safeguard against tubulointerstitial injury. *J Am Soc Nephrol*, 18, 1824-34.

THOMAS, M. E., HARRIS, K. P., WALLS, J., FURNESS, P. N. & BRUNSKILL, N. J. (2002) Fatty acids exacerbate tubulointerstitial injury in protein-overload proteinuria. *Am J Physiol Renal Physiol*, 283, F640-7.

THRAILKILL, K. M., NIMMO, T., BUNN, R. C., COCKRELL, G. E., MOREAU, C. S., MACKINTOSH, S., EDMONDSON, R. D. & FOWLKES, J. L. (2009) Microalbuminuria in type 1 diabetes is associated with enhanced excretion of the endocytic multiligand receptors megalin and cubilin. *Diabetes Care*, 32, 1266-8.

TIAN, W., ZHANG, Z. & COHEN, D. M. (2000) MAPK signaling and the kidney. *Am J Physiol Renal Physiol*, 279, F593-604.

TIMPL, R. & DZIADEK, M. (1986) Structure, development, and molecular pathology of basement membranes. *Int Rev Exp Pathol*, 29, 1-112.

TOJO, A. & ENDOU, H. (1992) Intrarenal handling of proteins in rats using fractional micropuncture technique. *Am J Physiol*, 263, F601-6.

TOWBIN, H., STAEBELIN, T. & GORDON, J. (1979) Electrophoretic transfer of proteins from polyacrylamide gels to nitrocellulose sheets: procedure and some applications. *Proc Natl Acad Sci U S A*, 76, 4350-4.

TRYGGVASON, K. (1999) Unraveling the mechanisms of glomerular ultrafiltration: nephrin, a key component of the slit diaphragm. *J Am Soc Nephrol*, 10, 2440-5.

UNGEWICKELL, A., WARD, M. E., UNGEWICKELL, E. & MAJERUS, P. W. (2004) The inositol polyphosphate 5-phosphatase Ocr1 associates with endosomes that are partially coated with clathrin. *Proc Natl Acad Sci U S A*, 101, 13501-6.

VAIDYA, V. S., OZER, J. S., DIETERLE, F., COLLINGS, F. B., RAMIREZ, V., TROTH, S., MUNIAPPA, N., THUDIUM, D., GERHOLD, D., HOLDER, D. J., BOBADILLA, N. A., MARRER, E., PERENTES, E., CORDIER, A., VONDERSCHER, J., MAURER, G., GOERING, P. L., SISTARE, F. D. & BONVENTRE, J. V. (2010) Kidney injury molecule-1 outperforms traditional biomarkers of kidney injury in preclinical biomarker qualification studies. *Nat Biotechnol*, 28, 478-85.

VAIDYA, V. S., RAMIREZ, V., ICHIMURA, T., BOBADILLA, N. A. & BONVENTRE, J. V. (2006) Urinary kidney injury molecule-1: a sensitive quantitative biomarker for early detection of kidney tubular injury. *Am J Physiol Renal Physiol*, 290, F517-29.

VAN TIMMEREN, M. M., BAKKER, S. J., VAIDYA, V. S., BAILLY, V., SCHUURS, T. A., DAMMAN, J., STEGEMAN, C. A., BONVENTRE, J. V. & VAN GOOR, H. (2006) Tubular kidney injury molecule-1 in protein-overload nephropathy. *Am J Physiol Renal Physiol*, 291, F456-64.

VAN TIMMEREN, M. M., VAIDYA, V. S., VAN REE, R. M., OTERDOOM, L. H., DE VRIES, A. P., GANS, R. O., VAN GOOR, H., STEGEMAN, C. A., BONVENTRE, J. V. & BAKKER, S. J. (2007a) High urinary excretion of kidney injury molecule-1 is an independent predictor of graft loss in renal transplant recipients. *Transplantation*, 84, 1625-30.

VAN TIMMEREN, M. M., VAN DEN HEUVEL, M. C., BAILLY, V., BAKKER, S. J., VAN GOOR, H. & STEGEMAN, C. A. (2007b) Tubular kidney injury molecule-1 (KIM-1) in human renal disease. *J Pathol*, 212, 209-17.

VARLAM, D. E., SIDDIQ, M. M., PARTON, L. A. & RUSSMANN, H. (2001) Apoptosis contributes to amphotericin B-induced nephrotoxicity. *Antimicrob Agents Chemother*, 45, 679-85.

VERHAVE, J. C., GANSEVOORT, R. T., HILLEGE, H. L., BAKKER, S. J., DE ZEEUW, D. & DE JONG, P. E. (2004) An elevated urinary albumin excretion predicts de novo development of renal function impairment in the general population. *Kidney Int Suppl*, S18-21.

VILASI, A., CUTILLAS, P. R., MAHER, A. D., ZIRAH, S. F., CAPASSO, G., NORDEN, A. W., HOLMES, E., NICHOLSON, J. K. & UNWIN, R. J. (2007) Combined proteomic and metabonomic studies in three genetic forms of the renal Fanconi syndrome. *Am J Physiol Renal Physiol*, 293, F456-67.

WAANDERS, F., VAIDYA, V. S., VAN GOOR, H., LEUVENINK, H., DAMMAN, K., HAMMING, I., BONVENTRE, J. V., VOGT, L. & NAVIS, G. (2009) Effect of renin-angiotensin-aldosterone system inhibition, dietary sodium restriction, and/or diuretics on urinary kidney injury molecule 1 excretion in nondiabetic proteinuric kidney disease: a post hoc analysis of a randomized controlled trial. *Am J Kidney Dis*, 53, 16-25.

WANG, A. H., GREGOIRE, S., ZIKA, E., XIAO, L., LI, C. S., LI, H., WRIGHT, K. L., TING, J. P. & YANG, X. J. (2005a) Identification of the ankyrin repeat proteins ANKRA and RFXANK as novel partners of class IIa histone deacetylases. *J Biol Chem*, 280, 29117-27.

WANG, P. X. & SANDERS, P. W. (2007) Immunoglobulin light chains generate hydrogen peroxide. *J Am Soc Nephrol*, 18, 1239-45.

WANG, Y., CAI, H., CEBOTARU, L., HRYCIW, D. H., WEINMAN, E. J., DONOWITZ, M., GUGGINO, S. E. & GUGGINO, W. B. (2005b) CIC-5: role in endocytosis in the proximal tubule. *Am J Physiol Renal Physiol*, 289, F850-62.

WANG, Y., CHEN, J., CHEN, L., TAY, Y. C., RANGAN, G. K. & HARRIS, D. C. (1997) Induction of monocyte chemoattractant protein-1 in proximal tubule cells by urinary protein. *J Am Soc Nephrol*, 8, 1537-45.

WANG, Y., RANGAN, G. K., TAY, Y. C. & HARRIS, D. C. (1999) Induction of monocyte chemoattractant protein-1 by albumin is mediated by nuclear factor kappaB in proximal tubule cells. *J Am Soc Nephrol*, 10, 1204-13.

WATKINS, P. J., BLAINEY, J. D., BREWER, D. B., FITZGERALD, M. G., MALINS, J. M., O'SULLIVAN, D. J. & PINTO, J. A. (1972) The natural history of diabetic renal disease. A follow-up study of a series of renal biopsies. *Q J Med*, 41, 437-56.

WEINMAN, E. J., EVANGELISTA, C. M., STEPLOCK, D., LIU, M. Z., SHENOLIKAR, S. & BERNARDO, A. (2001) Essential role for NHERF in cAMP-mediated inhibition of the Na⁺-HCO₃⁻ co-transporter in BSC-1 cells. *J Biol Chem*, 276, 42339-46.

WHALEY-CONNELL, A. T., MORRIS, E. M., REHMER, N., YAGHOUBIAN, J. C., WEI, Y., HAYDEN, M. R., HABIBI, J., STUMP, C. S. & SOWERS, J. R. (2007)

Albumin activation of NAD(P)H oxidase activity is mediated via Rac1 in proximal tubule cells. *Am J Nephrol*, 27, 15-23.

WIGHT, J. P., SALZANO, S., BROWN, C. B. & EL NAHAS, A. M. (1992) Natural history of chronic renal failure: a reappraisal. *Nephrol Dial Transplant*, 7, 379-83.

WILLIAMS, A. J., BAKER, F. & WALLS, J. (1987) Effect of varying quantity and quality of dietary protein intake in experimental renal disease in rats. *Nephron*, 46, 83-90.

WILLIAMS, M. E. (2005) Diabetic nephropathy: the proteinuria hypothesis. *Am J Nephrol*, 25, 77-94.

WILLIAMS, P. S., FASS, G. & BONE, J. M. (1988) Renal pathology and proteinuria determine progression in untreated mild/moderate chronic renal failure. *Q J Med*, 67, 343-54.

WILLNOW, T. E., ARMSTRONG, S. A., HAMMER, R. E. & HERZ, J. (1995) Functional expression of low density lipoprotein receptor-related protein is controlled by receptor-associated protein in vivo. *Proc Natl Acad Sci U S A*, 92, 4537-41.

WILLNOW, T. E., GOLDSTEIN, J. L., ORTH, K., BROWN, M. S. & HERZ, J. (1992) Low density lipoprotein receptor-related protein and gp330 bind similar ligands, including plasminogen activator-inhibitor complexes and lactoferrin, an inhibitor of chylomicron remnant clearance. *J Biol Chem*, 267, 26172-80.

WILLNOW, T. E., HILPERT, J., ARMSTRONG, S. A., ROHLMANN, A., HAMMER, R. E., BURNS, D. K. & HERZ, J. (1996a) Defective forebrain development in mice lacking gp330/megalin. *Proc Natl Acad Sci U S A*, 93, 8460-4.

WILLNOW, T. E., ROHLMANN, A., HORTON, J., OTANI, H., BRAUN, J. R., HAMMER, R. E. & HERZ, J. (1996b) RAP, a specialized chaperone, prevents ligand-induced ER retention and degradation of LDL receptor-related endocytic receptors. *EMBO J*, 15, 2632-9.

WOHLFARTH, V., DRUMM, K., MILDENBERGER, S., FREUDINGER, R. & GEKLE, M. (2003) Protein uptake disturbs collagen homeostasis in proximal tubule-derived cells. *Kidney Int Suppl*, S103-9.

WOLF, G., SCHROEDER, R., ZIYADEH, F. N. & STAHL, R. A. (2004) Albumin up-regulates the type II transforming growth factor-beta receptor in cultured proximal tubular cells. *Kidney Int*, 66, 1849-58.

WRONG, O. M., NORDEN, A. G. & FEEST, T. G. (1994) Dent's disease; a familial proximal renal tubular syndrome with low-molecular-weight proteinuria, hypercalciuria, nephrocalcinosis, metabolic bone disease, progressive renal failure and a marked male predominance. *QJM*, 87, 473-93.

YAMMANI, R. R., SEETHARAM, S. & SEETHARAM, B. (2001) Identification and characterization of two distinct ligand binding regions of cubilin. *J Biol Chem*, 276, 44777-84.

YANAGISAWA, J., YANAGI, Y., MASUHIRO, Y., SUZAWA, M., WATANABE, M., KASHIWAGI, K., TORIYABE, T., KAWABATA, M., MIYAZONO, K. & KATO, S. (1999) Convergence of transforming growth factor-beta and vitamin D signaling pathways on SMAD transcriptional coactivators. *Science*, 283, 1317-21.

YANG, Y. L., LIN, S. H., CHUANG, L. Y., GUH, J. Y., LIAO, T. N., LEE, T. C., CHANG, W. T., CHANG, F. R., HUNG, M. Y., CHIANG, T. A. & HUNG, C. Y. (2007) CD36 is a novel and potential anti-fibrogenic target in albumin-induced renal proximal tubule fibrosis. *J Cell Biochem*, 101, 735-44.

YARD, B. A., CHORIANOPOULOS, E., HERR, D. & VAN DER WOUDE, F. J. (2001) Regulation of endothelin-1 and transforming growth factor-beta1 production in cultured proximal tubular cells by albumin and heparan sulphate glycosaminoglycans. *Nephrol Dial Transplant*, 16, 1769-75.

YASUDA, J., WHITMARSH, A. J., CAVANAGH, J., SHARMA, M. & DAVIS, R. J. (1999) The JIP group of mitogen-activated protein kinase scaffold proteins. *Mol Cell Biol*, 19, 7245-54.

YU, H., CHEN, J. K., FENG, S., DALGARNO, D. C., BRAUER, A. W. & SCHREIBER, S. L. (1994) Structural basis for the binding of proline-rich peptides to SH3 domains. *Cell*, 76, 933-45.

YUSEFF, M. I., FARFAN, P., BU, G. & MARZOLO, M. P. (2007) A cytoplasmic PPPSP motif determines megalin's phosphorylation and regulates receptor's recycling and surface expression. *Traffic*, 8, 1215-30.

YUSUF, S., TEO, K. K., POGUE, J., DYAL, L., COPLAND, I., SCHUMACHER, H., DAGENAIS, G., SLEIGHT, P. & ANDERSON, C. (2008) Telmisartan, ramipril, or both in patients at high risk for vascular events. *N Engl J Med*, 358, 1547-59.

ZEISBERG, E. M., TARNAVSKI, O., ZEISBERG, M., DORFMAN, A. L., MCMULLEN, J. R., GUSTAFSSON, E., CHANDRAKER, A., YUAN, X., PU, W. T., ROBERTS, A. B., NEILSON, E. G., SAYEGH, M. H., IZUMO, S. & KALLURI, R.

(2007) Endothelial-to-mesenchymal transition contributes to cardiac fibrosis. *Nat Med*, 13, 952-61.

ZHAI, X. Y., NIELSEN, R., BIRN, H., DRUMM, K., MILDENBERGER, S., FREUDINGER, R., MOESTRUP, S. K., VERRAUST, P. J., CHRISTENSEN, E. I. & GEKLE, M. (2000) Cubilin- and megalin-mediated uptake of albumin in cultured proximal tubule cells of opossum kidney. *Kidney Int*, 58, 1523-33.

ZHANG, C., BAUDINO, T. A., DOWD, D. R., TOKUMARU, H., WANG, W. & MACDONALD, P. N. (2001) Ternary complexes and cooperative interplay between NCoA-62/Ski-interacting protein and steroid receptor coactivators in vitamin D receptor-mediated transcription. *J Biol Chem*, 276, 40614-20.

ZOJA, C., DONADELLI, R., COLLEONI, S., FIGLIUZZI, M., BONAZZOLA, S., MORIGI, M. & REMUZZI, G. (1998) Protein overload stimulates RANTES production by proximal tubular cells depending on NF-kappa B activation. *Kidney Int*, 53, 1608-15.

ZOU, Z., CHUNG, B., NGUYEN, T., MENTONE, S., THOMSON, B. & BIEMESDERFER, D. (2004) Linking receptor-mediated endocytosis and cell signaling: evidence for regulated intramembrane proteolysis of megalin in proximal tubule. *J Biol Chem*, 279, 34302-10.